DISSERTATION

# THE ROLE OF PROTEASES IN *PECTOBACTERIUM CAROTOVORUM* VIRULENCE

Submitted by

Maryam Mahdi Alaryan

Department of Agricultural Biology

In partial fulfillment of the requirements

For the Degree of Doctor of Philosophy

Colorado State University

Fort Collins, Colorado

Summer 2025

Doctoral Committee:

Advisor: Amy O. Charkowski

Jane Stewart
Robyn Roberts
Brad Borlee

Copyright by Maryam Mahdi Alaryan 2025

All Rights Reserved

ABSTRACT

THE ROLE OF PROTEASES IN *PECTOBACTERIUM CAROTOVORUM* VIRULENCE

This dissertation investigates the role of proteases in the virulence of *Pectobacterium carotovorum*, a significant bacterial pathogen responsible for economically devastating soft rot diseases in numerous plant hosts. Proteases are crucial enzymes that enable bacterial pathogens to degrade host tissues, thus facilitating infection and colonization. Despite extensive study, significant gaps persist regarding protease regulation, precise roles in virulence, and effective diagnostic and management strategies.

Initially, we thoroughly reviewed the current knowledge on bacterial proteases, particularly emphasizing their classification, regulatory pathways, and mechanisms involved in host interactions. Subsequently, we systematically optimized protease activity detection assays, leading to improved protocols for reliably identifying protease activity in *P. carotovorum*. These optimized assays provided foundational tools for accurately characterizing protease-related phenotypes.

To identify genetic factors controlling virulence, a mutant library of *P. carotovorum* WPP14 was constructed using mini-Tn5 transposon mutagenesis. Phenotypic screening identified critical mutations affecting protease production, motility, and pectate lyase activity, notably disruptions in *gacS*, *purM*, *metA*, and *prtW* genes. Transcriptomic analyses further confirmed extensive regulatory roles for these genes, highlighting their impact on secretion systems, metabolic pathways, and stress responses. Complementation experiments validated these genes' direct roles in regulating virulence-associated traits.

Functional evaluations of cloned proteases from *P. carotovorum* WPP14 were conducted to assess interactions with plant-derived inhibitors from *Solanum chacoense*. Experimental assays

revealed limited inhibitory effects, with measurable inhibition observed only for Lon protease under specific conditions. Complementary computational analyses using AlphaFold3 supported these findings, predicting weak interactions between most cloned proteases and the tested inhibitors. These results highlight the need for further refinement and optimization of protease inhibitors as a potential strategy for managing soft rot diseases.

Additionally, a comprehensive review of related soft rot pathogens *Dickeya* and *Musicola* outlined current diagnostic methods, biochemical differentiation techniques, and molecular identification tools, identifying limitations in existing methods. These findings underscore the need for enhanced diagnostic tools and methodologies to better detect and manage these pathogens effectively.

Collectively, this research advances the understanding of protease-mediated virulence mechanisms in *P. carotovorum*, identifies key genetic targets for potential disease management strategies, and provides improved methodologies for pathogen detection and virulence assessment. These insights lay critical groundwork for developing effective control measures against economically significant soft rot diseases.

# ACKNOWLEDGMENTS

I would like to express my deepest appreciation to my advisor, Dr. Amy Charkowski, for her invaluable guidance, unwavering support, and insightful feedback throughout my doctoral studies. Her mentorship, dedication, and expertise have significantly shaped my growth as a researcher and academic, and without her continuous assistance, this dissertation would not have been possible.

I am grateful to my doctoral committee members, Dr. Jane Stewart, Dr. Robyn Roberts, and Dr. Brad Borlee, for giving me this opportunity and for their patience, valuable suggestions, and feedback, which contributed to refining my research and improving the overall quality of this dissertation.

Special thanks to my colleagues Dr. Janak Joshi and Dr. Yuan Zeng, whose support and expertise were indispensable at the beginning of my research journey. Their generosity in sharing knowledge and experience greatly enhanced my laboratory skills and confidence. I also sincerely thank Dr. Aritra Roy Choudhury, who joined our lab later and generously provided valuable assistance and guidance whenever possible.

Finally, I want to express my heartfelt appreciation to my family and friends for their constant emotional support, patience, and encouragement during my studies. Their understanding and belief in my capabilities have been crucial in helping me achieve this academic milestone.

# DEDICATION

I dedicate this dissertation to the memory of my beloved father, whose unwavering belief in my abilities gave me strength even in moments when I doubted myself. To my spouse, daughters, and family, your endless love, patience, and support have inspired me every step of this journey.

TABLE OF CONTENTS

# Chapter 1 - Proteases and Their Role in Virulence of *Pectobacterium carotovorum*: A Comprehensive Review


## Summary

Proteases produced by *Pectobacterium carotovorum* represent critical virulent factors underlying soft rot diseases in various economically important crops. Bacterial proteases are classified based on their catalytic mechanisms and substrate specificity, playing essential roles in degrading plant structural proteins, promoting bacterial colonization, and compromising plant defenses. Extensive research on metalloproteases such as PrtW has elucidated their roles in tissue maceration and immune evasion. Regulatory systems controlling protease production, notably quorum sensing and the GacS/GacA two-component pathway, respond dynamically to environmental and host-derived signals, influencing protease expression. This chapter highlights significant knowledge gaps, including incomplete structural data for proteases, limited insights into protease-mediated disruption of host defense responses, and insufficient understanding of regulatory mechanisms under natural field conditions. Integrated approaches combining molecular biology, genomics, proteomics, and field-based research are essential to overcome these challenges and develop effective strategies for controlling soft rot diseases.


## Introduction

Soft rot diseases are among the most destructive bacterial diseases affecting many economically important crops worldwide, including potatoes, carrots, tomatoes, and ornamental plants (Charkowski, 2018). These diseases cause extensive maceration of plant tissues, leading to significant losses in crop yield and quality, and resulting in severe economic impacts globally (Mansfield et al., 2012). Among the pathogens responsible for soft rot, *Pectobacterium carotovorum* is particularly notable as a Gram-negative bacterium within the family

Pectobacteriaceae, known for its wide host range and aggressive disease-causing abilities (Adeolu et al., 2016).

The ability of *P. carotovorum* to cause disease largely depends on its production of extracellular enzymes that break down plant cell walls, enabling rapid infection and spread within host tissues. Of these enzymes, proteases are particularly significant, playing important roles in bacterial virulence, nutrient uptake, and the breakdown of host tissue (Charkowski et al., 2012; Joshi et al., 2022). Proteases degrade structural proteins in plant tissues and interfere with host defense responses, thus promoting bacterial colonization and survival in host plants (Misas-Villamil & Van der Hoorn, 2008).

Despite their importance, the molecular mechanisms controlling protease production and regulation in *P. carotovorum* remain incompletely understood. Recent genomic and transcriptomic studies have provided insights into protease regulation, highlighting the importance of quorum sensing, two-component regulatory systems such as the GacS/GacA pathway, and small RNA-based post-transcriptional regulation (Charkowski, 2018; Joshi et al., 2022). However, significant knowledge gaps remain, particularly regarding how these regulatory systems respond under natural environmental and host conditions.

This literature review will summarize the current understanding of proteases produced by *P. carotovorum*, including their classification, roles in disease, regulatory mechanisms, and implications for disease control. Emphasizing gaps in our current understanding, this chapter aims to highlight essential areas for future investigation to improve our grasp of protease-driven virulence and to support the development of practical disease management solutions.

## *Pectobacterium carotovorum*: Pathogen and Disease Overview

*Pectobacterium carotovorum* is a Gram-negative, rod-shaped bacterium belonging to the family Pectobacteriaceae. It is well known for causing soft rot disease in a wide range of plant hosts (Adeolu et al., 2016). Historically classified within the genus *Erwinia*, advances in genomic analysis have led to its current classification under the genus *Pectobacterium*, reflecting its distinct genomic and phylogenetic traits (Adeolu et al., 2016; Toth et al., 2003). Among the various species within the genus *Pectobacterium*, such as *P. atrosepticum*, *P. betavasculorum*, *P. wasabiae*, and *P. carotovorum* subsp. *brasiliense*, *P. carotovorum* is particularly notable for its widespread distribution and high aggressiveness, frequently causing significant economic losses in potatoes, carrots, tomatoes, cabbage, and various ornamental plants (Charkowski, 2015; Mansfield et al., 2012). Its ability to rapidly degrade plant tissues and infect numerous hosts, particularly potatoes, emphasizes the pathogen's adaptability and highlights the importance of thoroughly understanding its biology and virulence mechanisms to develop effective control and management strategies (Charkowski, 2015; Moleleki et al., 2017).

*P. carotovorum* is highly adaptable and frequently found in different environments, such as soil, surface water, and plant debris. This versatility helps the bacterium spread widely and effectively infect multiple plant hosts (Pérombelon, 2002). In addition, the genome of *P. carotovorum* contains a large number of genes that encode extracellular enzymes, various secretion systems, and regulatory components, all of which enhance its capacity to cause disease and thrive under diverse environmental conditions (Toth et al., 2003).

Infection by *P. carotovorum* typically begins through wounds or natural openings in plants, rapidly progressing to extensive tissue maceration characterized by softening, and liquefaction of plant tissues (Charkowski, 2018). The pathogen exhibits a wide host range, infecting numerous

economically important crops such as potatoes, carrots, cabbage, tomatoes, and several ornamental plants (Mansfield et al., 2012; Pérombelon, 2002).

The economic impact of soft rot diseases caused by *P. carotovorum* is substantial, leading to yield losses, reduced product quality, and increased costs associated with disease management and control (Charkowski, 2018). Therefore, it is crucial to understand the biology and pathogenic mechanisms behind *P. carotovorum*, especially the role of key virulence factors such as proteases, to help develop effective strategies to reduce the virulence and pathogenicity of the soft rot disease.

**Bacterial Proteases: General Classification and Function**

Proteases are enzymes that catalyze the breakdown of proteins by hydrolyzing peptide bonds. In bacterial pathogens, proteases serve crucial roles beyond simple nutrient acquisition; they are also key players in virulence and host interactions (Figaj et al., 2019). These enzymes are typically classified according to two primary criteria: the catalytic mechanism and the cleavage site specificity.

Based on catalytic mechanisms, proteases are classified into several groups, including serine proteases, metalloproteases, cysteine proteases, aspartic proteases, glutamic proteases, and threonine proteases (Ramírez-Larrota & Eckhard, 2022). Serine proteases contain serine residues in their active sites, which are essential for catalysis, while metalloproteases utilize metal ions (often zinc) at their catalytic centers (Feng et al., 2014; Page & Di Cera, 2008). Cysteine proteases employ cysteine residues for catalytic activity, and aspartic proteases contain essential aspartic acid residues within their catalytic sites (Hotson & Mudgett, 2004; Rawlings et al., 2018).

Proteases can also be distinguished based on their cleavage site specificity as either endopeptidases or exopeptidases. Endopeptidases cleave internal peptide bonds within a protein substrate, while exopeptidases remove terminal amino acids from either end of the protein

(Ramírez-Larrota & Eckhard, 2022). This classification provides additional insight into protease functions and their roles in pathogenicity. Overall, the biochemical diversity, distinct catalytic properties, and substrate specificities of proteases underline their critical roles in bacterial virulence and host-pathogen interactions.

**Proteases Produced by *Pectobacterium carotovorum* and Their Role in Virulence**

*P. carotovorum* produces a variety of extracellular proteases critical for its virulence, host interactions, and survival. Among these, the metalloprotease PrtW is the most extensively studied. PrtW is a zinc-dependent extracellular protease that facilitates extensive maceration of host tissues by degrading structural proteins, weakening plant cell integrity, and promoting bacterial colonization (Marits et al., 2002). This proteolytic activity is critical because it works together with other enzymes like pectinases and cellulases, accelerating the breakdown of plant cell walls and tissues, which in turn facilitates bacterial infection and spread (Marits et al., 1999).

Beyond its direct role in tissue degradation, PrtW also participates in bacterial immune evasion by degrading antimicrobial peptides produced by host plants, thereby impairing the plant's defense response (Misas-Villamil & Van der Hoorn, 2008). Recent findings on *Pectobacterium brasiliense Pb1692* have shown that protease inhibitors derived from plants can significantly reduce the activity of PrtW, resulting in decreased bacterial motility and reduced virulence. This highlights proteases as a valuable potential target for managing soft rot disease (Joshi et al., 2022).

Other proteases in *P. carotovorum*, including serine proteases (HtrA family), maintain bacterial membrane stability under stress conditions, facilitating bacterial adaptation and survival in hostile environments (Figaj et al., 2019). ATP-dependent proteases such as Lon and FtsH play crucial roles in protein quality control by degrading damaged or misfolded proteins, enabling bacterial resilience against oxidative and environmental stress (Figaj et al., 2020; Langklotz et al.,

2012). Moreover, proteases contribute significantly to biofilm formation, which helps the bacteria withstand harsh environmental conditions and evade plant immune responses, eventually enabling longer-lasting infections (Ramírez-Larrota & Eckhard, 2022).

**Regulation of Protease Production in *Pectobacterium carotovorum***

Protease production in *P. carotovorum* is tightly controlled through a complicated network of signaling pathways, responding dynamically to bacterial population density, environmental stimuli, and interactions with plant hosts. Quorum sensing, involving N-acyl homoserine lactone (AHL) signaling molecules, is a key regulatory mechanism controlling the expression of extracellular enzymes such as proteases. As bacterial populations increase, higher concentrations of AHL molecules trigger the expression of protease genes, synchronizing virulence factor production with bacterial growth stages and optimizing infection efficiency (Põllumaa et al., 2012).

Another major regulatory pathway influencing protease production is the GacS/GacA two-component system, a global regulator of virulence determinants. In this system, environmental cues are detected by the sensor kinase GacS, which then phosphorylates and activates the response regulator GacA. Activated GacA promotes the production of small regulatory RNAs, including RsmB, which interact with and neutralize the translational repressor RsmA. Thus, the pathogen becomes more virulent due to the significantly enhanced translation of extracellular enzymes, including proteases (Charkowski et al., 2012; Marits et al., 2002).

Environmental factors such as nutrient availability, temperature fluctuations, and plant-derived signals also notably influence protease expression. Protease gene expression increases under nutrient limitation or exposure to specific plant-derived compounds, helping the bacterium adapt effectively to challenging plant environments (Põllumaa et al., 2012). In addition,

temperature changes have been demonstrated to modulate protease production and secretion, influencing bacterial virulence under diverse climatic conditions encountered during infection (Kaczynska et al., 2021).

The complexity of protease regulation is summarized in Table 1, which lists various environmental, bacterial-derived, and host-derived signals known to influence protease production in *P. carotovorum*. This table emphasizes the intricate interactions and regulatory pathways critical to understanding and managing bacterial virulence.

**Table 1: Environmental, bacterial-derived, and host-derived signals influencing protease production in *Pectobacterium carotovorum***

| Signal Type | Specific Signal | Regulatory System(s) | Effect on Protease Production | Reference(s) |
|---|---|---|---|---|
| **Environmental** | Temperature | GacS/GacA, ArcAB | Modulates protease expression and secretion | Kaczynska et al., 2021 |
| **Environmental** | Oxygen availability | ArcAB | Alters protease production under anaerobic conditions | Babujee et al., 2012 |
| **Environmental** | Nutrient availability | ExpI/ExpR quorum sensing | Increases protease production at high bacterial density | Põllumaa et al., 2012; Fan et al., 2020 |
| **Bacterial-derived** | Acyl-homoserine lactones (AHLs) | ExpI/ExpR quorum sensing | Enhances protease production at high bacterial density | Charkowski, 2012; Põllumaa et al., 2012 |
| **Host-derived** | Pectate | KdgR | Increases expression of protease genes | Liu et al., 1999; Charkowski, 2012 |
| **Host-derived** | Salicylic acid | ExpI/ExpR quorum sensing, AHL synthase | Inhibits quorum sensing genes, reducing protease production and bacterial virulence | Joshi et al., 2020 |

## Insights from Genomics and Transcriptomics

Recent genomic and transcriptomic studies have enhanced our understanding of how protease genes are expressed and regulated in *the Pectobacterium* species. Although research in

this area is limited, comparative genomic studies have identified notable genetic variations among different Pectobacterium strains, especially concerning genes linked to virulence, including those encoding proteases (Arizala & Arif, 2019; Toth et al., 2015). These analyses demonstrate how adaptable these bacteria are across diverse hosts and environments, highlighting the potential influence of horizontal gene transfer on their virulent traits.

Recent transcriptomic studies have provided new information about how protease genes in *P. carotovorum* respond to environmental factors, such as nutrient availability and interactions with host plants. For example, during plant infection, protease gene expression levels change in response to host-derived signals and stress conditions within plant tissues (Fan et al., 2020). Furthermore, Sun et al. (2024) conducted transcriptomic comparisons between closely related bacterial strains under similar conditions, uncovering distinct patterns of protease gene expression. These findings highlight the differences in regulatory responses and adaptive strategies that are specific to each strain (Sun et al., 2024).

More studies focusing on gene regulatory networks and protease expression under conditions similar to field environments need to be conducted to uncover the role of proteases and expand our understanding of proteases in bacterial virulence. This could also lead to the identification of promising targets for improved management of soft rot diseases.

**Targeting Proteases for Disease Management: Current and Emerging Approaches**

Traditionally, managing soft rot diseases caused by Pectobacterium carotovorum has mainly depended on cultural methods, including sanitation, exclusion, using certified disease-free seeds, and proper water management (Charkowski, 2015). Despite ongoing research, these basic management practices have remained largely unchanged over time because of persistent difficulties in effectively controlling this pathogen (Charkowski, 2015; Czajkowski et al., 2011).

Chemical control options are limited and usually ineffective. Copper-based compounds are among the few chemical treatments available; however, their effectiveness is mostly limited to surface protection, and they cannot penetrate plant tissues to eliminate internal infections. Additionally, extensive use of copper treatments has led to bacterial resistance, further reducing their effectiveness (Bender & Cooksey, 1987; Czajkowski et al., 2011; Fan et al., 2022).

Due to these challenges, researchers have explored alternative approaches, such as biological control. For example, bacteriophages, viruses specifically infecting bacteria, have shown potential in reducing Pectobacterium populations. Studies have demonstrated that certain bacteriophages effectively lower bacterial populations and decrease virulence by reducing the production of harmful enzymes (Czajkowski, 2016; Kim et al., 2022). Nevertheless, practical applications of phage-based biocontrol still face challenges, including variability in their effectiveness under natural conditions and potential bacterial resistance.

Recently, protease inhibitors isolated from plants have emerged as an innovative and promising method to combat soft rot. Joshi et al. (2022) successfully isolated protein-based inhibitors from wild potato species *Solanum chacoense*. These inhibitors (specifically g28531 and g6571) significantly reduced bacterial protease activity, which in turn impaired bacterial motility and decreased the severity of the disease. Because these inhibitors directly interact with bacterial proteases, they protect plant tissues from damage and slow pathogen spread. Therefore, integrating these inhibitors into plant breeding programs or applying them directly to susceptible crops could significantly enhance resistance to soft rot diseases.

Overall, these different approaches represent ongoing efforts to manage *P. carotovorum* disease effectively. Combining multiple strategies and continuous research will be essential for achieving sustainable and successful control of the soft rot pathogen.

**Current Knowledge Gaps, Future Research Directions, and Recommendations**

Despite advances in understanding the role of proteases in the virulence of *P. carotovorum*, many challenges and critical knowledge gaps remain. One major challenge is the functional redundancy among proteases, in which many proteases share similar roles, making it difficult to pinpoint the exact contribution of each enzyme. This redundancy complicates the efforts to identify specific targets for developing effective inhibitors, emphasizing the need for more integrated research approaches.

Moreover, there is a significant lack of structural data for proteases produced by *P. carotovorum*, which limits our ability to design precise inhibitors and thoroughly understand their interactions with substrates (Feng et al., 2014). Expanding our knowledge about these biochemical properties and structural characteristics of these understudied proteases would be valuable in elucidating their specific roles in pathogenicity (Figaj et al., 2019; Joshi et al., 2022).

Another important gap is the incomplete knowledge of protease regulation under natural field conditions. Laboratory experiments have provided useful insights, but these findings often differ from actual conditions in the field. Factors such as temperature changes, nutrient availability, and plant-derived signals likely have significant impacts on protease expression and secretion, but these influences remain insufficiently explored (Fan et al., 2020; Kaczynska et al., 2021).

Additionally, interactions between bacterial proteases and plant immune systems require further investigation. While it is known that bacterial proteases contribute to immune evasion, the precise mechanisms by which they interact with plant defenses remain unclear (Misas-Villamil & Van der Hoorn, 2008). Clarifying these interactions could lead to new strategies for enhancing crop resistance.

Addressing these challenges will require a comprehensive and integrated research approach. Future studies should combine genomics, transcriptomics, proteomics, and structural biology to gain deeper insights. Furthermore, developing advanced methods to study protease activity directly in infected plant tissues will be critical. Closing these knowledge gaps can lead to improved management strategies, helping reduce the economic impacts of soft rot diseases caused by *P. carotovorum* (Arizala & Arif, 2019; Sun et al., 2024).

**Addressing Identified Gaps: Overview of Dissertation Chapters**

Although some critical gaps, such as detailed structural data for proteases, understanding of protease regulation under natural field conditions, and mechanisms underlying protease interactions with plant immune systems, still require further research, several key gaps identified above are systematically addressed in the following chapters.

***Chapter 2.*** Accurately measuring protease activity is essential for understanding bacterial virulence, but developing effective assays can be challenging due to incomplete or unclear methods in published literature. This chapter addresses difficulties encountered when using dry skim milk agar plates for protease assays, highlighting issues with insufficient recipe details and reproducibility. Various assay recipes were evaluated, and modifications were introduced to enhance clarity and reliability, providing practical guidance for future studies on protease-mediated virulence in *P. carotovorum*.M.M.A – Responsible for conducting all experiments and writing the entire chapter.

***Chapter 3.*** Identifying the roles of specific proteases in bacterial virulence is crucial for managing soft rot diseases caused by *P. carotovorum*. This chapter screens a mutant library of *P. carotovorum* WPP14 to identify mutants with altered protease production and regulation. Through comprehensive phenotypic analyses, this study clearly defines individual proteases and their

regulators involved in infection processes, virulence, and host interactions. These findings highlight key proteases and regulatory pathways that represent promising targets for disease control strategies.**Author contributions:** Y.Z. and J.J. prepared the *Pectobacterium carotovorum* WPP14 mutant library. M.M.A. conducted all experiments described in this chapter and wrote the entire chapter. A.O.C. edited the chapter.

***Chapter 4.*** Characterizing specific proteases involved in virulence is fundamental to improving soft rot management strategies; however, limited data on cloning and assessing these proteases pose challenges. This chapter addresses practical difficulties encountered during cloning and protease activity testing, emphasizing issues related to consistently obtaining active proteases, despite refining cloning methods and optimizing assay conditions established in Chapter 2. Despite experimental limitations, valuable preliminary data were obtained on cloned protease interactions with protease inhibitors from *Solanum chacoense*. Computational analyses further provided insights into potential inhibitor-protease interactions, offering foundational knowledge and practical recommendations for future research.M.M.A. – Responsible for cloning the proteases from *Pectobacterium carotovorum* WPP14, conducting all experiments, and writing the entire chapter.

- J.J**.** – Responsible for cloning the protease inhibitors.
- A.O.C. – Responsible for editing the chapter.

***Chapter 5.*** Accurate identification and characterization of *Dickeya* and *Musicola* species are essential due to their significance in soft rot diseases affecting economically important crops. This chapter provides a comprehensive review of both genera, emphasizing their biology, taxonomy, and diagnostic methods. It discusses current knowledge of their epidemiology and pathogenic interactions, highlighting critical gaps, especially regarding *Musicola*. Evaluations of

semi-selective media, biochemical differentiation assays, and PCR-based detection methods provide valuable insights for diagnosing and managing diseases caused by these pathogens, guiding future epidemiological and ecological research to enhance disease management.M.M.A. – Responsible for Table 4.

- A.O.C and J.J - Responsible for writing the entire chapter.

**Conclusions**

Proteases significantly contribute to the pathogenicity of *P. carotovorum*, primarily by degrading plant cell wall components and disrupting host defense mechanisms. While recent research has provided valuable insights into these processes, critical gaps still exist. Specifically, there is a need for detailed structural and biochemical analyses of understudied proteases, a clearer understanding of protease regulatory mechanisms under natural field conditions, and more precise knowledge regarding bacterial protease interactions with plant immune systems.

Although promising strategies such as protease inhibitors and biological control methods have emerged, practical implementation faces notable challenges, including redundancy among proteases and inconsistent effectiveness in field conditions. To overcome these obstacles, an integrated research approach combining molecular biology, genomics, proteomics, structural biology, and realistic field studies is required. The following chapters in this dissertation aim to address several of these identified knowledge gaps, providing foundational insights and practical methods to support the development of more effective and sustainable management strategies for soft rot diseases caused by *P. carotovorum.*

**References**


Adeolu, M., Alnajar, S., Naushad, S., & S. Gupta, R. (2016). Genome-based phylogeny and taxonomy of the '*Enterobacteriales*': proposal for *Enterobacterales* ord. nov. divided into the families *Enterobacteriaceae*, *Erwiniaceae* fam. nov., *Pectobacteriaceae* fam. nov., *Yersiniaceae* fam. nov., *Hafniaceae* fam. nov., *Morganellaceae* fam. nov., and *Budviciaceae* fam. nov. *International journal of systematic and evolutionary microbiology*, *66*(12), 5575-5599.

Arizala, D., & Arif, M. (2019). Genome-wide analyses revealed remarkable heterogeneity in pathogenicity determinants, antimicrobial compounds, and crispr-cas systems of complex phytopathogenic genus *Pectobacterium*. *Pathogens*, *8*(4), 247.

Bender, C., & Cooksey, D. (1987). Molecular cloning of copper resistance genes from *Pseudomonas syringae* pv. tomato. *Journal of Bacteriology*, *169*(2), 470-474.

Charkowski, A., Blanco, C., Yedidia, I., Charkowski, A., Blanco, C., Condemine, G., Expert, D., Franza, T., Hayes, C., Hugouvieux-Cotte-Pattat, N., Solanilla, E. L., Low, D., Moleleki, L., Pirhonen, M., Pitman, A., Perna, N., Reverchon, S., Rodríguez Palenzuela, P., San Francisco, M., & Toth, I. (2012). The role of secretion systems and small molecules in soft-rot enterobacteriaceae pathogenicity. *Annual review of phytopathology.*, *50*(1), 425-449.

Charkowski, A. O. (2015). Biology and control of *Pectobacterium* in potato. *American journal of potato research.*, *92*(2), 223-229.

Charkowski, A. O. (2018). The changing face of bacterial soft-rot diseases. *Annual review of phytopathology.*, *56*(1), 269-288.

Czajkowski, R. (2016). Bacteriophages of soft rot *Enterobacteriaceae*—a minireview. *FEMS Microbiology Letters*, *363*(2), fnv230.

Czajkowski, R., Perombelon, M. C., van Veen, J. A., & van der Wolf, J. M. (2011). Control of blackleg and tuber soft rot of potato caused by Pectobacterium and Dickeya species: a review. *Plant Pathology*, *60*(6), 999-1013.

Fan, J., Ma, L., Zhao, C., Yan, J., Che, S., Zhou, Z., Wang, H., Yang, L., & Hu, B. (2020). Transcriptome of *Pectobacterium carotovorum* subsp. *carotovorum* PccS1 infected in calla plants in vivo highlights a spatiotemporal expression pattern of genes related to virulence, adaptation, a. *Molecular Plant Pathology*, *21*(6), 871-891.

Fan, X. J., Saleem, T., & Zou, H. S. (2022). Copper resistance mechanisms in plant pathogenic bacteria. *Phytopathologia mediterranea.*, 131-140.

Feng, T., Nyffenegger, C., Højrup, P., Vidal-Melgosa, S., Yan, K.-P., Fangel, J. U., Meyer, A. S., Kirpekar, F., Willats, W. G., & Mikkelsen, J. D. (2014). Characterization of an extensin-modifying metalloprotease: N-terminal processing and substrate cleavage pattern of *Pectobacterium carotovorum* Prt1. *Applied microbiology and biotechnology*, *98*, 10077-10089.

Figaj, D., Ambroziak, P., Przepiora, T., & Skorko-Glonek, J. (2019). The role of proteases in the virulence of plant pathogenic bacteria. *International Journal of Molecular Sciences*, *20*(3), 672.

Figaj, D., Czaplewska, P., Przepióra, T., Ambroziak, P., Potrykus, M., & Skorko-Glonek, J. (2020). Lon protease is important for growth under stressful conditions and pathogenicity of the phytopathogen, bacterium *Dickeya solani*. *International Journal of Molecular Sciences*, *21*(10), 3687.

Hotson, A., & Mudgett, M. B. (2004). Cysteine proteases in phytopathogenic bacteria: identification of plant targets and activation of innate immunity. *Current opinion in plant biology.*, *7*(4), 384-390.

Joshi, J. R., Brown, K., Charkowski, A. O., & Heuberger, A. L. (2022). Protease inhibitors from *Solanum chacoense* inhibit *Pectobacterium* virulence by reducing bacterial protease activity and motility. *Molecular Plant-Microbe Interactions®. 35:825-834.*

Kaczynska, N., Lojkowska, E., Narajczyk, M., & Czajkowski, R. (2021). Genome-wide analyses of the temperature-responsive genetic loci of the pectinolytic plant pathogenic *Pectobacterium atrosepticum*. *International Journal of Molecular Sciences*, *22*(9), 4839.

Kim, H., Kim, M., Jee, S.-N., Heu, S., & Ryu, S. (2022). Development of a bacteriophage cocktail against *pectobacterium carotovorum* subsp. *carotovorum* and its effects on *Pectobacterium* virulence. *Applied and Environmental Microbiology*, *88*(19).

Langklotz, S., Baumann, U., & Narberhaus, F. (2012). Structure and function of the bacterial AAA protease FtsH. *Biochimica et Biophysica Acta (BBA) - Molecular Cell Research*, *1823*(1), 40-48.

Mansfield, J., Genin, S., Magori, S., Citovsky, V., Sriariyanum, M., Ronald, P., Dow, M., Verdier, V., Beer, S. V., & Machado, M. A. (2012). Top 10 plant pathogenic bacteria in molecular plant pathology. *Molecular Plant Pathology*, *13*(6), 614-629.

Marits, R., Köiv, V., Laasik, E., & Mäe, A. (1999). Isolation of an extracellular protease gene of *Erwinia carotovora* subsp. *carotovora* strain SCC3193 by transposon mutagenesis and the role of protease in phytopathogenicity. *Microbiology*, *145*(8), 1959-1966.

Marits, R., Tshuikina, M., Pirhonen, M., Laasik, E., & Mäe, A. (2002). Regulation of the expression of prtW:: gusA fusions in *Erwinia carotovora* subsp. *carotovora*. *Microbiology*, *148*(3), 835-842.

Misas-Villamil, J. C., & Van der Hoorn, R. A. (2008). Enzyme–inhibitor interactions at the plant–pathogen interface. *Current opinion in plant biology*, *11*(4), 380-388.

Moleleki, L. N., Pretorius, R. G., Tanui, C. K., Mosina, G., & Theron, J. (2017). A quorum sensing-defective mutant of *Pectobacterium carotovorum* ssp. *brasiliense* 1692 is attenuated in virulence and unable to occlude xylem tissue of susceptible potato plant stems. *Molecular Plant Pathology*, *18*(1), 32-44.

Page, M. J., & Di Cera, E. (2008). Serine peptidases: Classification, structure and function. *Cellular and Molecular Life Sciences*, *65*(7-8), 1220-1236.

Pérombelon, M. (2002). Potato diseases caused by soft rot erwinias: an overview of pathogenesis. *Plant Pathology*, *51*(1), 1-12.

Põllumaa, L., Alamäe, T., & Mäe, A. (2012). Quorum sensing and expression of virulence in *Pectobacteria*. *Sensors*, *12*(3), 3327-3349.

Ramírez-Larrota, J. S., & Eckhard, U. (2022). An introduction to bacterial biofilms and their proteases, and their roles in host infection and immune evasion. *Biomolecules*, *12*(2), 306.

Rawlings, N. D., Barrett, A. J., Thomas, P. D., Huang, X., Bateman, A., & Finn, R. D. (2018). The MEROPS database of proteolytic enzymes, their substrates and inhibitors in 2017 and a comparison with peptidases in the PANTHER database. *Nucleic Acids Research*, *46*(D1), D624-D632.

Sun, Y., Utpal, H., Wu, Y., Sun, Q., Feng, Z., Shen, Y., Zhang, R., Zhou, X., & Wu, J. (2024). Comparative genomic and transcriptome analyses of two *Pectobacterium brasiliense* strains revealed distinct virulence determinants and phenotypic features. *Frontiers in Microbiology*, *15*.

Toth, I., Humphris, S., Campbell, E., & Pritchard, L. (2015). Why genomics research on *Pectobacterium* and *Dickeya* makes a difference. *American Journal of Potato Research*, *92*(2), 218-222.

Toth, I. K., Bell, K. S., Holeva, M. C., & Birch, P. R. J. (2003). Soft rot *erwiniae*: from genes to genomes. *Molecular Plant Pathology*, *4*(1), 17-30.

## Chapter 2 - Optimization and Challenges in Refining Protease Activity Assays

### Summary

Proteases play crucial roles in host-microbe interactions and significantly contribute to the virulence of plant pathogens like *Pectobacterium carotovorum*; however, assays to detect and measure protease activity often lack reliability and comprehensive descriptions. In this study, I systematically optimized conditions for protease activity detection using the wild-type *Pectobacterium carotovorum* strain WPP14. By evaluating multiple parameters, including media composition, pH, incubation temperature, inoculum type, sterilization method, and incubation duration, I significantly improved assay sensitivity and reliability. These methodological enhancements facilitated a comprehensive and statistically validated characterization of protease activity in the wild-type WPP14. The findings from these optimized assays provided a robust foundation for future research on bacterial protease activity and virulence assessment.

### Introduction

Proteases are enzymes responsible for degrading proteins into peptides and amino acids, playing essential roles in numerous biological processes, including bacterial pathogenicity (Fedatto et al., 2006). In bacterial pathogens such as *Pectobacterium carotovorum*, proteases are major contributors to tissue degradation and host invasion (Figaj et al., 2019). By breaking down plant cell wall components, these enzymes facilitate bacterial colonization and are responsible for characteristic symptoms of soft rot diseases (Feng et al., 2014). Given their central role in bacterial virulence, accurate detection and measurement of protease activity are vital for understanding pathogenic mechanisms and developing effective disease management strategies (Joshi et al., 2022; Sakoh et al., 2005).

Skim milk agar is a widely used medium for detecting bacterial protease activity due to its affordability, ease of preparation, and broad laboratory availability. Proteolytic enzymes degrade casein, the predominant protein in milk, resulting in clear zones around bacterial colonies that indicate protease activity (Mukhia et al., 2021; Saggu et al., 2019). Despite its widespread adoption, traditional skim milk agar formulations (typically 1% milk concentration) have limitations, notably poor clarity and visibility of proteolytic halos. The medium often appears overly transparent or faint, complicating accurate identification and measurement of protease activity zones, particularly when bacteria produce low levels of proteases (Jones et al., 2017; Zhang et al., 2021).

In this study, skim milk medium derived from bovine milk was utilized for its established sensitivity in detecting protease activities of plant pathogens (Vermelho et al., 1996; Zhang et al., 2021). Additionally, gelatin-based medium, also sourced from bovine, was selected for its susceptibility to degradation by bacterial proteases, clearly indicating enzyme activity (Alnahdi S, 2012; Vermelho et al., 1996). Casein medium, another bovine-derived substrate, was employed due to its widespread usage in protease detection assays and its clarity in visualizing proteolysis (Vermelho et al., 1996; Zhang et al., 2021). Soybean protein isolate, a plant-based alternative with high protein content, was initially evaluated for protease assays due to its suitability and richness in protein (Tang, 2019; Xiang et al., 2014). However, assays employing soybean isolate medium showed no detectable protease activity for cloned proteases or wild-type *Pectobacterium carotovorum* WPP14. Investigations revealed substantial levels of Kunitz-type trypsin inhibitors naturally present in soybean isolate, significantly inhibiting proteolytic enzymes (Khan et al., 2022). Although these inhibitors can be partially reduced through processing, such as heat treatment or chemical modifications (Baker & Rackis, 1986), their complete removal is

challenging. Consequently, soybean protein isolate proved less suitable for protease assays under the tested conditions due to its inherent inhibitor content affecting bacterial protease detection reliability (De Oliveira et al., 2015; Wei et al., 2023).

Another critical parameter influencing protease detection is the pH of the assay medium. Proteases exhibit optimal enzymatic activity within specific pH ranges, which vary based on the bacterial species and protease types produced (García-Moyano et al., 2021; Zhang et al., 2021). Therefore, systematically evaluating different pH conditions is necessary to identify optimal conditions that enhance enzyme activity and improve halo visibility. Optimizing both milk concentration and pH are essential steps toward refining protease assays, thus increasing their reliability and sensitivity.

Additionally, significant challenges are encountered in medium preparation, particularly regarding sterilization methods. Autoclaving, although commonly employed, frequently results in coagulated milk with a brown or burnt appearance, adversely affecting assay clarity and accuracy. To overcome this limitation, microwaving was evaluated as an alternative sterilization method, resulting in consistently clearer media with fewer artifacts. Adjustments in medium preparation, milk concentration, pH, and sterilization methods collectively aim to enhance the sensitivity, clarity, and accuracy of protease detection.

This study addresses the specific methodological challenges encountered when developing protease activity assays using skim milk agar plates, highlighting the necessity of comprehensive and precise experimental conditions. By systematically modifying and optimizing assay parameters, this work provides clear and practical guidance for researchers. Ultimately, the optimized protocols outlined here support consistent and reproducible protease activity measurements, facilitating future investigations into bacterial virulence mechanisms.

## Materials and Methods

**Protease Assay Medium Preparation**. Several protease assay media were evaluated to enhance the sensitivity and accuracy of detecting protease activity in Pectobacterium carotovorum WPP14. These included traditional skim milk agar medium (Medium 1), composed of 1% dry skim milk and 0.8% agar per liter (pH ~7) (Chatterjee et al., 1995; Joshi et al., 2022), and a slightly modified skim milk medium (Medium 2) with an increased concentration of skim milk (2% dry skim milk, 1.5% agar per liter, pH ~7). Additionally, enhanced skim milk agar supplemented with additional nutrients (Medium 3) was prepared by combining 2% dry skim milk, 1.5% agar, 0.4% peptone, and 0.1% yeast extract per liter. Other protein-based media tested included gelatin-based medium (Medium 4; 2% gelatin, 1.5% agar, 0.4% peptone, 0.1% yeast extract per liter) and casein-based medium (Medium 5; 2% casein, 1.5% agar, 0.4% peptone, 0.1% yeast extract per liter), both prepared according to established protocols (Vermelho et al., 1996). All assay media were prepared by dissolving the protein source (skim milk, gelatin, or casein) in 500 mL of distilled water while separately dissolving the remaining components in an additional 500 mL of distilled water. Solutions were heated in a microwave until all the ingredients were completely dissolved without causing coagulation. Following dissolution, media solutions were sterilized either by autoclaving or microwaving. For media sterilized by autoclaving, microwave heating lasted only 1–2 minutes, just enough to achieve complete dissolution. In contrast, media sterilized solely by microwaving required 4–6 minutes in total, performed in one-minute intervals each. After each interval, media solutions were carefully removed, gently swirled to prevent boiling over or splashing, and then reheated. The microwave power setting was consistently maintained at 1000 watts (full power). After sterilization, antibiotics were added once media cooled sufficiently under sterile conditions in a biosafety cabinet, preventing microbial contamination. Finally, the solutions were combined

aseptically, allowed to cool further, and then poured into Petri dishes. Protease agar plates were prepared freshly for immediate use; however, if necessary, prepared plates could be stored at 4°C for up to one week.

**Protease Activity Assay.** To evaluate protease activity, 20 µL aliquots of bacterial samples were inoculated into wells (2 mm diameter) created in each assay plate using a sterile cork borer. Bacterial samples were prepared through three different approaches: unfiltered overnight culture supernatants used directly, filtered overnight culture supernatants (passed through 0.22 µm sterile filters), and sonicated or lysed bacterial cells. For the preparation of sonicated cells, overnight bacterial cultures were pelleted by centrifugation and washed in phosphate-buffered saline (PBS; pH 7.4). Cells were lysed on ice by sonication at 70 kHz using cycles of 30-second pulses, each followed by a 1-minute resting interval. This pulse-rest cycle was repeated five times, resulting in a cumulative sonication time of 2.5 minutes, a total resting time of 5 minutes, and an overall processing duration of 7 minutes and 30 seconds. Similarly, a longer protocol involved ten pulse-rest cycles, totaling 5 minutes of cumulative sonication, 10 minutes of resting intervals, and an overall duration of 15 minutes. Lysed samples were stored at −20 °C until they were assayed.

**Optimization of Protease Assay Conditions.** To systematically determine optimal assay conditions for accurate protease detection, several experimental parameters, including incubation temperature (18°C, room temperature (~25°C), and 37°C), medium pH (pH 5 adjusted with 4N HCl, neutral pH 7, and pH 8 adjusted using 1M NaOH), sterilization method (autoclaving versus microwaving), and incubation duration (24, 48, and 72 hours), were evaluated both individually and in combination. Plates were initially incubated and monitored for up to five days, with detailed observations systematically recorded starting from 24 hours. However, the main data analyses were primarily focused on results obtained during the first 72 hours. Protease activity was

quantified by photographing assay plates and measuring the clear zone (halo) areas using ImageJ software, version 1.54g (Rasband, 2025). These methodological refinements aimed to establish reliable, accurate, and reproducible protease activity detection protocols, facilitating the characterization of protease-producing bacterial strains.

**Statistical Analysis.** Statistical analyses of protease activities across different experimental conditions were performed using Type III ANOVA to evaluate the effects of incubation time, temperature, pH, inoculum type, and their interactions. Differences between specific groups or conditions were further analyzed using Tukey's honest significant difference (HSD) test. Results with a p-value less than 0.05 were considered statistically significant. All statistical analyses were conducted using R software, version 4.4.3 (R Core, 2025).

## Results

**Comparison of Protease Assay Media.** Five different medium formulations were evaluated for their effectiveness in detecting protease activity of *Pectobacterium carotovorum* WPP14: traditional skim milk agar (1%), modified skim milk agar (2%), enhanced skim milk agar supplemented with peptone and yeast extract, gelatin-based medium, and casein-based medium. Protease activity was systematically assessed across several key experimental parameters, including sterilization method, medium type, pH levels, incubation temperatures, incubation duration, and inoculum preparation methods. Each parameter was rigorously tested to determine its impact on assay sensitivity, clarity, and reproducibility.

**Effect of Sterilization Method on Protease Activity.** The sterilization method significantly influenced protease detection (ANOVA, $p < 0.001$), with microwaved media consistently yielding clearer and more distinct protease halos compared to autoclaved media across various tested conditions. Pairwise comparisons revealed that microwaving the medium

significantly enhanced protease activity measurements, with differences particularly prominent in enhanced skim milk agar (Medium 3) at alkaline conditions (pH 8) and extended incubation times (72h) (Figure 1).

Analyzing each medium individually further highlighted the advantages of microwaving over autoclaving. Enhanced skim milk agar (Medium 3) demonstrated notable improvements, showing significantly clearer halos and greater measurable protease activities at pH 7 and pH 8 ($p < 0.001$) (Figure 2). Statistically significant enhancements were also observed in traditional skim milk agar (Medium 1; pH 7 and pH 8), modified skim milk agar (Medium 2; pH 7), and gelatin-based medium (Medium 4; pH 7). Casein-based medium (Medium 5) was excluded from direct comparisons due to instability and medium separation upon autoclaving.

Given the significant effect of sterilization method demonstrated in Figure 1, we further illustrate this impact specifically using Medium 3 (enhanced skim milk agar with peptone and yeast extract), which exhibited the highest sensitivity and clarity in protease assays (Figure 2). Similar trends were consistently observed across other skim milk-based medium (Medium 1 and 2), although with slightly reduced magnitude (data not shown).

Visual evidence further supported the statistical findings regarding medium clarity influenced by sterilization methods (Figure 3). Microwaved media consistently exhibited enhanced clarity, appearing visibly lighter and without coagulation compared to autoclaved media, which demonstrated noticeable browning and undesirable aggregation. These physical differences significantly influenced the visibility and measurement of proteolytic activity. Specifically, traditional skim milk agar (Medium 1) showed a clear distinction; autoclaving resulted in severe coagulation and browning (Figure 3A), leading to ambiguous and irregular proteolytic halos that significantly hindered accurate measurement (Figure 3B). In contrast, microwaving produced a

consistently clear and smooth medium, facilitating distinct, measurable, and reproducible proteolytic halos (Figure 3C).

Overall, microwaving provided superior medium clarity and increased measurable protease activity, particularly in enhanced skim milk agar at alkaline pH, room temperature, and prolonged incubation, making it the recommended sterilization method for reliable protease detection.

**Effect of Incubation Time on Protease Activity.** Incubation time significantly influenced the ability to measure protease activity across all tested media (Figure 4). Optimal protease activity consistently occurred at extended incubation periods, peaking at 72 hours. This trend was statistically significant ($p < 0.001$) across media, temperatures, and pH conditions, highlighting incubation time as a crucial factor influencing assay sensitivity and reliability. Representative images further illustrate this trend, clearly showing progressively larger and clearer protease halos from 24 hours to 72 hours across traditional skim milk agar (Medium 1), modified skim milk agar (Medium 2), enhanced skim milk agar (Medium 3), gelatin-based medium (Medium 4), and casein-based medium (Medium 5), reinforcing the statistical findings and visually confirming the necessity of prolonged incubation for optimal protease detection (Figure 5).

**Effect of Medium Composition on Protease Activity.** To determine the optimal medium for detecting protease activity of *Pectobacterium carotovorum* WPP14, five distinct medium compositions were evaluated at different incubation temperatures, including room temperature (RT), 18°C, and 37°C. The comprehensive pairwise statistical analysis clearly demonstrated significant differences in measurable protease activity among the tested media at RT and 18°C (Figure 6).

Although assays were conducted at 37°C, minimal or negligible protease activity was consistently observed, indicating that the proteases produced by *Pectobacterium carotovorum*

WPP14 are not active or stable at this incubation temperature. Therefore, the final pairwise analysis included only statistically significant results obtained at RT and 18°C. Enhanced skim milk agar supplemented with peptone and yeast extract (Medium 3) consistently exhibited superior performance, showing significantly higher proteolytic activity compared to all other tested medium formulations ($p < 0.001$), particularly under alkaline conditions (pH 8) and prolonged incubation (72 hours). Modified skim milk agar (Medium 2) also notably outperformed traditional skim milk agar (Medium 1), gelatin-based medium (Medium 4), and casein-based medium (Medium 5), though it remained significantly less sensitive compared to Medium 3 ($p < 0.01$). Traditional skim milk agar (Medium 1) and gelatin-based medium (Medium 4) demonstrated intermediate proteolytic activity, while casein-based medium (Medium 5) showed the lowest sensitivity, due to the positive activity in the negative controls and medium instability during preparation.

These findings emphasize the critical role of medium composition and incubation temperature in protease detection sensitivity and accuracy. Enhanced skim milk agar supplemented with peptone and yeast extract (Medium 3) emerged as the optimal medium for robust, reproducible, and sensitive detection of protease activity from *P. carotovorum* WPP14.

***Moderate detection capability with basic skim milk formulation: Traditional Skim Milk Agar (Medium 1).*** Medium 1, composed of 1% skim milk, provided moderate sensitivity for detecting protease activity of *Pectobacterium carotovorum* WPP14 under optimized assay conditions (room temperature [RT], pH 8, using either supernatant or 10-minute lysed cell inoculum; Figure 7). Initial trials at pH 8 were hindered by medium opacity due to Tris-HCl buffering. Substituting Tris-HCl with NaOH and employing microwave sterilization significantly improved medium clarity, resulting in enhanced halo visibility and measurable proteolytic activity

(Figure 7.1 C2). Statistical analysis (Type III ANOVA) confirmed significant effects of incubation time, inoculum type, pH, and temperature on protease activity (all factors $p < 0.01$; Table 1). Tukey's post hoc test indicated significantly larger halos at pH 8 compared to pH 7 ($p < 0.05$), with maximal activity observed after 72 hours of incubation ($p < 0.01$). Activity was highest at RT, reduced at 18°C, and negligible at 37°C ($p < 0.001$). Among inoculum types, supernatant and 10-minute lysed cells consistently yielded significantly larger proteolytic halos than filter-sterile or 5-minute lysed cells ($p < 0.05$), as visually confirmed in Figure 7.

Additionally, assay plates demonstrated clear and progressively larger proteolytic halos using cell lysate inoculum at room temperature under both pH 7 (Figure 7.1 B1–B4) and pH 5 (Figure 7.1 A1–A4), particularly after prolonged incubation times (48–72 h). Notably, 10-minute sonicated cells showed detectable activity sooner (after 24 h incubation), whereas the 5-minute sonicated cells displayed clear activity only after 48 h incubation. Although clarity and halo measurements on Medium 1 at pH 8 were notably improved by substituting Tris-HCl buffer with NaOH and employing microwave sterilization (Figure 7.1 C2), the halos remained comparatively faint and less distinct than those observed under identical assay conditions using enriched formulations: Medium 2 (Figure 7.1 D), Medium 3 (Figure 7.1 E), and Medium 4 (Figure 7.1 F). This relatively limited sensitivity prompted the development and subsequent use of these enhanced media formulations.

***Enhanced detection with increased skim milk concentration: Modified Skim Milk Agar (Medium 2).*** Medium 2, containing 2% skim milk, significantly improved the detection of protease activity compared to traditional skim milk agar (Medium 1), especially under alkaline conditions and longer incubation durations (Figure 8). Statistical analysis (Type III ANOVA) revealed significant effects of incubation time, temperature, and pH on protease activity ($p < 0.05$; Table 2).

Tukey's post hoc comparisons confirmed significantly increased proteolytic halos with extended incubation, reaching maximum activity at 72 hours. Protease activity was consistently higher at room temperature (RT) and 18°C, whereas activity was minimal or negligible at 37°C. Furthermore, alkaline conditions (pH 8) clearly enhanced halo formation compared to neutral pH (pH 7). These quantitative observations are visually supported by representative assay plates (Figure 12B), demonstrating distinct, large proteolytic halos formed at RT and 18°C after 48 hours, particularly under alkaline (pH 8) conditions. In contrast, minimal or negligible halo formation was observed at 37°C, confirming the quantitative trends shown in Figure 8. Notably, the inoculum type (supernatant versus filter-sterile) did not significantly affect protease detection on Medium 2, indicating consistent and reliable sensitivity independent of inoculum preparation. Collectively, these results support Medium 2 as a more sensitive and reliable formulation than Medium 1, highlighting the importance of increased skim milk concentration and optimized assay conditions for accurate protease detection of *Pectobacterium carotovorum* WPP14.

***Robust and rapid protease detection at alkaline pH and moderate temperatures: Enriched Skim Milk Agar (Medium 3).*** Medium 3, formulated with 2% skim milk supplemented with peptone and yeast extract, markedly improved protease detection by *Pectobacterium carotovorum* WPP14 compared to traditional skim milk media (Figures 7 and 8). Proteolytic halos on Medium 3 appeared earlier, were larger, and exhibited improved clarity, making it highly effective for both rapid qualitative screening and precise quantitative assays. Specifically, visible halos formed as early as 24 hours at room temperature (RT), with optimal quantification clearly achieved at pH 8, using supernatant inoculum, after 72 hours at either RT or 18°C (Figure 9). Statistical analysis (Type III ANOVA) demonstrated highly significant effects of incubation time ($F = 219.61$, $p < 0.001$), inoculum type ($F = 217.75$, $p < 0.001$), pH ($F = 74.14$, $p < 0.001$), and

temperature ($F = 104.14$, $p < 0.001$; Table 3). Tukey's post hoc tests confirmed significantly greater proteolytic activity at pH 8 compared to pH 7 and 5 ($p < 0.001$), and notably higher activity at RT and 18°C compared to 37°C ($p < 0.001$). Supernatant inoculum consistently produced significantly larger halos than filter-sterile inoculum across conditions ($p < 0.001$). Significant interactions among incubation time, temperature, and pH (all $p < 0.001$) further highlighted their combined influence on protease activity.

These quantitative trends are strongly supported by representative assay plates (Figure 12C), clearly illustrating robust halo formation at pH 8 and RT or 18°C conditions (48h incubation), while minimal proteolytic activity was observed at 37°C. Additionally, negligible background activity was observed from negative controls (*E. coli*) under these conditions, affirming assay specificity. Together, these observations strongly support Medium 3 as the most sensitive and reliable formulation among those tested, recommended for rapid qualitative assessments (within 24h) and accurate quantitative protease detection (at 72h incubation).

***Clear detection of protease activity using gelatin-based medium (Medium 4).*** Medium 4, composed of gelatin supplemented with peptone and yeast extract, clearly supported measurable detection of protease activity by *Pectobacterium carotovorum* WPP14 at room temperature (RT) using supernatant inoculum (Figure 10). Statistical analysis (Type III ANOVA) indicated highly significant effects of both pH ($F = 66.76$, $p < 0.001$) and incubation time ($F = 482.17$, $p < 0.001$; Table 4). Tukey's post hoc tests confirmed significant increases in halo size over time, reaching maximum activity at 72 hours. Although protease activity was detectable at all tested pH levels, alkaline conditions (pH 8) consistently produced larger and clearer halos compared to neutral (pH 7) and acidic (pH 5) conditions ($p < 0.001$). These quantitative results are visually reinforced by representative assay plates (Figure 12D), demonstrating progressively larger proteolytic halos,

particularly under alkaline conditions. Although the gelatin-based medium effectively supported measurable protease activity, the resulting halos were comparatively faint and less distinct than those observed with enriched skim milk formulations (Medium 2 and Medium 3; Figure 12B and 12C). This suggests that Medium 4 is a suitable alternative when milk-based substrates are not feasible, but it offers lower clarity and contrast for precise quantitative measurements.

***Protease detection using casein-based medium under acidic and neutral conditions: Casein-Based Agar (Medium 5).*** Medium 5, composed of casein supplemented with peptone and yeast extract, supported detectable protease activity by *Pectobacterium carotovorum* WPP14 at room temperature (RT) using supernatant inoculum (Figure 11). Proteolytic halos were clearly measurable at acidic (pH 5) and neutral (pH 7) conditions, increasing progressively in size over time, and reaching maximum clarity at 72 hours incubation. Statistical analysis (Type III ANOVA) indicated significant effects of pH ($F = 132.44$, $p < 0.001$) and incubation time ($F = 42.66$, $p < 0.001$; Table 5). However, this pH significance was mainly driven by the absence of measurable activity at pH 8, where medium instability and irregular texture due to reactions between casein and alkaline buffer were observed.

Tukey's post hoc analysis indicated no significant difference between protease activities at pH 5 and pH 7 ($p = 0.938$), demonstrating similar performance under these conditions. Representative assay plates (Figure 12E) visually confirm the quantitative results, showing clearly defined halos at pH 5 after 24, 48, and 72 hours incubation. Despite clear halo formation, the halos were relatively faint and smaller compared to enriched skim milk-based formulations (Medium 2 and Medium 3; Figure 12B and 12C). Due to these limitations, including medium instability at alkaline conditions and modest halo clarity, Medium 5 may be best utilized primarily for detecting protease activity under acidic to neutral pH conditions when other substrates are not available.

**Summary of Medium Performance and Recommended Conditions**

Among the five media tested, Medium 3 (2% skim milk with peptone and yeast extract) consistently demonstrated the highest sensitivity and clarity for detecting protease activity by *P. carotovorum* WPP14. Statistical analyses confirmed significant effects of pH, temperature, incubation time, and inoculum type, with maximal activity observed under pH 8, room temperature (RT) or 18°C, and 72-hour incubation using supernatant as inoculum. Medium 1 and Medium 2 provided moderate detection, while Medium 4 and Medium 5 were more suitable under specific pH conditions. Based on these results, Medium 3 under alkaline pH and moderate temperatures is recommended as the most effective formulation for both quantitative and qualitative detection of *P. carotovorum* WPP14 protease activity.

**Discussion**

This study aimed to optimize and enhance the protease detection assay for *Pectobacterium carotovorum* WPP14 by evaluating five different medium formulations under various assay conditions. Our primary objective was to establish a straightforward, accurate, reproducible, and affordable method suitable for initial protease screening. We systematically determined the most effective medium composition and assay conditions, including incubation temperature, incubation time, pH, inoculum type, and sterilization method, to reliably detect protease activity in the wild-type strain.

**Medium Comparison and Recommended Conditions**

Enhanced skim milk agar supplemented with peptone and yeast extract (Medium 3) proved to be the most sensitive, effective, and reliable medium for protease detection, exhibiting clear halos within 24 hours at moderate temperatures (RT and 18°C) and alkaline conditions (pH 8). Its

high sensitivity compared to traditional skim milk agar (Medium 1) and modified skim milk (Medium 2) was statistically confirmed (ANOVA, $p < 0.001$) across multiple assay parameters. These findings align with previous studies demonstrating that nutrient-rich media containing peptone and yeast extract significantly enhance bacterial growth and extracellular enzyme secretion, improving protease assay sensitivity and reliability (Li et al., 2011; Secades & Guijarro, 1999; Vermelho et al., 1996). Medium 4 (gelatin-based) also performed well, offering balanced detection across varied conditions, though with lower sensitivity compared to Medium 3. In contrast, Medium 5 (casein-based) presented challenges due to substantial background activity from the negative control strain (*E. coli*), clearly visible in Figure 13, complicating interpretation of results. Similar nonspecific protease activity issues with casein substrates have been previously documented, reinforcing concerns about potential false-positive signals (Song et al., 2023; Zhang et al., 2021).

**Practical Implications and Future Applications**

The optimized assay presented in this study offers significant practical advantages, particularly in terms of simplicity, reproducibility, and substantial time-saving benefits. By clearly defining optimal assay conditions, this research eliminates the need for extensive preliminary trial-and-error experiments, allowing researchers to obtain accurate and reliable protease detection results faster. The established conditions can be effectively implemented in microbiology laboratories focusing on bacterial enzyme characterization and pathogenicity research. Furthermore, the assay's clarity and reproducibility facilitate its potential application in high-throughput screening settings, which is crucial for identifying bacterial strains with notable virulence traits or protease secretion capabilities. Future research could build upon these findings by employing genetic and molecular biology approaches, such as gene knockout or transcriptomic

analyses, to further understand the specific genetic and regulatory roles of proteases in bacterial pathogenicity and adaptation to different environments.

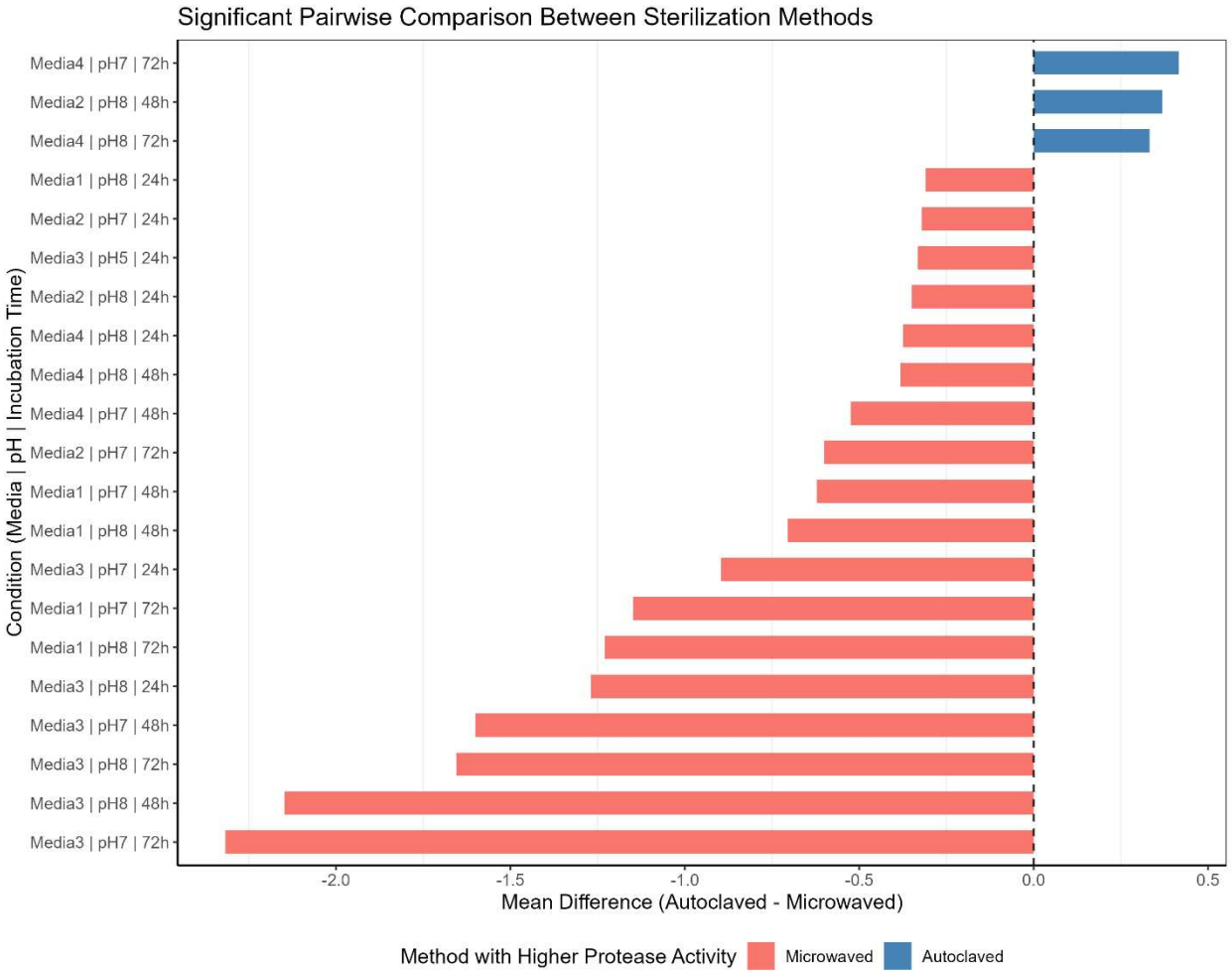


***Figure 1. Significant pairwise comparisons of sterilization methods (microwaving vs. autoclaving) on protease activity in* Pectobacterium carotovorum *WPP14 across media (1–4), pH levels, and incubation times (Tukey's HSD, adjusted* p *< 0.05).*** Red bars indicate significantly higher activity in microwaved media; blue bars indicate higher activity in autoclaved media. Microwaving generally provided superior protease detection, especially in Medium 3.

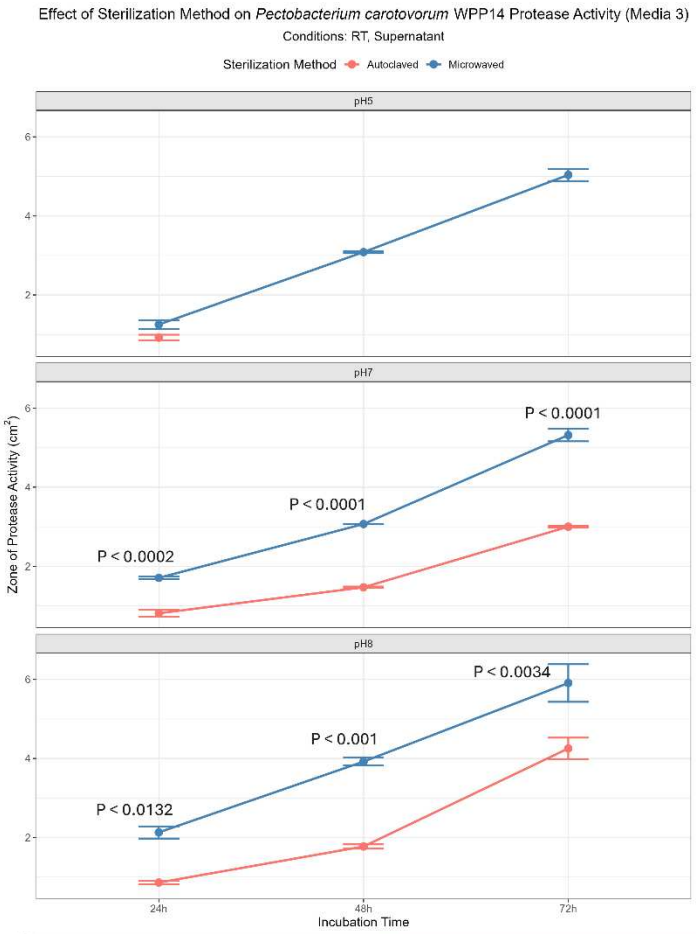


***Figure 2. Effect of Sterilization Method on Protease Activity in Enhanced Skim Milk Agar (Medium 3).*** Comparison of protease activity produced by wild-type *Pectobacterium carotovorum* WPP14 grown on Medium 3 sterilized by microwaving versus autoclaving. The results are shown across three pH conditions (pH 5, pH 7, and pH 8) at room temperature (RT) and incubation periods of 24, 48, and 72 hours. Significant differences (p-values indicated on plots) highlight superior protease activity detection in microwaved medium compared to autoclaved medium at neutral (pH 7) and alkaline (pH 8) conditions. The y-axis represents mean protease activity measured as the diameter (cm²) of the clearing zone surrounding bacterial growth, and the x-axis represents incubation time (hours).

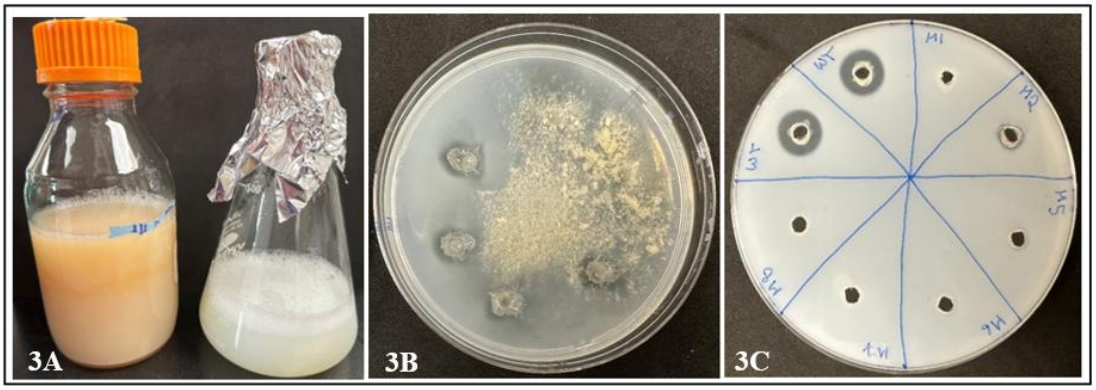


***Figure 3. Visual comparison of sterilization methods on skim milk agar medium clarity and protease detection.*** **(A)** Physical appearance of autoclaved (left) and microwaved (right) skim milk agar preparations, illustrating the severe browning and coagulation due to autoclaving. **(B)** Representative skim milk agar plate (Medium 1, autoclaved) inoculated with wild-type *P. carotovorum* WPP14, showing significant medium discoloration, aggregation, and irregular halo formation complicating accurate protease measurement. **(C)** Representative skim milk agar plate (Medium 1, microwaved) inoculated with wild-type *P. carotovorum* WPP14, clearly demonstrating improved medium clarity and well-defined proteolytic halos.

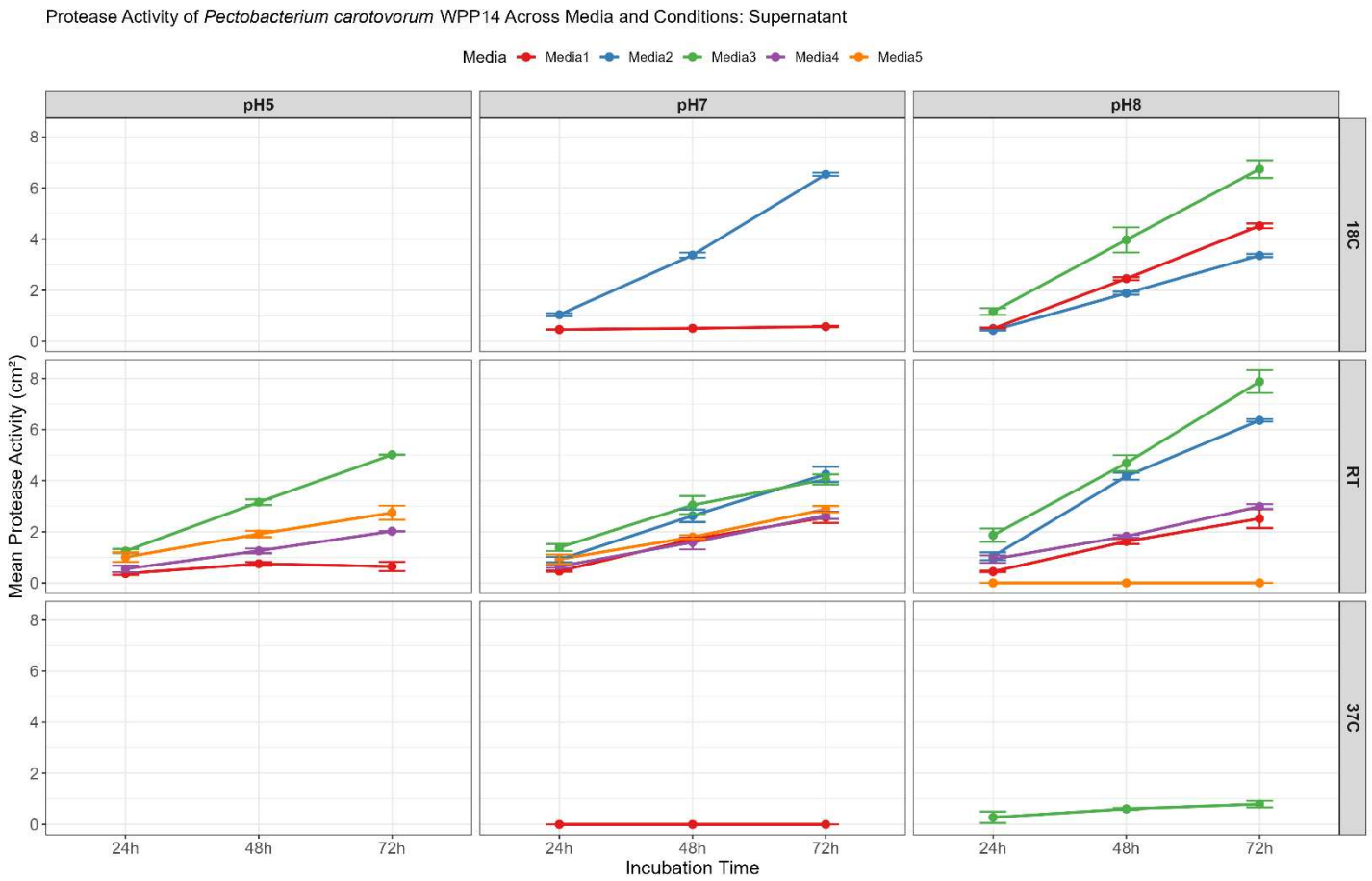


***Figure 4. Effect of incubation time on protease activity of Pectobacterium carotovorum WPP14.*** Protease activity significantly increased with prolonged incubation periods (24, 48, and 72 hours) across all tested media: traditional 1% skim milk agar (Medium 1), modified 2% skim milk agar (Medium 2), enhanced 2% skim milk agar with peptone and yeast (Medium 3), gelatin-based medium (Medium 4), and casein-based medium (Medium 5). This trend remained consistent across different incubation temperatures (18°C, room temperature, and 37°C) and pH levels (pH 5, 7, and 8), with maximal activities consistently observed at 72 hours. Statistical significance was determined by Tukey's test, with all trends shown being highly significant ($p < 0.001$).

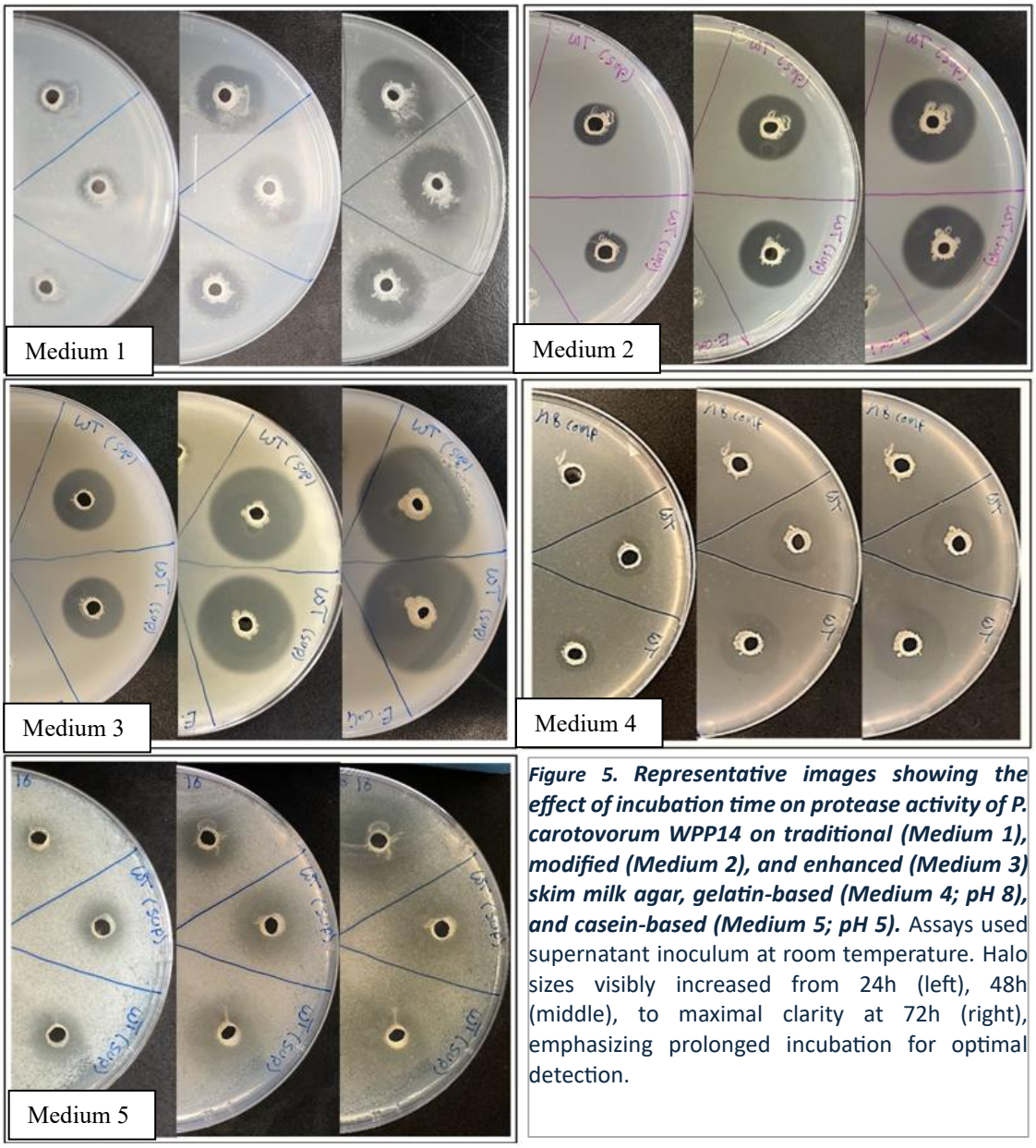


***Figure 5. Representative images showing the effect of incubation time on protease activity of P. carotovorum WPP14 on traditional (Medium 1), modified (Medium 2), and enhanced (Medium 3) skim milk agar, gelatin-based (Medium 4; pH 8), and casein-based (Medium 5; pH 5).*** Assays used supernatant inoculum at room temperature. Halo sizes visibly increased from 24h (left), 48h (middle), to maximal clarity at 72h (right), emphasizing prolonged incubation for optimal detection.

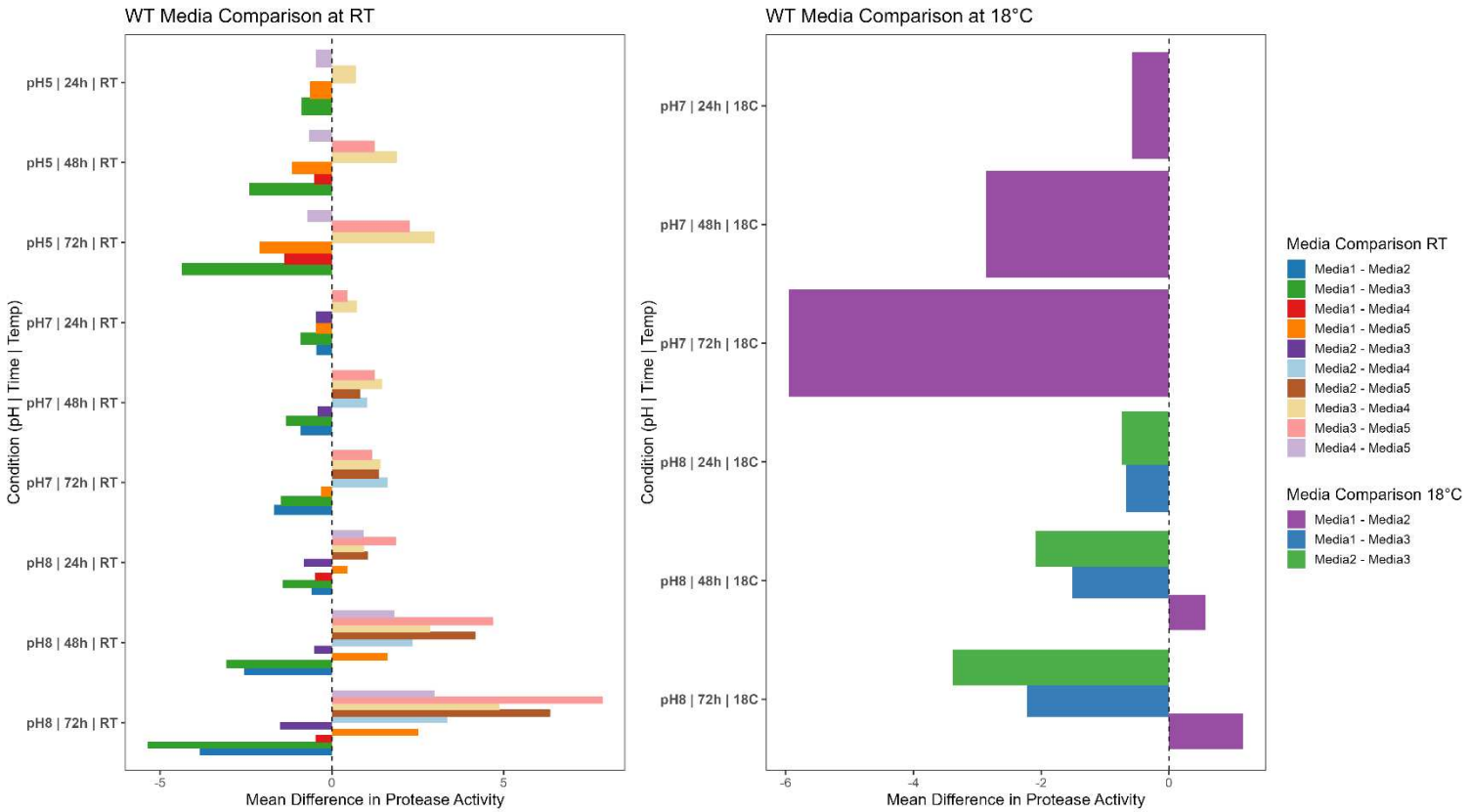


***Figure 6. Comprehensive pairwise comparisons of protease activity across different assay media: traditional skim milk agar (Medium 1), modified skim milk agar (Medium 2), enhanced skim milk agar supplemented with peptone and yeast extract (Medium 3), gelatin-based medium (Medium 4), and casein-based medium (Medium 5), evaluated at room temperature (RT) and 18°C.*** Pairwise comparisons indicate mean differences in protease activity (halo area in $cm^2$). Positive values indicate greater activity in the second-listed medium. Results clearly demonstrate enhanced skim milk agar (Medium 3) provided significantly greater sensitivity under optimal conditions (RT and 18°C). Statistical analysis was conducted using Tukey's HSD test (adjusted $p < 0.05$). **Note:** Although assays at 37°C were conducted, minimal protease activity was observed and thus results are not shown.

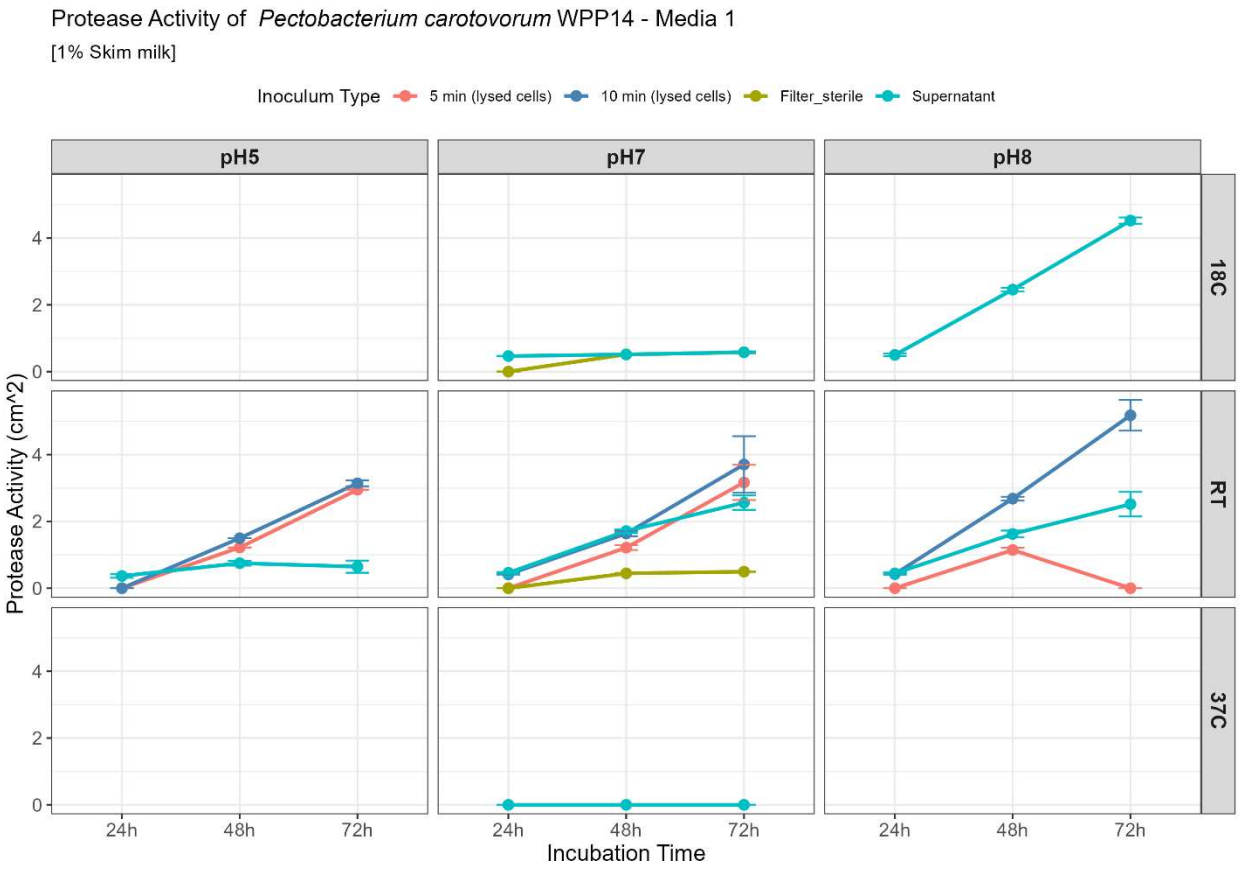


***Figure 7. Protease activity of Pectobacterium carotovorum WPP14 on Medium 1 (1% skim milk).*** Activity was assessed across inoculum types (5 min lysed cells, 10 min lysed cells, filter-sterilized, and supernatant), three temperatures (18°C, room temperature [RT], and 37°C), three pH values (5, 7, and 8), and three incubation durations (24h, 48h, and 72h). Type III ANOVA revealed significant effects of inoculum type, temperature, pH, and incubation time ($p < 0.05$). Tukey's post hoc analysis identified the highest protease activity under optimized conditions using 10-minute lysed cells or supernatant as inoculum, incubated for 72 hours at pH 8 and RT or 18°C. Data represent mean ± SD.

**Table 1. Type III ANOVA results for protease activity in Medium 1**

| Factor | Sum Sq | Df | F value | p-value |
|---|---|---|---|---|
| **Inoculum Type** | 27.48 | 3 | 14.29 | $3.90 \times 10^{-8}$ |
| **Incubation Time** | 90.85 | 2 | 70.89 | $9.94 \times 10^{-22}$ |
| **pH** | 8.97 | 2 | 6.99 | $1.29 \times 10^{-3}$ |
| **Temperature** | 9.82 | 2 | 7.66 | $7.08 \times 10^{-4}$ |
| **Residuals** | 41.72 | 65 | – | – |

*Table 1. Type III ANOVA results analyzing factors influencing protease activity in P. carotovorum WPP14 grown on Medium 1.* Tested factors include inoculum type, incubation time, pH, and temperature. All factors significantly influenced protease activity ($p < 0.05$), with incubation time and inoculum type showing particularly strong effects. Statistical significance was determined at $p < 0.05$.

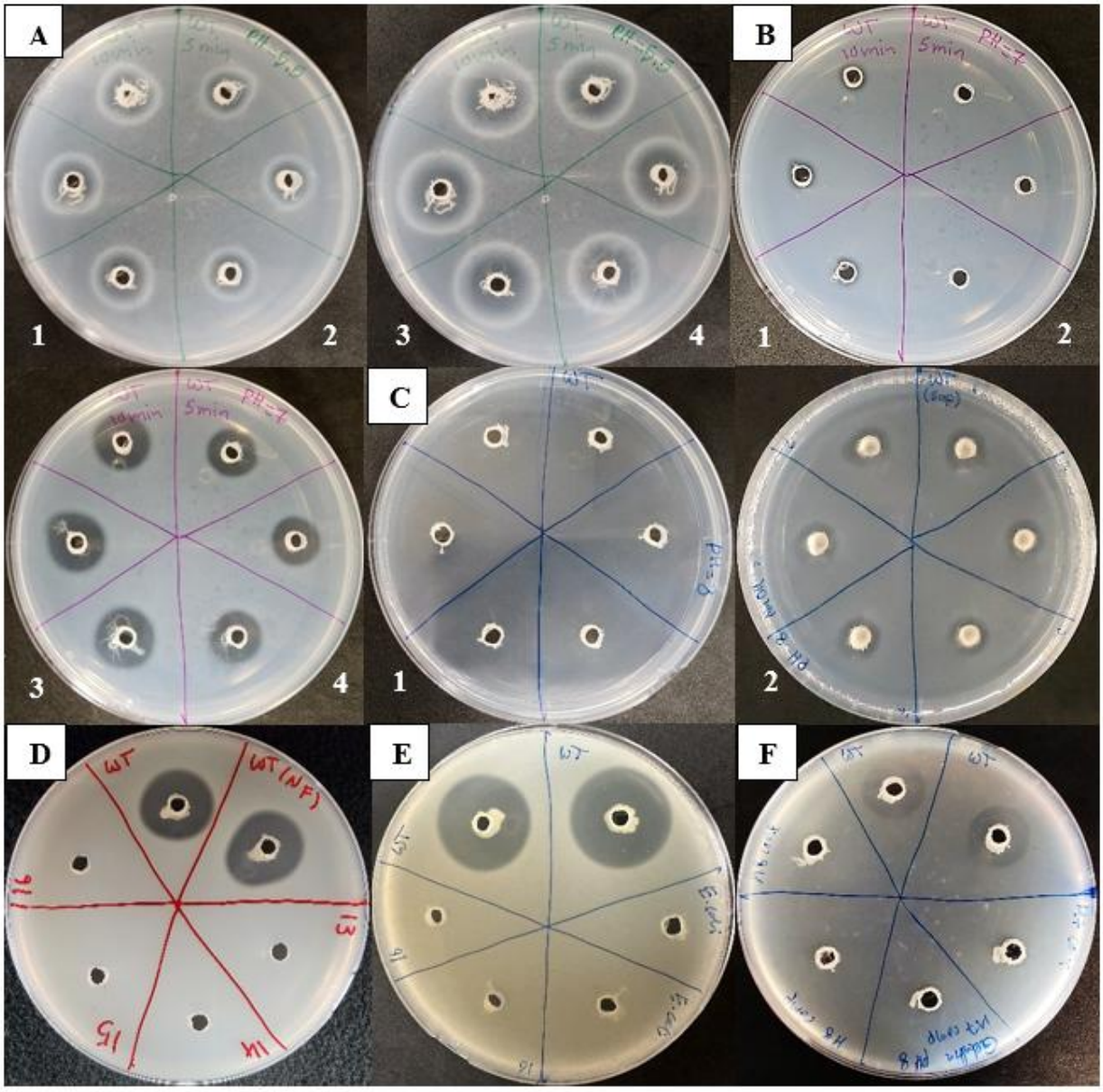


***Figure 7.1. Representative assay plates demonstrating protease activity of Pectobacterium carotovorum WPP14 under optimized conditions on Medium 1 (1% skim milk agar).*** Plates show activity at RT using cell lysate inoculum at pH 5 (A1–A4) and pH 7 (B1–B4) after incubation for 24, 48, or 72 h. Plates (C1–C2) illustrate improved clarity when substituting Tris-HCl buffer (C1) with NaOH buffer (C2) at pH 8. Comparative halo visibility across Medium 2 (D), Medium 3 (E), and Medium 4 (F) under identical conditions (RT, pH 8, supernatant inoculum, 48 h) highlights the limited sensitivity of Medium 1.

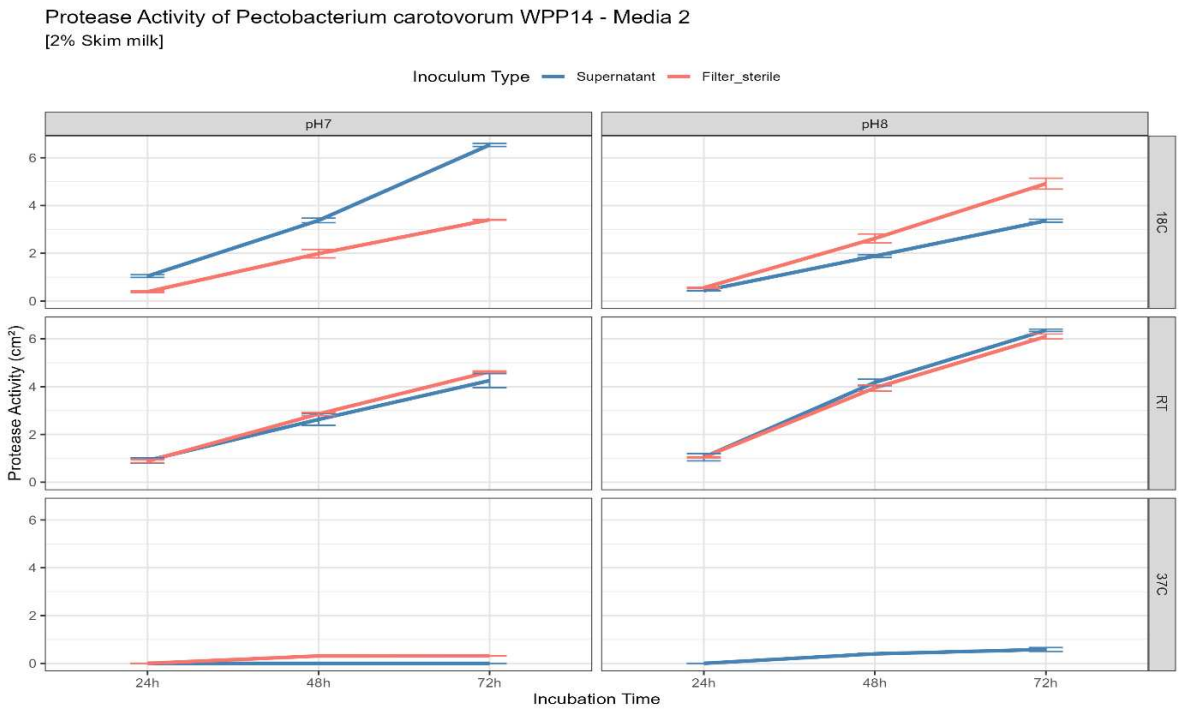


***Figure 8. Protease activity of Pectobacterium carotovorum WPP14 on modified skim milk agar (Medium 2; 2% skim milk).*** Activity was assessed across two inoculum types (supernatant and filter-sterile), three temperatures (18°C, room temperature [RT], and 37°C), two pH values (7 and 8), and three incubation durations (24h, 48h, and 72h). Type III ANOVA revealed significant effects of incubation time, temperature, and pH ($p < 0.05$), while inoculum type was not significant. Tukey's test indicated maximal protease activity at 72 hours, with increased halo sizes observed at pH 8 and under RT or 18°C. Protease activity was minimal at 37°C across all conditions. Data represent mean ± SD.

**Table 2. Type III ANOVA results for protease activity in Medium 2**

| Factor | Sum Sq | Df | F value | p-value |
|---|---|---|---|---|
| **Incubation Time** | 99.70 | 2 | 38.64 | $8.76 \times 10^{-12}$ |
| **Temperature** | 94.75 | 2 | 36.72 | $2.13 \times 10^{-11}$ |
| **pH** | 5.77 | 1 | 4.48 | $3.82 \times 10^{-2}$ |
| **Inoculum Type** | 1.29 | 1 | 1.00 | $3.20 \times 10^{-1}$ |
| **Residuals** | 83.86 | 65 | – | – |

*Table 2. Type III ANOVA results for factors influencing protease activity in P. carotovorum WPP14 grown on Medium 2. Tested factors include incubation time, temperature, pH, and inoculum type. Incubation time, temperature, and pH significantly affected protease activity ($p < 0.05$), while inoculum type did not show a significant effect. Statistical significance was determined at $p < 0.05$.*

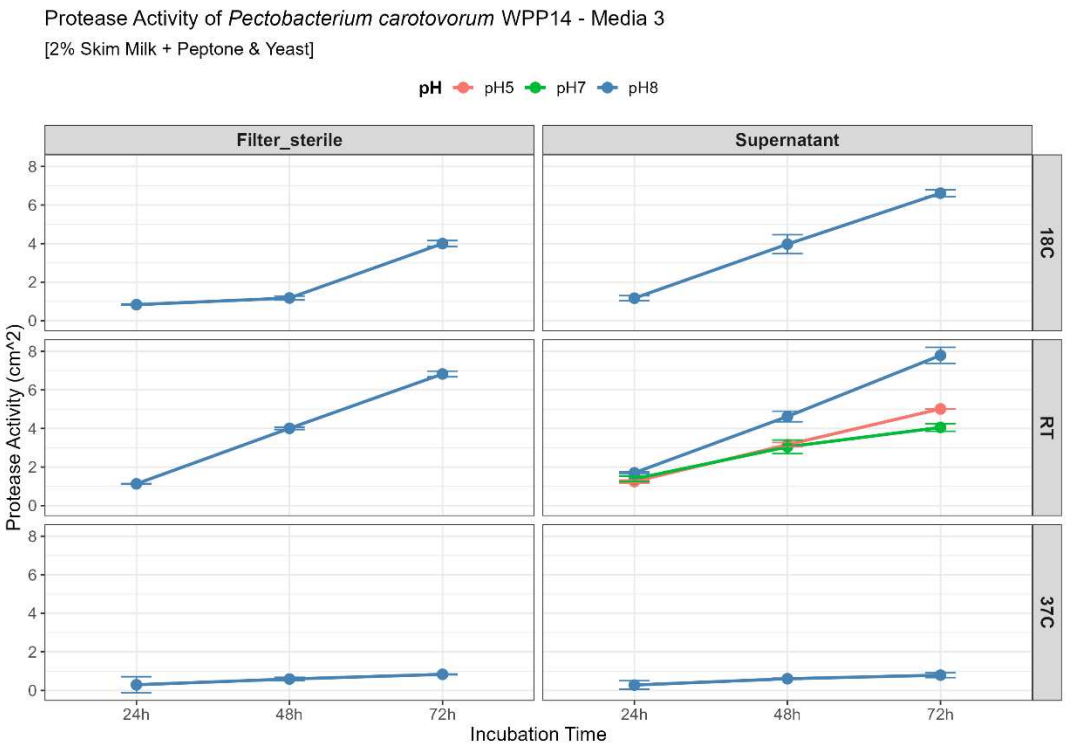


**Figure 9.** ***Protease activity of Pectobacterium carotovorum WPP14 on Medium 3 (2% skim milk agar with peptone and yeast extract).*** Activity was measured across inoculum types (supernatant, filter-sterilized), temperatures (18°C, room temperature [RT], 37°C), pH levels (5, 7, 8), and incubation durations (24h, 48h, 72h). Type III ANOVA revealed significant effects of incubation time, inoculum type, pH, and temperature ($p < 0.001$; Table 3). Tukey's test confirmed significantly higher protease activity at alkaline pH (pH 8 vs. pH 7 and 5), moderate temperatures (RT and 18°C vs. 37°C), and with supernatant inoculum (vs. filter-sterilized). Clear halos were already detectable after 24 hours for qualitative screening, with maximal halo sizes observed at 72 hours for quantitative measurements. Data are presented as mean ± SD.

**Table 3. Type III ANOVA results for protease activity in Medium 3**

| Factor | Sum Sq | Df | F value | p-value |
|---|---|---|---|---|
| **Incubation Time** | 163.8 | 2 | 219.61 | $< 2.2 \times 10^{-16}$ |
| **Inoculum Type** | 81.2 | 1 | 217.75 | $< 2.2 \times 10^{-16}$ |
| **pH** | 55.3 | 2 | 74.14 | $3.97 \times 10^{-17}$ |
| **Temperature** | 77.7 | 2 | 104.14 | $< 2.2 \times 10^{-16}$ |
| **Incubation Time:pH** | 18.8 | 4 | 12.61 | $7.03 \times 10^{-8}$ |
| **Incubation Time:Temp** | 24.5 | 4 | 16.42 | $4.38 \times 10^{-10}$ |
| **pH:Temperature** | 28.7 | 4 | 19.22 | $4.52 \times 10^{-11}$ |
| **Residuals** | 31.3 | 84 | - | - |

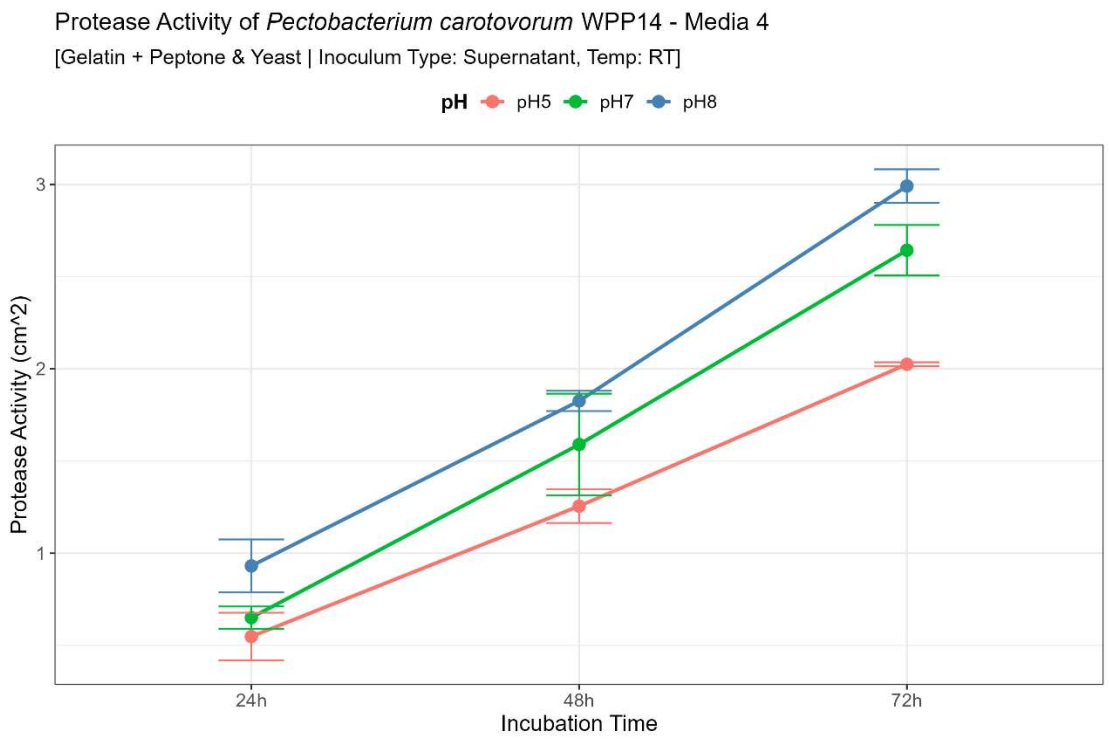


***Figure 10. Protease activity of Pectobacterium carotovorum WPP14 on Medium 4 (gelatin with peptone and yeast extract).*** Assays used supernatant inoculum at room temperature across pH 5, 7, and 8, and incubation times of 24h, 48h, and 72h. Type III ANOVA showed significant effects of pH and incubation time ($p < 0.001$; Table 4). Tukey's test confirmed highest activity at pH 8 and 72h. Data are mean ± SD.

**Table 4. Type III ANOVA results for protease activity in Medium 4**

| Factor | Sum Sq | Df | F value | p-value |
|---|---|---|---|---|
| **pH** | 3.69 | 2 | 66.76 | < 0.001 |
| **Incubation Time** | 26.68 | 2 | 482.17 | < 0.001 |
| **Residuals** | 1.19 | 43 | – | – |

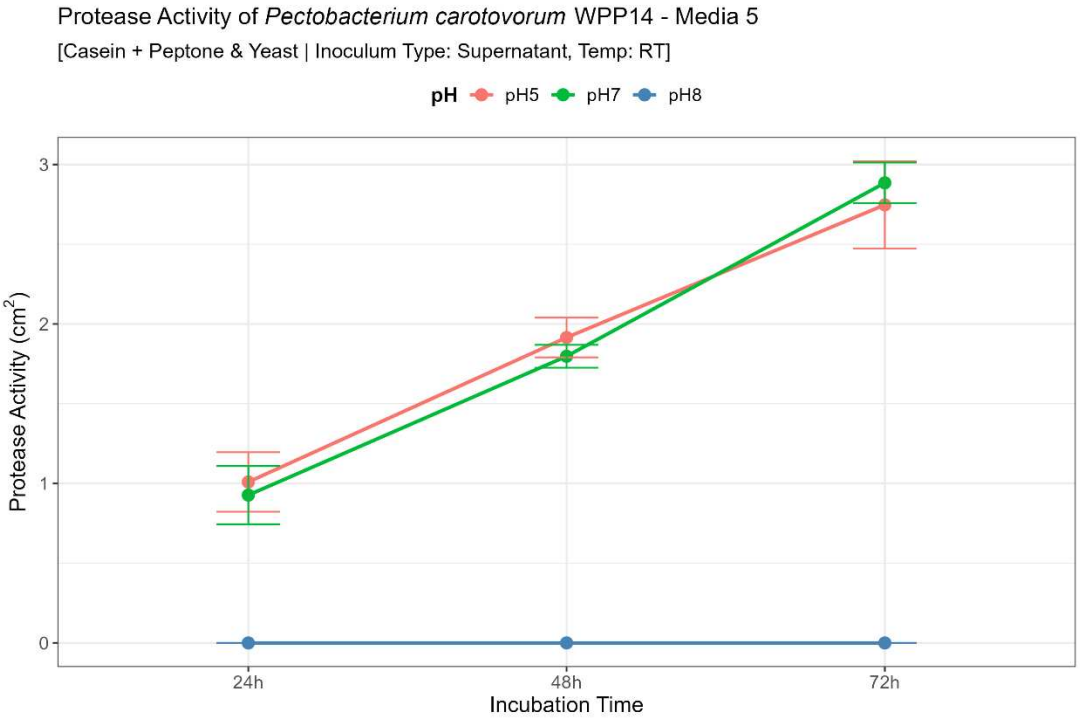


***Figure 11. Protease activity of Pectobacterium carotovorum WPP14 on casein-based Medium 5 (supernatant inoculum, RT) at pH 5, 7, and 8 over 24–72 h incubation.*** ANOVA indicated significant effects of pH and incubation time ($p < 0.001$), with similar activity at pH 5 and 7. Data represent mean ± SD.

**Table 5. Type III ANOVA results for protease activity in Medium 5**

| Factor | Sum Sq | Df | F value | p-value |
|---|---|---|---|---|
| **pH** | 42.43 | 2 | 132.44 | < 0.001 |
| **Incubation Time** | 13.66 | 2 | 42.66 | < 0.001 |
| **Residuals** | 7.85 | 49 | – | – |

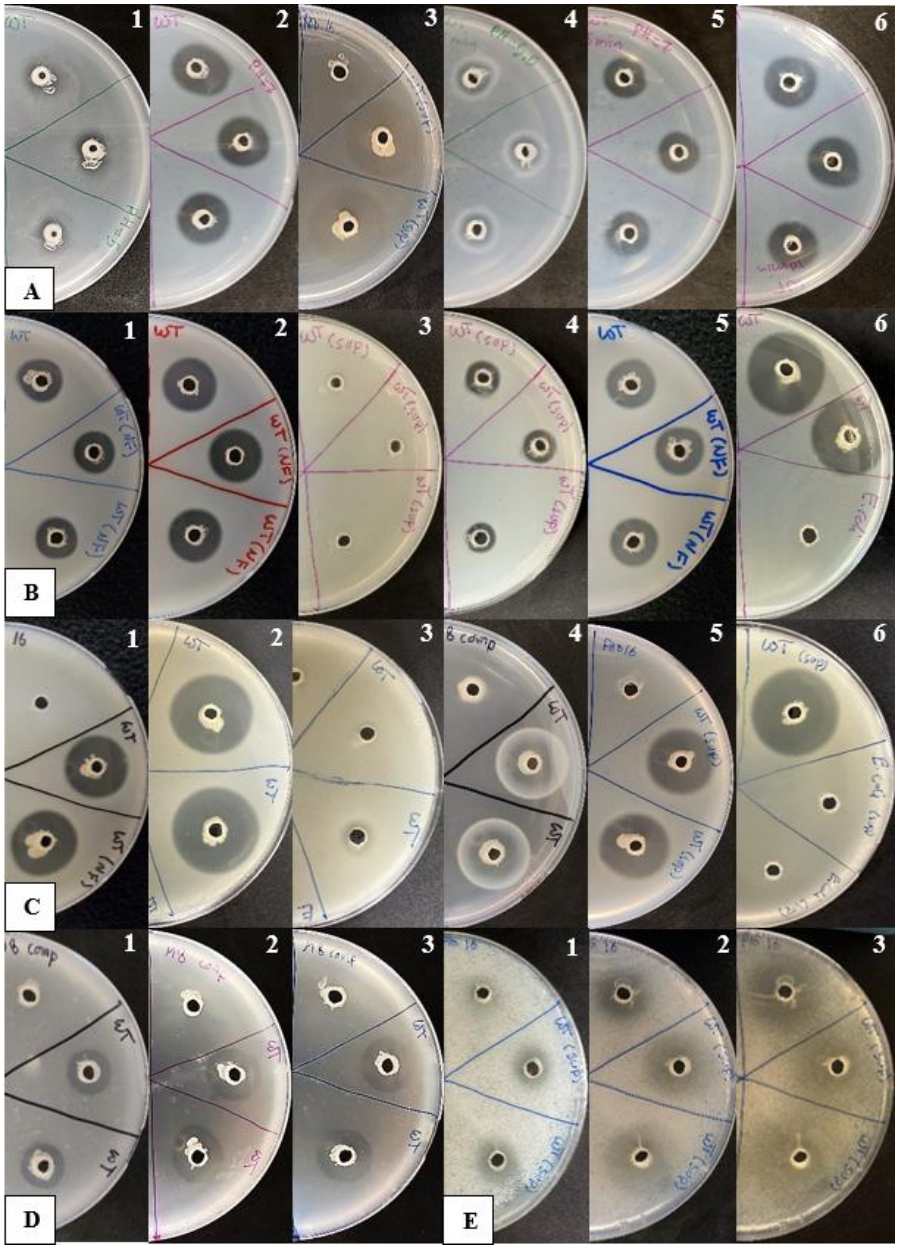


***Figure 12. Comparative protease activity assay plates for Pectobacterium carotovorum WPP14 across optimized media conditions. (*A) Medium** 1 (1% skim milk, RT, supernatant/cell lysate, 48h): A1, pH 5 (MES buffer); A2, pH 7; A3, pH 8 (NaOH); A4, pH 5 (5-min lysate); A5, pH 7 (5-min lysate); A6, pH 7 (10-min lysate). **(B) Medium 2** (2% skim milk, supernatant, 48h unless noted): B1, 18°C (pH 7); B2, RT (pH 7); B3, 37°C (pH 7); B4, 37°C (72h, pH 7); B5, 18°C (pH 8); B6, RT (pH 8). **(C) Medium 3** (2% skim milk + peptone + yeast, pH 8, supernatant, 48h): C1, 18°C; C2, RT; C3, 37°C; C4, RT (pH 5); C5, RT (pH 7); C6, RT (pH 8, showing negligible activity from *E. coli*). **(D) Medium 4** (gelatin + peptone + yeast, RT, supernatant, 48h): D1, pH 5; D2, pH 7; D3, pH 8. **(E) Medium 5** (casein + peptone + yeast, RT, pH 5, supernatant): E1, 24h; E2, 48h; E3, 72h.

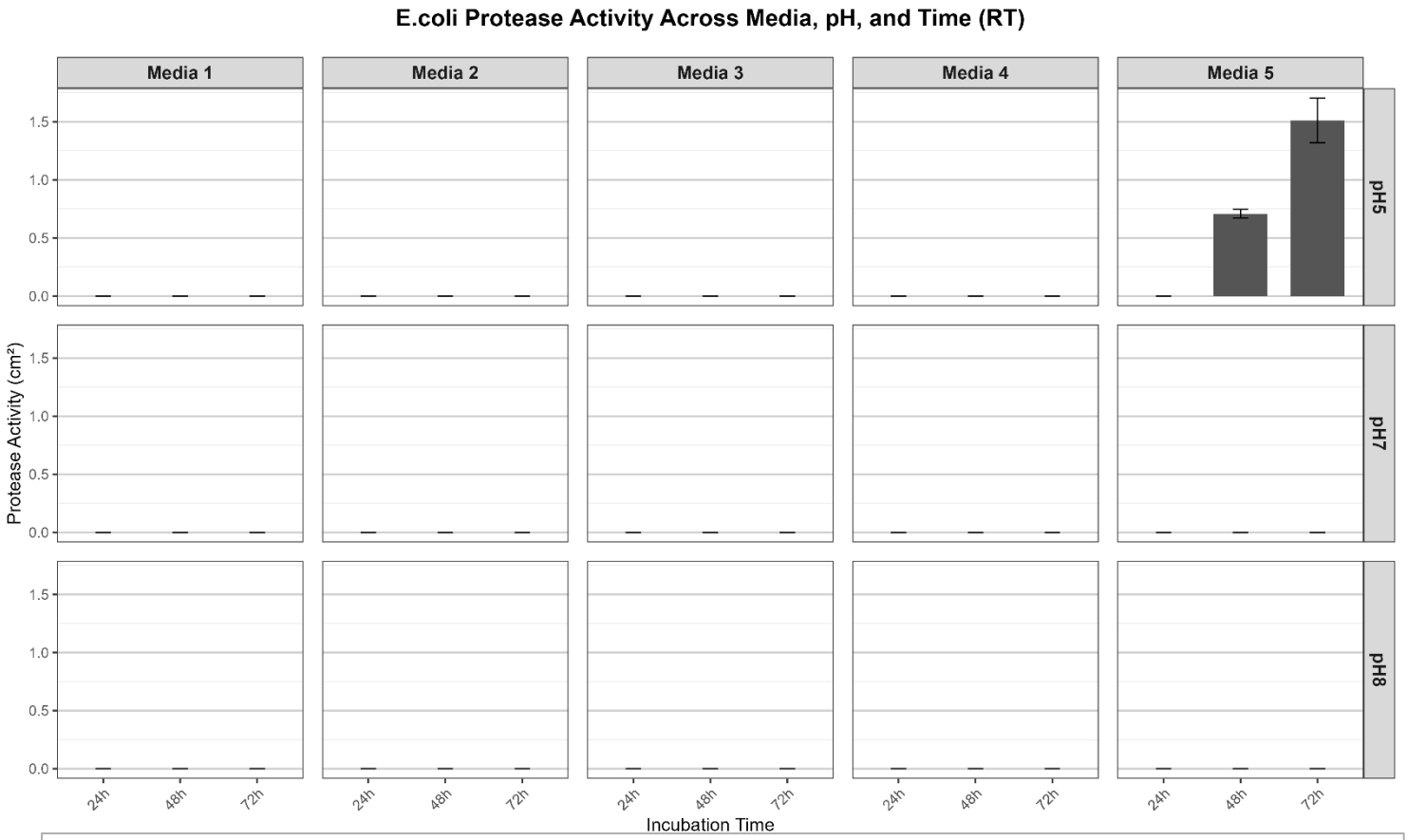


***Figure 13. Protease activity assay results demonstrating unexpected background activity of E. coli on Medium 5 (casein-based medium) at room temperature, pH 5, particularly after 48 and 72 hours of incubation.*** Ideally, *E. coli* should exhibit no protease activity and thus serves as a negative control. The observed false-positive result indicates that Medium 5 may not reliably differentiate true proteolytic activity, reducing its suitability as a selective assay medium compared to Media 1–4, which showed no activity from *E. coli* across all tested conditions.

**Table 6:** Comparative summary of protease activity, optimal assay conditions, and sterilization effectiveness across evaluated media formulations

| Media Type | WT WPP14 Activity | Temperature Effect | pH Effect | Sterilization Method |
|---|---|---|---|---|
| **Skim Milk (1%) (Medium 1)** | Moderate (+) | Optimal at RT | Detectable clearly at pH 5 and 7; unclear at pH 8 | Microwaving clearer than autoclaving |
| **Skim Milk (2%) (Medium 2)** | Moderate (+) | Optimal at RT and 18°C | Slightly better at alkaline (pH 8) | Microwaving is clearer than autoclaving |
| **Skim Milk (2%) + Peptone & Yeast Extract (Medium 3)** | High (+++) | Optimal at RT and 18°C (WT), RT and 37°C (clones) | Strongest at alkaline (pH 8) | Both methods are effective and clear with both methods |
| **Gelatin-Based (Medium 4)** | Moderate (+) | Optimal at RT | Broad activity across pH 5, 7, and 8 | Effective with both methods |
| **Casein-Based (Medium 5)** | Moderate (+) | Optimal at RT | Activity detected only at pH 5 | Microwaving only (autoclaving unusable) |

**References**


Alnahdi S, H. (2012). Isolation and screening of extracellular proteases produced by new isolated *Bacillus sp*. *Journal of Applied Pharmaceutical Science*, *Vol. 2 (9)*.

Baker, E. C., & Rackis, J. J. (1986). Preparation of unheated soy protein isolates with low trypsin inhibitor content. In (pp. 349-355). Springer US.

Chatterjee, A., Cui, Y. Y., Liu, Y., Dumenyo, C. K., & Chatterjee, A. K. (1995). Inactivation of rsmA leads to overproduction of extracellular pectinases, cellulases, and proteases in Erwinia carotovora subsp. carotovora in the absence of the starvation/cell density-sensing signal, N-(3-oxohexanoyl)-L-homoserine lactone. *Applied and environmental microbiology. 61:1959-1967.*

De Oliveira, C. F., Corrêa, A. P. F., Coletto, D., Daroit, D. J., Cladera-Olivera, F., & Brandelli, A. (2015). Soy protein hydrolysis with microbial protease to improve antioxidant and functional properties. *Journal of Food Science and Technology*, *52*(5), 2668-2678.

Fedatto, L. M., Silva-Stenico, M. E., Etchegaray, A., Pacheco, F. T., Rodrigues, J. L., & Tsai, S. M. (2006). Detection and characterization of protease secreted by the plant pathogen *Xylella fastidiosa*. *Microbiological Research*, *161*(3), 263-272.

Feng, T., Nyffenegger, C., Højrup, P., Vidal-Melgosa, S., Yan, K.-P., Fangel, J. U., Meyer, A. S., Kirpekar, F., Willats, W. G., & Mikkelsen, J. D. (2014). Characterization of an extensin-modifying metalloprotease: N-terminal processing and substrate cleavage pattern of *Pectobacterium carotovorum* Prt1. *Applied microbiology and biotechnology*, *98*, 10077-10089.

Figaj, D., Ambroziak, P., Przepiora, T., & Skorko-Glonek, J. (2019). The role of proteases in the virulence of plant pathogenic bacteria. *International Journal of Molecular Sciences*, *20*(3), 672.

García-Moyano, A., Diaz, Y., Navarro, J., Almendral, D., Puntervoll, P., Ferrer, M., & Bjerga, G. E. K. (2021). Two-step functional screen on multiple proteinaceous substrates reveals temperature-robust proteases with a broad-substrate range. *Applied microbiology and biotechnology*, *105*(8), 3195-3209.

Jones, K. M., Balalla, S., Theadom, A., Jackman, G., & Feigin, V. L. (2017). A systematic review of the worldwide prevalence of survivors of *Poliomyelitis* reported in 31 studies. *BMJ Open*, *7*(7), e015470.

Joshi, J. R., Brown, K., Charkowski, A. O., & Heuberger, A. L. (2022). Protease inhibitors from *Solanum chacoense* inhibit *Pectobacterium* virulence by reducing bacterial protease activity and motility. *Molecular Plant-Microbe Interactions®. 35:825-834.*

Khan, S., Arshad, S., Arif, A., Tanveer, R., Amin, Z. S., Abbas, S., Maqsood, A., Raza, M., Munir, A., Latif, A., Habiba, M., & Afzal, M. (2022). Trypsin inhibitor isolated from glycine max (*Soya bean*) extraction, purification, and characterization. *Dose-Response*, *20*(4).

Li, M., Liao, X., Zhang, D., Du, G., & Chen, J. (2011). Yeast extract promotes cell growth and induces production of polyvinyl alcohol-degrading enzymes. *Enzyme Research*, *2011*, 1-8.

Mukhia, S., Kumar, A., & Kumar, R. (2021). Generation of antioxidant peptides from soy protein isolate through psychrotrophic *Chryseobacterium sp.* derived alkaline broad temperature active protease. *LWT - Food Science and Technology*, *143*, 111152.

R Core, T. (2025). *R: A language and environment for statistical computing*. In (Version 4.4.3) [Computer software]. R Foundation for Statistical Computing.

Rasband, W. S. (2025). *ImageJ*. In (Version 1.54g) [Computer software]. U.S. National Institutes of Health.

Saggu, S. K., Jha, G., & Mishra, P. C. (2019). Enzymatic degradation of biofilm by metalloprotease from *Microbacterium sp. Sks10*. *Frontiers in bioengineering and biotechnology.*, *7*.

Sakoh, M., Ito, K., & Akiyama, Y. (2005). Proteolytic activity of htpx, a membrane-bound and stress-controlled protease from *Escherichia coli*. *Journal of Biological Chemistry*, *280*(39), 33305-33310.

Secades, P., & Guijarro, J. A. (1999). Purification and characterization of an extracellular protease from the fish pathogen *Yersinia ruckeri* and effect of culture conditions on production. *Applied and Environmental Microbiology*, *65*(9), 3969-3975.

Song, P., Zhang, X., Wang, S., Xu, W., Wang, F., Fu, R., & Wei, F. (2023). Microbial proteases and their applications. *Frontiers in Microbiology*, *14*.

Tang, C. (2019). Nanostructures of soy proteins for encapsulation of food bioactive ingredients. *Biopolymer Nanostructures for Food Encapsulation Purposes*, 247-285.

Vermelho, A. B., Meirelles, M. N. L., Lopes, A., Petinate, S. D. G., Chaia, A. A., & Branquinha, M. H. (1996). Detection of extracellular proteases from microorganisms on agar plates. *Memorias do Instituto Oswaldo Cruz*, *91*, 755-760.

Wei, M., Chen, P., Zheng, P., Tao, X., Yu, X., & Wu, D. (2023). Purification and characterization of aspartic protease from *Aspergillus niger* and its efficient hydrolysis applications in soy protein degradation. *Microbial Cell Factories*, *22*(1).

Xiang, Y., Herman, T., & Hartman, G. L. (2014). Utilizing soybean milk to culture soybean pathogens. *Advances in Microbiology*, *04*(02), 126-132.

Zhang, X., Shuai, Y., Tao, H., Li, C., & He, L. (2021). Novel method for the quantitative analysis of protease activity: The casein plate method and its applications. *ACS Omega*, *6*(5), 3675-3680.

## Chapter 3 - Genetic Analysis of Protease-Mediated Virulence in *Pectobacterium carotovorum* subsp. *carotovorum* WPP14


### Summary

*Pectobacterium carotovorum* is a major phytopathogen that causes soft rot diseases in many economically valuable crops, causing significant agricultural losses worldwide. Understanding the genetic basis of virulence in *P. carotovorum* is crucial for developing targeted strategies to reduce crop damage. In this study, we constructed a mutant library of *P. carotovorum* WPP14 using mini-Tn5 transposon mutagenesis. We screened for mutants with altered protease activity, pectate lyase activity, motility, and virulence with phenotypic assays. Disruptions in the sensor histidine kinase (*gacS)*, metabolic genes (*purM)* and (*metA)*, and the protease gene (*prtW)* significantly impaired these virulence-associated phenotypes. Transcriptomic analyses of these mutants revealed extensive changes in gene expression related to extracellular enzyme production, metabolic pathways, secretion systems, and motility regulation. The mutants were complemented to restore the wild-type phenotypes and confirm the critical roles of these genes in virulence regulation, where some of the mutants had complete restoration, and some had partial restoration. In addition, differentially expressed genes shared among the mutants highlighted the interconnection of proteolytic activity, secretion systems, and metabolic regulation in *Pectobacterium*. These findings elucidate the complex regulatory networks that govern virulence in *P. carotovorum* WPP14 and identify potential genetic targets for controlling soft rot diseases. This research enhances the fundamental understanding of bacterial pathogenesis and identifies key genetic factors that can be targeted to develop effective control measures against *P. carotovorum* in *Solanum tuberosum*.

## Introduction

Plant pathogenic bacteria employ diverse virulence factors to colonize and infect their hosts successfully. Among these, proteases play a crucial role in the virulence of *Pectobacterium carotovorum,* a significant gram-negative phytopathogenic bacterium that causes soft rot disease in numerous economically important crops (Charkowski et al., 2012; Li et al., 2019). The disease often manifests through the coordinated production of plant cell wall-degrading enzymes (PCWDEs), such as proteases, pectate lyases, and cellulases, which collectively degrade plant cell walls and facilitate bacterial colonization. While these enzymes are commonly produced in *Pectobacterium* strains associated with soft rot diseases, their expression and activity may vary depending on the specific strain and environmental conditions. (Feng et al., 2014; Figaj et al., 2020).

*Pectobacterium* virulent genes are regulated by a complex network that integrates plants, bacterial, and environmental signals. The GacS/GacA two-component system serves as a master regulator, controlling plant cell wall-degrading enzymes like proteases, pectate lyases, and other virulence determinants (Eriksson et al., 1998). This system is found in many Gram-negative bacteria, such as *Pectobacterium carotovorum*, *Dickeya dadantii*, *Pseudomonas aeruginosa*, and other related species. The GacS sensor kinase detects environmental signals, while the GacA response regulator activates the transcription of RsmB, which is a small regulatory RNA that relieves the repressive effects of RsmA, which allows for a coordinated expression of these enzymes (Cui et al., 2008). This cascade is crucial for the pathogen to break down the plant cell walls and initiate infection. Additionally, quorum sensing (QS) plays a critical role in regulating virulence gene expression in response to bacterial population density. Through the production of N-acyl-homoserine lactones (AHLs), *P. carotovorum* can sense its population density and

coordinate the expression of virulence factors accordingly, ensuring they are expressed at the right moment for effective infection (Joshi et al., 2020; Põllumaa et al., 2012). KdgM is another important regulatory protein that controls the production of enzymes responsible for degrading plant cell walls. By regulating pectate lyases, KdgM aids the pathogen to invade plant tissues and initiate infection (Charkowski et al., 2012). Plant-derived compounds, like p-coumaric acid, can also impact bacterial regulation. For example, Li et al. (2009) found that p-coumaric acid can repress the expression of genes related to the type III secretion system in *Dickeya dadantii*, suggesting that similar plant signals may affect regulatory pathways in *P. carotovorum*. Furthermore, a study by Moleleki et al. (2017) demonstrated that a quorum sensing-defective mutant of *P. carotovorum* ssp. *brasiliense* showed reduced virulence and failed to block xylem tissue in potatoes, which highlights the essential role of quorum sensing in virulence regulation. Overall, these systems, GacS/GacA, quorum sensing, RsmAB, KdgM, and external plant signals, work together to help *Pectobacterium* finely adjust its virulence in response to environmental conditions, demonstrating the complex regulation behind its pathogenicity.

*Pectobacterium carotovorum* relies on complex metabolic pathways to support its virulence and survival. Two crucial genes in its metabolic network, *purM* and *metA*, play significant roles in bacterial growth, stress adaptation, and pathogenicity. The *purM* gene is involved in de novo purine nucleotide biosynthesis, which is critical for DNA replication and energy production. In *Escherichia coli*, a dense network of binary interactions connects most purine nucleotide biosynthesis enzymes, suggesting the formation of a supramolecular complex (Gedeon et al., 2023). Disruptions in this network can affect purine nucleotide pools and bacterial fitness, highlighting the importance of proper interactions among these enzymes (Gedeon et al., 2023). While specific studies on *purM* in *P. carotovorum* are limited, research on other pathogens

provides valuable insights. For instance, in plant pathogenic fungi like *Magnaporthe oryzae*, the de novo purine nucleotide biosynthesis pathway is essential for fungal growth, development, and plant infection (Fernandez et al., 2013). Blocking this pathway inhibits the formation of penetration structures and invasive growth. The *metA* gene, encoding homoserine O-succinyltransferase, is involved in methionine biosynthesis. A recent study on *P. carotovorum* subsp. *carotovorum* Pcc21 showed that disruption of the methionine biosynthesis pathway significantly reduces virulence and the bacterium's ability to cause soft-rot disease in plants (Yu et al., 2023). The mutant strain exhibited impaired multiplication in hosts and downregulation of genes involved in methionine biosynthesis and transport. These metabolic pathways are likely integrated with other virulence factors, including quorum sensing, which coordinates bacterial behavior and infection processes (Cubitt et al., 2013). In *P. carotovorum* ssp. *brasiliense* 1692, inactivation of the quorum sensing gene *expI* led to reduced production of plant cell wall-degrading enzymes, inability to produce acyl homoserine lactone, and reduced virulence in potato tubers and stems (Moleleki et al., 2017). Although the specific regulatory mechanisms of *purM* and *metA* in *P. carotovorum* are not fully understood, their roles in the bacterium's virulence and overall survival make them promising targets for future disease control strategies. Further research is needed to elucidate the precise regulatory networks governing these pathways in *P. carotovorum* and their interactions with other virulence factors.

Proteases, particularly metalloproteases like PrtW, contribute significantly to *Pectobacterium* virulence through different mechanisms. These enzymes help the bacteria infect plants by degrading host proteins, facilitating plant cell wall maceration, and potentially interfering with the plant's defense mechanisms (Charkowski et al., 2012; Marits et al., 1999). The production of these proteases in *Pectobacterium* is tightly regulated by a combination of environmental and

internal factors, such as the availability of nutrients, stress responses, and the presence of other microorganisms competing for resources (Toth et al., 2003). Research in related *Pectobacterium* strains, such as *Pectobacterium brasiliense*, has shown that protease production is closely linked to the bacteria's growth and ability to infect. For example, the GacS/GacA two-component system has been shown to control the production of extracellular enzymes, including proteases, in *Pectobacterium* species (Cui et al., 2008; Li et al., 2019). In addition, quorum sensing mediated by N-acyl homoserine lactones (AHLs) also plays a role in regulating protease levels, as seen in *Pectobacterium* strains where disrupting quorum sensing leads to changes in protease production (Charkowski et al., 2012; Chatterjee et al., 1995). These findings suggest that protease regulation in *P. carotovorum* is likely connected to other important factors, including quorum sensing and the GacS/GacA system, that contribute significantly to *Pectobacterium* virulence (Cui et al., 2008; Toth et al., 2003).

However, much of our knowledge about protease regulation in *P. carotovorum* remains incomplete. Most of the existing models are based on genetic data from a single strain, particularly studies by Chatterjee et al. (1995). While these models have provided valuable insights, they are limited because they have not been validated across a broader range of strains or using more extensive genomic approaches. This creates a gap in our understanding, particularly regarding how strain-specific differences might influence regulatory processes. For example, the strain of *P. carotovorum* (WPP14) being studied here may display regulatory patterns that differ from those observed in earlier models.

The Type VI Secretion System (T6SS) is another key mechanism that plays an important role in regulating *Pectobacterium carotovorum* virulence. It is a needle-like structure used by *P. carotovorum* and other closely related *Pectobacterium* species to inject toxic proteins into

neighboring cells, including both bacterial and plant cells. This system plays a vital role in competition, tissue degradation, and survival. In *P. carotovorum*, the regulation of T6SS is influenced by global systems, including the Hfq RNA chaperone, which modulates T6SS expression and enzyme production in response to environmental cues (Wang et al., 2018). Studies in related *Pectobacterium* species like *P. brasiliense* and *P. atrosepticum* reveal that T6SS regulation is interconnected with stress response pathways and positively regulated by GacS/GacA (Li et al., 2019). The RpoS sigma factor also influences stress responses and virulence regulation. While much of our understanding of T6SS regulation in *P. carotovorum* is based on studies of related species, the exact mechanisms in *P. carotovorum* strain WPP14 require further investigation. Research in other pathogens, such as *P. brasiliense*, has demonstrated the role of T6SS in both bacterial competition and pathogenesis, providing insights into how T6SS might function in *P. carotovorum* (Bellieny-Rabelo et al., 2020). Understanding these regulatory interactions in more detail will be crucial for developing strategies to control soft-rot diseases and improve disease management practices for crop protection.

Despite our understanding of these major regulatory systems, significant gaps remain in our knowledge of *P. carotovorum* virulence, which remains incompletely understood. For instance, the connection between primary metabolism, the essential biochemical processes to maintain basic cellular functions, and virulence factor production remains poorly understood. Furthermore, while specific proteases like PrtW have been identified (Marits et al., 1999), their regulation and integration with other virulence networks require further investigation. To address this gap, we used transposon mutagenesis, a powerful tool for creating random gene disruptions, to create a high-quality mutant library of *Pectobacterium carotovorum* WPP14 to identify novel genes involved in virulence (Holeva et al., 2004b; Wilson et al., 1995). By generating a mutant library

and screening for altered protease phenotype, we uncovered essential genes and regulatory networks contributing to *Pectobacterium* virulence.

In this study, our goal was to investigate the role of proteases in the virulence of *Pectobacterium* to understand the mechanisms underlying its pathogenicity and to expand our understanding of the genetic factors contributing to *P. carotovorum* virulence by integrating the observed phenotypic data with genomic insights to unveil potential targets for disease control and management. Understanding the genetic factors of *P. carotovorum* virulence *provides a better grasp of how the bacteria cause the disease and develops* targeted strategies to reduce crop losses effectively. In addition, identifying key regulatory and metabolic genes involved in virulence can provide more insight into antimicrobial agents or the engineering of resistant plant varieties, thereby enhancing agricultural productivity and sustainability.

## Materials and Methods

### Bacterial strains, growth conditions, and plant materials.

The wild-type *Pectobacterium carotovorum* strain WPP14 was cultured in nutrient broth (NB) supplemented with chloramphenicol (Cm), while mutant strains were grown in NB containing spectinomycin (Sp) and Cm and incubated at 30°C with shaking (200 rpm). Mutants were cloned into the pGEM-T Easy vector and transformed into JM109 high-efficiency competent cells (Promega, USA). Complemented mutants were plated on Luria-Bertani (LB) agar (1% tryptone, 1% NaCl, 0.5% yeast extract, 1.5% agar per liter) supplemented with ampicillin (Amp) and incubated at 30°C. Protease activity was measured using skim milk agar (SM), containing 2% dry skim milk and 1.2% agar per liter, adjusted to pH 8 with 1M NaOH and incubated at room temperature for 48h (Chatterjee et al., 1995; Joshi et al., 2022). Semi-solid agar media (1% tryptone, 0.5% NaCl, and 0.3% agar per liter) was used for motility assays (Sivaranjani et al., 2016;

Sudarshan et al., 2021). Pectate lyase (Pel) activity was assessed following a modified protocol from (Jahn et al., 2008), using 1% polygalacturonic acid (PGA) (Sigma-Aldrich), 0.67% yeast extract, 2% agar, 0.38 mM $CaCl_2$, and 100 mM Tris-HCl at pH 8. Plates were incubated at room temperature for 24 hours, and halos were visualized using 4N HCl. Virulence assays were conducted on *Solanum tuberosum* (Gold Potatoes) sourced from local supermarkets, and stem inoculations were performed on Russet Norkotah. All assays were performed three times with five replicates for each mutant.

**Construction of *P. carotovorum* WPP14 mutant library.**

A mutant library of *P. carotovorum* WPP14 was created by random insertion of the mini-Tn5 transposon *Tn5SSgusA*, where the conjugation occurred between the donor bacteria *E. coli* S17-1//λpir (inserted into the vector pCAM140), and the recipient bacteria *P. carotovorum* WPP14 (chloramphenicol resistance; $Cm^r$) (Holeva et al., 2004a; Wilson et al., 1995; Yap et al., 2008). The bacteria were mixed in a 1:2 ratio, spotted onto nutrient agar (NA) plates, and incubated for 18h at room temperature. Sterile water ($sH_2O$) was added to the obtained mating spots to suspend them in the water and plate the diluted conjugation mixture onto NA supplemented with spectinomycin (Sp) and chloramphenicol (Cm). All the obtained colonies, which were about 7,960 *Tn5SSgusA* insertion mutants of *P. carotovorum* WPP14, were cultured in sterile 96-well plates filled with 200µl nutrient broth (NB) supplemented with Sp and Cm and incubated at 30ºC overnight with agitation (200 rpm) (Holeva et al., 2004a; Mee-Ngan Yap et al., 2008). The bacterial cells were harvested by centrifugation, resuspended in a 20% glycerol solution, and stored at -80°C for later analysis.

The whole genome paired-end sequencing was used to sequence the mutant libraries. Eight libraries were constructed using the Tn5 DNA Library Prep Kit, and the *Tn5SSgusA* insertion DNA

of the wild-type WPP14 mutants was extracted using QIAGEN DNeasy PowerSoil Pro Kit. The position of each transposon in the bacterial genome was determined by mapping the pair-end sequences to *P. carotovorum* WPP14 genome and the *Tn5SSgusA* sequence using the algorithm bwa-me.

**Phenotypic screening for the mutant library**

**Initial protease activity assays.** Skim-milk agar plates were used to screen the mutant library for protease (Prt) phenotype by assessing the mutant's ability to hydrolyze the milk protein, measured by the clear zone around the inoculum. The mutants were cultured in 200µl NB supplemented with Sp and Cm (1:1000 ratio NB: antibiotics) in sterile 96-well plates and incubated at 30°C with agitation (200 rpm) overnight. All protease activity assays were performed once the optical density at 600 nm reached ($OD_{600}$) ≥ four for all cultured mutants. Skim-milk agar plates were prepared by mixing 1% dry skim-milk and 0.8% agar, where a 2mm sterile core borer was used to make wells in the plates, and 20µl supernatant of the overnight mutant bacterial culture was applied. Protease plates were incubated at room temperature for 24h, and the results were taken by scanning the plates to measure the clear zone formed around the inoculum by ImageJ-1.54g (Joshi et al., 2022).

Mutants showing protease activity (both low and high) based on their mean ± standard deviation (SD) compared to the wild-type WPP14 were selected for a replicated protease assay with three replicates for each mutant. After confirming the mutant phenotype, they were cultured on nutrient agar plates (NA) supplemented with Sp and Cm to obtain single colonies and prepare a stock solution for each one. The stock solution was prepared by culturing the single colonies in NB with Sp and Cm (incubated at 30°C overnight with 200 rpm). The overnight cultures were

centrifuged, and the bacterial pellets were resuspended in 20% glycerol, flash-frozen with liquid nitrogen, and stored at -80$^{o}$C for later analysis.

**Pectate lyase activity assays**. Mutants with protease activity were also tested for pectate lyase activity (Pel), which was determined using polygalacturonic acid (PGA). Like protease assay, we used a 2mm sterile core borer to make wells, and 20µl of the overnight bacterial culture was applied. The plates were then incubated at RT overnight (20h), and to visualize the halos, 1 ml 4N HCL was applied to the plates. Enzyme activity was measured by scanning the plates to measure the clear area formed around the inoculum using ImageJ-1.54g.

***Motility Assays.*** Following Sivaranjani et al. 2016, semisolid tryptone media was used to determine mutants' swimming motility. Two microliters of the mutant's overnight culture (1 x $10^8$ CFU/ml) were inoculated in the center of the plates and incubated at 30°C for 15h. The results were taken by scanning the plates to measure the turbid area using ImageJ-1.54g.

**Virulence Assays.**

***Tuber Virulence.*** For tuber virulence assays, the tubers (Gold Potatoes) were surface sterilized by soaking them in sodium hypochlorite solution for 20 minutes and washed three times with water. Then, they were placed in the biosafety cabinet, sprayed with 70% ethanol, and left to dry for 30min (Joshi et al., 2022). Three concentrations were prepared for each mutant expressing protease phenotype by measuring their optical density ($OD_{600}$) at 600 nm absorbance for the overnight cultures ($10^8$, $10^6$, and $10^4$ CFU). Under aseptic conditions, holes were made in the tubers using a 20µl pipette tip, and they were inoculated with 10µl of each concentration. Inoculated tubers were sealed and placed in bags to prevent the wounds from drying, and they were incubated at 30°C for 48h. Macerated tissues were measured by cutting the tubers through the holes we made and gently scraping all the decayed tissues to weigh them (decayed tissue/g).

***Stem Inoculation*.** Following the (Taylor et al., 2021) protocol, Russet Norkotah tubers were used for stem inoculation virulence assay. After cutting the buds from the seed tubers, they were washed and planted in (6 cm x 9 cm x 11.5 cm, [L $^{xx}$ W $^{xx}$ H]) pots 1 cm below the surface level of the potting mix (Miracle-Gro Potting Mix; Marysville, OH 43041). After planting, the pots were placed in the lab growth chamber and irrigated by hand to saturation. The temperature was set to 24°C, with a 16h daylight setting. Before the plants were ready for inoculation in 3-4 days, all the mutants were cultured on NA media to obtain single colonies. Using a sterile toothpick, we gently made a vertical cut in the lower part of the stem, and two bacterial colonies (each around 5mm) were placed in the stem slit. After inoculation, the plants were monitored daily to record the results. We recorded the result for all the mutants for lesion length based on the first lesion that appeared on the WT (our positive control). To monitor disease progression, we took the result every day until none of the plants showed any change or symptoms; we waited for two days since the last observed change. If all the conditions remain unchanged, then the experiment is completed.

**Growth Assays.** The bacterial growth assay was performed by preparing overnight cultures of *P. carotovorum* mutant strains and the WT in nutrient broth (NB) at 30°C with shaking at 200 rpm. The overnight culture was then centrifuged, and the bacterial cells were resuspended in sterile water to prepare the inoculum. A 10 µL aliquot of the bacterial inoculum (10^8 CFU/mL) was added to 1 mL of fresh nutrient broth (NB). The culture was incubated at 30°C with shaking at 200 rpm for 15 hours. Following incubation, bacterial growth was assessed by serially diluting the culture and plating the dilutions onto NB agar plates. The number of colony-forming units (CFU) per milliliter was recorded to determine the bacterial multiplication (Joshi et al., 2022).

**Genome Sequencing and Mutant Complementation.** A draft genome was obtained for the mutants with significantly lower and higher proteases compared to the wild-type *P. carotovorum* WPP14 to identify the insertional sites of the mini-Tn5 transposon using Oxford Nanopore long-reads sequencing. The identified mutants were amplified using the primers listed in (Table 1) and cloned into the pGEM-T vector (Promega). After successfully cloning the mutants, we purified the plasmids using QIAprep Spin Miniprep Kit to construct complemented mutants by electroporation using Bio-rad Gene Pulser.

**Next Generation Sequencing: RNA-Sequencing.** Three biological replicates were prepared for the mutants M1(*gacS*::Tn5*)*, M2(*purM*::Tn5*)*, M6(*metA*::Tn5*)*, and M8(*prtW*::Tn5) and the WT(WPP14). Mutants and WT were streaked on NA plates supplemented with antibiotics and incubated overnight. After that, all the samples were grown in a potato extract medium, prepared by boiling 100g of peeled and washed potato in 500 ml of sterile $H_2O$. The boiled potatoes were filtered through a filter fabric, and the extract was autoclaved before use (Davis, 1933). Mutants and WT were cultured in the potato extract medium and incubated for 3h at 30°C. The optical density at 600 nm for all the samples was ($OD_{600} \geq 0.2$). Then, the samples were centrifuged at 8000xg for 5 min, and frozen cell pellets were sent to Azenta Life Sciences for RNA sequencing, library preparation, and data analysis to study the differentially expressed genes of the mutants compared to the wild type.

**Statistical Analysis.** All statistical analyses were conducted in R software (version 4.4.1), with methods selected based on data type, sample size, and distribution assumptions.

For protease activity, a t-test was initially used after data transformation to compare the WT and mutant groups, while ANOVA with Tukey's HSD was applied in the final analysis to

assess differences among WT, mutants, and complements. Levene's test was performed to check variance homogeneity before ANOVA.

For pectate lyase activity, Welch's one-way ANOVA with Dunnett's post-hoc test was used in the initial assay due to variance heterogeneity. In the final replicated assay, one-way ANOVA with Tukey's HSD was applied after confirming normality and equal variance. Bacterial motility was analyzed using one-way ANOVA with Tukey's HSD post-hoc test in both initial and final analyses, as the data met normality and variance assumptions, allowing for multiple comparisons. For tuber virulence, Two-Way ANOVA assessed the effects of mutation and inoculum level on tissue decay, and their interaction. Dunnett's test compared each mutant and its complement to WT, while Tukey's HSD evaluated differences among inoculum levels.

Lesion length for the stem inoculation assay was analyzed using the Kruskal-Wallis test with Dunn's post-hoc test, which provides a non-parametric alternative to one-way ANOVA. Further, Fisher's Exact Test with Bonferroni correction was used for disease progression, which is ideal for categorical data and adjusts for multiple comparisons. These methods were chosen to ensure accurate, valid, and robust statistical analysis based on the characteristics of each dataset.

## Results

### Phenotypic Characterization of *P. carotovorum* WPP14 Mutants

A mutant library was screened for protease activity to evaluate the impact of gene disruptions on the virulence factors. From a total of 88 (96-well) plates, 30 plates (2,880 mutants) were screened to assess protease phenotypes. Among these, 68 mutants that exhibited varying levels of protease activity, classified based on the mean ± standard deviation relative to the WT(WPP14), were chosen for further analysis. Of these, 18 mutants had increased protease

activity, 18 exhibited reduced activity, 25 had activity levels close to the WT average of 0.97 $cm^2$, and seven had no protease activity. From this pool, 11 mutants were selected for further analysis: four with the highest level of protease activity and all seven mutants that lacked protease activity.

Further assays, including replicated protease activity, pectate lyase activity, motility, and tuber virulence tests, were performed to narrow the mutant selection to 8 mutants, 6 with zero activity and 2 with high activity. The selected mutants were identified via Oxford Nanopore long-read sequencing as having insertions in *gacS*, *purM*, a hypothetical protein, a *lysR*-family transcriptional regulator, *cysJ*, *metA*, and *prtW* (designated as M1, M2, M3, M4, M5, M6, and M7/M8, respectively) (Table 1). Notably, two mutants (M7 and M8) are both *prtW* mutants with mini-Tn5 transposon insertions at different sites.

**Table 3.** Identified mutants with protease phenotype.

| Mutant | Identified genes | Product | Primers used for cloning |
|---|---|---|---|
| **M1** | *gacS* | Two-component sensor kinase response regulator | F: AATGTACTATCGATTGATCTCTTGGGTTGA<br>R: TTACGAATGCATAGGTTTGATATGCGGC |
| **M2** | *purM* | Phosphoribosylformylglycinamidine cyclo-ligase | F:CATTATCTCCCCATCGGCTAGTGGACGGAC<br>R: CTACTCGGCAGCATAGCCCTGTGG |
| **M3** | *yeaR* | Hypothetical protein-*ADT0000389* | F: ATGGAACGAATTGTTATACCCGCG<br>R: TTACCAGCCGCAGACGTTAGTGTC |
| **M4** | *lysR* | Transcriptional regulator | F: ATGGGACAATCTGATAGCTTTGA<br>R: TCACGTCTTAATAACTTGTGAAC |
| **M5** | *cysJ* | Sulfite reductase flavoprotein alpha-component | F: CGAGTACCGTCTGCAAAGAGGGCTGCAT<br>R: TTACCCTTCGTGCAGCCCGCATTC |
| **M6** | *metA* | Homoserine-O-succinyltransferase | F:AATATTTCCCTGAGTGATTCCTATGCGCTT<br>R: CTAGTCCAGCGTAGGGTTCATCCTACG |
| **M7/M8** | *prtW* | Metalloprotease | F: CAAATTCCTATATATTCGTTTGCAGAATA<br>R: TTAGTTTCTGCCGATCTTGTGG |

***Protease Activity Assay Results.*** The initial screening revealed a complete loss of protease activity (0.00 $cm^2$, $p \leq 0.02$) in the M1 (*gacS*::Tn5), M2 (*purM*::Tn5), M5 (*cysJ*::Tn5), M6 (*metA*::Tn5), M7 (*prtW*::Tn5), and M8 (*prtW*::Tn5) mutants compared to the wild-type (WT) (0.85 ± 0.08 $cm^2$). Repeated assays confirmed zero activity in M1, M7, and M8, while M2 and M6

exhibited minimal but significantly reduced activity (0.23 ± 0.004 cm² and 0.34 ± 0.02 cm², respectively) (Table 4, Figure.1). The variation in M2 and M6 activity levels between initial and final assays suggests complex regulatory networks affecting protease production.

Mutants M3 (yeaR::Tn5) and M4 (lysR::Tn5) demonstrated enhanced protease activity (1.22 ± 0.07 cm² and 1.13 ± 0.04 cm², respectively) compared to WT. However, our focus remained on reduced-activity mutants to understand essential regulatory mechanisms in virulence.

The consistent loss of protease activity in M1 (gacS::Tn5) and both prtW mutants (M7 and M8) indicates their essential role in protease activity. Complementation successfully restored protease activity in (M1comp) *gacS*::Tn5 (pGacS) (0.69 ± 0.09 cm²), (M2comp) *purM*::Tn5 (pPurM) (1.07 ± 0.09 cm²), and (M6comp) *metA*::Tn5 (pMetA) (1.24 ± 0.1 cm²), confirming the direct involvement of these genes in protease regulation. Complementation could not be achieved for M5 (*cysJ*::Tn5) and M7/M8 (*prtW*::Tn5) due to technical challenges. However, the identical phenotypes from independent insertions in *prtW* provide strong evidence for its role. Previous studies regarding prtW (metalloproteases) demonstrate its role and importance in *Pectobacterium* virulence (Charkowski et al., 2012; Marits et al., 2002).

***Pectate Lyase Activity Results***. Initial screening revealed significant reductions in pectate lyase activity across all mutants except M5 (*cysJ*::Tn5) and M6 (*metA*::Tn5) compared to WT (1.7 ± 0.08 cm²). M1 (*gacS*::Tn5), M2 (*purM*::Tn5), M3 (*yeaR*::Tn5), M4 (*lysR*::Tn5), M7 (*prtW*::Tn5), and M8 (*prtW*::Tn5) showed significant reductions ($p \leq 0.05$), with M1 (1.2 ± 0.09 cm²) and M2 (1.5 ± 0.06 cm²) exhibiting the most reduction (Table 2, Figure.2). However, M6 maintained activity levels comparable to WT (1.6 ± 0.27 cm²), suggesting that methionine metabolism does not directly influence pectate lyase production.

Final assays confirmed consistent reductions in pectate lyase activity, with M1 showing the most significant reduction (1.32 ± 0.14 cm²), followed by M2 (1.59 ± 0.06 cm²) and M8 (1.46 ± 0.08 cm²). Mutant complementation restored pectate lyase activity in M2comp (2.06 ± 0.17 cm²) and M6comp (2.19 ± 0.06 cm²), while M1comp showed only partial restoration (1.54 ± 0.10 cm²), suggesting that *gacS* influences multiple regulatory pathways.

***Motility Assays Results*.** The initial motility assay revealed significant reductions in swimming motility across all mutants compared to the wild type (WT) strain (19.0 ± 1.02 cm²). The most significant reductions were observed in M1 (*gacS*::Tn5), M2 (*purM*::Tn5), and M5 (*cysJ*::Tn5), with swimming motility of 5.7 ± 0.06 cm², 4.6 ± 1.43 cm², and 6.8 ± 2.24 cm², respectively. M7 (*prtW*::Tn5) and M8 (*prtW*::Tn5) also exhibited notable reductions (11.4 ± 2.52 cm² and 8.8 ± 2.60 cm², respectively), while M3 (*yeaR*::Tn5), M4 (*lysR*::Tn5), and M6 (*metA*::Tn5) displayed intermediate motility levels (13.0 ± 1.67 cm², 10.8 ± 2.32 cm², and 11.7 ± 0.91 cm², respectively) (Table 2, Fig 3). These findings suggest that while these genes contribute to motility regulation, the most significant effects were observed in *gacS* and *purM* disruptions, potentially due to their roles in global regulatory networks.

Final motility assays confirmed the initial reductions, with M1, M2, and M8 maintaining significantly lower motility compared to the WT. Complementation of these mutants restored motility to varying degrees. (M1comp) *gacS*::Tn5 (pGacS) exhibited complete restoration (27.7 ± 2.85 cm²), confirming the essential role of *gacS* in motility regulation. Interestingly, (M2comp) *purM*::Tn5 (pPurM) and (M6comp) *metA*::Tn5 (pMetA) displayed enhanced motility compared to WT(WPP14) (31.2 ± 2.62 cm² and 33.9 ± 0.9 cm², respectively) (Table 4, Fig 3), suggesting that disruptions in purine (M2) and methionine (M6) metabolism might trigger compensatory mechanisms that increase motility. The successful complementation of *gacS*, *purM*, and *metA*

further supports their involvement in motility regulation, potentially through signaling and metabolic pathways.

***Tuber Virulence. Assays Results.*** Initial virulence assays using an inoculum of $10^8$ CFU/ml revealed varying degrees of virulence attenuation compared to the WT(WPP14) (8.8 ± 0.8 gm). Among the mutants, M1 (*gacS*::Tn5) exhibited the most reduction in tuber maceration (1.7 ± 0.2 gm), followed by M2 (*purM*::Tn5) (2.8 ± 0.1 gm). M6 (*metA*::Tn5) showed a moderate reduction (5.8 ± 0.4 gm), while M7 (*prtW*::Tn5) and M8 (*prtW*::Tn5) maintained partial virulence (6.3 ± 0.3/0.4 gm). At lower inoculum levels ($10^6$ and $10^4$ CFU/ml), M1 and M2 continued to display significant reductions in virulence. Notably, M2 exhibited a complete loss of virulence at $10^4$ CFU/ml (0.00, p = 1.E-07), followed by M1 (1.3 ± 0.3 gm) (Table 3).

Complementation assays demonstrated varying degrees of virulence restoration. (M2comp) *purM*::Tn5 (pPurM) exhibited complete restoration at $10^8$ and $10^4$ CFU/ml (5.6 ± 0.6 gm and 2.2 ± 0.2 gm, respectively) (Table 5, Figure. 4). Similarly, (M6comp) *metA*::Tn5 (pMetA) displayed full virulence recovery across all inoculum levels (7.3 ± 0.8 gm, 4.8 ± 0.7 gm, and 2.0 ± 0.3 gm for $10^8$, $10^6$, and $10^4$ CFU/ml, respectively) (Table 5, Figure. 4). In contrast, (M1comp) *gacS*::Tn5 (pGacS) only exhibited partial recovery (2.2 ± 0.3 gm) at $10^8$ CFU/ml, indicating that *gacS* likely influences additional regulatory pathways beyond virulence restoration (Table 5, Figure. 4).

***Stem Inoculation Assays Results.*** Stem inoculation assays revealed significant differences in lesion length (Table 6, Figure. 5A) and disease progression (Table 7, Figure. 5B) among the tested mutants. The WT strain exhibited severe virulence, producing extensive lesions (1.5 ± 0.2 cm) and leading to significant disease progression, with 14 plants dead and one diseased out of 15 total plants.

M1 (*gacS*::Tn5) showed a complete loss of virulence, with no lesion formation (0 cm, $p < 0.0001$) and no signs of disease progression (15 healthy plants, p.adj = 1.5E-07), indicating its essential role in virulence regulation. Similarly, M2 (*purM*::Tn5) and M6 (*metA*::Tn5) exhibited severe reductions in lesion formation (0.04 ± 0.04 cm and 0.06 ± 0.06 cm, respectively, $p = 0.00001$), with significantly reduced disease progression. M2 resulted in 11 healthy plants and only four dead, whereas M6 showed 10 healthy, two diseased, and three dead, indicating their significant impact on *Pectobacterium* virulence attenuation.

M7 and M8 (*prtW*::Tn5) retained partial virulence, producing moderate lesions (0.5 ± 0.1 cm and 0.4 ± 0.1 cm) and showing variable disease progression. M7 caused seven plant deaths, while M8 resulted in two dead plants, suggesting that *prtW* is involved in virulence but may not be the sole contributor to stem infection.

Complementation assays partially restored virulence in (M1comp) *gacS*::Tn5 (pGacS), which exhibited 0.8 ± 0.2 cm lesions and a moderate increase in disease severity (two dead, eight diseased). (M2comp) *purM*::Tn5 (pPurM) and (M6comp) *metA*::Tn5 (pMetA) showed stronger restoration, producing lesion lengths of 0.7 ± 0.2 cm and 0.9 ± 0.2 cm, respectively, and increasing the number of dead plants (six and seven dead, respectively). These results confirm the involvement of *gacS*, *purM*, and *metA* in disease development, with *gacS* playing a more extensive regulatory role that may not be fully restored by complementation alone.

***Growth Curve Analysis.*** The growth curve analysis demonstrated that mutations in M1(*gacS::*Tn5), M2*(purM::*Tn5*),* M6*(metA::*Tn5), and M8(*prtW::*Tn5) did not significantly impair bacterial multiplication in nutrient broth (NB) cultures, as the mutants had similar growth patterns to the WT, particularly in the later stages (8–16 hours). These results indicate that the observed virulence defects are not due to general growth deficiencies but rather disruptions in

regulatory pathways affecting virulence-associated factors such as protease secretion, motility, and pectate lyase activity. These findings align with previous research showing that mutations in virulence regulators like *gacS* primarily affect pathogenicity mechanisms while maintaining normal growth capabilities (Jiang et al., 2016; Latour, 2020; Lebeau et al., 2008). The preserved growth patterns suggest that these mutations impact virulence pathways without compromising essential metabolic functions required for bacterial survival and proliferation (Latour, 2020).

A similar conclusion was drawn by Joshi et al. (2021), who reported that M6 metabolite extracts did not reduce bacterial multiplication in *Pectobacterium brasiliense* but instead inhibited the expression and activity of exoenzymes such as Prt, Pel, and Cel. Their study demonstrated that bacterial growth remained unaffected in the presence of these plant-derived metabolites, yet exoenzyme activity was significantly reduced due to quorum sensing (QS) inhibition (Joshi et al., 2021). This is consistent with our findings, as the mutants exhibited no significant differences in growth yet displayed significantly lower protease and pectate lyase activity. These results reinforce the idea that bacterial virulence can be attenuated without affecting overall growth.

Despite the differences in approach, our study involving a Tn5 mutant library screening and Joshi et al. (2021) focusing on plant-derived metabolites, both studies emphasize that virulence attenuation can occur independently of bacterial proliferation. This further supports the idea that targeting regulatory pathways can reduce bacterial pathogenicity without compromising survival.

**RNA-seq Analysis of Differentially Expressed Genes (DEGs)**

***M1 (gacS::Tn5) DEGs Analysis***. RNA-seq analysis of gacS::Tn5 mutant revealed extensive transcriptional changes compared to the WT (WPP14). Out of 4,262 annotated genes, a total of 392 differentially expressed genes (DEGs) were identified (padj < 0.05) using featureCounts from the Subread package and differential expression analysis with DESeq2. The volcano plot (Figure.

6B) illustrates the gene expression changes in the gacS mutant compared to the WT (WPP14), highlighting a large number of significantly differentially expressed genes. A substantial number of genes were strongly downregulated (blue), particularly those involved in secretion systems, motility, and virulence-associated exoenzymes. In contrast, a smaller subset of genes was upregulated (red), primarily associated with stress response and nutrient transport. Hierarchical clustering analysis confirmed distinct expression patterns between WT (WPP14) and mutant replicates, demonstrating major virulence-associated genes clustering together in their downregulation patterns (Figure. 6A). Major virulence-associated pathways were significantly downregulated, aligning with the observed phenotypes. A significant reduction was observed in genes encoding secretion systems, particularly the Type VI Secretion System (T6SS) (*tssB*, *tssC*, *tssF*, *tssG*, *tssE*, *tssK*, *tagH*, *tssJ*, *tssA*, *tssM*, *tssI*), with $\log_2$FoldChanges ranging from -3.08 to -7.03. Additionally, genes encoding T6SS effectors (hcp family proteins) and the energy-providing ATPase tssH (clpV) were significantly repressed ($\log_2$FoldChange -3.93 to -4.67). The Type I Secretion System (T1SS) was also affected, with prtD and prtF downregulated ($\log_2$FoldChange -2.22 to -2.11), correlating with the observed reduction in protease activity (0.00 $cm^2$, $p \leq 0.05$). Similarly, Type II (T2SS) and Type III Secretion System (T3SS) components (*gspG*, *gspL*, *gspM*, *gspH*, *hrpA*, *hrpN*, *sctV*, *sctT*) exhibited strong repression ($\log_2$FoldChange -2.98 to -3.48), suggesting a broad defect in protein secretion.

The suppression of these secretion systems correlates with the loss of extracellular enzyme activity, particularly the downregulation of pectate lyase genes (*pelA*, *pelB*, *pelI*, *pelN*, *pelZ*, *pehA*, *pelY*) and cellulase (*celV*) ($\log_2$FoldChange -5.04 to -2.93), as well as protease genes, including *prtW* ($\log_2$FoldChange -5.35). Additionally, kdgM, which encodes an oligogalacturonate-specific porin involved in pectin degradation, was also downregulated ($\log_2$FoldChange -1.37). This further

supports the impaired ability of the gacS mutant to degrade plant cell wall components. These gene expression changes correspond with the observed decline in pectate lyase activity ($1.2 \pm 0.09$ cm², $p = 7.04E-06$) and reduced protease activity, further supporting the role of gacS in controlling exoenzyme production. The downregulation of multiple pectate lyase genes, such as kdgM and pelY, indicates that gacS, in addition to producing these enzymes, also transports degradation byproducts, potentially limiting the mutant's ability to utilize pectin-derived carbon sources effectively.

Motility-related genes were also significantly affected, including *fliC* (flagellin, $log_2$FoldChange -1.74), *fliA* (sigma factor, $log_2$FoldChange -0.83), and *fliZ* (flagellar biosynthesis regulator, $log_2$FoldChange -1.52). Chemotaxis-related genes ADT-0000941, *cheM*, ADT-0000983, and ADT-0000266 ($log_2$FoldChange -2.68 to -0.56) were also downregulated. These findings correlate with the motility assays, where M1 exhibited significantly reduced movement ($5.7 \pm 0.06$ cm², $p < 0.0001$).

Additionally, quorum sensing (QS) genes were downregulated, including *expR* ($log_2$FoldChange -2.2) and carI ($log_2$FoldChange -1.85), known to regulate extracellular enzyme production and virulence factor expression in Pectobacterium (Joshi et al., 2016). The suppression of QS genes likely contributed to the loss of protease and pectate lyase activity.

Interestingly, while virulence-associated pathways were suppressed, stress response genes were upregulated. The phage shock protein operon (pspABCG; $log_2$FoldChange +3.13 to +4.09) and the urea ABC transporter (ADT-0001692; $log_2$FoldChange +4.29) were significantly induced, suggesting increased envelope stress and altered nitrogen metabolism in response to the *gacS* mutation.

Finally, the hinT gene, encoding a purine-related enzyme, was downregulated ($log_2$FoldChange -0.57), particularly relevant due to its connection to purine metabolism and its potential link to purM, the disrupted gene in M2.

Overall, these findings highlight the significant role of gacS in regulating multiple virulence pathways, including secretion, motility, quorum sensing, and exoenzyme production, contributing to the significant reduction observed in tuber maceration and stem inoculation assays.***M2 (purM::Tn5) DEGs Analysis.*** RNA-seq analysis of the *purM*::Tn5 mutant revealed significant transcriptional changes compared to the WT (WPP14), affecting metabolic pathways, stress responses, and virulence-associated functions. A total of 558 differentially expressed genes (DEGs) were identified (padj < 0.05) out of 4,291 annotated genes, highlighting substantial transcriptional adjustments. Hierarchical clustering analysis (Figure. 7A) confirmed distinct expression patterns between WT (WPP14) and mutant replicates, clearly demonstrating differential expression across numerous genes. The volcano plot (Figure. 7B) illustrates the distribution of these DEGs, indicating a slightly higher number of significantly upregulated genes (red dots) compared to downregulated genes (blue dots), suggesting that disruption of *purM* results primarily in activation of several regulatory and metabolic pathways alongside suppression of specific virulence-related functions.

***purM::Tn5 Disrupts Purine Metabolism.*** The loss of *purM* resulted in strong downregulation of *purM* (-1.85 $log_2$FC) and *purN* (-1.26 $log_2$FC), key enzymes in the de novo purine biosynthesis pathway, confirming a metabolic bottleneck in nucleotide synthesis. Several upstream purine biosynthesis genes were upregulated, including *purB, purE, purF, purD, purH, purT,* and *purK* ($log_2$FC ranging from +0.55 to +1.54), possibly as a compensatory response to restore purine levels. Additionally, *purR* (+1.08 $log_2$FC), a key regulator of purine metabolism,

was induced, indicating an attempt to modulate nucleotide biosynthesis under purine-limiting conditions. In contrast, *apt* (-0.46 $log_2$FC), involved in purine salvage, was downregulated, suggesting further constraints on nucleotide recycling. The *puuE* gene (+0.89 $log_2$FC), linked to purine catabolism, was upregulated, possibly reflecting a metabolic shift toward alternative sources of nucleotides.

***purM::Tn5 Impairs Motility and Chemotaxis*.** M2 exhibited significant downregulation of genes involved in chemotaxis and flagellar function. Chemotaxis-related genes *cheA* (-0.36 $log_2$FC), ADT-0002771 (-0.48 $log_2$FC), ADT-0000266 (-0.56 $log_2$FC), ADT-0004277 (-1.28 $log_2$FC), and ADT-0003246 (-0.87 $log_2$FC) were downregulated, indicating reduced bacterial responsiveness to environmental stimuli. Additionally, key flagellar genes *fliD* (-0.77 $log_2$FC), *motA* (-0.37 $log_2$FC), and ADT-0001931 (-0.85 $log_2$FC) were downregulated, correlating with the reduced motility observed in phenotypic assays. Flagellar assembly and chemotaxis are crucial for bacterial movement, host colonization, and pathogenicity, so their repression suggests a significant motility impairment in M2.

***purM::Tn5 Suppresses Secretion Systems and Virulence-Associated Enzymes.*** Several genes involved in protein degradation and processing were downregulated, including *pepT* (HER17_RS11655 -0.92$log_2$FC, HER17_RS13310 -0.52 $log_2$FC), *sprT* (-1.08 $log_2$FC), and *map* (-0.41 $log_2$FC), suggesting a reduction in proteolytic activity. This reduction in protease secretion may explain the decrease in extracellular protease activity observed in M2, which could impact its ability to degrade host proteins and facilitate infection. The Type VI Secretion System (T6SS) was also significantly downregulated (HER17_RS04920 -2.35, and HER17_RS00310 -2.69 $log_2$FC). Since it plays a role in bacterial competition and virulence, its suppression may weaken M2's ability to interact with host cells and compete with microbial flora. Furthermore, multiple pectate

lyase genes required for plant cell wall degradation were downregulated, including *pnl* (-1.43 $log_2$FC), *pelB* (-1.48 $log_2$FC), and *pelN* (-0.71 $log_2$FC). These enzymes facilitate tissue maceration in plant hosts, and their downregulation likely contributes to the reduced pectate lyase activity and attenuated virulence of M2 in tuber maceration and stem inoculation assays.

***purM::Tn5 Triggers Envelope Stress and Alters Metabolism.*** Several envelope stress response genes were strongly upregulated, including *pspA* (+4.3 $log_2$FC) and *pspF* (+0.72 $log_2$FC). The Phage Shock Protein (Psp) system is activated under stress conditions to help maintain membrane integrity, suggesting that M2 experiences increased envelope stress, likely due to metabolic disruptions. In addition, *metC* (-0.72 $log_2$FC), a gene involved in methionine biosynthesis, was downregulated, which might have a role in sulfur metabolism. This is particularly relevant in relation to the M6 (*metA*::Tn5) mutant, which is directly linked to methionine biosynthesis. These results highlight the extensive metabolic disruption and adaptive stress responses triggered by *purM* disruption, affecting bacterial virulence and overall fitness.

***M6 (metA::Tn5) DEGs Analysis*.** RNA-seq analysis of *metA*::Tn5 mutant revealed distinct transcriptional profiles compared to WT (WPP14). Principal component analysis clearly separated mutant and WT replicates (PC1: 79% variance, PC2: 11% variance), indicating reproducible, though limited, transcriptional differences. Out of 4,181 analyzed genes, only 20 differentially expressed genes (DEGs, padj < 0.05) were identified, suggesting that the *metA* mutation elicits a targeted transcriptional response rather than widespread effects.

Hierarchical clustering analysis (Figure. 8A) supported these findings, clearly illustrating distinct gene expression profiles differentiating WT and M6 replicates. Consistent with these observations, the volcano plot (Figure. 8B) exhibited fewer significantly upregulated (red dots) and downregulated (blue dots) genes compared to other mutants studied. Notably, upregulated

genes included a hypothetical protein (ADT-0000849, +1.55 $log_2$FC) and a methyl-accepting chemotaxis protein (ADT-0003843, +1.17 $log_2$FC). Downregulated genes primarily encompassed metabolic functions, including glycine dehydrogenase (*gcvP*, -1.34 $log_2$FC), phosphopantetheine-binding protein (-2.89 $log_2$FC), and glycerol-3-phosphate dehydrogenase (*glpC*, -1.22 $log_2$FC) (Table 10). Overall, the focused transcriptional alterations observed in M6 highlight a specialized regulatory role for *metA*, particularly in central metabolism, rather than broad virulence-associated pathways.

***M8 (prtW::Tn5) DEGs Analysis.*** The RNA-seq analysis of the *prtW*::Tn5 mutant revealed substantial transcriptional alterations compared to the WT strain. Principal component analysis (PC1: 72% variance, PC2: 17% variance) demonstrated a clear separation between conditions. Out of 4,202 annotated genes, 59 DEGs were identified (padj < 0.05), indicating moderate yet distinct transcriptional changes. The hierarchical clustering heatmap (Figure. 9A) revealed two major expression clusters: one comprising downregulated virulence factors, including pectate lyase, flagellin, and protease-related genes, and another comprising upregulated metabolic genes, particularly involved in glutamine and glycerol transport systems. The volcano plot (Figure. 9B) highlighted key differentially expressed genes, including additional virulence-associated factors that were significantly downregulated, such as a Type VI Secretion System (T6SS) effector (ADT-0005888, -2.66 $log_2$FC), *pnl* (-1.96 $log_2$FC), and flagellin (-1.33 $log_2$FC), all critical for host infection and competitive interactions.

The suppression of pectate lyase genes, notably *pnl* (-1.96 $log_2$FC), likely contributes to the reduced pectate lyase activity observed in M8, impairing its ability to degrade plant cell walls and effectively macerate host tissues. Additionally, *exuT* (-3.46 $log_2$FC), encoding a major facilitator superfamily (MFS) transporter involved in galacturonate transport, was also strongly

downregulated. Its reduced expression indicates both impaired pectin degradation and decreased capacity to utilize pectin-derived sugars, contributing to the mutant's weakened virulence and impaired host colonization capabilities.

In contrast, upregulated genes included the glutamine transport system genes *glnP* (+1.36 $log_2$FC), *glnQ* (+1.34 $log_2$FC), and *glnH* (+1.22 $log_2$FC), suggesting a shift in nitrogen metabolism. Additionally, a methyl-accepting chemotaxis protein (HER17_RS12775, +2.53 $log_2$FC) was induced, potentially indicating adaptation to altered environmental sensing mechanisms. The glycerol metabolism pathway was also affected, with upregulation of glycerol-3-phosphate transporter *glpT* (+1.68 $log_2$FC) and glycerol-3-phosphate dehydrogenase *glpD* (+1.57 $log_2$FC), indicating a metabolic shift towards alternative carbon sources. Overall, the transcriptional profile of M8 suggests that *prtW* disruption impacts protease-mediated virulence functions while inducing metabolic adaptations potentially compensating for the loss of extracellular proteolytic activity.

**Shared Differentially Expressed Genes (DEGs) Among Multiple Mutants**

***M1 (gacS) and M2 (purM).*** RNA-seq analysis identified 117 differentially expressed genes (DEGs) shared between M1 and M2 mutants (Figure. 10A), suggesting overlapping regulatory disruptions resulting from *gacS* and *purM* mutations. Many of these transcriptional changes impact virulence-associated pathways, metabolic processes, and stress responses. Several genes involved in pectate degradation showed consistent downregulation, including *pelB* (-4.45 $log_2$FC in M1, -1.48 $log_2$FC in M2), *pelN* (-2.23 $log_2$FC in M1, -0.71 $log_2$FC in M2), and *pnl* (-3.11 $log_2$FC in M1, -1.43 $log_2$FC in M2), suggesting a reduction in pectate lyase activity, which may impair host tissue maceration. Additionally, the flagellar gene *fliC* was repressed in both mutants, indicating potential defects in motility. Similarly, the Type VI Secretion System (T6SS)

effectors (ADT-0005888) were significantly downregulated, potentially weakening bacterial competition and virulence.

In addition to virulence factors, shared metabolic alterations were observed. The MFS transporter *exuT* was strongly downregulated in both M1 (-3.72 $log_2$FC) and M2 (-2.92 $log_2$FC), suggesting an impaired ability to transport pectin-derived sugars, a key carbon source during plant infection. Several ABC transporter genes (ADT-0001694, ADT-0000532, ADT-0003722) were upregulated, possibly as compensatory mechanisms for disrupted metabolic pathways. Additionally, *hinT*, encoding a purine nucleoside phosphoramidase, was downregulated in both mutants, potentially affecting purine metabolism.

Both M1 and M2 also exhibited signs of envelope stress, as evidenced by the upregulation of the phage shock protein (Psp) system (*pspA, pspB, pspC, pspG*), indicating stress responses likely triggered by metabolic disruptions. Similarly, osmotic stress regulators (*osmB, betI*) were differentially expressed, suggesting adaptive responses to external stress conditions.

These shared transcriptional changes indicate that *gacS* and *purM* mutations result in overlapping deficiencies in virulence-related pathways, including pectate degradation, motility, and secretion systems, while also triggering metabolic adaptations and increased stress responses, highlighting their interconnected regulatory roles.

***M1 (gacS) and M6 (metA).*** RNA-seq analysis identified four DEGs shared between M1 and M6 mutants, involving chemotaxis, secondary metabolism, and uncharacterized functions. Notably, two methyl-accepting chemotaxis proteins (ADT-0000027 and ADT-0003843) were upregulated (M1: +0.78 and +1.25 $log_2$FC; M6: +0.51 and +1.17 $log_2$FC), indicating potential shifts in environmental sensing and motility regulation. Conversely, genes related to secondary

metabolism and unknown functions, such as ADT-0003365, encoding a phosphopantetheine-binding protein (M1: -3.57 $log_2$FC, M6: -2.89 $log_2$FC), and ADT-0003330, an uncharacterized protein, were downregulated. These shared DEGs suggest distinct but overlapping roles for *gacS* and *metA* in influencing chemotaxis and metabolic processes.

***M1 (gacS) and M8 (prtW).*** Several DEGs were identified between M1 and M8 mutants (Figure. 11A, B), highlighting potential functional overlap in virulence regulation and metabolic processes. Among the most significant changes, *prtW*, encoding a serralysin metalloprotease, was strongly downregulated in both mutants. Additionally, *inh*, a protease inhibitor of the Omp19 family, was repressed, potentially altering protease regulation and bacterial stress adaptation.

Flagellar motility was affected in both mutants, indicated by the downregulation of *fliC* (Figure. 11B), possibly contributing to reduced bacterial movement. Similarly, *exuT* was significantly suppressed, suggesting impaired uptake of pectin-derived sugars, consistent with reduced pectate lyase activity observed. Type VI Secretion System components (*hcp* and PAAR domain-containing protein) showed consistent downregulation, weakening bacterial competition.

Other shared DEGs included *oppA* and *aapJ*, consistently upregulated in M1 and M8, indicating metabolic shifts to alternative nutrient sources. Meanwhile, *cysK* and *ilvC* were downregulated, suggesting disruptions in sulfur and branched-chain amino acid metabolism.

***M2 (purM) and M6 (metA).*** Shared DEGs indicated disruptions in metabolic pathways, chemotaxis, and protease activity. Genes involved in chemotaxis (ADT-0003843) were upregulated (M2: +1.00 $log_2$FC; M6: +1.17 $log_2$FC), suggesting adaptive environmental responses. Genes related to amino acid metabolism (*ilvD*, *ilvA*, *ilvE*) and glycerol metabolism (*glpC*) were downregulated, alongside the glycine cleavage system (*gcvP*, *gcvT*) and nucleotide metabolism

(*udp*), highlighting significant metabolic alterations. The zinc-dependent metalloprotease (*sprT*) was similarly downregulated, potentially impairing protein turnover.

***M2 (purM) and M8 (prtW).*** The overlapping DEGs between M2 and M8 mutants (Figure. 11) suggest consistent disruptions in virulence-related pathways, particularly motility, protease activity, and pectin degradation. Key virulence-associated genes, such as *pnl*, *exuT*, and *fliC*, were significantly downregulated, potentially limiting their infection capabilities. Protease activity was also affected, with *sprT* downregulation indicating reduced proteolytic activity. T6SS components were consistently downregulated, weakening bacterial competition. Metabolic shifts included increased expression of glycerol metabolism genes (*glpT, glpD*) and amino acid transporters (*aapJ*), suggesting adaptations to alternative nutrients.

***All Mutants (M1, M2, M6, M8).*** Comprehensive comparisons across all mutants revealed both shared and unique transcriptional changes (Figure. 12A–C). Downregulated DEGs indicated consistent metabolic disruptions and reduced virulence-related functions (Figure. 12B), while upregulated genes reflected adaptive or compensatory responses due to pathway disruptions (Figure. 12C). For instance, methyl-accepting chemotaxis proteins and phosphopantetheine-binding proteins showed consistent differential expression across mutants, indicating shifts in bacterial motility regulation and secondary metabolism.

**Discussion**

This study examines how virulence is regulated in *Pectobacterium carotovorum* WPP14. Through differential gene expression analysis and phenotypic assays, we identified essential regulators and metabolic pathways controlling bacterial virulence and uncovered overlapping regulatory networks controlled by *gacS*, *purM*, and *prtW*. Our study reveals that PrtW functions

as a regulator, influencing multiple virulence-related pathways beyond protease degradation. By characterizing the mutants, we identified key genes involved in pectate lyase synthesis, protease production, bacterial motility, and overall plant pathogenicity. These findings provide new insights into the molecular mechanisms governing *P. carotovorum* pathogenesis.

The transcriptomic and phenotypic analyses of *P. carotovorum* WPP14 mutants highlight complex regulatory networks controlling protease production and virulence. The varying degrees of complementation success among mutants, particularly the incomplete restoration in M1 (*gacS*::Tn5), suggest intricate regulatory hierarchies. The partial restoration of phenotypes in M1comp suggests that *gacS* regulatory effects involve complex feedback loops that cannot be fully restored by expressing *gacS* on a plasmid. This observation aligns with previous studies demonstrating the role of the GacS/GacA system in coordinating multiple virulence pathways (Charkowski et al., 2012; Cui et al., 2001; Parkins et al., 2001).

The partial restoration of phenotypes in M1comp suggests that *gacS* regulation involves intricate feedback loops that cannot be fully restored by simply reintroducing the gene on a plasmid. *GacS* is a key sensor kinase in the *GacS/GacA* two-component system, which controls various virulence traits such as exoenzyme production, motility, and secretion systems. When *gacS* is disrupted, it affects multiple pathways simultaneously. However, plasmid-based expression does not completely reverse these effects, likely due to the complexity of its regulatory network.

A possible reason for this could be that GacS is part of a complex regulatory network that relies on specific signaling interactions. Reintroducing the gene alone might not be enough to fully restore its function if other key components remain unregulated. Additionally, factors like post-translational modifications or precise expression timing may be missing in the plasmid-based system, preventing complete recovery of its regulatory effects. Prior studies have shown that

GacS/GacA integrates environmental and metabolic signals to coordinate virulence, mainly through small regulatory RNAs (sRNAs) in the *rsm* pathway (Latour, 2020). However, our findings suggest that *gacS* in *P. carotovorum* also regulates additional pathways beyond the known RsmA mechanism, which could explain why M1comp does not fully restore wild-type virulence.

The GacS/GacA two-component system is a global regulator that controls diverse virulence factors, including extracellular enzymes, motility, quorum sensing, and type VI secretion. In *P. carotovorum*, GacS/GacA influences multiple regulatory networks, including the *rsm* pathway, which modulates the expression of pectate lyases, cellulases, and proteases (Charkowski et al., 2012; Cui et al., 2001). However, our study did not detect differential regulation of RsmA or other *rsm*-associated genes, suggesting that GacS may regulate virulence through multiple pathways. In particular, our findings reveal new regulatory interactions between GacS and genes involved in metabolic adaptation, stress response, and protein secretion systems. Notably, the downregulation of *kdgM* and *pel* genes in the *gacS* mutant suggests that GacS not only controls exoenzyme production but also influences the transport and utilization of pectin degradation products. These results expand current knowledge of GacS function in *P. carotovorum*, suggesting that its role in virulence extends beyond known *rsm*-mediated mechanisms.

The predominance of upregulated genes in M2 (*purM*::Tn5) highlights metabolic adaptations to purine biosynthesis disruption. The strong up-regulation of stress response genes and enhanced transport systems suggests the activation of compensatory mechanisms when purine metabolism is impaired. These results indicate that PurM is not only essential for nucleotide biosynthesis but also plays a broader role in bacterial function, including regulating virulence factor production. Similar observations have been reported previously, where mutations in purine biosynthesis genes reduced bacterial virulence (Lee, 2013). In addition, studies in related bacteria,

such as *Staphylococcus aureus*, have shown that de novo purine biosynthesis is crucial for intracellular growth and virulence phenotypes. Disruptions in purine metabolism can lead to metabolic changes and impact bacterial pathogenicity, highlighting the significance of purine biosynthesis pathways in bacterial metabolism and virulence (Allwood et al., 2011; Goncheva et al., 2020).

In *P. carotovorum*, pectate lyases are crucial for breaking down plant cell walls and enabling infection. Studies have shown that their expression is tightly regulated by multiple control systems, such as *kdgR*, *hexA*, and the *rsm* pathway. Our findings show significant downregulation of pectate lyase genes in multiple mutants, reinforcing the importance of these regulatory mechanisms in virulence control. The focused transcriptional response in M6 (*metA*::Tn5) suggests that *metA* primarily affects metabolic pathways rather than acting as a broad virulence regulator (Yu et al., 2023). The relatively mild virulence attenuation observed in M6, compared to M1 or M2, may be due to the limited number of differentially expressed genes with significant adjusted p-values. These patterns collectively reveal a hierarchical regulatory network where global regulators (GacS), metabolic pathways (PurM), and specific enzymes (MetA) contribute differentially to virulence regulation.

Our study also provides new insights into the regulatory role of PrtW. Inactivation of *prtW* led to differential expression of genes involved in motility, type VI secretion, and carbohydrate metabolism. Additionally, *prtW* inactivation resulted in the downregulation of *sprT*, a zinc-dependent metalloprotease, and *pnl*, a pectate lyase gene, further linking PrtW to protease activity and pectin degradation. These results support previous research on bacterial proteases while also expanding our understanding by revealing that *prtW* plays a broader regulatory role beyond a protease coding gene (Joshi et al., 2022). Joshi et al. (2022) further supports this regulatory role,

as their study demonstrated that protease inhibitors from *Solanum chacoense* suppressed multiple virulence traits in *P. carotovorum*, including reduced motility, decreased secretion of extracellular enzymes, and impaired infection capability. This was consistent with our findings. the absence of *prtW* resulted in significant transcriptional changes impacting key virulence-related pathways. These observations lend additional support to the concept that *prtW* role extends beyond protease activity, and it functions as a regulator that plays a wider role in *P. carotovorum's* pathogenic capabilities.

Identifying shared transcriptional patterns among mutants, particularly in stress response and metabolic pathways, suggests coordinated regulation of virulence factors. The consistent upregulation of stress response genes across mutants indicates that disruption of virulence pathways triggers compensatory mechanisms to maintain cellular homeostasis (Joly et al., 2010). The preservation of normal growth patterns despite significant virulence attenuation suggests that these mutations specifically target virulence pathways without compromising essential cellular functions (Eriksson et al., 1998; Marits et al., 1999). These findings expand our understanding of protease regulation in *P. carotovorum* WPP14 and identify several regulatory pathways that could be targeted for disease control strategies. The complex interplay between metabolic and regulatory networks revealed by this study provides new insights into bacterial adaptation and virulence regulation.

**Implications and Future Directions**

Our research highlights the essential roles of *gacS*, *purM*, *metA*, and *prtW* in modulating virulence and adaptive responses in *P. carotovorum* WPP14. Although each gene performs distinct functions, they also intersect within overlapping regulatory networks. Investigating these interactions provides deeper insights into the intricate molecular mechanisms underlying bacterial

pathogenicity and may offer novel strategies for managing soft rot disease. Future research should aim to elucidate the precise regulatory mechanisms by which these genes influence virulence factor expression and evaluate their viability as targets for disease control. Additionally, further functional characterization of the hypothetical proteins identified with significant adjusted p-values in our study could uncover previously unrecognized virulence determinants, potentially revealing new regulatory elements or components of critical pathways involved in bacterial virulence and adaptive responses.

***Table 2.*** *Initial Results: Comparison of WT and Mutant Means for Protease (t-test on transformed data), Pectate Lyase (Welch's ANOVA with Dunnett's Post-Hoc Test), and Motility (One-way ANOVA with Tukey's post-hoc test).*

| **WPP14 mutants** | **Protease activity** ($cm^2$) | | **Pectate lyase** ($cm^2$) | | **Motility** ($cm^2$) | |
|---|---|---|---|---|---|---|
| | mean±sd | p-value | mean±sd | p-value | mean±sd | p-value |
| **WT(WPP14)** | 0.85±0.08 | ≤ 0.05 | 1.7±0.08 | ≤ 0.05 | 19.0±1.02 | ≤ 0.05 |
| **M1** (*gacS*::Tn5) | 0.00 | 0.00002*** [1] | 1.2±0.09 | 7.04E-06*** | 5.7±0.06 | < 0.0001**** |
| **M2** (*purM*::Tn5) | 0.00 | 0.00002*** | 1.5±0.06 | 0.002** | 4.6±1.43 | < 0.0001**** |
| **M3** (*yeaR*::Tn5) | 1.22±0.07 | 0.01** [2] | 1.5±0.08 | 0.003** | 13.0±1.67 | 0.02* |
| **M4** (*lysR*::Tn5) | 1.13±0.04 | 0.02* | 1.4±0.12 | 0.004** | 10.8±2.32 | 0.0009*** |
| **M5** (*cysJ*::Tn5) | 0.00 | 0.00002*** | 1.5±0.22 | 0.1 (ns) | 6.8±2.24 | <0.0001**** |
| **M6** (*metA*::Tn5) | 0.00 | 0.00002*** | 1.6±0.27 | 0.2 **(ns)** [3] | 11.7±0.91 | 0.003** |
| **M7** (*prtW*::Tn5) | 0.00 | 0.00002*** | 1.5±0.15 | 0.04* | 11.4±2.52 | 0.002** |
| **M8** (*prtW*::Tn5) | 0.00 | 0.00002*** | 1.4±0.10 | 0.003** | 8.8±2.60 | < 0.0001*** |

[1] *p-value * = significantly decreased activity*
[2] *p-value * = significantly increased activity*
[3] *p-value (ns) = not significant*

***Table 3.*** *Initial tuber virulence results: Comparison of the WT mean with the mutants, analyzed by two-way ANOVA followed by Dunnett's post hoc test.*

| **WPP14 mutants** | **$10^8$** | | **$10^6$** | | **$10^4$** | |
|---|---|---|---|---|---|---|
| | Mean(gm)±sd | p-value | Mean(gm)±sd | p-value | Mean(gm)±sd | p-value |
| **WT(WPP14)** | 8.8±0.8 | ≤ 0.05 | 5.2±0.4 | ≤ 0.05 | 4.9±0.4 | ≤ 0.05 |
| **M1** *(gacS*::Tn5) | 1.7±0.2 | 5.E-14*** | 1.5±0.2 | 5.E-05 *** | 1.3±0.3 | 0.0001*** |
| **M2** *(purM*::Tn5) | 2.8±0.1 | 1.E-10*** | 2.7±0.3 | 0.01 * | 0.00 | 1.E-07*** |
| **M3** *(yeaR*::Tn5) | 7.8±0.3 | 0.7$^{(ns)}$ | 6.1±0.5 | 0.8$^{(ns)}$ | 4.3±0.6 | 0.9$^{(ns)}$ |
| **M4** *(lysR*::Tn5) | 8.2±0.4 | 0.9$^{(ns)}$ | 6.1±0.5 | 0.8$^{(ns)}$ | 4.3±0.5 | 0.9$^{(ns)}$ |
| **M5** *(cysJ*::Tn5) | 6.1±0.4 | 0.01** | 4.9±0.8 | 0.9$^{(ns)}$ | 2.5±0.5 | 0.02* |
| **M6** *(metA*::Tn5) | 5.8±0.4 | 0.002** | 7.8±1.4 | 0.01* | 2.1±0.3 | 0.004** |
| **M7** *(prtW*::Tn5) | 6.3±0.3 | 0.02* | 5.4±0.7 | 0.9$^{(ns)}$ | 5.3±0.5 | 0.9$^{(ns)}$ |
| **M8** *(prtW*::Tn5) | 6.3±0.4 | 0.02* | 5.2±0.4 | 0.9$^{(ns)}$ | 3.3±0.4 | 0.2$^{(ns)}$ |

***Table 4.*** *Results of replicated assays of WPP14 mutants and their complemented strains compared to the WT. One-way ANOVA was used to analyze the data followed by Tukey HSD test for all assays (protease activity, motility, and pectate lyase).*

| **WPP14 mutants** | **Protease activity** ($cm^2$) | | **Pectate lyase** ($cm^2$) | | **Motility** ($cm^2$) | |
|---|---|---|---|---|---|---|
| | mean±sd | p-value | mean±sd | p-value | mean±sd | p-value |
| **WT(WPP14)** | 0.93±0.04 | ≤ 0.05 | 2.15±0.13 | ≤ 0.05 | 23.4±0.9 | ≤ 0.05 |
| **M1(** *gacS*::Tn5) | 0.00 | 4.3e-15 **** | 1.32±0.14 | 0.00001**** | 7.11±1.41 | 1.E-12**** |
| **M2(***purM*::Tn5) | 0.23±0.004 | 1.8e-13 **** | 1.59±0.06 | 0.00001**** | 4.98±1.24 | 6.2E-14**** |
| **M6(***metA*::Tn5) | 0.34±0.02 | 9.8e-12 **** | 1.61±0.11 | 0.00001**** | 13.7±0.77 | 1.E-07**** |
| **M7(***prtW*::Tn5) | 0.00 | 4.3e-15 **** | 1.54±0.08 | 0.00004**** | 17.9±0.9 | 0.0001*** |
| **M8(***prtW*::Tn5) | 0.00 | 4.3e-15 **** | 1.46±0.08 | 0.00001**** | 12.7±1.10 | 2.E-08**** |
| **M1comp**(*gacS*::Tn5(pGacS)) | 0.69±0.12 | 4.0e-04** | 1.54±0.10 | 0.00004 **** | 27.7±2.85 | 0.7* |
| **M2comp**(*purM*::Tn5(pPurM)) | 1.07±0.09 | 0.02* | 2.06±0.17 | 1 (ns) | 31.2±2.62 | 2.E-04*** |
| **M6comp**(*metA*::Tn5(pMetA)) | 1.24±0.1 | 5.4e-06*** | 2.19±0.06 | 1 (ns) | 33.9±0.9 | 1.E-06*** |

***Table 5. Tuber virulence assay**: a comparison of the wild type (WT) mean with the mutants and their complements in tuber tissue decay using three different inoculum levels ($10^8$, $10^6$, and $10^4$ cfu/ml). The data were collected from three independent experiments and were analyzed using Welch's one-way ANOVA with the Games-Howell multiple comparisons test.*

| **WPP14 mutants** | **$10^8$** | | **$10^6$** | | **$10^4$** | |
|---|---|---|---|---|---|---|
| | mean(gm)±sd | p-value | mean(gm)±sd | p-value | mean(gm)±sd | p-value |
| **WT(WPP14)** | 7.6±0.7 | ≤ 0.05 | 5.4±0.4 | ≤ 0.05 | 3.7±0.6 | ≤ 0.05 |
| **M1(***gacS***::Tn5)** | 2.6±0.5 | <0.0001*** | 2.2±0.4 | 0.0004*** | 0.2±0.1 | 0.0005*** |
| **M2(***purM***::Tn5)** | 2.9±0.4 | <0.0001*** | 1.7±0.3 | <0.0001**** | 0.3±0.1 | 0.0007*** |
| **M6(***metA***::Tn5)** | 4.9±0.3 | 0.04* | 3.7±0.4 | 0.2(ns) | 1.0±0.3 | 0.01* |
| **M7(***prtW***::Tn5)** | 4.4±0.4 | 0.01* | 3.1±0.6 | 0.07(ns) | 1.2±0.3 | 0.01* |
| **M8(***prtW***::Tn5)** | 4.4±0.5 | 0.01* | 4.3±0.6 | 0.8(ns) | 1.4±0.4 | 0.04* |
| **M1comp**(*gacS*::Tn5(pGacS)) | 2.2±0.3 | <0.0001*** | 1.4±0.3 | <0.0001**** | 0.8±0.2 | 0.003** |
| **M2comp**(*purM*::Tn5(pPurM)) | 5.6±0.6 | 0.4(ns) | 3.3±0.4 | 0.04* | 2.2±0.5 | 0.5(ns) |
| **M6comp**(*metA*::Tn5(pMetA)) | 7.3±0.8 | 1(ns) | 4.8±0.7 | 1(ns) | 2.0±0.3 | 0.2(ns) |

**Table 6.** Stem Inoculation Lesion Length[4]

| **WPP14 mutants** | **Stem Inoculation (Lesion length – cm)** | |
|---|---|---|
| | mean±sd | p-value ≤ 0.05 |
| **WT(WPP14)** | 1.5±0.2 | |
| **M1(***gacS*::Tn5) | 0 | <0.0001 **** |
| **M2(***purM*::Tn5) | 0.04±0.04 | <0.0001 **** |
| **M6(***metA*::Tn5) | 0.06±0.06 | 0.00001 *** |
| **M7(***prtW*::Tn5) | 0.5±0.1 | 0.004 ** |
| **M8(***prtW*::Tn5) | 0.4±0.1 | 0.001 ** |
| **M1comp**(*gacS*::Tn5(pGacS)) | 0.8±0.2 | $0.2^{(ns)}$ |
| **M2comp**(*purM*::Tn5(pPurM)) | 0.7±0.2 | $0.08^{(ns)}$ |
| **M6comp**(*metA*::Tn5(pMetA)) | 0.9±0.2 | $1^{(ns)}$ |

[4] •Lesion length data from stem inoculation (average of three independent experiments).
•Five replicates per strain in each experiment (total of 15 replicates per strain).
•Measurements recorded upon appearance of the first lesion on WT-inoculated plants (usually after 1–2 days).
•Statistical analysis: Kruskal-Wallis followed by Dunn's post hoc test.

**Table 7.** Disease Progression Following Stem Inoculation[5]

| **WPP14 mutants** | **Stem Inoculation** | | | |
|---|---|---|---|---|
| | **Healthy** | **Diseased** | **Dead** | **p. adj** |
| **WT(WPP14)** | 0 | 1 | 14 | **+Ctrl** |
| **H2O** (-Ctrl) | 15 | 0 | 0 | 1.5E-07*** |
| **M1**(*gacS*::Tn5) | 15 | 0 | 0 | 1.5E-07*** |
| **M2**(*purM*::Tn5) | 11 | 0 | 4 | 6.E-04*** |
| **M6**(*metA*::Tn5) | 10 | 2 | 3 | 3.4E-04*** |
| **M7**(*prtW*::Tn5) | 6 | 2 | 7 | 0.1(ns) |
| **M8**(*prtW*::Tn5) | 8 | 5 | 2 | 1.1E-04*** |
| **M1comp** (*gacS*::Tn5(pGacS)) | 5 | 8 | 2 | 2.6E-04*** |
| **M2comp** (*purM*::Tn5(pPurM)) | 1 | 8 | 6 | 0.3(ns) |
| **M6comp** (*metA*::Tn5(pMetA)) | 3 | 5 | 7 | 7.7E-04*** |

[5] •Comparison of WT (positive control), water (negative control), and mutants to assess disease progression.
•Each strain had 5 replicates per experiment, with a total of 15 replicates per strain across three independent experiments.
•Observations started one day post-inoculation, continued daily, and ceased two days after no further changes were noted post the last observed change (death or symptoms).
•Statistical analysis conducted using Fisher's exact test (p-value ≤ 0.05).

**Table 8: M1 (*gacS*::Tn5)** Differentially Expressed Genes (DEGs). $log_2$FoldChange > 0 Upregulated, and $log_2$FoldChange < 0 Downregulated

| # | Locus Tag (NCBI) | $Log_2FC$ | padj | Gene Name | Affected Pathway |
|---|---|---|---|---|---|
| 1 | HER17_RS18115 | 0.84 | 3.30E-02 | ADT-0003375 | ABC transport |
| 2 | HER17_RS09900 | 1.07 | 4.90E-02 | ADT-0002843 | ABC transport |
| 3 | HER17_RS09895 | 1.25 | 6.00E-04 | ADT-0000532 | ABC transport |
| 4 | HER17_RS06755 | 1.59 | 1.60E-02 | ADT-0000785 | ABC transport |
| 5 | HER17_RS06765 | 1.61 | 5.70E-03 | ADT-0003039 | ABC transport |
| 6 | HER17_RS13925 | 2.22 | 1.10E-02 | ADT-0003722 | ABC transport |
| 7 | HER17_RS09190 | 4.14 | 1.10E-02 | ADT-0001694 | ABC transport |
| 8 | HER17_RS10175 | -3.57 | 2.30E-17 | ADT-0000543 | ABC transport |
| 9 | HER17_RS07625 | -2.42 | 1.80E-04 | ADT-0006294 | ABC transport |
| 10 | HER17_RS02510 | -1.25 | 8.00E-04 | ADT-0003159 | ABC transport |
| 11 | HER17_RS09320 | -1.16 | 2.60E-04 | ADT-0002823 | ABC transport |
| 12 | HER17_RS02515 | -1.14 | 3.20E-03 | ADT-0003160 | ABC transport |
| 13 | HER17_RS18040 | -5.02 | 2.10E-20 | budA | Acetoin biosynthesis |
| 14 | HER17_RS22070 | -2.23 | 2.80E-17 | hecA1 | Adhesion and virulence |
| 15 | HER17_RS06255 | -0.69 | 9.00E-03 | ADT-0001992 | Alcohol metabolism |
| 16 | HER17_RS06220 | -2.28 | 5.50E-04 | ADT-0004111 | Amide metabolism |
| 17 | HER17_RS01940 | -0.74 | 1.00E-03 | ADT-0001090 | Amino acid export |
| 18 | HER17_RS05620 | 1.78 | 1.20E-02 | ADT-0000851 | Amino acid export |
| 19 | HER17_RS18785 | -1.96 | 3.70E-13 | ADT-0005416 | Amino acid metabolism |
| 20 | HER17_RS09850 | -1.57 | 2.70E-03 | ADT-0003838 | Amino acid metabolism |
| 21 | HER17_RS13855 | 1.09 | 4.50E-02 | tdcB | Amino acid metabolism |
| 22 | HER17_RS20860 | 1.44 | 4.60E-02 | ycjG | Amino acid metabolism |
| 23 | HER17_RS07030 | 1.73 | 2.70E-02 | hisJ | Amino acid transport |
| 24 | HER17_RS20290 | 2.01 | 3.00E-03 | aapJ | Amino acid transport |
| 25 | HER17_RS03060 | 2.06 | 5.70E-04 | ADT-0002166 | Amino acid transport |
| 26 | HER17_RS15785 | 2.05 | 2.80E-02 | amtB | Ammonium transport |
| 27 | HER17_RS21585 | -2.55 | 2.60E-04 | asnA | Asparagine biosynthesis |
| 28 | HER17_RS16100 | -1.94 | 1.00E-04 | ansB1 | Asparagine metabolism |
| 29 | HER17_RS20265 | -1.11 | 6.30E-06 | ADT-0003458 | ATP-dependent processes |
| 30 | HER17_RS03930 | -2.06 | 9.00E-03 | ipdC | Auxin biosynthesis |
| 31 | HER17_RS05000 | -0.88 | 5.60E-03 | ADT-0002061 | Bacteriocin resistance |
| 32 | HER17_RS21760 | -1.18 | 1.00E-03 | ADT-0002302 | Biofilm formation |
| 33 | HER17_RS13450 | -0.92 | 4.80E-02 | bioC | Biotin biosynthesis |
| 34 | HER17_RS01100 | -1.06 | 8.10E-06 | ilvC | Branched-chain amino acid biosynthesis |
| 35 | HER17_RS18035 | -5.04 | 8.40E-19 | alsS | Butanediol metabolism |
| 36 | HER17_RS15665 | -1.29 | 5.20E-13 | ADT-0005485 | Carbohydrate binding |
| 37 | HER17_RS21210 | -3.88 | 2.20E-06 | ADT-0002334 | Carbohydrate binding and potential virulence |
| 38 | HER17_RS12570 | -0.71 | 4.10E-03 | ADT-0001885 | Carbohydrate metabolism |
| 39 | HER17_RS05085 | 0.71 | 2.50E-02 | yqaB | Carbohydrate metabolism |

| | | | | | |
|---|---|---|---|---|---|
| 40 | HER17_RS07390 | 0.94 | 2.90E-02 | ADT-0003027 | Carbohydrate metabolism |
| 41 | HER17_RS00555 | 1.53 | 3.70E-02 | otnC | Carbohydrate metabolism |
| 42 | HER17_RS17050 | 2.31 | 1.10E-02 | manD | Carbohydrate metabolism |
| 43 | HER17_RS08965 | 1.14 | 3.60E-02 | licT | Carbohydrate metabolism regulation |
| 44 | HER17_RS17380 | 1.46 | 1.20E-02 | ADT-0001409 | Carbohydrate transport |
| 45 | HER17_RS10350 | 1.74 | 2.40E-03 | ascF | Carbohydrate transport |
| 46 | HER17_RS06075 | 1.95 | 3.00E-02 | ADT-0001995 | Carbohydrate transport |
| 47 | HER17_RS19765 | 3.73 | 1.70E-02 | ADT-0000115 | Carbohydrate transport |
| 48 | HER17_RS20230 | -2.32 | 9.50E-27 | cah | Carbon dioxide metabolism |
| 49 | HER17_RS05535 | 0.46 | 3.80E-02 | can | Carbon dioxide metabolism |
| 50 | HER17_RS03180 | 0.89 | 1.20E-02 | ftsA | Cell division |
| 51 | HER17_RS01595 | 0.89 | 4.10E-02 | ADT-0003198 | Cell division |
| 52 | HER17_RS07490 | 2.27 | 3.70E-02 | ADT-0004066 | Cell wall biogenesis |
| 53 | HER17_RS16825 | -2.99 | 1.10E-07 | ADT-0001333 | Cell wall biosynthesis |
| 54 | HER17_RS18240 | -2.42 | 2.80E-02 | ADT-0003369 | Cell wall degradation |
| 55 | HER17_RS09620 | -1.86 | 2.30E-03 | ADT-0002424 | Cell wall degradation |
| 56 | HER17_RS12895 | -0.79 | 2.90E-02 | mepS | Cell wall metabolism |
| 57 | HER17_RS16635 | 0.61 | 4.30E-02 | mltC | Cell wall metabolism |
| 58 | HER17_RS06820 | -2.4 | 2.70E-09 | ADT-0004091 | Cell wall protection |
| 59 | HER17_RS20980 | -1.64 | 4.90E-13 | ADT-0001246 | Cell wall protection |
| 60 | HER17_RS01090 | -0.73 | 4.50E-04 | ADT-0002252 | Cell wall protection |
| 61 | HER17_RS09510 | -2.93 | 9.70E-08 | celV | Cellulose degradation |
| 62 | HER17_RS14035 | -2.68 | 1.50E-03 | ADT-0000941 | Chemotaxis |
| 63 | HER17_RS08535 | -2.07 | 1.10E-11 | cheM | Chemotaxis |
| 64 | HER17_RS03050 | -0.69 | 7.50E-03 | ADT-0000983 | Chemotaxis |
| 65 | HER17_RS16065 | -0.56 | 3.00E-02 | ADT-0000266 | Chemotaxis |
| 66 | HER17_RS21115 | 0.78 | 5.60E-03 | ADT-0000027 | Chemotaxis |
| 67 | HER17_RS09925 | 1.25 | 9.30E-05 | ADT-0003843 | Chemotaxis |
| 68 | HER17_RS03415 | -1.23 | 3.90E-02 | cutC | Choline metabolism |
| 69 | HER17_RS16730 | -2.35 | 1.40E-18 | ADT-0002484 | Chromosome partitioning |
| 70 | HER17_RS21745 | -0.94 | 1.90E-06 | ADT-0001200 | Cofactor biosynthesis |
| 71 | HER17_RS19590 | -2.69 | 7.50E-07 | cas2e | CRISPR-Cas system |
| 72 | HER17_RS19595 | -2.68 | 2.00E-05 | cas1e | CRISPR-Cas system |
| 73 | HER17_RS19600 | -2.31 | 3.10E-03 | cas6e | CRISPR-Cas system |
| 74 | HER17_RS19630 | -2.02 | 2.00E-05 | cas3 | CRISPR-Cas system |
| 75 | HER17_RS19610 | -2 | 6.30E-03 | cas7e | CRISPR-Cas system |
| 76 | HER17_RS19605 | -2 | 1.10E-02 | cas5e | CRISPR-Cas system |
| 77 | HER17_RS03560 | -1.71 | 3.20E-05 | cas6f | CRISPR-Cas system |
| 78 | HER17_RS19615 | -1.64 | 2.50E-02 | casB | CRISPR-Cas system |
| 79 | HER17_RS19620 | -1.48 | 4.30E-02 | casA | CRISPR-Cas system |
| 80 | HER17_RS03565 | -1.4 | 6.60E-04 | ADT-0003608 | CRISPR-Cas system |
| 81 | HER17_RS04225 | -0.71 | 8.20E-03 | ADT-0002087 | Cyclic di-GMP signaling |
| 82 | HER17_RS17170 | -1.86 | 4.40E-03 | cysK | Cysteine biosynthesis |

| | | | | | |
|---|---|---|---|---|---|
| 83 | HER17_RS15810 | 1.45 | 1.80E-02 | ADT-0001518 | Cysteine biosynthesis |
| 84 | HER17_RS19635 | -2.47 | 3.50E-10 | ADT-0001311 | Cytoskeleton |
| 85 | HER17_RS12540 | 0.64 | 1.30E-02 | deoR | Deoxyribonucleotide metabolism regulation |
| 86 | HER17_RS11040 | 0.49 | 2.10E-02 | hns | DNA organization |
| 87 | HER17_RS07345 | -0.77 | 1.50E-03 | ADT-0000752 | DNA recombination |
| 88 | HER17_RS18370 | -1.16 | 1.30E-03 | ADT-0003364 | DNA regulation |
| 89 | HER17_RS10530 | -0.98 | 2.70E-07 | ogt | DNA repair |
| 90 | HER17_RS03660 | 0.43 | 3.90E-02 | dnaB | DNA replication |
| 91 | HER17_RS04770 | 1.62 | 2.80E-02 | ADT-0005889 | DNA replication |
| 92 | HER17_RS19340 | -0.96 | 1.30E-03 | ADT-0003519 | DNA restriction |
| 93 | HER17_RS19335 | -0.84 | 4.80E-02 | ADT-0003518 | DNA restriction |
| 94 | HER17_RS08430 | -1.13 | 1.50E-04 | ADT-0000439 | DNA uptake and transformation |
| 95 | HER17_RS07655 | -3.63 | 1.50E-40 | ADT-0003765 | DNA/RNA metabolism |
| 96 | HER17_RS17200 | -0.83 | 5.80E-05 | ADT-0002545 | Efflux transport |
| 97 | HER17_RS17205 | -0.77 | 1.10E-03 | macB | Efflux transport |
| 98 | HER17_RS13155 | -1.29 | 2.80E-05 | ADT-0004004 | Electron transfer |
| 99 | HER17_RS09525 | 3.13 | 2.40E-02 | pspB | Envelope stress response |
| 100 | HER17_RS09530 | 3.31 | 8.40E-03 | pspC | Envelope stress response |
| 101 | HER17_RS03675 | 3.34 | 9.70E-03 | pspG | Envelope stress response |
| 102 | HER17_RS09520 | 4.09 | 2.40E-03 | pspA | Envelope stress response |
| 103 | HER17_RS20985 | -0.66 | 7.90E-03 | ADT-0003433 | Fatty acid metabolism |
| 104 | HER17_RS08355 | -0.66 | 1.50E-02 | fliA | Flagellar gene regulation |
| 105 | HER17_RS08035 | -1.74 | 7.10E-11 | fliC | Flagellar motility |
| 106 | HER17_RS08360 | -1.52 | 8.90E-07 | fliZ | Flagellar regulation |
| 107 | HER17_RS08890 | 0.56 | 3.20E-02 | apbE | Flavin metabolism |
| 108 | HER17_RS01025 | 1.96 | 2.40E-02 | ytfR | Galactofuranose transport |
| 109 | HER17_RS01030 | 1.97 | 9.00E-03 | ytfT | Galactofuranose transport |
| 110 | HER17_RS19915 | 0.78 | 1.60E-02 | gltD | Glutamate biosynthesis |
| 111 | HER17_RS16200 | -1.43 | 1.10E-04 | ADT-0000258 | Glutathione metabolism |
| 112 | HER17_RS13500 | -0.8 | 3.50E-03 | gsiC | Glutathione transport |
| 113 | HER17_RS13505 | -0.78 | 5.30E-03 | gsiB | Glutathione transport |
| 114 | HER17_RS13495 | -0.66 | 2.70E-02 | gsiD | Glutathione transport |
| 115 | HER17_RS11555 | 1.37 | 3.30E-03 | ugpB | Glycerol-3-phosphate transport |
| 116 | HER17_RS11550 | 0.94 | 2.70E-02 | ADT-0001821 | Glycerophospholipid metabolism |
| 117 | HER17_RS16790 | -1.81 | 2.90E-06 | ADT-0003329 | Glycosylation |
| 118 | HER17_RS16795 | -1.72 | 4.90E-06 | ADT-0001339 | Glycosylation |
| 119 | HER17_RS10150 | -3.48 | 1.30E-12 | ADT-0003861 | Hemolysin secretion and virulence |
| 120 | HER17_RS17060 | -1.67 | 3.80E-02 | ADT-0001438 | Hydrolase activity |
| 121 | HER17_RS19475 | 1.58 | 2.30E-02 | ADT-0001319 | Hydrolase activity |
| 122 | HER17_RS17750 | -0.94 | 7.10E-08 | yjcE | Ion transport and pH regulation |
| 123 | HER17_RS06760 | 1.43 | 5.40E-03 | ADT-0003038 | Iron transport |
| 124 | HER17_RS15015 | 2.54 | 1.50E-03 | ADT-0001560 | Iron transport |

| | | | | | |
|---|---|---|---|---|---|
| 125 | HER17_RS17785 | 0.53 | 1.60E-02 | lpxP | Lipid A biosynthesis |
| 126 | HER17_RS18630 | -0.89 | 8.60E-05 | ADT-0003351 | Lipid metabolism |
| 127 | HER17_RS16805 | -1.41 | 3.70E-03 | ADT-0001337 | LPS biosynthesis |
| 128 | HER17_RS20790 | 0.61 | 1.20E-02 | ADT-0003441 | LPS biosynthesis |
| 129 | HER17_RS06855 | -0.51 | 2.30E-02 | mlaA | Membrane lipid homeostasis |
| 130 | HER17_RS15610 | -1.02 | 7.20E-13 | ADT-0001532 | Membrane organization |
| 131 | HER17_RS15615 | -0.88 | 9.60E-05 | ADT-0001531 | Membrane organization |
| 132 | HER17_RS16820 | -2.02 | 1.30E-04 | ADT-0001334 | Membrane structure |
| 133 | HER17_RS04610 | -1.64 | 1.10E-06 | ADT-0004163 | Membrane structure |
| 134 | HER17_RS04605 | -1.53 | 9.70E-04 | ADT-0004164 | Membrane structure |
| 135 | HER17_RS12825 | -1.07 | 1.20E-05 | ADT-0001889 | Metabolism |
| 136 | HER17_RS10705 | -1 | 2.50E-03 | ydfG | Metabolism |
| 137 | HER17_RS10675 | -0.84 | 8.70E-05 | pptA | Metabolism |
| 138 | HER17_RS05360 | 1.11 | 2.80E-03 | ADT-0002053 | Methylation |
| 139 | HER17_RS06770 | 1.27 | 4.20E-03 | ADT-0000784 | Molybdate transport |
| 140 | HER17_RS09220 | -0.67 | 3.80E-02 | norM | Multidrug efflux |
| 141 | HER17_RS15515 | -0.65 | 1.60E-02 | HER17_RS15515 | NAD metabolism |
| 142 | HER17_RS12265 | -1.16 | 4.30E-03 | HER17_RS12265 | Nitrogen compound metabolism |
| 143 | HER17_RS16380 | -1.14 | 9.60E-05 | ADT-0001471 | Nitrogen compound metabolism |
| 144 | HER17_RS08995 | -1.5 | 3.50E-05 | nrfA | Nitrogen metabolism |
| 145 | HER17_RS09005 | -1.43 | 1.60E-02 | nrfC | Nitrogen metabolism |
| 146 | HER17_RS09000 | -1.42 | 1.40E-02 | nrfB | Nitrogen metabolism |
| 147 | HER17_RS09010 | -1.37 | 3.20E-02 | nrfD | Nitrogen metabolism |
| 148 | HER17_RS16980 | -1.57 | 5.70E-04 | ADT-0001445 | Nucleobase transport |
| 149 | HER17_RS03255 | 1.22 | 1.50E-03 | tsx | Nucleoside transport |
| 150 | HER17_RS14005 | -0.66 | 3.80E-02 | amn | Nucleotide metabolism |
| 151 | HER17_RS12535 | 1.18 | 5.50E-05 | deoC | Nucleotide metabolism |
| 152 | HER17_RS11025 | 0.73 | 1.00E-02 | oppA | Oligopeptide transport |
| 153 | HER17_RS08385 | 1.78 | 3.10E-02 | betI | Osmotic stress response |
| 154 | HER17_RS09400 | 2.44 | 1.60E-02 | osmB | Osmotic stress response |
| 155 | HER17_RS09860 | -2.71 | 4.10E-06 | ADT-0003840 | Oxidation-reduction processes |
| 156 | HER17_RS09865 | -2.48 | 5.60E-06 | ADT-0003841 | Oxidation-reduction processes |
| 157 | HER17_RS09845 | -2.11 | 4.90E-04 | ADT-0003837 | Oxidation-reduction processes |
| 158 | HER17_RS08605 | -1.2 | 7.00E-03 | ADT-0000449 | Oxidation-reduction processes |
| 159 | HER17_RS16440 | 0.81 | 1.50E-03 | ADT-0001464 | Oxidation-reduction processes |
| 160 | HER17_RS03670 | 1.2 | 1.40E-02 | ADT-0002596 | Oxidation-reduction processes |
| 161 | HER17_RS09580 | -1.08 | 6.40E-04 | tpx | Oxidative stress response |
| 162 | HER17_RS01900 | -5.04 | 4.70E-46 | pelA | Pectate degradation and virulence |
| 163 | HER17_RS01895 | -4.45 | 1.60E-52 | pelB | Pectate degradation and virulence |
| 164 | HER17_RS10130 | -3.5 | 4.90E-09 | hrpW | Pectate degradation and virulence (T3SS) |
| 165 | HER17_RS16135 | -3.26 | 1.60E-16 | pelI | Pectate degradation and virulence |
| 166 | HER17_RS14235 | -3.11 | 3.20E-16 | pnl | Pectate degradation and virulence |

| | | | | | |
|---|---|---|---|---|---|
| 167 | HER17_RS12080 | -2.23 | 4.40E-08 | pelN | Pectate degradation and virulence |
| 168 | HER17_RS01890 | -2.19 | 3.50E-03 | pelC | Pectate degradation and virulence |
| 169 | HER17_RS01885 | -1.84 | 4.50E-08 | pelZ | Pectate degradation and virulence |
| 170 | HER17_RS10180 | -1.37 | 3.20E-05 | pelY | Pectate degradation and virulence |
| 171 | HER17_RS10185 | -1.37 | 7.10E-03 | KdgM | Pectin degradation |
| 172 | HER17_RS16130 | -3.1 | 1.10E-11 | pehA | Pectin degradation and virulence |
| 173 | HER17_RS13175 | -3.19 | 1.50E-12 | ADT-0002133 | Phage-related functions |
| 174 | HER17_RS13165 | -3.17 | 4.00E-39 | ADT-0002134 | Phage-related functions |
| 175 | HER17_RS13150 | -3.1 | 8.70E-15 | ADT-0004003 | Phage-related functions |
| 176 | HER17_RS22080 | -3.09 | 9.00E-18 | No hits | Phage-related functions |
| 177 | HER17_RS13160 | -3.09 | 4.40E-24 | ADT-0002135 | Phage-related functions |
| 178 | HER17_RS13115 | -1.79 | 2.10E-04 | ADT-0002137 | Phage-related functions |
| 179 | HER17_RS13110 | -1.5 | 3.30E-04 | ADT-0003999 | Phage-related functions |
| 180 | HER17_RS21925 | -1.48 | 1.00E-09 | ADT-0003997 | Phage-related functions |
| 181 | HER17_RS13140 | -1.35 | 2.70E-08 | ADT-0002136 | Phage-related functions |
| 182 | HER17_RS13100 | -1.17 | 1.10E-08 | ADT-0003997 | Phage-related functions |
| 183 | HER17_RS13105 | -1.17 | 4.20E-04 | ADT-0003998 | Phage-related functions |
| 184 | HER17_RS07290 | -0.93 | 4.30E-02 | ADT-0001867 | Phage-related functions |
| 185 | HER17_RS18535 | 1.61 | 1.00E-02 | ADT-0006169 | Phage-related functions |
| 186 | HER17_RS20250 | 2.02 | 7.40E-04 | NF033153 | Phage-related functions |
| 187 | HER17_RS18540 | 2.13 | 9.20E-03 | ADT-0006232 | Phage-related functions |
| 188 | HER17_RS20245 | 2.18 | 1.40E-02 | ADT-0003456 | Phage-related functions |
| 189 | HER17_RS18530 | 2.39 | 2.50E-02 | gpM | Phage-related functions |
| 190 | HER17_RS05250 | 2.7 | 4.30E-02 | ADT-0006232 | Phage-related functions |
| 191 | HER17_RS13945 | 0.74 | 3.40E-02 | cdh | Phospholipid metabolism |
| 192 | HER17_RS10095 | -3.1 | 5.00E-11 | hrpN | Plant cell wall interaction and virulence |
| 193 | HER17_RS16810 | -1.17 | 1.10E-03 | ADT-0001336 | Polysaccharide biosynthesis |
| 194 | HER17_RS16815 | -2.13 | 1.00E-02 | ADT-0001335 | Polysaccharide biosynthesis and export |
| 195 | HER17_RS13470 | -2.26 | 1.00E-06 | celB | Polysaccharide degradation |
| 196 | HER17_RS13220 | -2.4 | 8.50E-27 | inh | Protease inhibition |
| 197 | HER17_RS02675 | -1.44 | 6.80E-10 | yggG | Protein degradation |
| 198 | HER17_RS06740 | -1.28 | 1.50E-04 | outO | Protein degradation |
| 199 | HER17_RS09570 | -1 | 4.40E-03 | ADT-0000521 | Protein degradation |
| 200 | HER17_RS20740 | -0.39 | 2.00E-02 | secB | Protein export |
| 201 | HER17_RS01975 | -0.5 | 4.90E-03 | fkpA | Protein folding |
| 202 | HER17_RS03235 | 1.21 | 9.00E-03 | hofC | Protein transport |
| 203 | HER17_RS04915 | -3.35 | 2.20E-12 | ADT-0000876 | Protein-protein interactions |
| 204 | HER17_RS04935 | -1.55 | 6.20E-07 | ADT-0002064 | Protein-protein interactions |
| 205 | HER17_RS13225 | -5.35 | 2.60E-52 | prtW | Proteolysis and virulence |
| 206 | HER17_RS08705 | -0.57 | 4.60E-02 | hinT | Purine metabolism |
| 207 | HER17_RS21045 | -2.2 | 5.40E-16 | expR | Quorum sensing |

| | | | | | |
|---|---|---|---|---|---|
| 208 | HER17_RS21050 | -1.85 | 1.50E-06 | carI | Quorum sensing |
| 209 | HER17_RS20960 | -1.04 | 1.10E-04 | ADT-0003431 | Quorum sensing |
| 210 | HER17_RS05495 | 2.5 | 2.90E-02 | nrdH | Redox homeostasis |
| 211 | HER17_RS11075 | 1.68 | 2.90E-03 | No hits | RNA regulation |
| 212 | HER17_RS08895 | 2.25 | 1.00E-02 | rprA | RNA regulation |
| 213 | HER17_RS14835 | 2.9 | 1.20E-02 | No seq | RNA regulation |
| 214 | HER17_RS18265 | -3.57 | 2.10E-05 | ADT-0003365 | Secondary metabolism |
| 215 | HER17_RS04990 | -2.34 | 1.40E-13 | pvcA | Secondary metabolism |
| 216 | HER17_RS18275 | -1.35 | 8.80E-03 | ADT-0002501 | Secondary metabolism |
| 217 | HER17_RS10005 | -2.96 | 4.70E-06 | ADT-0002852 | Signal transduction |
| 218 | HER17_RS03820 | -2.55 | 2.00E-06 | ADT-0002112 | Signal transduction |
| 219 | HER17_RS16975 | -1.63 | 9.90E-06 | ADT-0001446 | Signal transduction |
| 220 | HER17_RS13380 | -1.18 | 2.80E-06 | ADT-0001918 | Stress response |
| 221 | HER17_RS10520 | -1.13 | 9.60E-05 | uspE | Stress response |
| 222 | HER17_RS07685 | -1.27 | 3.40E-06 | iraP | Stress response regulation |
| 223 | HER17_RS14510 | -0.42 | 4.10E-02 | galF | Sugar nucleotide biosynthesis |
| 224 | HER17_RS19290 | 1.04 | 2.00E-04 | ADT-0002449 | Sulfate transport |
| 225 | HER17_RS09855 | -1.98 | 4.30E-04 | ADT-0003839 | Sulfur metabolism |
| 226 | HER17_RS04245 | -0.93 | 7.80E-03 | cysH | Sulfur metabolism |
| 227 | HER17_RS04240 | -0.8 | 2.80E-02 | cysI | Sulfur metabolism |
| 228 | HER17_RS10870 | -0.89 | 8.40E-03 | cysB | Sulfur metabolism regulation |
| 229 | HER17_RS11610 | -0.63 | 2.70E-02 | icd | TCA cycle |
| 230 | HER17_RS20405 | 0.81 | 2.00E-03 | thiH | Thiamine biosynthesis |
| 231 | HER17_RS19625 | -1.67 | 3.90E-04 | ADT-0005961 | Toxin-antitoxin system |
| 232 | HER17_RS04890 | -4.67 | 4.00E-28 | ADT-0003094 | Transcriptional regulation |
| 233 | HER17_RS09270 | -2.37 | 8.60E-06 | slyA | Transcriptional regulation |
| 234 | HER17_RS11585 | -1 | 1.70E-04 | ADT-0002905 | Transcriptional regulation |
| 235 | HER17_RS02670 | -0.83 | 6.00E-04 | ADT-0002189 | Transcriptional regulation |
| 236 | HER17_RS04830 | -0.76 | 7.10E-03 | ADT-0004156 | Transcriptional regulation |
| 237 | HER17_RS00085 | -0.73 | 1.30E-02 | ADT-0001195 | Transcriptional regulation |
| 238 | HER17_RS03335 | 0.67 | 2.50E-02 | ADT-0000969 | Transcriptional regulation |
| 239 | HER17_RS18375 | 1.07 | 6.00E-03 | No seq | Transcriptional regulation |
| 240 | HER17_RS07120 | 1.2 | 1.50E-04 | lrhA | Transcriptional regulation |
| 241 | HER17_RS20900 | 1.71 | 4.60E-02 | ADT-0000036 | Transcriptional regulation |
| 242 | HER17_RS19760 | 2.27 | 5.00E-02 | ADT-0000116 | Transcriptional regulation |
| 243 | HER17_RS09175 | 2.34 | 1.90E-02 | ADT-0001691 | Transcriptional regulation |
| 244 | HER17_RS03870 | -1.01 | 4.30E-03 | prfH | Translation termination |
| 245 | HER17_RS18720 | -3.72 | 4.00E-07 | ADT-0000166 | Transmembrane transport |
| 246 | HER17_RS08750 | 2.19 | 1.30E-03 | ADT-0005548 | Transmembrane transport |
| 247 | HER17_RS08745 | 2.2 | 4.50E-03 | ADT-0001665 | Transmembrane transport |
| 248 | HER17_RS11560 | 3.23 | 4.00E-09 | ADT-0001822 | Transmembrane transport |
| 249 | HER17_RS12340 | -0.68 | 1.80E-02 | serS | tRNA aminoacylation |
| 250 | HER17_RS18225 | -0.88 | 1.60E-02 | No seq | tRNA processing |

| | | | | | |
|---|---|---|---|---|---|
| 251 | HER17_RS04105 | -1.14 | 8.20E-03 | barA | Two-component signal transduction |
| 252 | HER17_RS13215 | -2.22 | 1.50E-13 | prtD | Type I secretion system (T1SS) |
| 253 | HER17_RS13205 | -2.11 | 1.30E-15 | prtF | Type I secretion system (T1SS) |
| 254 | HER17_RS13210 | -1.96 | 4.40E-10 | ADT-0005642 | Type I secretion system (T1SS) |
| 255 | HER17_RS02520 | -1.3 | 1.50E-03 | ADT-0003162 | Type I secretion system (T1SS) |
| 256 | HER17_RS06700 | -3.18 | 3.80E-08 | gspG | Type II secretion system (T2SS) |
| 257 | HER17_RS06725 | -3.13 | 9.60E-22 | gspL | Type II secretion system (T2SS) |
| 258 | HER17_RS06730 | -2.98 | 6.30E-13 | gspM | Type II secretion system (T2SS) |
| 259 | HER17_RS06705 | -2.93 | 6.80E-10 | gspH | Type II secretion system (T2SS) |
| 260 | HER17_RS06710 | -2.85 | 7.20E-09 | gspI | Type II secretion system (T2SS) |
| 261 | HER17_RS06695 | -2.49 | 5.10E-07 | gspF | Type II secretion system (T2SS) |
| 262 | HER17_RS06715 | -2.38 | 7.60E-08 | gspJ | Type II secretion system (T2SS) |
| 263 | HER17_RS06735 | -2.3 | 2.30E-08 | outN | Type II secretion system (T2SS) |
| 264 | HER17_RS06690 | -2.16 | 3.30E-05 | gspE | Type II secretion system (T2SS) |
| 265 | HER17_RS06720 | -2.16 | 1.60E-06 | gspK | Type II secretion system (T2SS) |
| 266 | HER17_RS06685 | -1.82 | 2.20E-03 | gspD | Type II secretion system (T2SS) |
| 267 | HER17_RS06665 | -1.36 | 4.20E-06 | gspB | Type II secretion system (T2SS) |
| 268 | HER17_RS06660 | -1.31 | 2.10E-09 | gspS | Type II secretion system (T2SS) |
| 269 | HER17_RS09990 | -3.08 | 7.40E-05 | hrpP | Type III secretion system (T3SS) |
| 270 | HER17_RS10045 | -2.94 | 8.00E-08 | hrpA | Type III secretion system (T3SS) |
| 271 | HER17_RS09970 | -2.82 | 1.60E-02 | sctT | Type III secretion system (T3SS) |
| 272 | HER17_RS09995 | -2.67 | 2.00E-03 | hrpO | Type III secretion system (T3SS) |
| 273 | HER17_RS10070 | -2.44 | 1.10E-02 | hrpF | Type III secretion system (T3SS) |
| 274 | HER17_RS10140 | -2.17 | 2.30E-06 | ADT-0001742 | Type III secretion system (T3SS) |
| 275 | HER17_RS10010 | -2.15 | 3.20E-04 | sctV | Type III secretion system (T3SS) |
| 276 | HER17_RS09985 | -2.01 | 4.20E-05 | sctQ | Type III secretion system (T3SS) |
| 277 | HER17_RS10195 | -1.94 | 1.80E-05 | ADT-0002735 | Type III secretion system (T3SS) |
| 278 | HER17_RS10055 | -1.82 | 1.20E-03 | sctJ | Type III secretion system (T3SS) |
| 279 | HER17_RS09980 | -1.78 | 1.40E-02 | sctR | Type III secretion system (T3SS) |
| 280 | HER17_RS10050 | -1.58 | 4.40E-03 | hrpB | Type III secretion system (T3SS) |
| 281 | HER17_RS10000 | -1.57 | 7.70E-03 | sctN | Type III secretion system (T3SS) |
| 282 | HER17_RS10135 | -3.22 | 8.70E-07 | ADT-0005575 | Type III secretion system (T3SS) effector |
| 283 | HER17_RS10015 | -3.48 | 3.10E-10 | sctW | Type III secretion system (T3SS) regulation |
| 284 | HER17_RS04880 | -5.19 | 4.00E-26 | icmH | Type IVB secretion system |
| 285 | HER17_RS04840 | -7.03 | 1.40E-49 | tssB | Type VI secretion system (T6SS) |
| 286 | HER17_RS04845 | -6.78 | 3.00E-51 | tssC | Type VI secretion system (T6SS) |
| 287 | HER17_RS04855 | -6.26 | 1.20E-47 | tssF | Type VI secretion system (T6SS) |
| 288 | HER17_RS04860 | -6.1 | 5.90E-29 | tssG | Type VI secretion system (T6SS) |
| 289 | HER17_RS04900 | -4.42 | 1.80E-31 | tssA | Type VI secretion system (T6SS) |
| 290 | HER17_RS04895 | -3.65 | 2.10E-14 | vasI | Type VI secretion system (T6SS) |
| 291 | HER17_RS04910 | -3.55 | 2.30E-17 | ADT-0005808 | Type VI secretion system (T6SS) |

| | | | | | |
|---|---|---|---|---|---|
| 292 | HER17_RS04905 | -3.27 | 3.20E-12 | tssM | Type VI secretion system (T6SS) |
| 293 | HER17_RS00305 | -3.08 | 1.10E-09 | tssI | Type VI secretion system (T6SS) |
| 294 | HER17_RS04925 | -2.93 | 2.20E-13 | ADT-0005804 | Type VI secretion system (T6SS) |
| 295 | HER17_RS04595 | -2.25 | 1.90E-09 | ADT-0005804 | Type VI secretion system (T6SS) |
| 296 | HER17_RS13440 | -2.11 | 1.40E-09 | ADT-0003690 | Type VI secretion system (T6SS) |
| 297 | HER17_RS10120 | -1.94 | 8.90E-07 | No seq | Type VI secretion system (T6SS) |
| 298 | HER17_RS20720 | -1.83 | 5.80E-07 | ADT-0000046 | Type VI secretion system (T6SS) |
| 299 | HER17_RS04620 | -1.38 | 5.00E-04 | ADT-0005815 | Type VI secretion system (T6SS) |
| 300 | HER17_RS20135 | -1.36 | 2.40E-10 | ADT-0005385 | Type VI secretion system (T6SS) |
| 301 | HER17_RS04930 | -1.35 | 8.90E-04 | ADT-0004153 | Type VI secretion system (T6SS) |
| 302 | HER17_RS04850 | -5.66 | 1.90E-34 | tssE | Type VI secretion system (T6SS) baseplate assembly |
| 303 | HER17_RS04875 | -5.63 | 1.20E-23 | tssK | Type VI secretion system (T6SS) baseplate assembly |
| 304 | HER17_RS00310 | -5.82 | 6.70E-14 | ADT-0005888 | Type VI secretion system (T6SS) effector delivery |
| 305 | HER17_RS04920 | -4.67 | 6.90E-18 | ADT-0005888 | Type VI secretion system (T6SS) effector delivery |
| 306 | HER17_RS07650 | -4.1 | 5.10E-26 | ADT-0005385 | Type VI secretion system (T6SS) effector delivery |
| 307 | HER17_RS16205 | -3.93 | 6.90E-24 | ADT-0000257 | Type VI secretion system (T6SS) effector delivery |
| 308 | HER17_RS18020 | -3.27 | 1.20E-11 | ADT-0000146 | Type VI secretion system (T6SS) effector delivery |
| 309 | HER17_RS04885 | -4.83 | 2.50E-32 | tssH (clpV) | Type VI secretion system (T6SS) energy provision |
| 310 | HER17_RS04870 | -5.97 | 2.50E-30 | tssJ | Type VI secretion system (T6SS) membrane complex |
| 311 | HER17_RS04865 | -6 | 1.10E-38 | tagH | Type VI secretion system (T6SS) regulation |
| 312 | HER17_RS02535 | -5.16 | 3.70E-19 | ADT-0004237 | Unknown |
| 313 | HER17_RS18270 | -3.47 | 1.10E-05 | ADT-0002500 | Unknown |
| 314 | HER17_RS13170 | -3.08 | 5.40E-14 | ADT-0001904 | Unknown |
| 315 | HER17_RS18030 | -3.02 | 8.50E-27 | ADT-0003381 | Unknown |
| 316 | HER17_RS02530 | -3.02 | 4.00E-09 | ADT-0004236 | Unknown |
| 317 | HER17_RS16835 | -2.95 | 5.00E-04 | ADT-0003330 | Unknown |
| 318 | HER17_RS19130 | -2.85 | 5.00E-08 | ADT-0002434 | Unknown |
| 319 | HER17_RS18025 | -2.81 | 1.10E-09 | ADT-0003380 | Unknown |
| 320 | HER17_RS18255 | -2.78 | 8.40E-03 | ADT-0003367 | Unknown |
| 321 | HER17_RS07630 | -2.68 | 1.50E-06 | ADT-0004373 | Unknown |
| 322 | HER17_RS07660 | -2.62 | 6.10E-08 | ADT-0003766 | Unknown |
| 323 | HER17_RS06445 | -2.48 | 2.20E-13 | ADT-0003046 | Unknown |
| 324 | HER17_RS04940 | -2.48 | 3.80E-06 | ADT-0002063 | Unknown |
| 325 | HER17_RS07620 | -2.45 | 3.80E-04 | ADT-0004372 | Unknown |
| 326 | HER17_RS05275 | -2.38 | 1.10E-08 | ADT-0003319 | Unknown |

| | | | | | |
|---|---|---|---|---|---|
| 327 | HER17_RS07645 | -2.33 | 2.70E-15 | ADT-0005861 | Unknown |
| 328 | HER17_RS06815 | -2.2 | 3.50E-09 | ADT-0004090 | Unknown |
| 329 | HER17_RS04815 | -2.17 | 1.00E-11 | ADT-0004387 | Unknown |
| 330 | HER17_RS09610 | -2.15 | 3.70E-06 | ADT-0003493 | Unknown |
| 331 | HER17_RS03860 | -2.1 | 7.20E-11 | ADT-0002608 | Unknown |
| 332 | HER17_RS03590 | -2.06 | 1.00E-08 | ADT-0000949 | Unknown |
| 333 | HER17_RS03865 | -2.06 | 2.90E-07 | ADT-0002609 | Unknown |
| 334 | HER17_RS16215 | -2.04 | 7.70E-08 | ADT-0003583 | Unknown |
| 335 | HER17_RS04600 | -2.04 | 6.20E-10 | ADT-0002239 | Unknown |
| 336 | HER17_RS13435 | -2.01 | 4.00E-08 | ADT-0003689 | Unknown |
| 337 | HER17_RS06825 | -2 | 9.30E-05 | ADT-0004092 | Unknown |
| 338 | HER17_RS13560 | -1.99 | 1.30E-04 | ADT-0003769 | Unknown |
| 339 | HER17_RS00300 | -1.94 | 3.50E-02 | ADT-0002998 | Unknown |
| 340 | HER17_RS10125 | -1.84 | 2.60E-04 | ADT-0000542 | Unknown |
| 341 | HER17_RS06450 | -1.8 | 1.70E-09 | ADT-0004101 | Unknown |
| 342 | HER17_RS20715 | -1.79 | 4.10E-07 | No seq | Unknown |
| 343 | HER17_RS21770 | -1.78 | 6.10E-06 | ADT-0002300 | Unknown |
| 344 | HER17_RS19135 | -1.72 | 2.90E-02 | ADT-0002435 | Unknown |
| 345 | HER17_RS10680 | -1.69 | 2.00E-02 | ADT-0003874 | Unknown |
| 346 | HER17_RS07815 | -1.65 | 1.70E-06 | ADT-0004382 | Unknown |
| 347 | HER17_RS03600 | -1.59 | 7.50E-03 | ADT-0002592 | Unknown |
| 348 | HER17_RS05690 | -1.55 | 4.30E-02 | ADT-0000847 | Unknown |
| 349 | HER17_RS04615 | -1.54 | 1.10E-06 | ADT-0004162 | Unknown |
| 350 | HER17_RS04825 | -1.54 | 1.30E-04 | ADT-0004155 | Unknown |
| 351 | HER17_RS05270 | -1.5 | 1.50E-03 | ADT-0006185 | Unknown |
| 352 | HER17_RS10105 | -1.5 | 3.50E-02 | ADT-0001740 | Unknown |
| 353 | HER17_RS07930 | -1.43 | 6.50E-05 | ADT-0005537 | Unknown |
| 354 | HER17_RS17520 | -1.39 | 1.00E-03 | ADT-0003400 | Unknown |
| 355 | HER17_RS21765 | -1.35 | 4.50E-05 | ADT-0002301 | Unknown |
| 356 | HER17_RS20125 | -1.32 | 6.20E-10 | ADT-0002390 | Unknown |
| 357 | HER17_RS12970 | -1.28 | 2.70E-02 | ADT-0000716 | Unknown |
| 358 | HER17_RS19195 | -1.26 | 3.00E-02 | ADT-0001326 | Unknown |
| 359 | HER17_RS16210 | -1.24 | 8.50E-04 | ADT-0002573 | Unknown |
| 360 | HER17_RS04945 | -1.21 | 1.90E-02 | ADT-0002062 | Unknown |
| 361 | HER17_RS13705 | -1.15 | 4.60E-03 | ADT-0003725 | Unknown |
| 362 | HER17_RS22060 | -1.14 | 4.70E-02 | ADT-0004110 | Unknown |
| 363 | HER17_RS17515 | -1.13 | 3.10E-02 | ADT-0003399 | Unknown |
| 364 | HER17_RS00585 | -1.08 | 4.40E-04 | ADT-0002276 | Unknown |
| 365 | HER17_RS05030 | -1.05 | 4.70E-02 | ADT-0003088 | Unknown |
| 366 | HER17_RS10110 | -1.05 | 8.20E-03 | ADT-0001741 | Unknown |
| 367 | HER17_RS11600 | -1.02 | 3.10E-04 | ADT-0003910 | Unknown |
| 368 | HER17_RS10115 | -0.99 | 5.10E-03 | No hits | Unknown |
| 369 | HER17_RS19570 | -0.98 | 4.30E-02 | ADT-0005397 | Unknown |

| | | | | | |
|---|---|---|---|---|---|
| 370 | HER17_RS04060 | -0.97 | 1.60E-05 | ADT-0002654 | Unknown |
| 371 | HER17_RS20955 | -0.95 | 1.20E-02 | No seq | Unknown |
| 372 | HER17_RS06175 | -0.94 | 7.90E-03 | ADT-0003048 | Unknown |
| 373 | HER17_RS17790 | -0.94 | 2.30E-05 | ADT-0002527 | Unknown |
| 374 | HER17_RS02540 | -0.9 | 3.00E-02 | ADT-0003166 | Unknown |
| 375 | HER17_RS19330 | -0.89 | 9.90E-03 | No hits | Unknown |
| 376 | HER17_RS10390 | -0.85 | 3.80E-05 | ADT-0000555 | Unknown |
| 377 | HER17_RS03540 | -0.84 | 9.50E-05 | ADT-0002587 | Unknown |
| 378 | HER17_RS06235 | -0.82 | 9.60E-05 | ADT-0003054 | Unknown |
| 379 | HER17_RS16725 | -0.81 | 1.10E-02 | ADT-0002485 | Unknown |
| 380 | HER17_RS10765 | -0.76 | 7.60E-05 | ADT-0003868 | Unknown |
| 381 | HER17_RS13565 | -0.73 | 6.40E-04 | ADT-0002756 | Unknown |
| 382 | HER17_RS10985 | -0.55 | 2.60E-02 | No hits | Unknown |
| 383 | HER17_RS19110 | 0.38 | 2.40E-02 | ADT-0000147 | Unknown |
| 384 | HER17_RS03935 | 1.26 | 4.80E-02 | ADT-0000930 | Unknown |
| 385 | HER17_RS04710 | 1.74 | 8.00E-03 | ADT-0002065 | Unknown |
| 386 | HER17_RS18925 | 1.89 | 1.60E-02 | ADT-0003529 | Unknown |
| 387 | HER17_RS08740 | 2.09 | 7.80E-03 | ADT-0000467 | Unknown |
| 388 | HER17_RS02500 | -3.65 | 2.90E-17 | ADT-0001022 | Unknown |
| 389 | HER17_RS09180 | 4.29 | 5.80E-05 | ADT-0001692 | Urea transport |
| 390 | HER17_RS16985 | -2.93 | 2.00E-19 | avrM | Virulence |
| 391 | HER17_RS06800 | -2.62 | 1.50E-13 | ADT-0000781 | Virulence |
| 392 | HER17_RS14810 | 1.13 | 5.60E-03 | zitB | Zinc transport |

**Table 9: M2 (*purM*::Tn5)** Differentially Expressed Genes (DEGs). $log_2$FoldChange > 0 Upregulated, and $log_2$FoldChange < 0 Downregulated

| # | Locus Tag (NCBI) | $Log_2$FC | padj | Gene Name | Affected Pathway |
|---|---|---|---|---|---|
| 1 | HER17_RS13925 | 2.04 | 2.60E-02 | ADT-0003722 | ABC transport |
| 2 | HER17_RS00920 | 1.55 | 2.70E-02 | ADT-0004310 | ABC transport |
| 3 | HER17_RS09870 | 1.07 | 2.90E-02 | ADT-0001730 | ABC transport |
| 4 | HER17_RS00900 | 2.04 | 3.00E-02 | ADT-0001163 | ABC transport |
| 5 | HER17_RS13985 | 0.99 | 4.90E-02 | ADT-0003745 | ABC transport |
| 6 | HER17_RS09190 | 4.51 | 3.30E-04 | ADT-0001694 | ABC transport |
| 7 | HER17_RS18115 | 1.13 | 2.70E-03 | ADT-0003375 | ABC transport |
| 8 | HER17_RS09185 | 3.31 | 5.40E-04 | ADT-0001693 | ABC transport |
| 9 | HER17_RS16900 | 1.65 | 2.60E-05 | ADT-0000228 | ABC transport |
| 10 | HER17_RS09895 | 1.88 | 5.60E-03 | ADT-0000532 | ABC transport |
| 11 | HER17_RS13350 | 1.28 | 1.00E-02 | ADT-0001916 | ABC transport |
| 12 | HER17_RS00895 | 1.93 | 9.30E-03 | ADT-0001164 | ABC transport |
| 13 | HER17_RS14260 | 1.14 | 1.20E-04 | ADT-0001595 | ABC transport |
| 14 | HER17_RS15010 | 1.35 | 3.90E-03 | ADT-0001561 | ABC transport |
| 15 | HER17_RS00750 | 2.58 | 2.30E-02 | ADT-0001174 | ABC transport |
| 16 | HER17_RS09590 | -0.49 | 4.10E-03 | ADT-0002421 | ABC transport |

| | | | | | |
|---|---|---|---|---|---|
| 17 | HER17_RS02795 | 0.68 | 2.70E-02 | thrA | Amino acid biosynthesis |
| 18 | HER17_RS05620 | 1.69 | 2.20E-03 | ADT-0000851 | Amino acid export |
| 19 | HER17_RS17845 | 0.98 | 2.10E-02 | ADT-0003391 | Amino acid export |
| 20 | HER17_RS17770 | 0.58 | 4.50E-02 | ADT-0003397 | Amino acid metabolism |
| 21 | HER17_RS20860 | 1.35 | 2.10E-02 | ycjG | Amino acid metabolism |
| 22 | HER17_RS12390 | 0.51 | 2.60E-02 | ADT-0005627 | Amino acid metabolism |
| 23 | HER17_RS09875 | 0.52 | 4.20E-02 | ADT-0003842 | Amino acid metabolism |
| 24 | HER17_RS20410 | 0.92 | 2.40E-02 | ADT-0000075 | Amino acid metabolism |
| 25 | HER17_RS07410 | 0.78 | 2.20E-02 | ADT-0003025 | Amino acid metabolism |
| 26 | HER17_RS13855 | 1.21 | 1.20E-04 | No hits | Amino acid metabolism |
| 27 | HER17_RS20305 | 1.49 | 7.30E-06 | ADT-0000081 | Amino acid transport |
| 28 | HER17_RS20285 | -0.44 | 2.70E-02 | ADT-0002371 | Amino acid transport |
| 29 | HER17_RS15195 | 1.45 | 2.60E-03 | ADT-0002647 | Amino acid transport |
| 30 | HER17_RS20300 | 1.39 | 3.30E-02 | ADT-0002373 | Amino acid transport |
| 31 | HER17_RS20295 | 1.27 | 1.00E-02 | ADT-0002372 | Amino acid transport |
| 32 | HER17_RS20290 | 2.03 | 6.10E-05 | ADT-0000082 | Amino acid transport |
| 33 | HER17_RS03060 | 2.33 | 1.70E-05 | ADT-0002166 | Amino acid transport |
| 34 | HER17_RS01405 | -0.93 | 5.90E-04 | rhtB | Amino acid transport |
| 35 | HER17_RS11455 | 0.69 | 4.60E-02 | ADT-0000635 | Amino acid transport |
| 36 | HER17_RS15105 | 0.97 | 1.70E-02 | nagB | Amino sugar metabolism |
| 37 | HER17_RS15785 | 1.69 | 2.00E-03 | amtB | Ammonium transport |
| 38 | HER17_RS13550 | 1.03 | 8.70E-03 | ADT-0001929 | Anion transport |
| 39 | HER17_RS19290 | 1.07 | 3.70E-04 | ADT-0002449 | Anion transport |
| 40 | HER17_RS03265 | -0.57 | 2.00E-02 | ampE | Antibiotic resistance regulation |
| 41 | HER17_RS20635 | -0.4 | 4.50E-02 | argE | Arginine biosynthesis |
| 42 | HER17_RS02705 | 1.33 | 3.60E-04 | argO | Arginine transport |
| 43 | HER17_RS14480 | 1.6 | 9.80E-03 | ADT-0001583 | Aromatic amino acid biosynthesis |
| 44 | HER17_RS20115 | 2.57 | 1.40E-07 | aaeX | Aromatic compound efflux |
| 45 | HER17_RS20110 | 2.1 | 1.70E-06 | aaeA | Aromatic compound efflux |
| 46 | HER17_RS20105 | 1.7 | 9.70E-04 | aaeB | Aromatic compound efflux |
| 47 | HER17_RS10280 | 0.83 | 3.20E-02 | ADT-0002745 | Arsenic resistance |
| 48 | HER17_RS21585 | -2.71 | 6.70E-05 | asnA | Asparagine biosynthesis |
| 49 | HER17_RS18835 | -1.19 | 1.50E-03 | aspA | Aspartate metabolism |
| 50 | HER17_RS21705 | 0.89 | 2.60E-03 | ADT-0004361 | Benzoate transport |
| 51 | HER17_RS12545 | 0.72 | 9.10E-03 | ADT-0001881 | Beta-lactam resistance |
| 52 | HER17_RS08585 | 1.14 | 5.00E-05 | bssS | Biofilm formation |
| 53 | HER17_RS08490 | 1.51 | 1.80E-04 | ADT-0001656 | Biofilm formation and acid resistance |
| 54 | HER17_RS13455 | -0.97 | 5.00E-03 | bioF | Biotin biosynthesis |
| 55 | HER17_RS13465 | -0.9 | 2.60E-03 | bioA | Biotin biosynthesis |
| 56 | HER17_RS10730 | -0.49 | 6.50E-04 | bioD | Biotin biosynthesis |
| 57 | HER17_RS13450 | -1 | 3.40E-02 | bioC | Biotin biosynthesis |

| | | | | | |
|---|---|---|---|---|---|
| 58 | HER17_RS01075 | -0.59 | 2.50E-05 | ilvD | Branched-chain amino acid biosynthesis |
| 59 | HER17_RS01100 | -0.87 | 9.60E-07 | ilvC | Branched-chain amino acid biosynthesis |
| 60 | HER17_RS01070 | -0.8 | 5.50E-05 | ilvE | Branched-chain amino acid metabolism |
| 61 | HER17_RS15665 | -0.81 | 2.70E-03 | ADT-0005485 | Carbohydrate binding |
| 62 | HER17_RS06210 | 1 | 4.30E-02 | ADT-0004109 | Carbohydrate binding |
| 63 | HER17_RS00550 | 1.36 | 3.90E-02 | otnI | Carbohydrate metabolism |
| 64 | HER17_RS00555 | 2.14 | 6.90E-03 | otnC | Carbohydrate metabolism |
| 65 | HER17_RS00560 | 2.91 | 1.50E-03 | otnK | Carbohydrate metabolism |
| 66 | HER17_RS06070 | 1.5 | 4.20E-02 | ADT-0001996 | Carbohydrate metabolism |
| 67 | HER17_RS07380 | 0.8 | 3.90E-02 | No seq | Carbohydrate metabolism |
| 68 | HER17_RS17305 | 0.97 | 4.20E-02 | ADT-0001414 | Carbohydrate metabolism |
| 69 | HER17_RS17050 | 1.81 | 3.70E-02 | manD | Carbohydrate metabolism |
| 70 | HER17_RS03450 | 2.28 | 1.30E-03 | dtnK | Carbohydrate metabolism |
| 71 | HER17_RS07390 | 1.24 | 8.00E-05 | ADT-0003027 | Carbohydrate metabolism |
| 72 | HER17_RS08050 | 1.28 | 2.40E-02 | ADT-0002766 | Carbohydrate metabolism |
| 73 | HER17_RS18645 | -0.82 | 5.30E-03 | ADT-0000170 | Carbohydrate metabolism |
| 74 | HER17_RS17365 | 0.92 | 3.60E-02 | ADT-0001412 | Carbohydrate metabolism |
| 75 | HER17_RS00565 | 2.77 | 6.10E-03 | ltnD | Carbohydrate metabolism |
| 76 | HER17_RS10690 | 1.06 | 4.70E-02 | ADT-0003872 | Carbohydrate metabolism |
| 77 | HER17_RS14510 | -0.5 | 5.30E-03 | galF | Carbohydrate metabolism |
| 78 | HER17_RS18710 | -1.55 | 2.70E-02 | uxaB1 | Carbohydrate metabolism |
| 79 | HER17_RS14465 | -0.52 | 9.50E-03 | licT | Carbohydrate metabolism regulation |
| 80 | HER17_RS18650 | -1 | 1.70E-02 | ADT-0001354 | Carbohydrate transport |
| 81 | HER17_RS11835 | 1.56 | 4.60E-02 | ADT-0000654 | Carbohydrate transport |
| 82 | HER17_RS19165 | 1.34 | 3.50E-02 | rhaT | Carbohydrate transport |
| 83 | HER17_RS14255 | 1.35 | 7.60E-05 | uhpC | Carbohydrate transport |
| 84 | HER17_RS18720 | -2.92 | 1.40E-03 | exuT | Carbohydrate transport |
| 85 | HER17_RS19770 | 3.59 | 2.70E-02 | ADT-0000114 | Carbohydrate transport |
| 86 | HER17_RS19775 | 2.02 | 2.80E-02 | ADT-0000113 | Carbohydrate transport |
| 87 | HER17_RS06075 | 2.01 | 7.90E-03 | ADT-0001995 | Carbohydrate transport |
| 88 | HER17_RS19285 | 1.02 | 2.10E-02 | ADT-0002448 | Carbon dioxide metabolism |
| 89 | HER17_RS02260 | -0.56 | 9.10E-03 | ADT-0002204 | Carbon dioxide metabolism |
| 90 | HER17_RS17160 | -0.5 | 6.30E-04 | zipA | Cell division |
| 91 | HER17_RS01595 | 0.95 | 4.70E-02 | ADT-0003198 | Cell division |
| 92 | HER17_RS12045 | -0.54 | 2.40E-04 | ldtD | Cell wall biosynthesis |
| 93 | HER17_RS19890 | -0.35 | 4.50E-02 | mtgA | Cell wall biosynthesis |
| 94 | HER17_RS18240 | -2.15 | 1.30E-02 | ADT-0003369 | Cell wall degradation |
| 95 | HER17_RS12895 | -0.73 | 1.50E-02 | mepS | Cell wall metabolism |
| 96 | HER17_RS20980 | -0.57 | 1.80E-02 | ADT-0001246 | Cell wall protection |
| 97 | HER17_RS01090 | -0.66 | 4.30E-03 | ADT-0002252 | Cell wall protection |

| | | | | | |
|---|---|---|---|---|---|
| 98 | HER17_RS09285 | 1.03 | 8.60E-03 | ADT-0000500 | Cell wall protection |
| 99 | HER17_RS08835 | -0.53 | 2.90E-03 | nlpC | Cell wall remodeling |
| 100 | HER17_RS08100 | -0.36 | 5.70E-03 | cheA | Chemotaxis |
| 101 | HER17_RS08110 | -0.48 | 5.30E-03 | ADT-0002771 | Chemotaxis |
| 102 | HER17_RS16065 | -0.56 | 1.20E-02 | ADT-0000266 | Chemotaxis |
| 103 | HER17_RS01625 | -1.28 | 5.30E-03 | ADT-0004277 | Chemotaxis |
| 104 | HER17_RS00535 | -0.87 | 2.50E-10 | ADT-0003246 | Chemotaxis |
| 105 | HER17_RS15080 | -0.69 | 3.00E-02 | ADT-0001555 | Chemotaxis |
| 106 | HER17_RS04000 | 1.1 | 3.90E-02 | ADT-0002104 | Chemotaxis |
| 107 | HER17_RS09925 | 1 | 3.10E-05 | ADT-0003843 | Chemotaxis |
| 108 | HER17_RS10980 | 0.89 | 9.60E-03 | ADT-0000598 | Chemotaxis |
| 109 | HER17_RS01655 | 1.26 | 8.20E-03 | ADT-0001104 | CoA metabolism |
| 110 | HER17_RS20495 | -0.38 | 3.00E-02 | coaA | Coenzyme A biosynthesis |
| 111 | HER17_RS07015 | 1.2 | 2.50E-03 | cvpA | Colicin V production |
| 112 | HER17_RS11895 | 0.67 | 4.40E-02 | cutC | Copper homeostasis |
| 113 | HER17_RS00395 | 0.6 | 3.90E-02 | ADT-0004341 | Cyclic di-GMP signaling |
| 114 | HER17_RS08845 | 2.46 | 1.10E-09 | ADT-0001672 | Cyclic di-GMP signaling |
| 115 | HER17_RS11575 | 0.78 | 4.70E-03 | ADT-0003909 | Cyclic di-GMP signaling |
| 116 | HER17_RS17170 | -0.95 | 1.30E-02 | cysK | Cysteine biosynthesis |
| 117 | HER17_RS15810 | 1.53 | 7.70E-05 | ADT-0001518 | Cysteine biosynthesis |
| 118 | HER17_RS09030 | -0.5 | 3.70E-02 | ccmA | Cytochrome c biogenesis |
| 119 | HER17_RS09050 | -0.62 | 1.60E-04 | ccmE | Cytochrome c biogenesis |
| 120 | HER17_RS12540 | 0.44 | 6.10E-03 | deoR | Deoxyribonucleotide metabolism regulation |
| 121 | HER17_RS09140 | 0.71 | 4.50E-02 | ADT-0005553 | Dicarboxylate transport |
| 122 | HER17_RS13085 | -0.62 | 2.80E-04 | ybiB | DNA binding |
| 123 | HER17_RS18370 | -0.63 | 3.90E-02 | ADT-0003364 | DNA binding |
| 124 | HER17_RS20920 | -0.63 | 2.00E-02 | dinD | DNA damage response |
| 125 | HER17_RS19310 | 1.29 | 9.90E-03 | ADT-0003515 | DNA damage response |
| 126 | HER17_RS07610 | 1.07 | 2.20E-02 | ADT-0004369 | DNA processing |
| 127 | HER17_RS10440 | 1.26 | 1.90E-07 | ADT-0003764 | DNA recombination |
| 128 | HER17_RS19430 | 0.64 | 3.20E-04 | ADT-0003484 | DNA recombination |
| 129 | HER17_RS05050 | 0.73 | 4.90E-02 | recX | DNA recombination |
| 130 | HER17_RS19085 | 0.74 | 2.20E-02 | radA | DNA repair |
| 131 | HER17_RS17105 | 1.12 | 3.80E-02 | ADT-0001432 | DNA repair |
| 132 | HER17_RS10530 | -0.63 | 3.50E-03 | ogt | DNA repair |
| 133 | HER17_RS15770 | 0.7 | 2.40E-02 | ADT-0001519 | DNA repair |
| 134 | HER17_RS05755 | -0.4 | 3.20E-03 | ung | DNA repair |
| 135 | HER17_RS13795 | 0.69 | 4.50E-02 | ADT-0003710 | DNA repair and transcription regulation |
| 136 | HER17_RS11230 | 1.74 | 1.40E-09 | ADT-0001798 | DNA replication |
| 137 | HER17_RS17510 | 1.03 | 6.20E-04 | ADT-0005889 | DNA replication |
| 138 | HER17_RS04770 | 1.92 | 1.10E-06 | ADT-0005889 | DNA replication |

| | | | | | |
|---|---|---|---|---|---|
| 139 | HER17_RS10750 | 1.07 | 1.70E-03 | tus | DNA replication termination |
| 140 | HER17_RS22065 | -0.82 | 2.60E-03 | No seq | DNA restriction |
| 141 | HER17_RS21945 | -0.85 | 2.90E-02 | No seq | DNA restriction |
| 142 | HER17_RS05485 | 0.75 | 5.30E-03 | nrdE | DNA synthesis |
| 143 | HER17_RS05490 | 2.28 | 3.40E-06 | nrdI | DNA synthesis |
| 144 | HER17_RS02240 | -0.42 | 2.60E-02 | ADT-0003178 | DNA topology |
| 145 | HER17_RS19850 | 0.64 | 2.20E-03 | No seq | DNA transposition |
| 146 | HER17_RS16105 | 0.8 | 2.00E-02 | ADT-0000262 | Drug efflux |
| 147 | HER17_RS17110 | 0.46 | 4.90E-02 | ADT-0002547 | Drug efflux |
| 148 | HER17_RS14790 | 1.58 | 3.00E-02 | ADT-0002674 | Efflux transport |
| 149 | HER17_RS05865 | -0.4 | 2.60E-02 | aggA | Efflux transport |
| 150 | HER17_RS13155 | -1.14 | 4.50E-05 | ADT-0004004 | Electron transfer |
| 151 | HER17_RS21750 | -0.88 | 2.40E-02 | hydN | Electron transfer |
| 152 | HER17_RS11595 | -0.88 | 4.20E-02 | ADT-0002907 | Electron transfer |
| 153 | HER17_RS17065 | -2.68 | 4.10E-02 | ADT-0001437 | Electron transfer |
| 154 | HER17_RS15085 | -0.32 | 4.30E-02 | fldA | Electron transfer |
| 155 | HER17_RS08580 | 0.74 | 4.50E-02 | ADT-0003793 | Electron transport chain |
| 156 | HER17_RS10600 | 1.14 | 4.90E-03 | ADT-0001763 | Electron transport chain |
| 157 | HER17_RS15880 | -0.57 | 3.10E-02 | cyoB | Electron transport chain |
| 158 | HER17_RS15890 | -0.53 | 3.20E-02 | ADT-0000278 | Electron transport chain |
| 159 | HER17_RS01190 | 0.65 | 1.20E-02 | wzyE | Enterobacterial common antigen biosynthesis |
| 160 | HER17_RS00670 | 1.52 | 1.20E-10 | cpxP | Envelope stress response |
| 161 | HER17_RS09525 | 3.56 | 3.90E-09 | pspB | Envelope stress response |
| 162 | HER17_RS09530 | 3.82 | 1.10E-13 | pspC | Envelope stress response |
| 163 | HER17_RS03675 | 3.79 | 1.00E-17 | pspG | Envelope stress response |
| 164 | HER17_RS04685 | -0.39 | 3.20E-02 | frsA | Ester hydrolysis |
| 165 | HER17_RS04640 | 1.85 | 4.90E-03 | fadE | Fatty acid beta-oxidation |
| 166 | HER17_RS00340 | 2.44 | 6.50E-09 | ADT-0004347 | Fatty acid biosynthesis |
| 167 | HER17_RS00345 | 1.44 | 2.20E-02 | ADT-0004346 | Fatty acid biosynthesis |
| 168 | HER17_RS20555 | 1.91 | 5.20E-04 | fadA | Fatty acid metabolism |
| 169 | HER17_RS06885 | 0.7 | 1.60E-02 | fadI | Fatty acid metabolism |
| 170 | HER17_RS20550 | 1.87 | 4.10E-03 | fadB | Fatty acid metabolism |
| 171 | HER17_RS11275 | 2.14 | 1.50E-07 | fadD | Fatty acid metabolism |
| 172 | HER17_RS09680 | 0.57 | 9.60E-03 | ADT-0003498 | Fimbrial assembly |
| 173 | HER17_RS08160 | 0.43 | 4.70E-02 | flgA | Flagellar assembly |
| 174 | HER17_RS08305 | -0.77 | 1.90E-03 | fliD | Flagellar assembly |
| 175 | HER17_RS08035 | -0.85 | 1.40E-02 | ADT-0001931 | Flagellar assembly |
| 176 | HER17_RS08090 | -0.37 | 3.50E-02 | motA | Flagellar motor function |
| 177 | HER17_RS13270 | -0.46 | 4.30E-02 | ADT-0001913 | Flavin metabolism |
| 178 | HER17_RS19920 | -0.98 | 1.20E-02 | ADT-0003466 | Formaldehyde metabolism |
| 179 | HER17_RS09880 | 0.86 | 3.70E-02 | ADT-0002841 | GABA metabolism |
| 180 | HER17_RS01025 | 2.24 | 1.10E-02 | ytfR | Galactofuranose transport |

| | | | | | |
|---|---|---|---|---|---|
| 181 | HER17_RS01030 | 2.26 | 5.60E-03 | ytfT | Galactofuranose transport |
| 182 | HER17_RS06380 | -0.56 | 2.00E-03 | galR | Galactose metabolism regulation |
| 183 | HER17_RS01915 | -0.64 | 4.00E-02 | crp | Global transcriptional regulation |
| 184 | HER17_RS01455 | 1.3 | 3.20E-02 | ADT-0004306 | Gluconate metabolism |
| 185 | HER17_RS03045 | 1.42 | 1.10E-06 | sgrT | Glucose transport regulation |
| 186 | HER17_RS07250 | -0.63 | 2.70E-03 | ADT-0000756 | Glutamine metabolism |
| 187 | HER17_RS05630 | -0.66 | 4.40E-02 | ADT-0003073 | Glutathione metabolism |
| 188 | HER17_RS13255 | -0.64 | 1.90E-02 | ADT-0000724 | Glutathione metabolism |
| 189 | HER17_RS01430 | -0.79 | 2.50E-02 | glpA | Glycerol metabolism |
| 190 | HER17_RS01440 | -1.46 | 1.20E-04 | glpC | Glycerol metabolism |
| 191 | HER17_RS01435 | -1.23 | 1.80E-04 | glpB | Glycerol metabolism |
| 192 | HER17_RS01510 | 3.1 | 3.00E-11 | glpD | Glycerol metabolism |
| 193 | HER17_RS01530 | -0.44 | 9.20E-03 | glpR | Glycerol metabolism regulation |
| 194 | HER17_RS01425 | 1.01 | 6.90E-03 | glpT | Glycerol transport |
| 195 | HER17_RS17995 | -1.31 | 6.90E-03 | gcvP | Glycine cleavage system |
| 196 | HER17_RS18005 | -1.05 | 1.10E-05 | gcvT | Glycine metabolism |
| 197 | HER17_RS18000 | -1.05 | 2.50E-03 | gcvH | Glycine metabolism |
| 198 | HER17_RS00725 | -0.71 | 1.10E-04 | pfkA | Glycolysis |
| 199 | HER17_RS11175 | 2.31 | 5.20E-03 | ADT-0000613 | Glycolysis |
| 200 | HER17_RS19780 | 2.25 | 2.20E-03 | ADT-0002399 | Glycolysis |
| 201 | HER17_RS15895 | -0.46 | 3.50E-02 | cyoE | Heme biosynthesis |
| 202 | HER17_RS21450 | -0.63 | 1.00E-02 | hemN | Heme biosynthesis |
| 203 | HER17_RS01310 | -0.37 | 9.50E-03 | hemD | Heme biosynthesis |
| 204 | HER17_RS08855 | 1.51 | 2.00E-04 | ADT-0000471 | Heme transport |
| 205 | HER17_RS09040 | -0.52 | 2.70E-02 | ccmC | Heme transport |
| 206 | HER17_RS07930 | -0.57 | 1.50E-02 | ADT-0005537 | Histidine biosynthesis |
| 207 | HER17_RS20250 | 2.44 | 6.90E-09 | No hits | Host-pathogen interaction |
| 208 | HER17_RS14320 | 1.1 | 6.90E-03 | ADT-0003706 | Hydrolase activity |
| 209 | HER17_RS06780 | -0.43 | 3.60E-02 | ADT-0000783 | Hydrolase activity |
| 210 | HER17_RS07550 | -0.83 | 1.90E-02 | ADT-0003013 | Hydrolase activity |
| 211 | HER17_RS20670 | -0.76 | 1.90E-04 | ADT-0001265 | Hydrolase activity |
| 212 | HER17_RS01935 | -0.68 | 6.10E-03 | ADT-0004258 | Hydrolase activity |
| 213 | HER17_RS03695 | 0.8 | 4.20E-04 | ADT-0002122 | Hydrolase activity |
| 214 | HER17_RS04195 | -0.45 | 3.10E-02 | ADT-0003118 | Hydrolase activity |
| 215 | HER17_RS11450 | 0.76 | 4.10E-02 | ADT-0000634 | Hydrolase activity |
| 216 | HER17_RS13900 | 0.85 | 4.20E-02 | ADT-0002703 | Intermembrane transport |
| 217 | HER17_RS01370 | 1.77 | 2.10E-04 | corA | Ion transport |
| 218 | HER17_RS02850 | 1.22 | 2.40E-04 | nhaA | Ion transport |
| 219 | HER17_RS17750 | -0.59 | 1.70E-04 | ADT-0001388 | Ion transport |
| 220 | HER17_RS21225 | 1.21 | 2.30E-03 | No hits | Iron acquisition |
| 221 | HER17_RS05615 | 0.83 | 1.20E-02 | fhuB | Iron transport |
| 222 | HER17_RS14265 | 0.96 | 3.90E-04 | ADT-0001594 | Iron transport |
| 223 | HER17_RS15015 | 2.94 | 1.60E-08 | ADT-0001560 | Iron transport |

| | | | | | |
|---|---|---|---|---|---|
| 224 | HER17_RS17255 | 2.05 | 2.20E-04 | ADT-0003559 | Iron transport |
| 225 | HER17_RS14065 | 1.39 | 3.00E-03 | ADT-0001613 | Iron transport |
| 226 | HER17_RS17620 | 1.78 | 1.30E-08 | ADT-0001399 | Iron transport |
| 227 | HER17_RS03340 | 0.9 | 6.90E-03 | ADT-0004201 | Iron transport |
| 228 | HER17_RS07220 | 1.28 | 4.30E-02 | ADT-0003954 | Iron uptake |
| 229 | HER17_RS01545 | -0.36 | 1.30E-02 | nfuA | Iron-sulfur cluster assembly |
| 230 | HER17_RS06010 | 1.78 | 2.00E-02 | iscR | Iron-sulfur cluster assembly regulation |
| 231 | HER17_RS01080 | -0.5 | 3.70E-04 | ilvA | Isoleucine biosynthesis |
| 232 | HER17_RS17785 | 0.47 | 2.30E-03 | lpxP | Lipid A biosynthesis |
| 233 | HER17_RS03760 | -0.48 | 9.40E-03 | aas | Lipid metabolism |
| 234 | HER17_RS00445 | -0.68 | 4.50E-02 | ADT-0001186 | Lipid metabolism |
| 235 | HER17_RS11055 | 1.11 | 1.40E-02 | rssA | Lipid metabolism |
| 236 | HER17_RS18155 | -0.68 | 1.00E-02 | ADT-0000184 | Lipid transport |
| 237 | HER17_RS08840 | -0.6 | 3.50E-03 | lplA | Lipoic acid metabolism |
| 238 | HER17_RS01340 | -0.47 | 3.90E-02 | dapF | Lysine biosynthesis |
| 239 | HER17_RS06365 | -1.96 | 1.50E-02 | malE | Maltose transport |
| 240 | HER17_RS12525 | -0.87 | 2.80E-04 | ADT-0001880 | Membrane structure |
| 241 | HER17_RS08955 | -0.32 | 3.80E-02 | ADT-0000479 | Membrane structure |
| 242 | HER17_RS11280 | 2.14 | 1.30E-17 | ADT-0003900 | Membrane structure |
| 243 | HER17_RS15540 | -0.45 | 2.90E-02 | menC | Menaquinone biosynthesis |
| 244 | HER17_RS05760 | -1.11 | 2.40E-10 | grcA | Metabolic processes |
| 245 | HER17_RS07470 | 1.59 | 2.10E-06 | ADT-0004067 | Metabolic processes |
| 246 | HER17_RS20100 | 1 | 9.70E-03 | ADT-0001287 | Metabolic processes |
| 247 | HER17_RS10675 | -0.62 | 5.90E-03 | pptA | Metabolic processes |
| 248 | HER17_RS03345 | 1.06 | 4.30E-02 | ADT-0000968 | Metal homeostasis regulation |
| 249 | HER17_RS10275 | 1.22 | 3.00E-02 | ADT-0000411 | Metal homeostasis regulation |
| 250 | HER17_RS17405 | 0.6 | 2.60E-03 | ADT-0003546 | Metal ion transport |
| 251 | HER17_RS08400 | 0.73 | 2.30E-03 | ADT-0000438 | Metal resistance |
| 252 | HER17_RS18690 | 1.54 | 1.10E-09 | ADT-0000168 | Metal resistance |
| 253 | HER17_RS07355 | -0.86 | 6.70E-03 | ADT-0001936 | Methionine salvage pathway |
| 254 | HER17_RS05360 | 1.03 | 5.30E-04 | ADT-0002053 | Methylation |
| 255 | HER17_RS14820 | 1.98 | 4.50E-05 | nadA | NAD biosynthesis |
| 256 | HER17_RS17415 | -0.6 | 9.70E-04 | nadK | NAD metabolism |
| 257 | HER17_RS15515 | -0.57 | 2.50E-03 | ADT-0002630 | NAD metabolism |
| 258 | HER17_RS09505 | 1.24 | 4.90E-07 | ADT-0002418 | NAD metabolism |
| 259 | HER17_RS14815 | 1.56 | 1.20E-03 | pnuC | NAD precursor transport |
| 260 | HER17_RS17125 | 2.53 | 6.60E-20 | norR | Nitric oxide response |
| 261 | HER17_RS13525 | -1.14 | 3.40E-02 | ADT-0000736 | Nitro compound reduction |
| 262 | HER17_RS08995 | -1.43 | 3.00E-05 | nrfA | Nitrogen metabolism |
| 263 | HER17_RS09005 | -1.15 | 3.50E-02 | nrfC | Nitrogen metabolism |
| 264 | HER17_RS09000 | -1.22 | 2.20E-02 | nrfB | Nitrogen metabolism |
| 265 | HER17_RS15790 | 1.79 | 2.60E-02 | glnK | Nitrogen metabolism |

| | | | | | |
|---|---|---|---|---|---|
| 266 | HER17_RS11480 | 2.37 | 2.00E-04 | ADT-0002904 | Nitrous oxide response |
| 267 | HER17_RS17780 | 1.36 | 8.70E-03 | ADT-0002526 | Nucleobase transport |
| 268 | HER17_RS17755 | 0.94 | 1.30E-02 | ADT-0001387 | Nucleobase transport |
| 269 | HER17_RS21400 | 2.18 | 7.50E-04 | ADT-0000011 | Nucleobase transport |
| 270 | HER17_RS16085 | 1.48 | 2.40E-03 | ADT-0002580 | Nucleoside transport |
| 271 | HER17_RS04455 | 1.17 | 4.80E-02 | ADT-0002080 | Nucleoside transport |
| 272 | HER17_RS14005 | -0.52 | 4.00E-03 | amn | Nucleotide metabolism |
| 273 | HER17_RS16395 | -0.57 | 2.70E-02 | ppnN | Nucleotide metabolism |
| 274 | HER17_RS20665 | -0.96 | 3.50E-03 | udp | Nucleotide metabolism |
| 275 | HER17_RS14115 | 0.87 | 4.70E-02 | ADT-0001608 | Osmotic stress response |
| 276 | HER17_RS04505 | 0.99 | 2.30E-02 | proV | Osmotic stress response |
| 277 | HER17_RS09400 | 2.2 | 7.80E-04 | osmB | Osmotic stress response |
| 278 | HER17_RS21355 | 0.94 | 2.90E-03 | ADT-0003409 | Outer membrane structure |
| 279 | HER17_RS14310 | 3.39 | 2.40E-05 | ADT-0002034 | Oxidation-reduction processes |
| 280 | HER17_RS10705 | -0.82 | 7.20E-04 | ydfG | Oxidation-reduction processes |
| 281 | HER17_RS03670 | 1.51 | 4.30E-06 | ADT-0002596 | Oxidation-reduction processes |
| 282 | HER17_RS09435 | 0.91 | 4.70E-03 | ADT-0001561 | Oxidation-reduction processes |
| 283 | HER17_RS14120 | 1.35 | 3.70E-02 | ADT-0003737 | Oxidation-reduction processes |
| 284 | HER17_RS20180 | -0.64 | 6.60E-04 | ADT-0000092 | Oxidation-reduction processes |
| 285 | HER17_RS07400 | 1.1 | 1.30E-02 | ADT-0001935 | Oxidation-reduction processes |
| 286 | HER17_RS16605 | -0.57 | 3.90E-02 | ADT-0003344 | Oxidation-reduction processes |
| 287 | HER17_RS14295 | 1.88 | 6.10E-03 | ADT-0003702 | Oxidation-reduction processes |
| 288 | HER17_RS08770 | 0.96 | 1.00E-02 | ADT-0003808 | Oxidation-reduction processes |
| 289 | HER17_RS10790 | -0.69 | 2.70E-02 | ADT-0002867 | Oxidation-reduction processes |
| 290 | HER17_RS14300 | 2.37 | 1.20E-03 | ADT-0003703 | Oxidation-reduction processes |
| 291 | HER17_RS14305 | 1.97 | 1.60E-02 | ADT-0003704 | Oxidation-reduction processes |
| 292 | HER17_RS21790 | 1.62 | 5.60E-05 | ADT-0002299 | Oxidation-reduction processes |
| 293 | HER17_RS17045 | 1.13 | 3.60E-02 | ADT-0001440 | Oxidation-reduction processes |
| 294 | HER17_RS08825 | -0.61 | 4.10E-02 | ADT-0001671 | Oxidative stress response |
| 295 | HER17_RS01920 | -0.51 | 1.10E-02 | ADT-0003186 | Oxidative stress response |
| 296 | HER17_RS16005 | -0.36 | 3.70E-02 | ADT-0000269 | Oxidative stress response |
| 297 | HER17_RS21110 | -0.53 | 4.00E-02 | sodA | Oxidative stress response |
| 298 | HER17_RS09580 | -0.7 | 1.50E-02 | tpx | Oxidative stress response |
| 299 | HER17_RS11160 | 2.95 | 2.40E-04 | ADT-0002881 | Oxygen binding |
| 300 | HER17_RS14235 | -1.43 | 2.10E-06 | pnl | Pectin degradation |
| 301 | HER17_RS01895 | -1.48 | 4.90E-02 | pelB | Pectin degradation |
| 302 | HER17_RS12080 | -0.71 | 2.90E-02 | pelN | Pectin degradation |
| 303 | HER17_RS17315 | 1.92 | 5.10E-04 | rpiB | Pentose phosphate pathway |
| 304 | HER17_RS17320 | 1.08 | 2.10E-03 | tal | Pentose phosphate pathway |
| 305 | HER17_RS13510 | 0.55 | 3.20E-02 | ADT-0003696 | Peptide transport |
| 306 | HER17_RS11020 | 0.35 | 2.20E-02 | oppA | Peptide transport |
| 307 | HER17_RS03260 | -0.46 | 3.00E-02 | ampD | Peptidoglycan recycling |
| 308 | HER17_RS18535 | 1.54 | 2.50E-03 | ADT-0006169 | Phage assembly |

| | | | | | |
|---|---|---|---|---|---|
| 309 | HER17_RS13160 | -2.05 | 2.70E-10 | ADT-0002135 | Phage assembly |
| 310 | HER17_RS13150 | -1.93 | 3.20E-14 | ADT-0004003 | Phage assembly |
| 311 | HER17_RS13105 | -0.78 | 1.70E-02 | ADT-0003998 | Phage assembly |
| 312 | HER17_RS13100 | -0.62 | 1.10E-02 | ADT-0003997 | Phage assembly |
| 313 | HER17_RS18975 | -0.98 | 1.70E-04 | ADT-0003524 | Phage assembly |
| 314 | HER17_RS13165 | -2.05 | 3.10E-10 | ADT-0002134 | Phage assembly |
| 315 | HER17_RS13140 | -1.16 | 3.30E-04 | ADT-0002136 | Phage assembly |
| 316 | HER17_RS07825 | 1.58 | 6.90E-03 | ADT-0003298 | Phage assembly |
| 317 | HER17_RS07290 | -0.71 | 3.90E-02 | ADT-0001867 | Phage assembly |
| 318 | HER17_RS21925 | -0.72 | 1.40E-02 | ADT-0003997 | Phage assembly |
| 319 | HER17_RS18900 | 1.17 | 7.20E-06 | iteA | Phage defense |
| 320 | HER17_RS18545 | 1.97 | 2.40E-02 | ADT-0005875 | Phage DNA packaging |
| 321 | HER17_RS07875 | 1.58 | 3.90E-02 | ADT-0005875 | Phage DNA packaging |
| 322 | HER17_RS18530 | 2.53 | 5.90E-03 | ADT-0005945 | Phage DNA packaging |
| 323 | HER17_RS12670 | 1.6 | 4.30E-02 | ADT-0004398 | Phage DNA packaging |
| 324 | HER17_RS13110 | -1.02 | 2.00E-03 | ADT-0003999 | Phage-related functions |
| 325 | HER17_RS13175 | -1.7 | 7.20E-04 | ADT-0002133 | Phage-related functions |
| 326 | HER17_RS22080 | -2.46 | 8.10E-15 | No hits | Phage-related functions |
| 327 | HER17_RS18540 | 2.14 | 9.50E-06 | ADT-0006232 | Phage-related functions |
| 328 | HER17_RS05250 | 2.1 | 2.00E-02 | ADT-0006232 | Phage-related functions |
| 329 | HER17_RS07870 | 1.51 | 1.40E-02 | ADT-0006232 | Phage-related functions |
| 330 | HER17_RS13115 | -1.21 | 1.80E-03 | ADT-0002137 | Phage-related functions |
| 331 | HER17_RS01580 | 0.93 | 2.40E-02 | ADT-0001107 | Phosphate metabolism |
| 332 | HER17_RS11950 | 0.54 | 1.00E-02 | ADT-0000660 | Phosphate metabolism |
| 333 | HER17_RS04005 | -0.58 | 2.70E-02 | plsY | Phospholipid biosynthesis |
| 334 | HER17_RS13945 | 0.72 | 9.50E-05 | ADT-0000405 | Phospholipid metabolism |
| 335 | HER17_RS03245 | -0.58 | 2.40E-02 | ppdD | Pilus assembly |
| 336 | HER17_RS16540 | -0.79 | 4.60E-02 | ppdC | Pilus assembly |
| 337 | HER17_RS06090 | 0.4 | 4.90E-02 | pilW | Pilus assembly |
| 338 | HER17_RS13475 | -0.42 | 4.60E-02 | ADT-0000731 | Programmed cell death |
| 339 | HER17_RS20490 | 0.77 | 4.30E-02 | ADT-0003448 | Protein acetylation |
| 340 | HER17_RS18150 | -0.62 | 1.60E-02 | ADT-0000185 | Protein acetylation |
| 341 | HER17_RS14475 | 1.99 | 2.80E-04 | ADT-0003664 | Protein activation |
| 342 | HER17_RS13080 | -0.63 | 9.50E-03 | ADT-0003994 | Protein degradation |
| 343 | HER17_RS11655 | -0.92 | 1.10E-02 | pepT | Protein degradation |
| 344 | HER17_RS13310 | -0.52 | 2.00E-04 | pepT | Protein degradation |
| 345 | HER17_RS02650 | -1.08 | 1.80E-08 | sprT | Protein degradation |
| 346 | HER17_RS18665 | 0.99 | 2.80E-04 | spy | Protein folding |
| 347 | HER17_RS09060 | -0.53 | 1.90E-02 | dsbE | Protein folding |
| 348 | HER17_RS06920 | -0.61 | 3.70E-04 | sixA | Protein modification |
| 349 | HER17_RS20660 | -0.55 | 3.00E-03 | ADT-0000050 | Protein modification |
| 350 | HER17_RS16340 | -0.41 | 3.10E-02 | map | Protein processing |
| 351 | HER17_RS08480 | 1.09 | 3.50E-06 | yccA | Protein quality control |

| | | | | | |
|---|---|---|---|---|---|
| 352 | HER17_RS10340 | 1.31 | 1.10E-03 | ADT-0002746 | Protein secretion |
| 353 | HER17_RS20595 | -0.54 | 1.20E-02 | tatA | Protein secretion |
| 354 | HER17_RS00740 | 1.49 | 1.20E-02 | ADT-0004319 | Protein secretion |
| 355 | HER17_RS15765 | 1.02 | 4.30E-03 | ffs | Protein targeting |
| 356 | HER17_RS03235 | 1.36 | 5.30E-03 | hofC | Protein transport |
| 357 | HER17_RS04935 | -0.7 | 2.40E-02 | ADT-0002064 | Protein-protein interactions |
| 358 | HER17_RS06475 | 1.1 | 2.40E-03 | purE | Purine biosynthesis |
| 359 | HER17_RS06470 | 0.91 | 1.10E-02 | purK | Purine biosynthesis |
| 360 | HER17_RS11635 | 0.55 | 2.70E-02 | purB | Purine biosynthesis |
| 361 | HER17_RS07020 | 0.87 | 3.30E-02 | purF | Purine biosynthesis |
| 362 | HER17_RS20335 | 1.37 | 3.20E-03 | purH | Purine biosynthesis |
| 363 | HER17_RS11770 | 1.54 | 2.60E-03 | purT | Purine biosynthesis |
| 364 | HER17_RS06160 | 0.62 | 3.50E-04 | guaA | Purine biosynthesis |
| 365 | HER17_RS20340 | 1.17 | 1.30E-02 | purD | Purine biosynthesis |
| 366 | HER17_RS15465 | -1.85 | 7.20E-10 | purM | Purine biosynthesis |
| 367 | HER17_RS05910 | 0.99 | 9.50E-03 | purL | Purine biosynthesis |
| 368 | HER17_RS15470 | -1.26 | 1.30E-18 | purN | Purine biosynthesis |
| 369 | HER17_RS17765 | 0.89 | 1.10E-02 | puuE | Purine catabolism |
| 370 | HER17_RS08705 | -0.72 | 5.00E-04 | hinT | Purine metabolism |
| 371 | HER17_RS09235 | 1.08 | 3.50E-03 | purR | Purine metabolism regulation |
| 372 | HER17_RS15710 | -0.46 | 3.90E-02 | apt | Purine salvage |
| 373 | HER17_RS14040 | 1.64 | 2.40E-05 | ygjG | Putrescine metabolism |
| 374 | HER17_RS12785 | 1.25 | 3.20E-02 | ptrR | Putrescine metabolism regulation |
| 375 | HER17_RS02895 | 0.73 | 2.20E-02 | carA | Pyrimidine biosynthesis |
| 376 | HER17_RS05005 | -0.54 | 2.10E-02 | grxB | Redox homeostasis |
| 377 | HER17_RS05495 | 3.22 | 5.10E-10 | nrdH | Redox homeostasis |
| 378 | HER17_RS09325 | 0.75 | 4.20E-03 | ribA | Riboflavin biosynthesis |
| 379 | HER17_RS21550 | 1.38 | 2.60E-02 | ADT-0000004 | Ribose metabolism |
| 380 | HER17_RS09335 | 2.34 | 1.80E-03 | ADT-0002824 | Ribose transport |
| 381 | HER17_RS21545 | 1.2 | 1.60E-03 | rbsA | Ribose transport |
| 382 | HER17_RS15745 | 0.93 | 2.70E-03 | ADT-0001523 | Ribosome assembly |
| 383 | HER17_RS21465 | 0.8 | 3.70E-02 | yihA | Ribosome biogenesis |
| 384 | HER17_RS18220 | 0.64 | 2.20E-02 | rimP | Ribosome biogenesis |
| 385 | HER17_RS11925 | -0.57 | 2.80E-04 | rimJ | Ribosome modification |
| 386 | HER17_RS00840 | -0.47 | 3.20E-02 | rraA | RNA metabolism regulation |
| 387 | HER17_RS08610 | -0.45 | 7.70E-03 | rne | RNA processing |
| 388 | HER17_RS03835 | -0.55 | 1.50E-03 | rnr | RNA processing |
| 389 | HER17_RS20075 | -0.35 | 2.90E-03 | rapZ | RNA processing |
| 390 | HER17_RS08895 | 2.05 | 3.60E-02 | rprA | RNA regulation |
| 391 | HER17_RS11075 | 1.44 | 3.00E-03 | No seq | RNA regulation |
| 392 | HER17_RS14835 | 3.16 | 4.90E-03 | No seq | RNA regulation |
| 393 | HER17_RS11715 | 0.95 | 2.50E-02 | rsmF | rRNA modification |
| 394 | HER17_RS10900 | 0.63 | 4.30E-02 | rluB | rRNA modification |

| | | | | | |
|---|---|---|---|---|---|
| 395 | HER17_RS18265 | -3.06 | 8.20E-04 | ADT-0003365 | Secondary metabolism |
| 396 | HER17_RS07210 | -0.45 | 3.70E-02 | ADT-0003953 | Secondary metabolism |
| 397 | HER17_RS18275 | -1.22 | 4.30E-02 | ADT-0002501 | Secondary metabolism |
| 398 | HER17_RS12290 | -0.66 | 4.10E-02 | serC | Serine biosynthesis |
| 399 | HER17_RS16960 | 0.76 | 3.80E-02 | fhuE | Siderophore transport |
| 400 | HER17_RS17740 | 1.63 | 1.10E-02 | ADT-0001390 | Signal transduction |
| 401 | HER17_RS11050 | 0.96 | 4.50E-02 | rssB | Signal transduction |
| 402 | HER17_RS05500 | 0.89 | 5.00E-02 | speD | Spermidine biosynthesis |
| 403 | HER17_RS11210 | -0.81 | 1.40E-02 | ADT-0002884 | Unknown |
| 404 | HER17_RS13380 | -0.55 | 1.70E-02 | ADT-0001918 | Stress response |
| 405 | HER17_RS02360 | 1.57 | 4.50E-04 | ADT-0001032 | Stress response |
| 406 | HER17_RS19060 | 1.25 | 3.40E-02 | osmY | Stress response |
| 407 | HER17_RS09515 | 0.72 | 1.10E-03 | pspF | Stress response |
| 408 | HER17_RS09520 | 4.3 | 4.60E-13 | pspA | Stress response |
| 409 | HER17_RS19050 | 1.47 | 3.60E-04 | ADT-0001330 | Stress response |
| 410 | HER17_RS10520 | -0.99 | 2.50E-07 | uspE | Stress response |
| 411 | HER17_RS03040 | -0.66 | 1.60E-03 | sgrR | Sugar metabolism regulation |
| 412 | HER17_RS19690 | -0.72 | 3.50E-02 | metC | Sulfur metabolism |
| 413 | HER17_RS13030 | 2.77 | 2.00E-04 | ADT-0001900 | Sulfur metabolism |
| 414 | HER17_RS10870 | -0.84 | 1.40E-03 | cysB | Sulfur metabolism regulation |
| 415 | HER17_RS14930 | -0.77 | 1.50E-02 | sucA | TCA cycle |
| 416 | HER17_RS06860 | 1.2 | 1.40E-02 | mqo | TCA cycle |
| 417 | HER17_RS20405 | 0.99 | 7.20E-07 | thiH | Thiamine biosynthesis |
| 418 | HER17_RS06265 | 1.47 | 6.20E-03 | thiD | Thiamine biosynthesis |
| 419 | HER17_RS20380 | 1 | 8.30E-04 | thiC | Thiamine biosynthesis |
| 420 | HER17_RS20385 | 1.4 | 6.60E-03 | thiE | Thiamine biosynthesis |
| 421 | HER17_RS20400 | 0.82 | 1.20E-02 | ADT-0001274 | Thiamine biosynthesis |
| 422 | HER17_RS00335 | 2.62 | 2.40E-12 | ADT-0004348 | Thiamine metabolism |
| 423 | HER17_RS09550 | 2.35 | 2.70E-03 | ADT-0003491 | Toxin biosynthesis |
| 424 | HER17_RS09500 | 1.23 | 9.50E-06 | ADT-0002417 | Toxin-antitoxin system |
| 425 | HER17_RS00675 | 1.71 | 2.60E-02 | ADT-0004328 | Toxin-antitoxin system |
| 426 | HER17_RS00680 | 1.48 | 3.30E-02 | ADT-0004327 | Toxin-antitoxin system |
| 427 | HER17_RS04800 | 1.09 | 1.50E-02 | ADT-0006384 | Toxin-antitoxin system |
| 428 | HER17_RS04805 | 1.16 | 2.70E-03 | ADT-0003303 | Toxin-antitoxin system |
| 429 | HER17_RS19230 | 0.66 | 2.90E-02 | ADT-0003510 | Toxin-antitoxin system |
| 430 | HER17_RS19305 | 1.07 | 1.50E-02 | ADT-0003514 | Toxin-antitoxin system |
| 431 | HER17_RS05780 | 0.61 | 2.70E-02 | rpoE | Transcription regulation |
| 432 | HER17_RS00485 | 1.35 | 2.30E-08 | rpoH | Transcription regulation |
| 433 | HER17_RS20375 | -0.66 | 3.50E-03 | rsd | Transcription regulation |
| 434 | HER17_RS04695 | -0.78 | 4.10E-05 | crl | Transcription regulation |
| 435 | HER17_RS21780 | 1.43 | 4.90E-04 | ADT-0004354 | Transcription regulation |
| 436 | HER17_RS16885 | 2.11 | 7.70E-06 | ADT-0002478 | Transcription regulation |
| 437 | HER17_RS14315 | 1.62 | 4.00E-04 | ADT-0002684 | Transcription regulation |

| | | | | | |
|---|---|---|---|---|---|
| 438 | HER17_RS16870 | 1.21 | 4.70E-04 | ADT-0002477 | Transcription regulation |
| 439 | HER17_RS04140 | 0.84 | 1.30E-04 | ADT-0003120 | Transcription regulation |
| 440 | HER17_RS19760 | 2.75 | 1.40E-03 | ADT-0000116 | Transcription regulation |
| 441 | HER17_RS08385 | 1.21 | 4.20E-02 | betI | Transcription regulation |
| 442 | HER17_RS18855 | -0.67 | 3.90E-02 | ADT-0001340 | Transcription regulation |
| 443 | HER17_RS13930 | 1.31 | 3.60E-03 | ADT-0002707 | Transcriptional regulation |
| 444 | HER17_RS21345 | -0.65 | 2.80E-02 | ADT-0002321 | Transcriptional regulation |
| 445 | HER17_RS16840 | 1.73 | 3.20E-04 | ADT-0003331 | Transcriptional regulation |
| 446 | HER17_RS13235 | -0.7 | 1.30E-03 | ADT-0002988 | Transcriptional regulation |
| 447 | HER17_RS00865 | -0.77 | 2.50E-04 | cytR | Transcriptional regulation |
| 448 | HER17_RS12840 | 0.77 | 4.70E-03 | yieE | Transcriptional regulation |
| 449 | HER17_RS18885 | 2.37 | 5.60E-06 | ADT-0003531 | Transcriptional regulation |
| 450 | HER17_RS17855 | 2.19 | 2.40E-03 | ADT-0003392 | Transcriptional regulation |
| 451 | HER17_RS19240 | -0.45 | 3.40E-02 | ADT-0003512 | Transcriptional regulation |
| 452 | HER17_RS18880 | 1.92 | 3.00E-02 | ADT-0002471 | Transcriptional regulation |
| 453 | HER17_RS04665 | 1.25 | 9.60E-04 | ADT-0000893 | Transcriptional regulation |
| 454 | HER17_RS07395 | 1.46 | 1.40E-04 | ADT-0000751 | Transcriptional regulation |
| 455 | HER17_RS11585 | -0.58 | 3.40E-02 | ADT-0002905 | Transcriptional regulation |
| 456 | HER17_RS11820 | 1.32 | 4.90E-04 | ADT-0003618 | Transcriptional regulation |
| 457 | HER17_RS06865 | 0.93 | 3.80E-03 | ADT-0003036 | Transcriptional regulation |
| 458 | HER17_RS04830 | -0.56 | 3.30E-02 | ADT-0004156 | Transcriptional regulation |
| 459 | HER17_RS09440 | 0.92 | 3.30E-02 | ADT-0001160 | Transcriptional regulation |
| 460 | HER17_RS20900 | 1.57 | 7.50E-03 | ADT-0000036 | Transcriptional regulation |
| 461 | HER17_RS10740 | 1.09 | 4.20E-02 | ADT-0002869 | Transcriptional regulation |
| 462 | HER17_RS09175 | 3.28 | 1.70E-17 | ADT-0001691 | Transcriptional regulation |
| 463 | HER17_RS15575 | -0.41 | 2.00E-02 | rcsB | Transcriptional regulation |
| 464 | HER17_RS05390 | -1.01 | 1.60E-02 | raiA | Translation regulation |
| 465 | HER17_RS09395 | 1.6 | 7.70E-03 | yciH | Translation regulation |
| 466 | HER17_RS03715 | 0.91 | 2.00E-02 | ADT-0003617 | Transmembrane transport |
| 467 | HER17_RS15055 | -0.87 | 7.40E-03 | ADT-0001556 | Transmembrane transport |
| 468 | HER17_RS01460 | 1.14 | 3.20E-04 | ADT-0001116 | Transmembrane transport |
| 469 | HER17_RS00025 | -0.5 | 7.00E-03 | ADT-0001196 | Transmembrane transport |
| 470 | HER17_RS12335 | 0.39 | 1.40E-02 | ADT-0000685 | Transmembrane transport |
| 471 | HER17_RS10215 | 1.9 | 2.40E-02 | ADT-0002736 | Transmembrane transport |
| 472 | HER17_RS19025 | 1.68 | 3.40E-03 | ADT-0001331 | Transmembrane transport |
| 473 | HER17_RS19550 | 1.67 | 1.00E-03 | ADT-0002416 | Transmembrane transport |
| 474 | HER17_RS19960 | 0.66 | 3.00E-02 | ADT-0002380 | Transmembrane transport |
| 475 | HER17_RS17040 | 0.87 | 4.70E-02 | ADT-0003562 | Transmembrane transport |
| 476 | HER17_RS08745 | 1.43 | 2.70E-03 | ADT-0001665 | Transmembrane transport |
| 477 | HER17_RS21775 | 0.99 | 6.20E-04 | ADT-0003262 | Transmembrane transport |
| 478 | HER17_RS13990 | 0.73 | 2.60E-02 | ADT-0001618 | Transmembrane transport |
| 479 | HER17_RS10610 | -0.63 | 1.40E-03 | ADT-0001764 | Transmembrane transport |
| 480 | HER17_RS08750 | 1.8 | 2.10E-03 | ADT-0005548 | Transmembrane transport |

| | | | | | |
|---|---|---|---|---|---|
| 481 | HER17_RS07195 | 1.29 | 1.60E-04 | treC | Trehalose metabolism |
| 482 | HER17_RS12340 | -0.64 | 1.30E-03 | serS | tRNA aminoacylation |
| 483 | HER17_RS02025 | 0.43 | 2.40E-02 | tusB | tRNA modification |
| 484 | HER17_RS11625 | 0.32 | 2.30E-02 | mnmA | tRNA modification |
| 485 | HER17_RS10685 | -1.47 | 3.80E-03 | ADT-0003873 | tRNA processing |
| 486 | HER17_RS14290 | 3.53 | 7.40E-03 | No seq | tRNA processing |
| 487 | HER17_RS01210 | -0.69 | 2.90E-02 | No seq | tRNA processing |
| 488 | HER17_RS08485 | 2.22 | 4.70E-04 | No seq | tRNA processing |
| 489 | HER17_RS01015 | 1.23 | 5.90E-03 | No seq | tRNA processing |
| 490 | HER17_RS10930 | -0.47 | 2.00E-03 | trpCF | Tryptophan biosynthesis |
| 491 | HER17_RS04920 | -2.35 | 2.10E-02 | ADT-0005888 | Type VI secretion system |
| 492 | HER17_RS00310 | -2.69 | 2.60E-02 | ADT-0005888 | Type VI secretion system |
| 493 | HER17_RS06490 | -0.95 | 1.70E-04 | ADT-0001973 | Unknown |
| 494 | HER17_RS19830 | 0.36 | 3.90E-02 | ADT-0000110 | Unknown |
| 495 | HER17_RS10710 | -0.39 | 8.60E-04 | ynfB | Unknown |
| 496 | HER17_RS19055 | 1.91 | 1.20E-15 | ADT-0001329 | Unknown |
| 497 | HER17_RS19295 | 0.71 | 3.20E-03 | ADT-0001325 | Unknown |
| 498 | HER17_RS02605 | 0.96 | 1.50E-02 | ADT-0001017 | Unknown |
| 499 | HER17_RS03935 | 1.5 | 6.60E-04 | ADT-0000930 | Unknown |
| 500 | HER17_RS18255 | -2.15 | 3.80E-02 | ADT-0003367 | Unknown |
| 501 | HER17_RS18925 | 1.42 | 4.60E-02 | ADT-0003529 | Unknown |
| 502 | HER17_RS03355 | 0.76 | 1.10E-02 | ADT-0000967 | Unknown |
| 503 | HER17_RS15970 | -0.45 | 3.70E-02 | ADT-0000271 | Unknown |
| 504 | HER17_RS09625 | -0.84 | 2.00E-04 | ADT-0000523 | Unknown |
| 505 | HER17_RS04300 | -0.43 | 7.40E-03 | ADT-0003116 | Unknown |
| 506 | HER17_RS09170 | 3.44 | 2.50E-14 | ADT-0000495 | Unknown |
| 507 | HER17_RS00690 | 0.49 | 4.00E-02 | ADT-0004326 | Unknown |
| 508 | HER17_RS19190 | -0.95 | 1.80E-02 | ADT-0002442 | Unknown |
| 509 | HER17_RS16775 | 0.91 | 6.20E-03 | ADT-0005463 | Unknown |
| 510 | HER17_RS01345 | -0.38 | 1.00E-02 | ADT-0001129 | Unknown |
| 511 | HER17_RS15265 | 1.21 | 2.70E-02 | ybeD | Unknown |
| 512 | HER17_RS02235 | -0.33 | 2.30E-02 | smg | Unknown |
| 513 | HER17_RS21795 | 1.9 | 2.20E-08 | ADT-0003260 | Unknown |
| 514 | HER17_RS16955 | 1.42 | 2.70E-02 | ADT-0001447 | Unknown |
| 515 | HER17_RS04060 | -0.6 | 4.70E-04 | ADT-0002654 | Unknown |
| 516 | HER17_RS08740 | 1.84 | 3.70E-04 | ADT-0000467 | Unknown |
| 517 | HER17_RS16880 | 3.26 | 2.60E-09 | ADT-0005461 | Unknown |
| 518 | HER17_RS04740 | 3.39 | 1.00E-02 | ADT-0003414 | Unknown |
| 519 | HER17_RS20950 | 1.55 | 9.80E-03 | ADT-0000033 | Unknown |
| 520 | HER17_RS09205 | 2.13 | 5.60E-03 | ADT-0006304 | Unknown |
| 521 | HER17_RS07640 | 0.97 | 2.70E-02 | ADT-0003279 | Unknown |
| 522 | HER17_RS20245 | 2.84 | 2.70E-07 | ADT-0003456 | Unknown |
| 523 | HER17_RS04765 | 1.56 | 3.50E-03 | ADT-0003456 | Unknown |

| | | | | | |
|---|---|---|---|---|---|
| 524 | HER17_RS06175 | -1.03 | 1.40E-04 | ADT-0003048 | Unknown |
| 525 | HER17_RS00655 | -0.51 | 4.20E-02 | ADT-0003237 | Unknown |
| 526 | HER17_RS09535 | 1.39 | 6.30E-07 | ADT-0003488 | Unknown |
| 527 | HER17_RS11600 | -0.71 | 3.90E-02 | ADT-0003910 | Unknown |
| 528 | HER17_RS13170 | -2.59 | 3.20E-14 | ADT-0001904 | Unknown |
| 529 | HER17_RS10680 | -1.81 | 7.70E-03 | ADT-0003874 | Unknown |
| 530 | HER17_RS09600 | 1.39 | 4.90E-04 | ADT-0005561 | Unknown |
| 531 | HER17_RS21915 | 1.18 | 3.00E-03 | ADT-0000849 | Unknown |
| 532 | HER17_RS12715 | 1.77 | 3.10E-06 | ADT-0003291 | Unknown |
| 533 | HER17_RS16875 | 1.76 | 7.20E-04 | ADT-0005462 | Unknown |
| 534 | HER17_RS16835 | -2.7 | 1.50E-03 | ADT-0003330 | Unknown |
| 535 | HER17_RS14015 | 1.15 | 3.50E-02 | ADT-0002727 | Unknown |
| 536 | HER17_RS18270 | -3.66 | 1.60E-04 | ADT-0002500 | Unknown |
| 537 | HER17_RS01475 | -0.36 | 4.50E-02 | ADT-0004278 | Unknown |
| 538 | HER17_RS10390 | -0.48 | 1.20E-02 | ADT-0000555 | Unknown |
| 539 | HER17_RS22140 | 1.53 | 8.90E-03 | ypfM | Unknown |
| 540 | HER17_RS07820 | 0.77 | 3.80E-02 | ADT-0003299 | Unknown |
| 541 | HER17_RS16890 | 1.61 | 1.30E-03 | ADT-0003573 | Unknown |
| 542 | HER17_RS15775 | 1.41 | 4.90E-05 | ADT-0000288 | Unknown |
| 543 | HER17_RS15020 | 1.19 | 3.80E-02 | ADT-0000344 | Unknown |
| 544 | HER17_RS12075 | -0.95 | 3.20E-02 | ADT-0001855 | Unknown |
| 545 | HER17_RS11920 | -0.45 | 1.00E-02 | ADT-0002924 | Unknown |
| 546 | HER17_RS10975 | -0.51 | 1.80E-03 | ADT-0000597 | Unknown |
| 547 | HER17_RS10880 | -0.74 | 2.30E-02 | ADT-0000586 | Unknown |
| 548 | HER17_RS08850 | 1.37 | 1.90E-07 | ADT-0001673 | Unknown |
| 549 | HER17_RS12940 | 1.97 | 1.20E-12 | ADT-0001896 | Unknown |
| 550 | HER17_RS07095 | -1.2 | 3.60E-02 | ADT-0000772 | Unknown |
| 551 | HER17_RS11090 | 0.66 | 2.70E-03 | ADT-0001791 | Unknown |
| 552 | HER17_RS09195 | 2.62 | 2.80E-03 | ADT-0003824 | Urea metabolism |
| 553 | HER17_RS09210 | 1.73 | 6.90E-03 | uca | Urea metabolism |
| 554 | HER17_RS09180 | 5.44 | 4.00E-13 | ADT-0001692 | Urea transport |
| 555 | HER17_RS14700 | -0.56 | 4.50E-02 | ADT-0000378 | Vitamin B6 metabolism |
| 556 | HER17_RS21080 | 1.46 | 2.30E-02 | xylF | Xylose transport |
| 557 | HER17_RS21075 | 2.03 | 6.10E-03 | ADT-0001237 | Xylose transport |

**Table 10: M6 (*metA*::Tn5)** Differentially Expressed Genes (DEGs). $log_2$FoldChange > 0 Upregulated, and $log_2$FoldChange < 0 Downregulated

| # | Locus Tag (NCBI) | $Log_2$FC | padj | Gene Name | Affected Pathway |
|---|---|---|---|---|---|
| 1 | HER17_RS01405 | -0.71 | 2.30E-02 | rhtB | Amino acid transport |
| 2 | HER17_RS01075 | -0.65 | 2.90E-04 | ilvD | Branched-chain amino acid biosynthesis |
| 3 | HER17_RS01080 | -0.56 | 2.90E-04 | ilvA | Branched-chain amino acid biosynthesis |
| 4 | HER17_RS01070 | -0.72 | 4.00E-04 | ilvE | Branched-chain amino acid metabolism |
| 5 | HER17_RS21115 | 0.51 | 4.00E-02 | ADT-0000027 | Chemotaxis |
| 6 | HER17_RS09925 | 1.17 | 1.20E-03 | ADT-0003843 | Chemotaxis |
| 7 | HER17_RS17995 | -1.34 | 6.40E-03 | gcvP | Glycine metabolism |
| 8 | HER17_RS18005 | -0.78 | 2.50E-02 | gcvT | Glycine metabolism |
| 9 | HER17_RS01440 | -1.22 | 2.40E-02 | glpC | Glycerol metabolism |
| 10 | HER17_RS00725 | -0.55 | 1.80E-02 | pfkA | Glycolysis |
| 11 | HER17_RS02285 | 1.4 | 9.70E-05 | metA | Methionine biosynthesis |
| 12 | HER17_RS20665 | -1.04 | 3.30E-02 | udp | Nucleotide metabolism |
| 13 | HER17_RS18265 | -2.89 | 3.40E-02 | ADT-0003365 | Secondary metabolism |
| 14 | HER17_RS18975 | -0.71 | 1.70E-02 | ADT-0003524 | Phage assembly |
| 15 | HER17_RS02650 | -0.88 | 2.70E-02 | sprT | Protein degradation |
| 16 | HER17_RS11210 | -0.84 | 1.70E-02 | ADT-0002884 | Unknown |
| 17 | HER17_RS16835 | -2.99 | 2.40E-02 | ADT-0003330 | Unknown |
| 18 | HER17_RS05035 | -1.12 | 2.30E-02 | ADT-0002059 | Unknown |
| 19 | HER17_RS04300 | -0.49 | 3.40E-02 | ADT-0003116 | Unknown |
| 20 | HER17_RS21915 | 1.55 | 3.30E-02 | ADT-0000849 | Unknown |

**Table 11: M8 (*prtW*::Tn5)** Differentially Expressed Genes (DEGs). $log_2$FoldChange > 0 Upregulated, and $log_2$FoldChange < 0 Downregulated

| # | Locus Tag (NCBI) | $Log_2FC$ | padj | Gene Name | Affected Pathway |
|---|---|---|---|---|---|
| 1 | HER17_RS12560 | -1.38 | 2.00E-02 | ADT-0001884 | ABC transport |
| 2 | HER17_RS16455 | -1.46 | 9.40E-03 | ADT-0002577 | ABC transport |
| 3 | HER17_RS16460 | -1 | 9.70E-03 | ADT-0002578 | ABC transport |
| 4 | HER17_RS02730 | -0.81 | 1.40E-02 | ADT-0002186 | Alcohol metabolism |
| 5 | HER17_RS16465 | -1.32 | 4.20E-02 | ADT-0003580 | Amino acid metabolism |
| 6 | HER17_RS20290 | 1.46 | 2.70E-02 | aapJ | Amino acid transport |
| 7 | HER17_RS01100 | -0.54 | 4.20E-02 | ilvC | Branched-chain amino acid biosynthesis |
| 8 | HER17_RS13815 | -0.83 | 2.30E-02 | ADT-0003712 | Carbohydrate metabolism |
| 9 | HER17_RS18710 | -1.99 | 4.20E-02 | uxaB1 | Carbohydrate metabolism |
| 10 | HER17_RS13260 | 1.35 | 4.10E-03 | pbpG | Cell wall metabolism |
| 11 | HER17_RS12775 | 2.41 | 2.40E-08 | ADT-0001887 | Chemotaxis |
| 12 | HER17_RS17170 | -1.6 | 9.70E-03 | cysK | Cysteine biosynthesis |
| 13 | HER17_RS12975 | 1.14 | 3.40E-03 | yejK | DNA organization |
| 14 | HER17_RS13060 | 1 | 4.20E-02 | dps | DNA protection |
| 15 | HER17_RS12850 | 1.6 | 2.30E-05 | nfo | DNA repair |
| 16 | HER17_RS08035 | -1.33 | 2.90E-04 | ADT-0001931 | Flagellar motility |
| 17 | HER17_RS12770 | 1.09 | 9.70E-03 | folE | Folate biosynthesis |
| 18 | HER17_RS12790 | 0.98 | 2.20E-07 | adhC | Formaldehyde detoxification |
| 19 | HER17_RS12795 | 0.92 | 4.40E-06 | fghA | Formaldehyde detoxification |
| 20 | HER17_RS18720 | -3.46 | 1.30E-03 | exuT | Galacturonate transport |
| 21 | HER17_RS13065 | 1.22 | 9.30E-04 | glnH | Glutamine transport |
| 22 | HER17_RS13070 | 1.36 | 9.10E-06 | glnP | Glutamine transport |
| 23 | HER17_RS13075 | 1.34 | 2.40E-04 | glnQ | Glutamine transport |
| 24 | HER17_RS01430 | 1.46 | 2.80E-02 | glpA | Glycerol metabolism |
| 25 | HER17_RS01510 | 1.57 | 4.30E-02 | glpD | Glycerol metabolism |
| 26 | HER17_RS01425 | 1.68 | 1.00E-02 | glpT | Glycerol metabolism |
| 27 | HER17_RS13020 | 1.1 | 1.40E-02 | EstC | Hydrolase activity |
| 28 | HER17_RS12985 | 1.43 | 8.00E-04 | yejM | LPS biosynthesis |
| 29 | HER17_RS21365 | 0.84 | 1.90E-02 | eptB | LPS modification |
| 30 | HER17_RS13650 | 1.15 | 3.50E-02 | ADT-0003732 | Metal stress response |
| 31 | HER17_RS07355 | -1.13 | 8.80E-03 | ADT-0001936 | Methionine salvage pathway |
| 32 | HER17_RS12945 | 1.31 | 3.90E-02 | bcr | Multidrug efflux |
| 33 | HER17_RS14235 | -1.96 | 1.80E-05 | pnl | Pectin degradation |
| 34 | HER17_RS11025 | 0.72 | 9.40E-03 | oppA | Peptide transport |
| 35 | HER17_RS11005 | 0.57 | 2.10E-02 | oppD | Peptide transport |
| 36 | HER17_RS12890 | 1.33 | 4.90E-02 | ADT-0000709 | Phosphate metabolism |
| 37 | HER17_RS13220 | -1.45 | 2.40E-02 | inh | Protease inhibition |
| 38 | HER17_RS13225 | -4.48 | 8.50E-20 | prtW | Protein degradation |
| 39 | HER17_RS02650 | -0.91 | 3.40E-03 | sprT | Protein degradation |
| 40 | HER17_RS04915 | -1.97 | 4.70E-02 | ADT-0000876 | Protein-protein interactions |

| | | | | | |
|---|---|---|---|---|---|
| 41 | HER17_RS12785 | 1.29 | 2.40E-02 | ptrR | Putrescine metabolism regulation |
| 42 | HER17_RS12755 | 1.12 | 4.40E-03 | rimO | Ribosome modification |
| 43 | HER17_RS12920 | 1.28 | 4.70E-02 | ADT-0000711 | Solute transport |
| 44 | HER17_RS19655 | -1.87 | 2.60E-05 | scrB | Sucrose metabolism |
| 45 | HER17_RS19650 | -1.94 | 7.90E-04 | ADT-0002393 | Sucrose transport |
| 46 | HER17_RS13030 | 2.85 | 1.40E-02 | ADT-0001900 | Sulfur metabolism |
| 47 | HER17_RS05780 | 0.67 | 8.60E-03 | rpoE | Transcription regulation |
| 48 | HER17_RS13040 | 1.41 | 5.50E-11 | ADT-0001901 | Transmembrane transport |
| 49 | HER17_RS10745 | -0.86 | 2.40E-02 | ynfM | Transmembrane transport |
| 50 | HER17_RS04930 | -1.14 | 1.10E-02 | ADT-0004153 | Type VI secretion system |
| 51 | HER17_RS04920 | -2.66 | 6.80E-03 | ADT-0005888 | Type VI secretion system |
| 52 | HER17_RS12980 | 1.47 | 2.10E-04 | ADT-0000717 | Unknown |
| 53 | HER17_RS05690 | -1.74 | 1.40E-02 | ADT-0000847 | Unknown |
| 54 | HER17_RS12940 | 1.61 | 9.40E-03 | ADT-0001896 | Unknown |
| 55 | HER17_RS13025 | 1.32 | 7.10E-09 | ADT-0001899 | Unknown |
| 56 | HER17_RS04940 | -1.88 | 3.90E-04 | ADT-0002063 | Unknown |
| 57 | HER17_RS03965 | 1.14 | 3.50E-04 | ADT-0002106 | Unknown |
| 58 | HER17_RS12845 | 1.96 | 2.00E-03 | ADT-0002975 | Unknown |
| 59 | HER17_RS12780 | 2.53 | 3.40E-13 | ADT-0005637 | Unknown |

**Table 12.** Shared Differentially Expressed Genes (DEGs) between mutants M1(*gacS*), M2(*purM*), and M8(*prtW*).

| Locus Tag (NCBI) | Gene Name | Regulation | Product | Pathway |
|---|---|---|---|---|
| HER17_RS01100 | ilvC | ↓ | ketol-acid reductoisomerase | Branched-chain amino acid biosynthesis |
| HER17_RS04920 | ADT-0005888 | ↓ | Hcp family type VI secretion system effector | Type VI secretion system |
| HER17_RS08035 | ADT-0001931 | ↓ | flagellin (*fliC*) | Flagellar motility |
| HER17_RS14235 | pnl | ↓ | pectate lyase | Pectin Degradation |
| HER17_RS17170 | cysK | ↓ | cysteine synthase A | Cysteine biosynthesis |
| HER17_RS18720 | exuT | ↓ | MFS transporter | Galacturonate transport |
| HER17_RS20290 | aapJ | ↑ | amino acid ABC transporter substrate-binding protein | Amino acid transport |

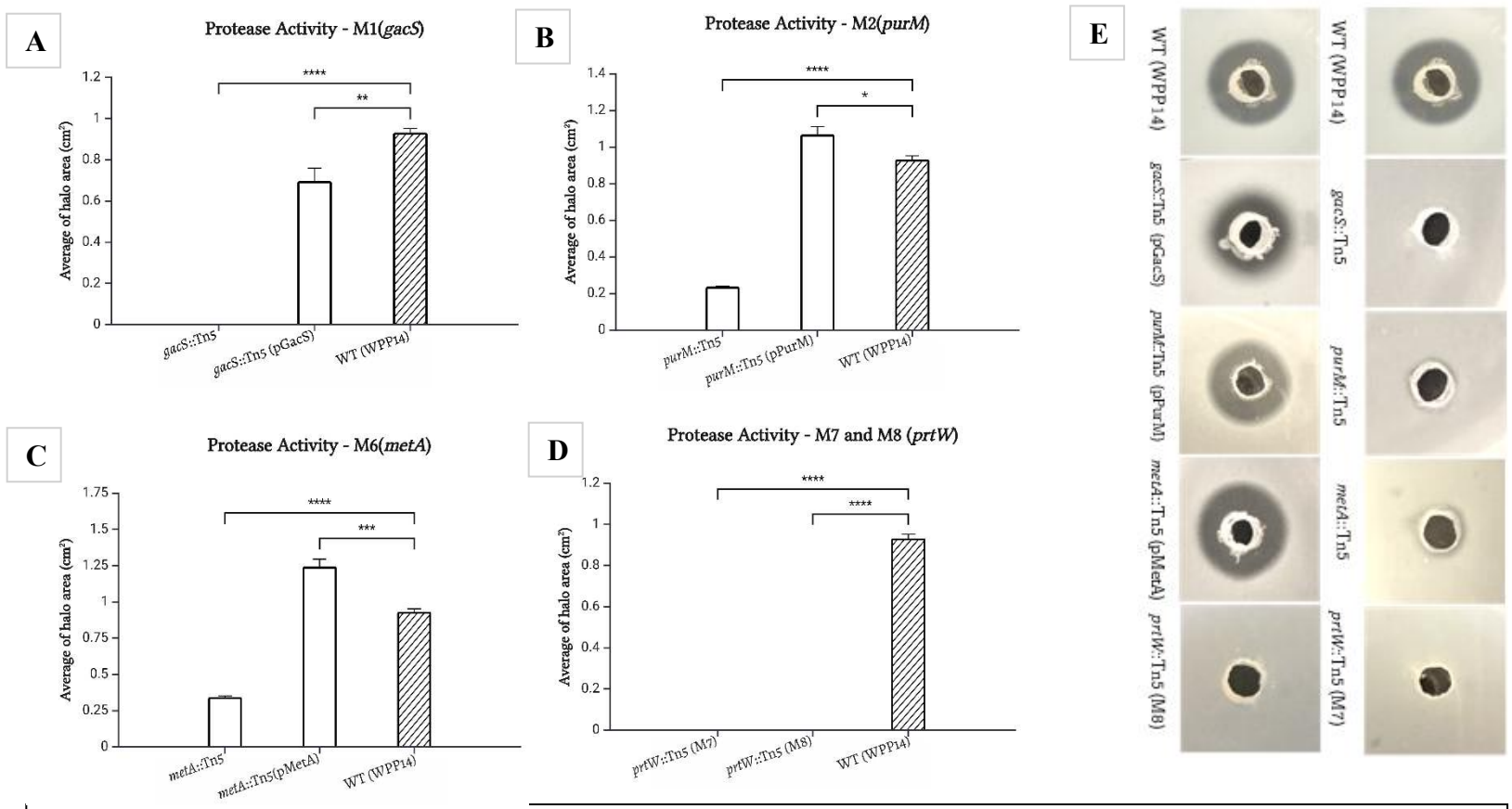


**Figure 1. Protease activity of Pectobacterium carotovorum WPP14 (WT) and Mutants. (A-D)** Protease activity for mutants M1 (gacS), M2 (purM), M6 (metA), and M8 (prtW) was measured as the average halo zone (cm²) on skim milk agar plates. Both gacS (M1) and prtW (M7 and M8) mutants exhibited a complete loss of protease activity ($p < 0.0001$) compared to WT, while purM (M2) and metA (M6) mutants showed a significant reduction. Complementation restored protease activity, with *gacS*::Tn5(pGacS), *purM*::Tn5(pPurM), and *metA*::Tn5(pMetA) displaying partial to near-complete recovery. Statistical significance was determined using one-way ANOVA followed by Tukey's HSD test. The data represent the average results of three independent experiments, with each experiment including three replicates per strain. **(E)** Representative images of protease activity assays showing halo formation for WT, mutants, and their complemented strains. The clear halos indicate proteolytic activity, absent in M1 (*gacS*), M7 & M8 (*prtW*), and significantly reduced in M2 (*purM*) and M6 (*metA*), further confirming the protease assay results.

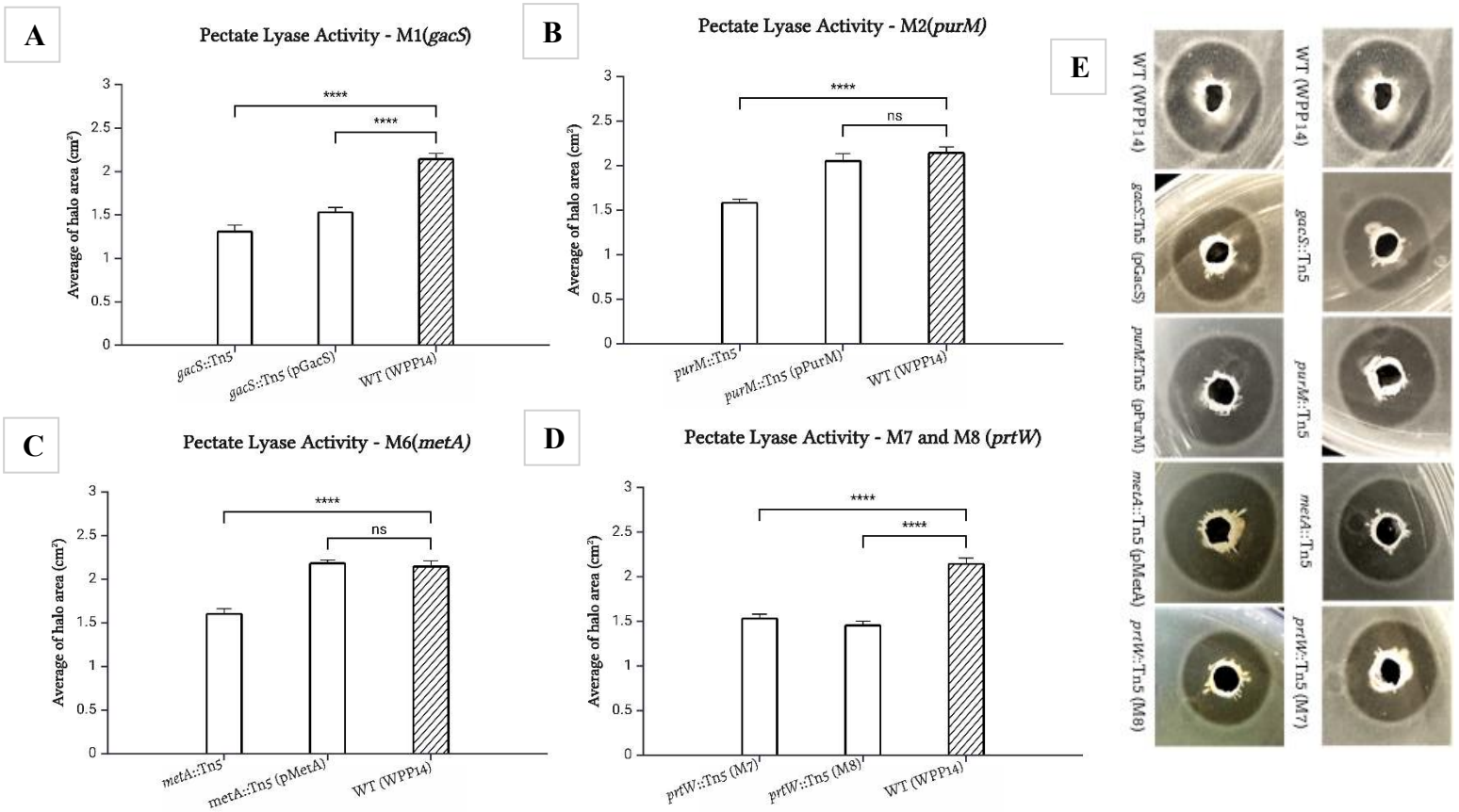


**Figure 2. Pectate lyase activity of *Pectobacterium carotovorum* WPP14 (WT) and mutants. (A-D)** Pectate lyase activity for mutants M1 (*gacS*), M2 (*purM*), M6 (*metA*), and M7 / M8 (*prtW*), measured as halo zones (cm²) on PGA agar. All mutants showed reduced activity, with the most significant reduction in M1 (*gacS*) and M8 (*prtW*). Complementation fully restored activity in *purM*::Tn5(pPurM) and *metA::*Tn5(pMetA), while *gacS::*Tn5(pGacS) showed partial restoration. Data represent the mean of three independent experiments with three replicates per strain. **(E)** Representative images of pectate lyase activity assays. Clear halos indicate pectate lyase activity, which was reduced in all mutants, particularly in M1 (*gacS*) and M8 (*prtW*), supporting their role in pectate lyase virulence.

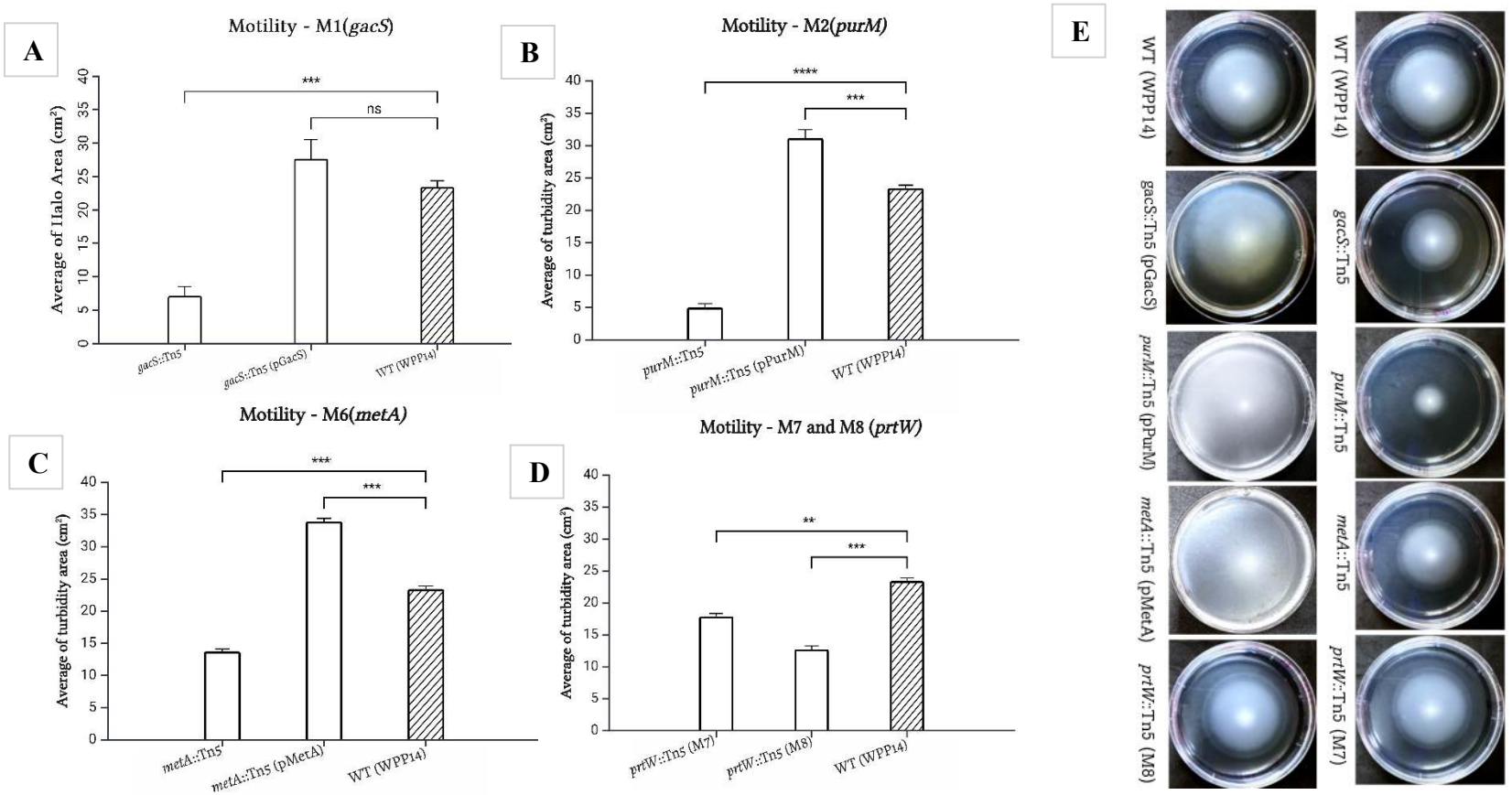


**Figure 3. Motility assay of *Pectobacterium carotovorum* WPP14 (WT) and mutants. (A–D)** Motility of mutants M1 (*gacS*), M2 (*purM*), M6 (*metA*), and M7/M8 (*prtW*) were significantly reduced compared to WT, as determined by one-way ANOVA with Tukey's post hoc test, suggesting their involvement in motility regulation. The most significant reduction was observed in M2 (*purM*), followed by M1 (*gacS*). **(E)** Representative images of motility assays show the reduced motility of the mutants compared to WT. Complementation of all mutants fully restored motility to WT levels.

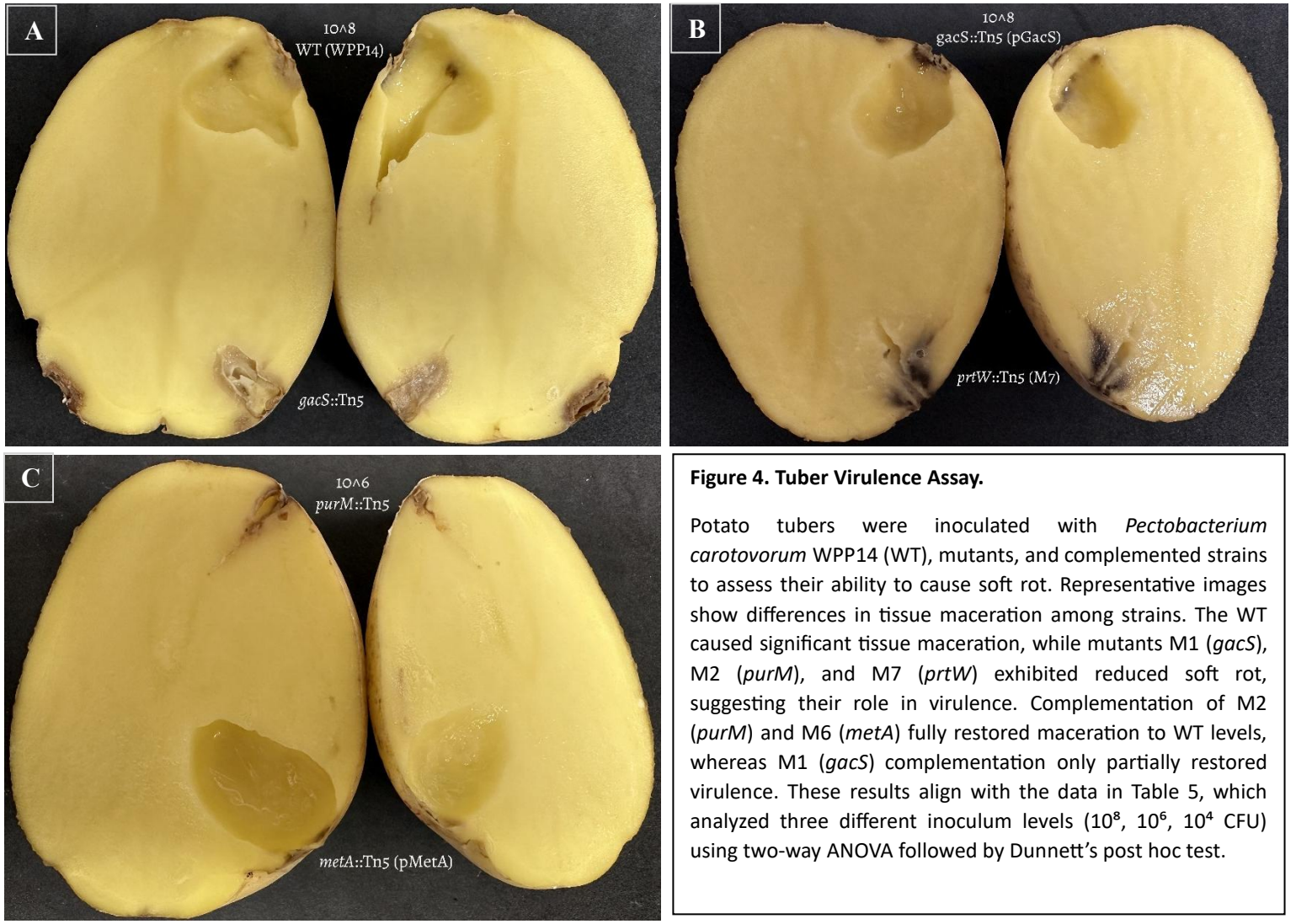


**Figure 4. Tuber Virulence Assay.**

Potato tubers were inoculated with *Pectobacterium carotovorum* WPP14 (WT), mutants, and complemented strains to assess their ability to cause soft rot. Representative images show differences in tissue maceration among strains. The WT caused significant tissue maceration, while mutants M1 (*gacS*), M2 (*purM*), and M7 (*prtW*) exhibited reduced soft rot, suggesting their role in virulence. Complementation of M2 (*purM*) and M6 (*metA*) fully restored maceration to WT levels, whereas M1 (*gacS*) complementation only partially restored virulence. These results align with the data in Table 5, which analyzed three different inoculum levels ($10^8$, $10^6$, $10^4$ CFU) using two-way ANOVA followed by Dunnett's post hoc test.

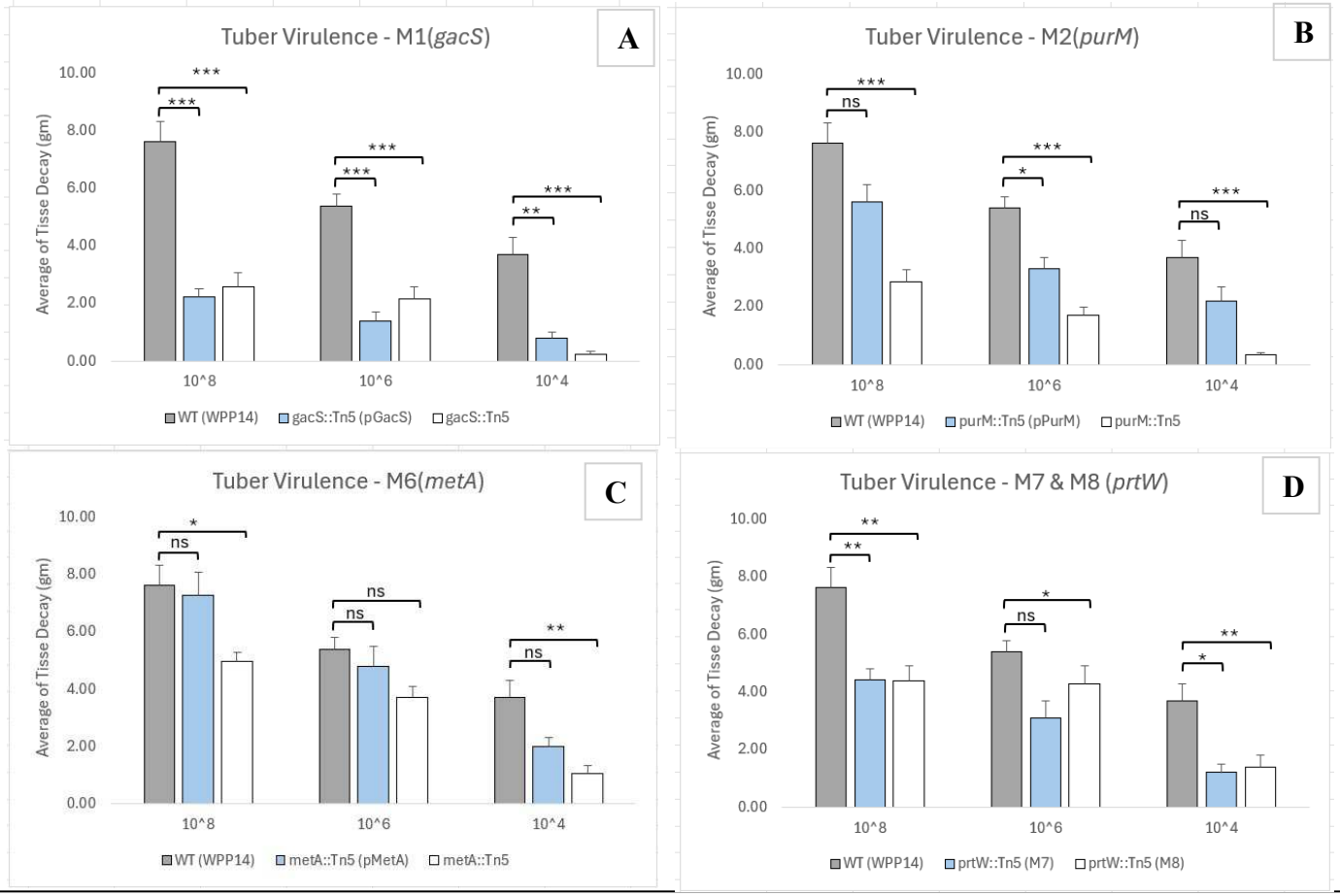


**Figure 4. Tuber Virulence Assay.** The average tissue maceration caused by *Pectobacterium carotovorum* WPP14 wild-type (WT) mutants and their complemented strains was quantified at three different inoculum levels ($10^8$, $10^6$, and $10^4$ CFU). (A–D) Graphs show the mean tissue decay (gm) for each mutant and its complemented strain. Mutants M1 (*gacS*), M2 (*purM*), M6 (*metA*), and M7/M8 (*prtW*) exhibited significantly reduced virulence compared to WT, with the strongest reduction observed in M1 (*gacS*), particularly at the lowest inoculum level ($10^4$ CFU). The most severe impairment in tissue maceration occurred in M1 (*gacS*) and M2 (*purM*), confirming their role in virulence regulation. Complementation of M2 (*purM*) and M6 (*metA*) fully restored virulence to WT levels, whereas M1 (*gacS*) complementation only partially restored maceration. Statistical significance was determined using two-way ANOVA followed by Dunnett's post hoc test ($p \leq 0.05$). These results align with the qualitative observations in Figure 3 and the summary data in Table 5.

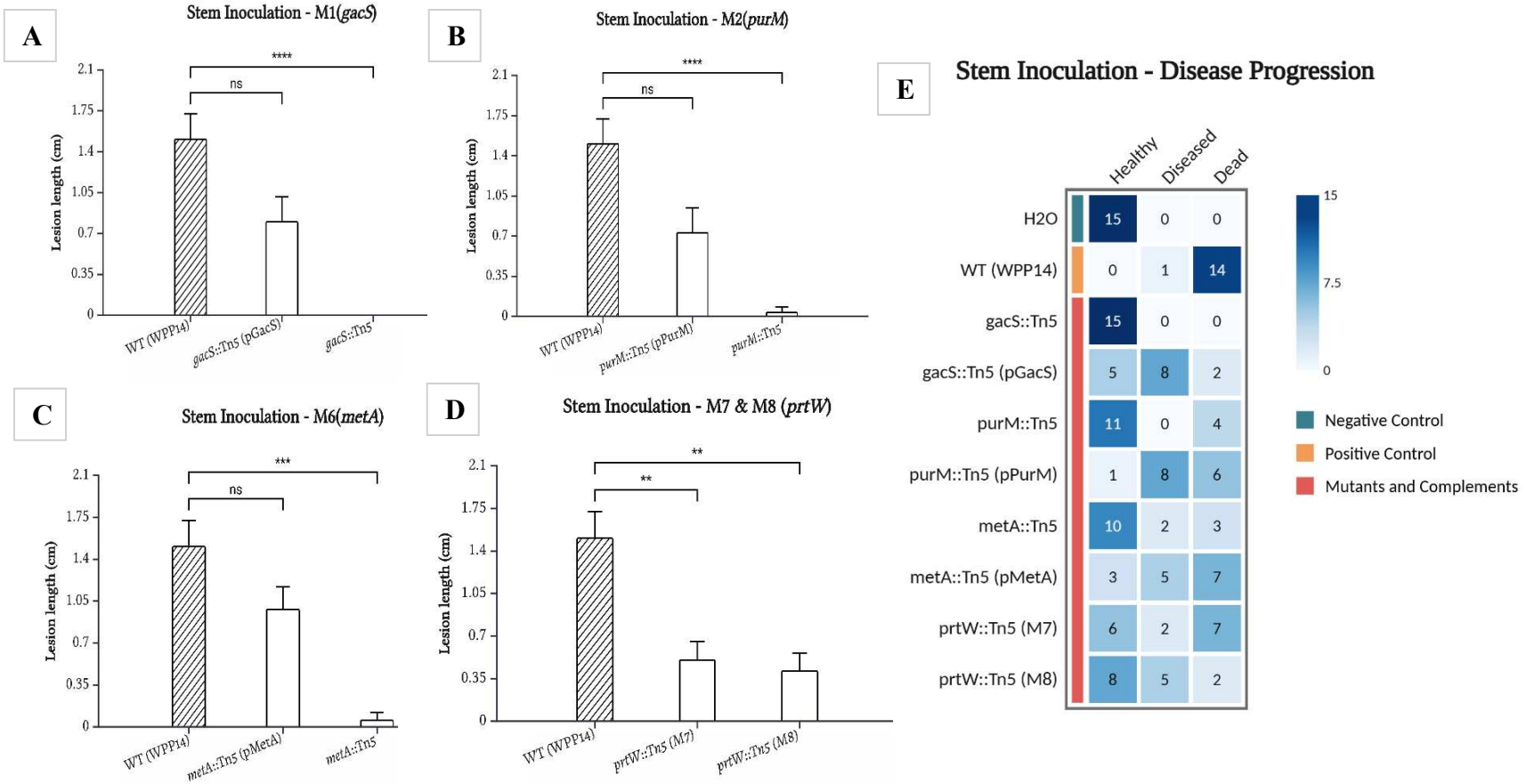


**Figure 5-1. Stem Inoculation Assay.** Lesion length measurements **(A-D)** and disease progression **(E)** were assessed in potato stems inoculated with WT, mutants, and complemented strains. Stem lesion formation was significantly reduced in all mutants compared to WT, with M1 (*gacS*) and M2 (*purM*) showing the most significant reduction in virulence, as indicated by minimal lesion formation and a higher proportion of healthy plants. Complementation of M2 (*purM*) and M6 (*metA*) fully restored the WT phenotype, while M1 (*gacS*) complementation was only partially restored. Statistical significance was determined using the Kruskal-Wallis test, followed by Dunn's post hoc test for lesion length and Fisher's exact test for disease progression ($p \leq 0.05$).


**Figure 5-2. Stem Inoculation: Disease Progression.** Representative images of potato stems inoculated with WT (*WPP14*), mutant M2 (*purM*::Tn5), and its complemented strain *purM*::Tn5(pPurM) at Day 1 and Day 2 post-inoculation. Stems were inoculated with two freshly cultured colonies (~5 mm each) from NA plates. WT-inoculated plants started showing symptoms from Day 1 and exhibited severe wilting and disease symptoms (stem rot and browning of the stem) by Day 2. In contrast, M2 (*purM*::Tn5) remained healthy with no visible disease symptoms. M2 complementation *purM*::Tn5(pPurM) restored virulence, leading to disease symptoms almost similar to the WT.

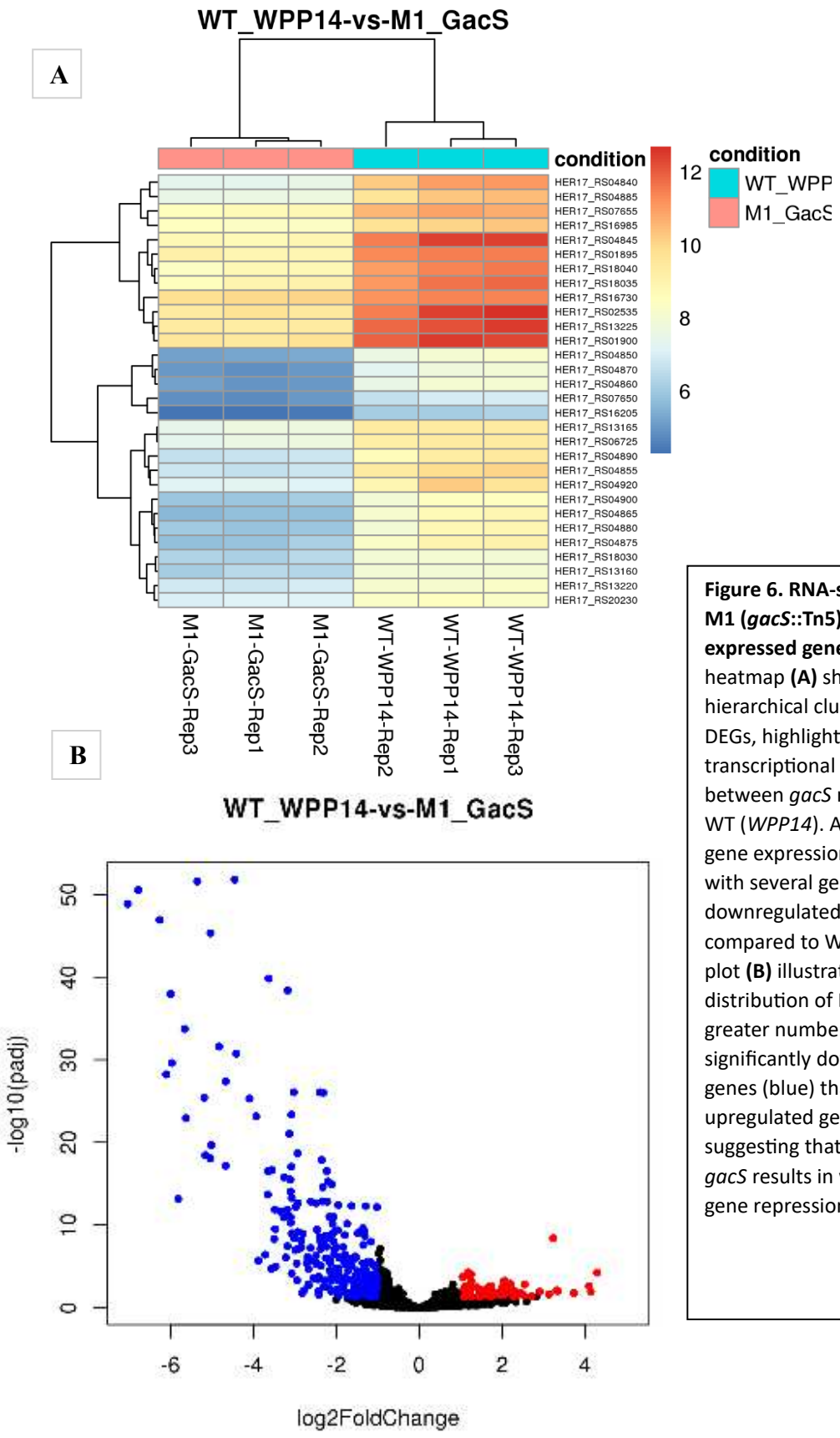


**Figure 6. RNA-seq analysis of M1 (*gacS*::Tn5) differentially expressed genes (DEGs).** The heatmap **(A)** shows hierarchical clustering of DEGs, highlighting distinct transcriptional differences between *gacS* mutant and WT (*WPP14*). A clear shift in gene expression is observed, with several genes strongly downregulated in the mutant compared to WT. The volcano plot **(B)** illustrates the overall distribution of DEGs, with a greater number of significantly downregulated genes (blue) than upregulated genes (red), suggesting that disrupting *gacS* results in widespread gene repression.

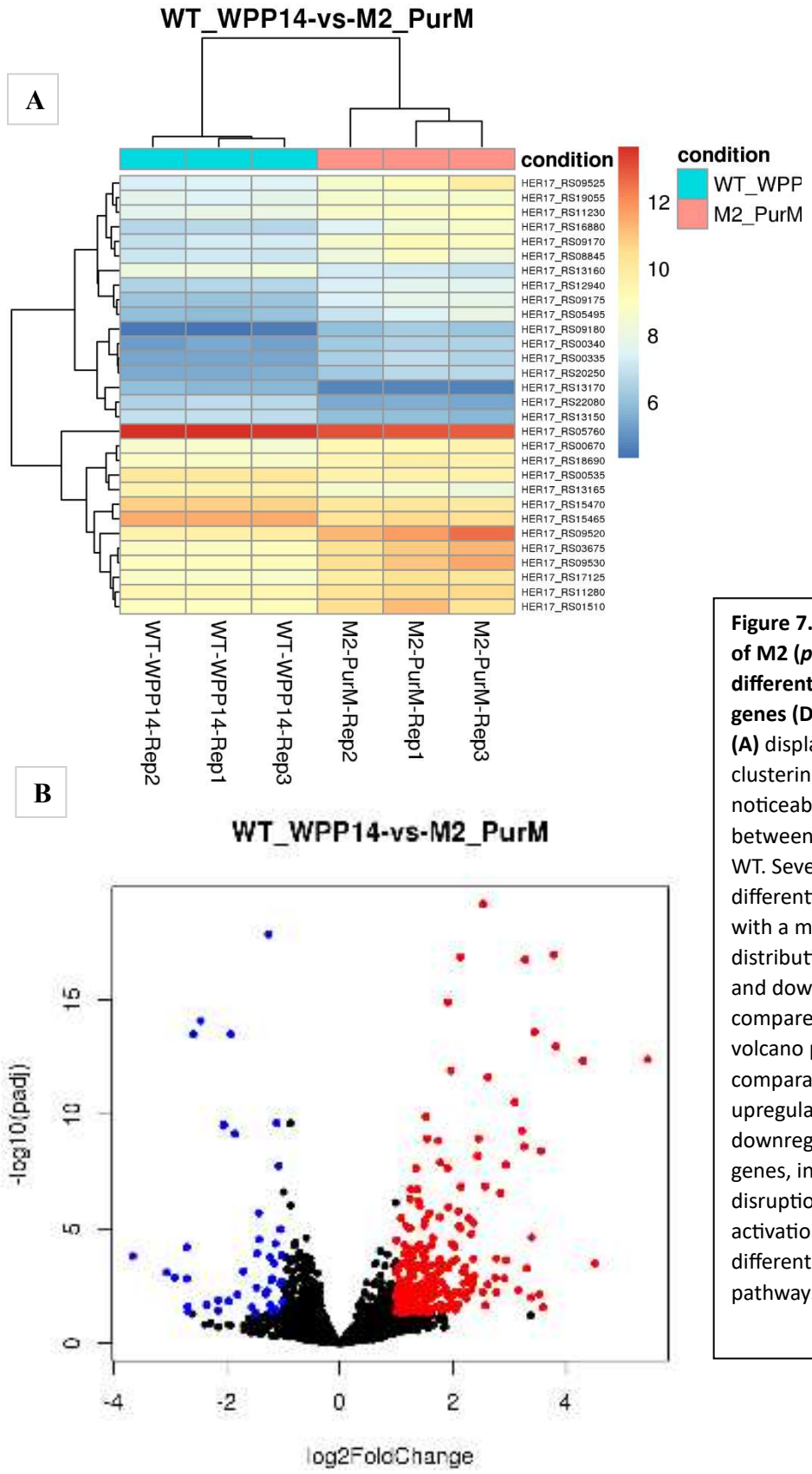


**Figure 7. RNA-seq analysis of M2 (*purM*::Tn5) differentially expressed genes (DEGs).** The heatmap **(A)** displays hierarchical clustering of DEGs, showing noticeable differences between purM mutant and WT. Several genes are differentially expressed, with a more balanced distribution of upregulated and downregulated genes compared to *gacS*. The volcano plot **(B)** reveals a comparable number of upregulated (red) and downregulated (blue) genes, indicating that *purM* disruption leads to both activation and repression of different regulatory pathways.

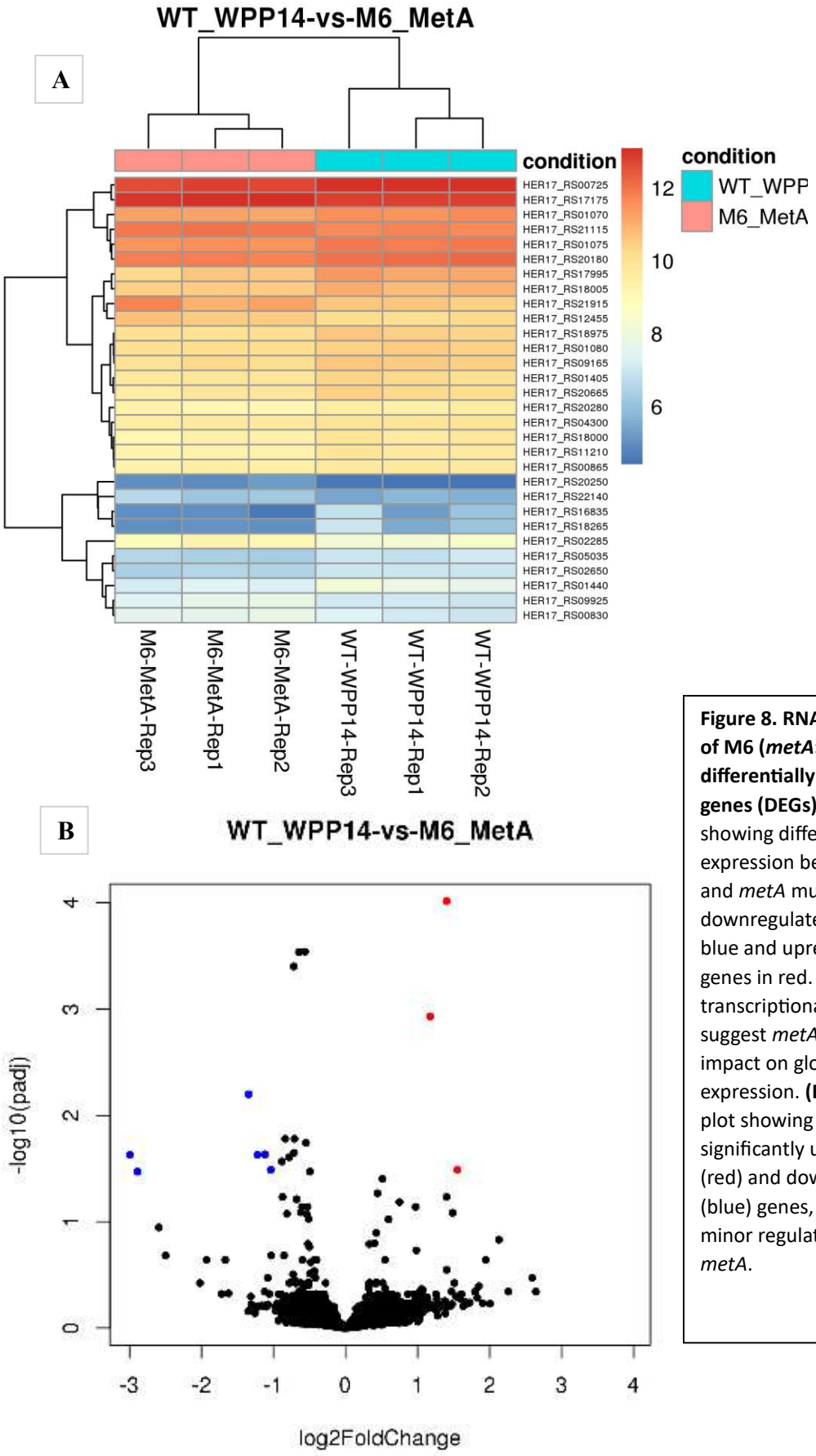


**Figure 8. RNA-seq analysis of M6 (*metA*::Tn5) differentially expressed genes (DEGs). (A)** Heatmap showing differential gene expression between WT and *metA* mutant, with downregulated genes in blue and upregulated genes in red. Minimal transcriptional changes suggest *metA* has a limited impact on global gene expression. **(B)** Volcano plot showing few significantly upregulated (red) and downregulated (blue) genes, indicating a minor regulatory role for *metA*.

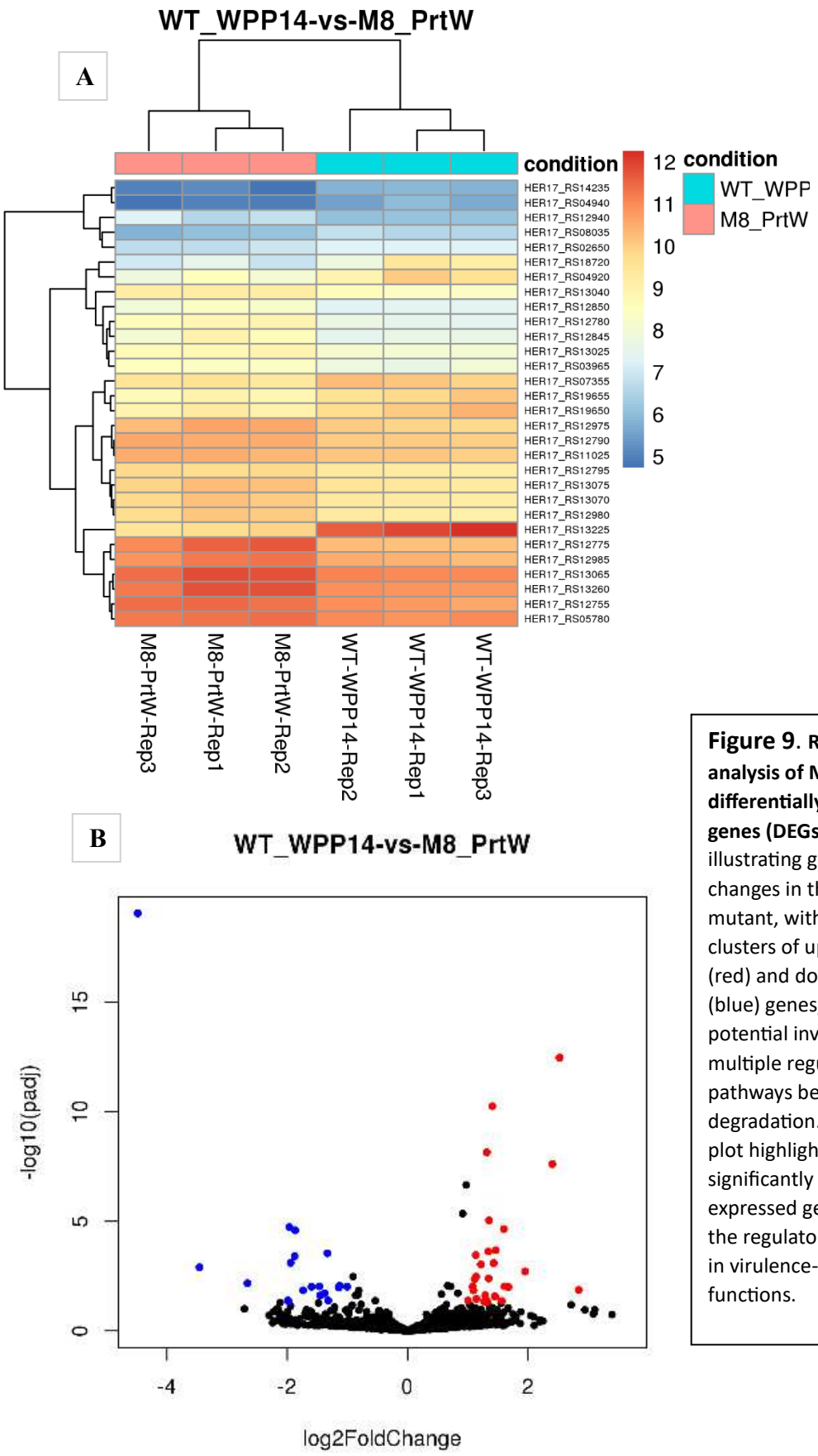


**Figure 9. RNA-seq analysis of M8 (*prtW*::Tn5) differentially expressed genes (DEGs). (A)** Heatmap illustrating gene expression changes in the *prtW* mutant, with distinct clusters of upregulated (red) and downregulated (blue) genes, suggesting its potential involvement in multiple regulatory pathways beyond protein degradation. **(B)** Volcano plot highlighting significantly differentially expressed genes, reflecting the regulatory role of *prtW* in virulence-related functions.

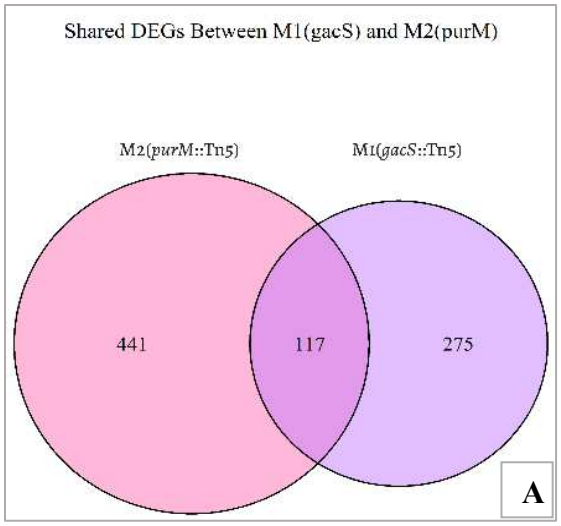


**Figure 10. Venn diagrams illustrating the overlap of differentially expressed genes (DEGs) between mutants M1 (*gacS*::Tn5) and M2 (*purM*::Tn5). (A)** Total DEGs identified between M1 and M2 mutants, reflecting both shared and unique gene regulation potentially influencing their distinct roles in bacterial virulence and metabolism.

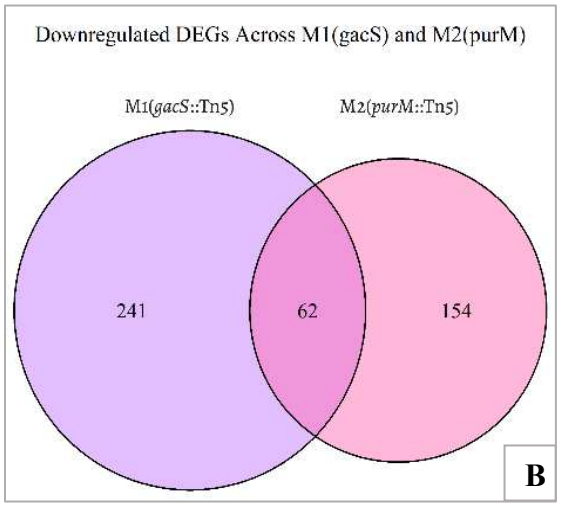


**Figure 10. (B)** Specifically, downregulated DEGs shared and unique between M1 and M2, highlighting genes potentially contributing to reduced virulence and metabolic shifts.

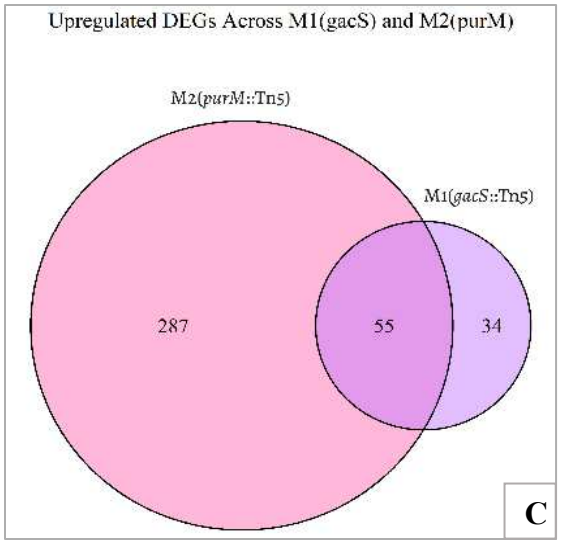


**Figure 10. (C)** Upregulated DEGs shared and unique between the two mutants, emphasizing genes potentially associated with compensatory mechanisms or adaptive responses in *Pectobacterium carotovorum* under altered regulatory states caused by *gacS* and *purM* mutations.

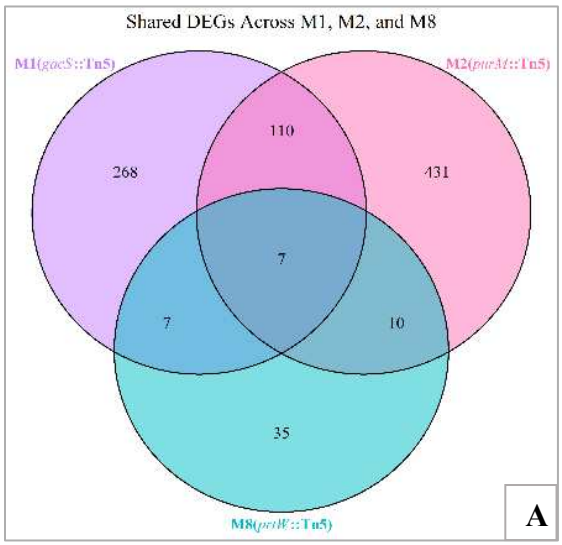


**Figure 11. Venn diagrams illustrating the overlap and distinctions of differentially expressed genes (DEGs) among mutants M1 (*gacS*::Tn5), M2 (*purM*::Tn5), and M8 (*prtW*::Tn5). (A)** Combined DEGs showing shared and unique regulatory responses across all three mutants, potentially influencing overall virulence, metabolic regulation, and proteolytic activities.

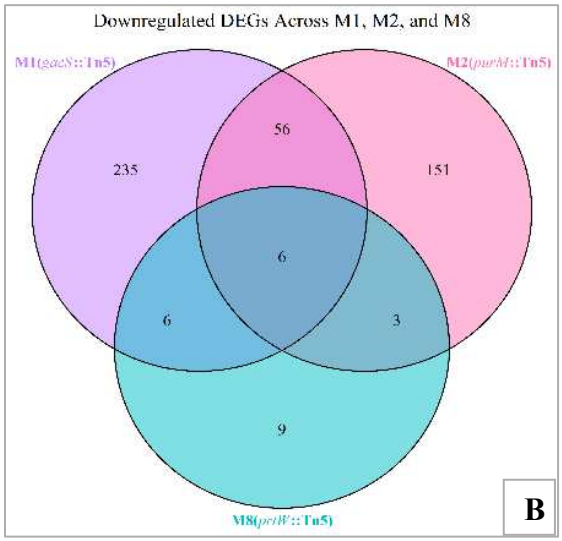


**Figure 11. (B)** Specific overlap and uniqueness among downregulated DEGs, suggesting genes involved in diminished metabolic or pathogenic capabilities common or specific to these mutations.

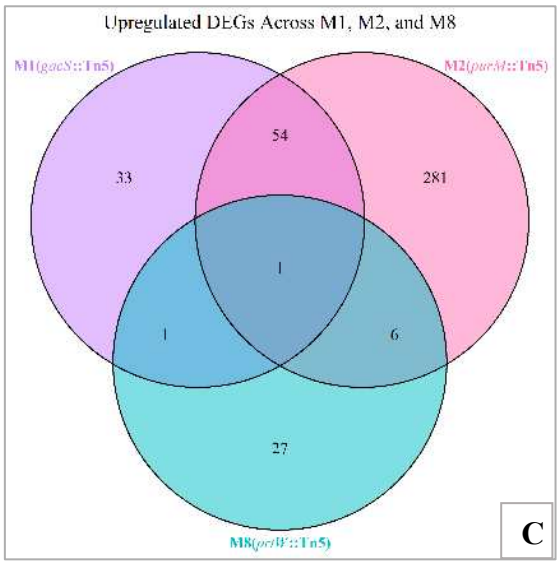


**Figure 11. (c)** Specific overlap and uniqueness among upregulated DEGs indicate potential compensatory or adaptive genetic responses to disruptions in *gacS*, *purM*, and *prtW* gene functions.

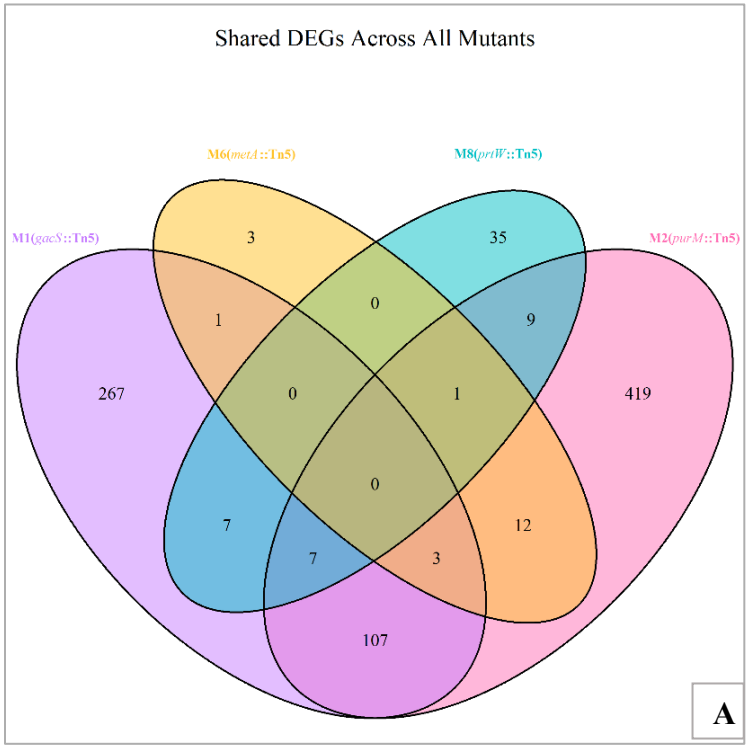


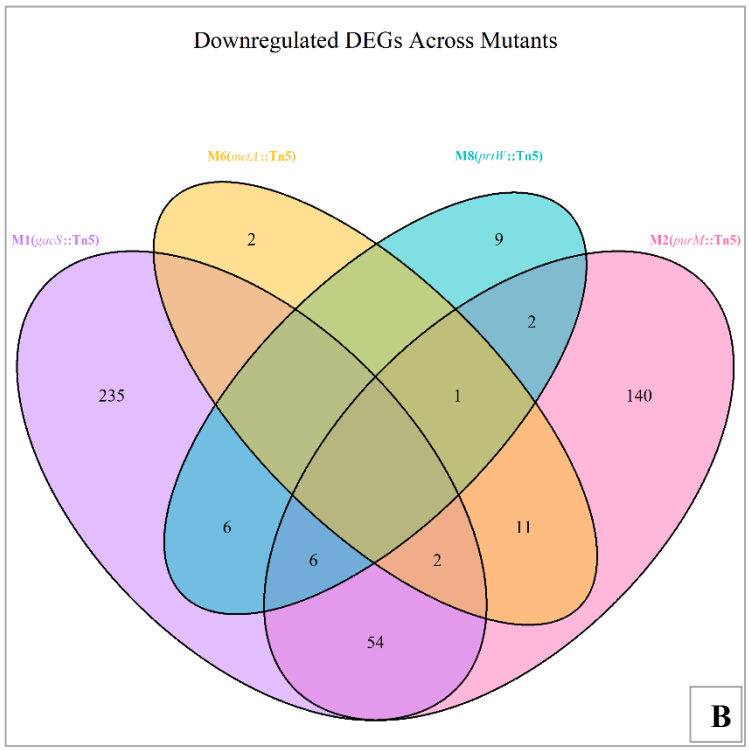


**Figure 12. Venn diagrams displaying shared and distinct differentially expressed genes (DEGs) across mutants M1 (*gacS*::Tn5), M2 (*purM*::Tn5), M6 (*metA*::Tn5), and M8 (*prtW*::Tn5). (A)** Overall DEGs highlighting common and unique gene expression changes among all mutants, reflecting their collective and individual influences on metabolic pathways, regulatory networks, and pathogenicity. **(B)** Downregulated DEGs specifically illustrating potential reduction in gene functions related to bacterial metabolism, virulence, or regulatory pathways as a result of these mutations.

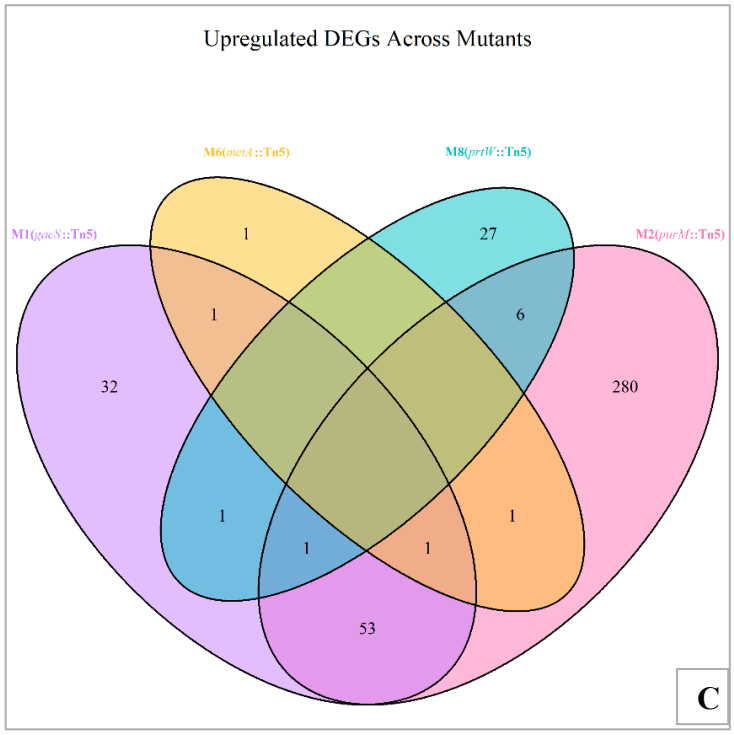


**Figure 12. (C)** Upregulated DEGs emphasizing genes potentially activated as adaptive or compensatory responses due to disruption of the *gacS*, *purM*, *metA*, and *prtW* pathways.

**References**


Allwood, E. M., Devenish, R. J., Prescott, M., Adler, B., & Boyce, J. D. (2011). Strategies for Intracellular survival of *Burkholderia pseudomallei*. *Frontiers in Microbiology*, *2*.

Bellieny-Rabelo, D., Nkomo, N. P., Shyntum, D. Y., & Moleleki, L. N. (2020). Horizontally acquired quorum-sensing regulators recruited by the phop regulatory network expand the host adaptation repertoire in the phytopathogen *Pectobacterium brasiliense*. *mSystems*, *5*(1).

Charkowski, A., Blanco, C., Yedidia, I., Charkowski, A., Blanco, C., Condemine, G., Expert, D., Franza, T., Hayes, C., Hugouvieux-Cotte-Pattat, N., Solanilla, E. L., Low, D., Moleleki, L., Pirhonen, M., Pitman, A., Perna, N., Reverchon, S., Rodríguez Palenzuela, P., San Francisco, M., & Toth, I. (2012). The role of secretion systems and small molecules in soft-rot Enterobacteriaceae pathogenicity. *Annual review of phytopathology.*, *50*(1), 425-449.

Chatterjee, A., Cui, Y. Y., Liu, Y., & Dumenyo, C. K. (1995). Inactivation of rsmA leads to overproduction of extracellular pectinases, cellulases, and proteases in *Erwinia carotovora* subsp. *carotovora* in the absence of the starvation/cell density-sensing signal, N-(3-oxohexanoyl)-L-homoserine lactone. *Applied and environmental microbiology.*, *61*(5), 1959-1967.

Cubitt, M. F., Hedley, P. E., Williamson, N. R., Morris, J. A., Campbell, E., Toth, I. K., & Salmond, G. P. C. (2013). A metabolic regulator modulates virulence and quorum sensing signal production in *Pectobacterium atrosepticum*. *Molecular Plant-Microbe Interactions®*, *26*(3), 356-366.

Cui, Y., Chatterjee, A., & Chatterjee, A. K. (2001). Effects of the two-component system comprising gaca and gacs of *Erwinia carotovora* subsp. *carotovora* on the production of global regulatory rsmb rna, extracellular enzymes, and harpin ecc. *Molecular plant-microbe interactions : MPMI.*, *14*(4), 516-526.

Cui, Y., Chatterjee, A., Yang, H., & Chatterjee, A. K. (2008). Regulatory network controlling extracellular proteins in *Erwinia carotovora* subsp. *carotovora*: Flhdc, the master regulator of flagellar genes, activates *rsmb* regulatory rna production by affecting *gaca* and *hexa* (*lrha*) expr. *Journal of Bacteriology*, *190*(13), 4610-4623.

Davis, W. H. (1933). Potato tubers as a culture medium for phytopathogenic bacteria and fungi. *Proceedings of the Iowa Academy of Science*, *40*(1), 57-65.

Eriksson, A. R. B., Andersson, R. A., Pirhonen, M., & Palva, E. T. (1998). Two-component regulators involved in the global control of virulence in *Erwinia carotovora* subsp. *carotovora*. *Molecular plant-microbe interactions : MPMI.*, *11*(8), 743-752.

Feng, T., Nyffenegger, C., Højrup, P., Vidal-Melgosa, S., Yan, K.-P., Fangel, J. U., Meyer, A. S., Kirpekar, F., Willats, W. G., & Mikkelsen, J. D. (2014). Characterization of an extensin-modifying metalloprotease: N-terminal processing and substrate cleavage pattern of *Pectobacterium carotovorum* Prt1. *Applied microbiology and biotechnology*, *98*, 10077-10089.

Fernandez, J., Yang, K. T., Cornwell, K. M., Wright, J. D., & Wilson, R. A. (2013). Growth in rice cells requires de novo purine biosynthesis by the blast fungus *Magnaporthe oryzae*. *Scientific Reports*, *3*(1).

Figaj, D., Czaplewska, P., Przepióra, T., Ambroziak, P., Potrykus, M., & Skorko-Glonek, J. (2020). Lon protease is important for growth under stressful conditions and pathogenicity of the phytopathogen, bacterium *Dickeya solani*. *International Journal of Molecular Sciences*, *21*(10), 3687.

Gedeon, A., Karimova, G., Ayoub, N., Dairou, J., Giai Gianetto, Q., Vichier-Guerre, S., Vidalain, P. O., Ladant, D., & Munier-Lehmann, H. (2023). Interaction network among *de novo* purine nucleotide biosynthesis enzymes in *Escherichia coli*. *The FEBS Journal*, *290*(12), 3165-3184.

Goncheva, M. I., Flannagan, R. S., & Heinrichs, D. E. (2020). *De Novo* purine biosynthesis is required for Intracellular growth of *staphylococcus aureus* and for the hypervirulence Phenotype of a *purR* Mutant. *Infection and Immunity*, *88*(5).

Holeva, M. C., Bell, K. S., Hyman, L. J., Avrova, A. O., Whisson, S. C., Birch, P. R., & Toth, I. K. (2004a). Use of a pooled transposon mutation grid to demonstrate roles in disease development for *Erwinia carotovora* subsp. *aroseptica* putative type iii secreted effector (dspe/a) and helper (hrpn) proteins. *Molecular plant-microbe interactions : MPMI*, *17*(9).

Holeva, M. C., Bell, K. S., Hyman, L. J., Avrova, A. O., Whisson, S. C., Birch, P. R., & Toth, I. K. (2004b). Use of a Pooled Transposon Mutation Grid to Demonstrate Roles in Disease Development for *Erwinia carotovora* subsp. *atroseptica* Putative Type III Secreted Effector (DspE/A) and Helper (HrpN) Proteins. *Molecular plant-microbe interactions : MPMI*, *17*(9).

Jahn, C. E., Willis, D. K., & Charkowski, A. O. (2008). The flagellar sigma factor flia is required for *Dickeya dadantii* virulence. *Molecular Plant-Microbe Interactions®*, *21*(11), 1431-1442.

Jiang, X., Zghidi-Abouzid, O., Oger-Desfeux, C., Hommais, F., Greliche, N., Muskhelishvili, G., Nasser, W., & Reverchon, S. (2016). Global transcriptional response of *Dickeya dadantii* to environmental stimuli relevant to the plant infection. *Environmental Microbiology*, *18*(11), 3651-3672.

Joly, N., Engl, C., Jovanovic, G., Huvet, M., Toni, T., Sheng, X., Stumpf, M. P. H., & Buck, M. (2010). Managing membrane stress: the phage shock protein (Psp) response, from molecular mechanisms to physiology. *FEMS Microbiology Reviews*, *34*(5), 797-827.

Joshi, J. R., Brown, K., Charkowski, A. O., & Heuberger, A. L. (2022). Protease inhibitors from *Solanum chacoense* inhibit *Pectobacterium* virulence by reducing bacterial protease activity and motility. *Molecular Plant-Microbe Interactions®. 35:825-834.*

Joshi, J. R., Khazanov, N., Khadka, N., Charkowski, A. O., Burdman, S., Carmi, N., Yedidia, I., & Senderowitz, H. (2020). Direct binding of salicylic acid to *Pectobacterium* N-acyl-homoserine lactone synthase. *ACS chemical biology. 15:1883-1891.*

Joshi, J. R., Yao, L., Charkowski, A. O., & Heuberger, A. L. (2021). Metabolites from wild potato inhibit virulence factors of the soft rot and blackleg pathogen *Pectobacterium brasiliense*. *Molecular Plant-Microbe Interactions*®, *34*(1), 100-109.

Latour, X. (2020). The evanescent gacs signal. *Microorganisms*, *8*(11), 1746.

Lebeau, A., Reverchon, S., Gaubert, S., Kraepiel, Y., Simond-Côte, E., Nasser, W., & Van Gijsegem, F. (2008). The GacA global regulator is required for the appropriate expression of *Erwinia chrysanthemi* 3937 pathogenicity genes during plant infection. *Environmental Microbiology*, *10*(3), 545-559.

Lee, D. H., Lim, A., Lee, J., Roh, E., Jung, K., Choi, M., Oh, C., Ryu, S., Yun, J., & Heu, S. . (2013). Characterization of genes required for the pathogenicity of *Pectobacterium carotovorum* subsp. *carotovorum* Pcc21 in Chinese cabbage. *Microbiology*, *159(Pt 7), 1487.*

Li, L., Yuan, L., Shi, Y., Xie, X., Chai, A., Wang, Q., & Li, B. (2019). Comparative genomic analysis of Pectobacterium carotovorum subsp. brasiliense SX309 provides novel insights into its genetic and phenotypic features. *BMC Genomics*, *20*(1).

Marits, R., Köiv, V., Laasik, E., & Mäe, A. (1999). Isolation of an extracellular protease gene of *Erwinia carotovora* subsp. *carotovora* strain SCC3193 by transposon mutagenesis and the role of protease in phytopathogenicity. *Microbiology*, *145*(8), 1959-1966.

Marits, R., Tshuikina, M., Pirhonen, M., Laasik, E., & Mäe, A. (2002). Regulation of the expression of prtW:: gusA fusions in *Erwinia carotovora* subsp. *carotovora*. *Microbiology*, *148*(3), 835-842.

Mee-Ngan Yap, Ching-Hong Yang, & Amy, O. C. (2008). The response regulator hrpy of *Dickeya dadantii* 3937 regulates virulence genes not linked to the hrp cluster. *Molecular plant-microbe interactions : MPMI*.

Moleleki, L. N., Pretorius, R. G., Tanui, C. K., Mosina, G., & Theron, J. (2017). A quorum sensing-defective mutant of *Pectobacterium carotovorum* ssp. *brasiliense* 1692 is attenuated in virulence and unable to occlude xylem tissue of susceptible potato plant stems. *Molecular Plant Pathology*, *18*(1), 32-44.

Parkins, M. D., Ceri, H., & Storey, D. G. (2001). *Pseudomonas aeruginosa* GacA, a factor in multihost virulence, is also essential for biofilm formation. *Molecular Microbiology*, *40*(5), 1215-1226.

Põllumaa, L., Alamäe, T., & Mäe, A. (2012). Quorum sensing and expression of virulence in *Pectobacteria*. *Sensors*, *12*(3), 3327-3349.

Sivaranjani, M., Krishnan, S. R., Kannappan, A., Ramesh, M., & Ravi, A. V. (2016). Curcumin from Curcuma longa affects the virulence of *Pectobacterium wasabiae* and *P. carotovorum* subsp *carotovorum* via quorum sensing regulation. *European journal of plant pathology /*, *146*(4), 793-806.

Sudarshan, S., Hogins, J., Ambagaspitiye, S., Zimmern, P., & Reitzer, L. (2021). Nutrient and energy pathway requirements for surface motility of nonpathogenic and uropathogenic *Escherichia coli*. *Journal of Bacteriology*, *203*(11).

Taylor, D., Charkowski, A. O., & Zeng, Y. (2021). Laboratory assays used to rank potato cultivar tolerance to blackleg showed that tuber vacuum infiltration results correlate with field observations. *Plant Disease*, *105*(3), 585-591.

Toth, I. K., Bell, K. S., Holeva, M. C., & Birch, P. R. J. (2003). Soft rot *Erwiniae*: from genes to genomes. *Molecular Plant Pathology*, *4*(1), 17-30.

Wang, C., Pu, T., Lou, W., Wang, Y., Gao, Z., Hu, B., & Fan, J. (2018). Hfq, a RNA chaperone, contributes to virulence by regulating plant cell wall–degrading enzyme production, Type VI secretion system expression, bacterial competition, and suppressing host defense

response in *Pectobacterium carotovorum*. *Molecular Plant-Microbe Interactions®*, *31*(11), 1166-1178.

Wilson, K. J., Sessitsch, A., Corbo, J. C., Giller, K. E., Akkermans, A. D., & Jefferson, R. A. (1995). Beta-glucuronidase (gus) transposons for ecological and genetic studies of *Rhizobia* and other gram-negative bacteria. *Microbiology (Reading, England)*, *141 ( Pt 7)*.

Yap, M.-N., Yang, C.-H., & Charkowski, A. O. (2008). The response regulator hrpy of *Dickeya dadantii* 3937 regulates virulence genes not linked to the *hrp* cluster. *Molecular Plant-Microbe Interactions®*, *21*(3), 304-314.

Yu, S., Kang, J., Chung, E.-H., & Lee, Y. (2023). Disruption of the metc gene affects methionine biosynthesis in *Pectobacterium carotovorum* subsp. *carotovorum* pcc21 and reduces soft-rot disease. *The Plant Pathology Journal*, *39*(1), 62-74.

# Chapter 4 - Functional Evaluation of Cloned *Pectobacterium carotovorum* WPP14 Proteases and Potential Plant-Derived Inhibitors in Controlling Soft Rot Disease


## Summary

Proteases play crucial roles in the virulence of *Pectobacterium carotovorum*, including the degradation of plant cell wall components, facilitating bacterial colonization, and impairing plant immune responses. Given their significant impact on the bacterium's pathogenic potential and contribution to the severity of soft rot disease, understanding these proteases is critical. This chapter describes proteases cloned from the wild-type strain *P. carotovorum* WPP14, encompassing three main enzyme classes: metalloproteases, serine proteases, and threonine proteases. The primary objective for cloning these proteases was to evaluate their susceptibility to protease inhibitors derived from wild potato (*Solanum chacoense*), previously characterized by Joshi et al. (2022). Each protease is presented in detail, including known functions in pathogenicity, optimal biochemical conditions, such as pH and temperature. When direct information on *Pectobacterium* is limited, relevant comparative information from studies involving closely related bacterial species is provided. Additionally, protease inhibitors from wild potato species are discussed due to their demonstrated efficacy in reducing bacterial protease activity, motility, and virulence, suggesting their potential utility for managing bacterial infections. Overall, this chapter offers valuable insights into the characterization of proteases from *P. carotovorum*, laying the groundwork for future research into targeted protease inhibitor-based strategies aimed at controlling bacterial virulence and managing soft rot diseases.

## Introduction

Proteases are enzymes that catalyze the hydrolysis of peptide bonds and play essential roles in numerous biological processes. They are classified into different categories based on their catalytic mechanisms and active site residues, including serine proteases, metalloproteases, cysteine proteases, aspartic proteases, and threonine proteases. Each class exhibits distinct structural features, mechanisms of action, and physiological roles, significantly affecting bacterial adaptation, physiology, and virulence (Figaj et al., 2019; Page & Di Cera, 2008).

In this study, we cloned 14 proteases from *P. carotovorum* WPP14, primarily representing metalloproteases and serine proteases. Metalloproteases, including Prt1, PrtW, BepA, M20, M48, and PepB, degrade extracellular proteins, facilitate nutrient acquisition, bacterial colonization, and host tissue degradation, which are critical processes for virulence. Metalloproteases typically require metal ions such as $Zn^{2+}$ or $Ca^{2+}$ as cofactors for their catalytic activity (Feng et al., 2014; Figaj et al., 2019). For example, Prt1 and PrtW are extracellular metalloproteases secreted outside the bacterial cell, requiring $Zn^{2+}$ and $Ca^{2+}$ for their activity. BepA is a membrane-associated metalloprotease involved in membrane protein turnover and response to environmental stress (Narita et al., 2013). M20 and M48 proteases are cytoplasmic and periplasmic, respectively, facilitating intracellular protein processing and bacterial adaptation under stress conditions. PepB is a leucine aminopeptidase dependent on manganese ions, localized within the cytoplasm.

Serine proteases, such as PtrB, Lon, ClpP, DegQ, DegS, S8/S53, and S33, play pivotal roles in protein quality control, stress responses, and regulation of bacterial virulence. Lon and ClpP are ATP-dependent serine proteases involved in degrading misfolded proteins within the cytoplasm, thus maintaining cellular homeostasis under stress (Figaj et al., 2020). DegQ and DegS are periplasmic and inner-membrane serine proteases, respectively, crucial for sensing and

responding to membrane stress and environmental changes (Sawa et al., 2011). PtrB and S8/S53 have both exo- and endo-peptidase activities, with PtrB functioning optimally at alkaline conditions (Moreno Amador et al., 2019), whereas S33 is associated with membrane structures.

Threonine proteases, including members of the ClpYQ protease complex (also known as HslUV), play an important role in protein turnover and stress adaptation, both of which are essential for bacterial survival during challenging conditions such as host infection. HslU, in particular, acts as the ATPase component that helps recognize and unfold damaged or abnormal proteins, delivering them to the proteolytic subunit HslV for degradation, thereby maintaining cellular homeostasis under stress (Gur et al., 2011).

L-asparaginase is an amidohydrolase that catalyzes the hydrolysis of L-asparagine into L-aspartate and ammonia. While it is not a protease, its role in nitrogen metabolism and stress response makes it a relevant enzyme in bacterial physiology. In *P. carotovorum*, L-asparaginase has been purified and characterized, showing optimal enzymatic activity at alkaline pH, specifically within the range of 8.0 to 10.0 (Kumar et al., 2011). Its inclusion in this study broadens the investigation of hydrolytic enzymes that may be involved in the adaptation and virulence mechanisms of the pathogen.

Despite their recognized importance, the specific roles of many of these proteases in *P. carotovorum*, a highly aggressive soft rot pathogen, remain understudied. Therefore, investigating the properties of these proteases, including their optimal pH, temperature, and regulatory mechanisms, is crucial for a better understanding of their roles in virulence and pathogenicity.

Joshi et al. (2022) recently identified and characterized protease inhibitors derived from *Solanum chacoense*. Their study demonstrated that these inhibitors effectively reduce bacterial protease activity and motility, significantly attenuating the virulence of *Pectobacterium* species

(Joshi et al., 2022). Among these inhibitors, g6571 exhibited promising potential, making it an ideal candidate for detailed investigation. The primary goal of this study was to experimentally evaluate the efficacy of the plant-derived protease inhibitor g6571 against cloned proteases from *P. carotovorum* WPP14. Experimental assays were complemented by structural predictions using AlphaFold to predict potential interactions and provide insights into inhibitory mechanisms. Due to time constraints and technical challenges associated with experimentally validating all potential interactions, this integrated approach efficiently identifies and visualizes likely inhibitor–protease interactions and mechanisms. This approach aims to validate potential strategies for managing bacterial virulence and controlling soft rot diseases.

## Materials and Methods

**Protease PCR Cloning.** Protease genes were cloned from *P. carotovorum* strain WPP14. Each protease gene was amplified using gene-specific primer sets detailed in Table 1. PCRs were performed using GoTaq DNA polymerase (Promega, USA) following the manufacturer's protocol.

The PCR conditions included an initial denaturation at 95°C for 2 minutes, followed by 34 cycles consisting of denaturation at 95°C for 30 seconds, annealing at 56°C for 30 seconds, and extension at 72°C for 1 minute and 20 seconds. The annealing temperature and extension time were occasionally modified based on the primer length and amplicon size to optimize amplification. Initially, the standard annealing temperature of 56°C did not yield clear amplification for some proteases; however, adjusting the annealing temperature and extension times according to the primer and target gene resolved these issues and resulted in successful amplification. The PCR cycles were followed by a final extension step at 72°C for 5 minutes and subsequently held at 4°C indefinitely.

PCR products were analyzed by agarose gel electrophoresis to confirm successful amplification. Initially, positive PCR products (without promoter or ribosome binding site sequences) were cloned into the pGEM-T Easy vector and transformed into chemically competent *E. coli* DH5α cells. Subsequently, redesigned PCR products (containing promoter and ribosome binding site sequences for enhanced expression) were similarly cloned into the pGEM-T Easy vector but transformed into high-efficiency chemically competent *E. coli* JM109 cells according to the manufacturer's protocol (Promega, USA). For both cloning experiments, positive transformants were selected on LB agar plates supplemented with ampicillin, IPTG, and X-Gal. Correct insertion of cloned fragments was verified by colony PCR and sequencing.

**Table 1.** Primers used for cloning *Pectobacterium carotovorum* WPP14 proteases into pGEM-T Easy vector.

| Cloned Protease | Forward Primer (5'-3') | Reverse Primer (5'-3') | Length (bp) |
|---|---|---|---|
| *prt1* | GATGAGCGTTTTCAAGGAGATGAGGTATGA | TCATAGGAACTCCTGCCGAACCTC | 1,055 |
| *prtw* | ATGGCTTTACGAGATCAAGATA | TCACACGATAAAATCGGT | 1,431 |
| *ptrb* | AACCTTATACCTGATCGGGTTGTGAAAAAT | TTACCAGCAAATGCGGATAGCGTTGC | 2,030 |
| *lon* | ATGAACCCTGAGCGTTCC | CTATTTTGCCTTGGCTTTGG | 2,403 |
| *clpp* | GGTCAGGCAACGAGTTAAATCACTGCGTTG | TTACCCACGGTTAGTGAATACGGAG | 935 |
| *degq* | CTTTCCCCTCTCTTGTTCTACGCTTAAAAC | TTAACGTAGCAGCAGATAAATTGTTTCTTC | 1,591 |
| *degs* | CGGCAGCTTAACTGGCCAGAA | TTATTGGGTAGGGAATTCCTGAATC | 1,218 |
| *bepa* | TAGATTGATCTCTGTGAGATGAGATTTCTT | TCAGGATTTCTGGTACTGGCGG | 1,615 |
| M20 | CGCATACGTAGATACACCTGCACGCCTGAA | TTAGCGGGAGGACAGCTGTTCTAAA | 1,235 |
| S8/S53 | ATGCAACATACATTAGAAATACT | TCATGTCCGAATTCTGACAT | 2,294 |
| L-asparaginase | TTCCGGTCTCTCCGCCCCTGATTTAG | TTAGCGATAGATATCGGCGACGGGAA | 1,008 |
| s33 | GAAGCATGCCCCTGAATCACGTTCTGTATT | TTAATGATAACGCGCAAAGTGCGCCA | 1,168 |
| M48 | CTAAGGCAGGAATATGAATATTGAGGGGCA | TTAGTGCTTATTCATCTCGCTTTC | 1,051 |
| *pepb* | TGGCAGGAATACCTATTATCGGAGAAGCAC | CTATTTGGCGTTGCTCAGCAGGAGGTTA | 1,339 |
| *hs1U* | GGATCAACTATGTCTGAAATGACCC | TTATAAGATAAATCGACTCAGATCTTCATC | 1,341 |

**Protease Activity Assay.** The protease activity of the cloned proteases was evaluated using skim milk agar plates to assess their capability to degrade milk proteins. Initially, cloned proteases were cultured overnight in nutrient broth (NB) supplemented with ampicillin at 37°C with shaking at 200 rpm to ensure optimal growth and protease production. Following incubation, the bacterial

cultures were prepared in three different forms: filter-sterilized supernatants, supernatants resuspended with bacterial pellets, and sonicated bacterial cells.

Twenty microliters (20 µL) of each prepared sample were then inoculated into wells created on skim milk agar plates composed of 0.8% agar and 1% dry skim milk (Joshi et al., 2022). To investigate the effect of environmental conditions on protease activity, plates were incubated at three temperatures (room temperature ~25°C, 18°C, and 37°C) and prepared at different pH levels (neutral pH ~7, acidic pH 5 adjusted with HCl, and alkaline pH 8 adjusted with NaOH). The plates were incubated for 24 to 72 hours, and proteolytic activity was observed by the formation of clear halos around wells. The diameter of these halos was measured using ImageJ software (version 1.54g) (Rasband, 2025).

Several modifications and alternative approaches were explored to overcome challenges encountered with the initial skim milk media preparation. The initial issues included media coagulation and discoloration after autoclaving, resulting in inconsistent and unclear halos. To resolve these problems, an alternative method using a microwave was employed, which improved clarity but introduced contamination risks due to the absence of sterilization. To mitigate this, antibiotics (ampicillin) were added to prevent contamination.

Additionally, to enhance visual clarity and consistency, a modified skim milk recipe with a higher concentration of milk (2% skim milk, 1.5% agar per liter) was used. For successful autoclaving, agar and milk were separately dissolved in equal halves of the total water volume, heated in the microwave, and autoclaved independently. After sterilization, solutions were carefully mixed and poured into plates after cooling.

Further assays were conducted using additional protein substrates, including casein agar and gelatin plates. These substrates were prepared following a general recipe (per liter) adapted

from established protocols (Vermelho et al., 1996): 15 g agar, 1 g yeast extract, and 4 g peptone dissolved in 500 mL of water; separately, 12 g protein source (skim milk, casein, or gelatin) dissolved in another 500 mL of water. Both solutions were either autoclaved separately or microwaved for approximately 4 minutes each, cooled before mixing, and then supplemented with antibiotics prior to plate preparation.

**Assessment of Protease Inhibitor Activity.** The effectiveness of protease inhibitors (PIs) against cloned proteases was evaluated using inhibitors previously characterized and cloned from *Solanum chacoense* (Joshi et al., 2022). Among the available inhibitors (g18987, g28531, g39249, g40384, and g6571), the PI with the highest inhibition activity (g6571) was selected for further analysis.

Protease inhibitors previously cloned from *Solanum chacoense* were transformed into *Escherichia coli* DH5α cells [DH5α(pG6571)]. Protease genes from *P. carotovorum* WPP14 were cloned into two separate strains of *E. coli* depending on the cloning strategy used: initially, protease genes (e.g., *prtW*) cloned without promoters or ribosome binding sites (RBS) were transformed into *E. coli* DH5α cells, while redesigned protease constructs containing promoters and RBS sequences for enhanced expression were cloned into *E. coli* JM109 cells [JM109(pPrtW)]. Both cloned protease-expressing strains and inhibitor-expressing strains were cultured overnight in nutrient broth at 30°C with shaking at 200 rpm. Overnight bacterial cultures were prepared into three forms for inhibitor assays: unfiltered culture supernatants, filter-sterilized supernatants, and lysed cell suspensions. Lysed cell suspensions were prepared by centrifuging bacterial cultures, resuspending cell pellets in phosphate-buffered saline (PBS, pH 7.4), and lysing cells by sonication to release intracellular proteases into the solution.

The protease solution was mixed with the protease inhibitor solution in different volume ratios (g6571:PrtW): 0:1, 1:1, 1:10, 10:1, and 1:0. Subsequently, each mixture was tested using the

previously described skim milk agar plate method for protease activity. Proteolytic activity was indicated by the formation of clear halos around inoculated wells. Effective inhibition by protease inhibitors was determined by the reduction or absence of halo formation compared to the protease-only control.

**Prediction of Protease-Inhibitor Interactions Using AlphaFold3.** To complement experimental assays, AlphaFold3 was used to predict structural interactions between cloned proteases and protease inhibitors. Protein sequences of both proteases and inhibitors were used as inputs for AlphaFold3, which predicted their potential interactions, binding sites, and structural compatibility. These computational predictions provided additional insights into possible inhibitory mechanisms.

## Results

### Preliminary Evaluation of Cloned Protease Activity

This study initially aimed to evaluate cloned proteases from *P.carotovorum* WPP14, specifically assessing whether their protease activity could be inhibited by protease inhibitors previously cloned from *Solanum chacoense*. In Chapter 2, five assay media formulations (Medium 1: traditional 1% skim milk; Medium 2: modified 2% skim milk; Medium 3: enriched skim milk agar supplemented with peptone and yeast extract; Medium 4: gelatin-based medium supplemented with peptone and yeast extract; and Medium 5: casein-based medium) were systematically optimized and validated for robust detection of wild-type protease activity. Here, these previously optimized media conditions were employed to evaluate the activity of 14 cloned protease genes, initially cloned without *P. carotovorum* promoter or ribosome binding site (RBS) sequences. Preliminary assays using Medium 1 (traditional skim milk, pH 7) initially revealed limited detectable activity only for proteases DegQ and PtrB. Subsequent assays using the

optimized media formulations identified broader protease activity, particularly for eight clones on Medium 3 and Medium 4; however, these initial results exhibited inconsistent reproducibility upon repeated testing.

To attempt to address reproducibility issues, primers were redesigned to include promoters and ribosome binding sites (RBS) for improved expression and translation. Despite successful cloning, confirmed by PCR and sequencing, assays using these redesigned constructs produced no detectable protease activity on any tested medium. Thus, the cloned protease activity data presented here represent preliminary findings from the initial cloning strategy, emphasizing observed activity trends rather than definitive quantitative conclusions.

***Cloned Protease Activity on Medium 1: Low Activity Detected for DegQ and PtrB.*** On Medium 1 (1% skim milk, RT, supernatant), the overall activity detected from cloned proteases was low and variable. Statistical analysis (ANOVA, $p < 0.05$) revealed a significant interaction among strain, incubation time, and pH. Among tested clones, DegQ exhibited modest but detectable activity at both pH 5 and pH 7 after extended incubation periods (72 hours), while PtrB showed detectable activity only at pH 7. No significant difference was observed between DegQ and PtrB activity levels at pH 7 ($p = 0.521$). Despite these observations, results obtained with Medium 1 displayed limited reproducibility and sensitivity for reliably detecting cloned protease activity, particularly when compared with Medium 3 and Medium 4. Medium 3 (enriched skim milk agar supplemented with peptone and yeast extract) consistently produced clearer, stronger, and more reproducible halos across multiple cloned proteases at varying pH conditions, demonstrating substantially improved sensitivity. Similarly, Medium 4 (gelatin-based medium) reliably indicated enzymatic activity across diverse conditions, especially after prolonged incubation times. Data presented in Figure 1 clearly summarizes the protease activity across tested

strains on Medium 1, highlighting its limited effectiveness in detecting cloned protease activity compared to Medium 3 and Medium 4.

***Cloned Protease Activity on Medium 2: No Detectable Activity from Redesigned Constructs.*** On Medium 2 (2% skim milk, RT, supernatant), no protease activity was detected for any of the cloned proteases expressed using the redesigned constructs containing promoters and ribosome binding sites (RBS). In contrast, the wild-type strain produced clear, strong, and reproducible proteolytic halos at both pH 7 and pH 8, especially following prolonged incubation (72 hours). These observations reinforce Medium 2's enhanced sensitivity and suitability for wild-type protease detection, while underscoring its limitations for reliably detecting protease activity from cloned genes expressed via plasmid-based systems. As no cloned protease activity was measurable under these conditions.

***Cloned Protease Activity on Medium 3: Activity Detected Across pH Conditions with Extended Incubation.*** Medium 3 (2% skim milk supplemented with peptone and yeast extract, RT, supernatant) facilitated clear and distinct detection of cloned protease activity across multiple cloned proteases originally derived from *P. carotovorum* WPP14. Several cloned proteases, including DegQ, DegS, PtrB, ClpP, Lon, M20, S8/S53, and BepA, exhibited measurable halos at all tested pH levels (5, 7, and 8), particularly following prolonged incubation periods (72 hours). Statistical analysis (ANOVA, $p < 0.001$) identified incubation time as the primary significant factor influencing cloned protease detection, whereas pH and its interaction with incubation time were not statistically significant. Data presented in Figure 2 clearly highlights Medium 3’s sensitivity and robustness in reliably detecting cloned protease activity. However, due to variability observed in these preliminary assays, results should be interpreted cautiously.

***Cloned Protease Activity on Medium 4: Reliable Detection Across Clones Enhanced by Extended Incubation.*** Medium 4 (gelatin-based medium supplemented with peptone and yeast extract, RT, supernatant) facilitated reliable detection of protease activity across multiple individually cloned proteases. Notable cloned proteases, including DegQ, DegS, PtrB, ClpP, Lon, M20, S8/S53, and BepA, exhibited clear and distinct halos at all tested pH levels (5, 7, and 8), particularly after prolonged incubation periods (72 hours). Medium 4 consistently indicated enzymatic activity of cloned proteases across diverse conditions. Statistical analysis (ANOVA, $p < 0.001$) identified incubation time as the primary significant factor influencing detection of cloned protease activity, whereas pH and its interaction with incubation time were not statistically significant. Data shown in Figure 3 clearly demonstrates Medium 4's reliability and robustness for screening cloned proteases. Although slightly lower in sensitivity compared to enriched skim milk agar formulations, Medium 4 remains a suitable and dependable alternative for protease activity assays, particularly when milk-based media are not optimal.

***Cloned Protease Activity on Medium 5: Activity Detected at pH 5 but Confounded by Background.*** Medium 5 (casein-based medium supplemented with peptone and yeast extract, RT, supernatant) showed apparent protease activity for all cloned proteases exclusively at pH 5, notably at incubation durations of 48h and 72h. However, significant background proteolytic activity was also observed from the negative control (*E. coli*) under identical conditions. This background signal confounds interpretation and raises uncertainty as to whether observed halos truly reflect activity from the cloned proteases or from host-associated caseinolytic enzymes. No cloned protease activity was detectable at pH 7 or pH 8, despite the clear and consistent activity from the wild-type strain at pH 5 and pH 7 (Figure 4). Consequently, Medium 5 was considered unreliable for accurate evaluation of cloned protease activity.

**Table 2. Summary of activity of cloned proteases on five media. Results for cloned proteases showed inconsistencies and should be considered preliminary.**

| Media Type | WT WPP14 Activity | Cloned Proteases Activity | Temperature Effect | pH Effect | Sterilization Method |
|---|---|---|---|---|---|
| Skim Milk (1%) (Medium 1) | Moderate (+) | Mostly negative; limited (+) activity (PtrB, DegQ) | Optimal at RT | Detectable clearly at pH 5 and 7; unclear at pH 8 | Microwaving clearer than autoclaving |
| Skim Milk (2%) (Medium 2) | Moderate (+) | Mostly negative; negligible detection | Optimal at RT and 18°C | Slightly better at alkaline (pH 8) | Microwaving is clearer than autoclaving |
| Skim Milk (2%) + Peptone & Yeast Extract (Medium 3) | High (+++) | Positive detection for multiple clones at RT | Optimal at RT and 18°C (WT), RT and 37°C (clones) | Strongest at alkaline (pH 8) | Both methods are effective and clear with both methods |
| Gelatin-Based (Medium 4) | Moderate (+) | Positive detection for multiple clones | Optimal at RT | Broad activity across pH 5, 7, and 8 | Effective with both methods |
| Casein-Based (Medium 5) | Moderate (+) | Positive but uncertain due to background from E. coli control | Optimal at RT | Activity detected only at pH 5 | Microwaving only (autoclaving unusable) |

**Protease Inhibitor Activity.** Protease inhibitor (PI) assays evaluated the effectiveness of the cloned plant-derived inhibitor g6571 from *Solanum chacoense* against cloned proteases DegQ, DegS, PtrB, ClpP, Lon, M20, S8/S53, and BepA using skim milk agar at pH 8. A slight reduction in proteolytic activity was observed for Lon protease with inhibitor g6571. Specifically, at 72 h incubation, Lon activity decreased from 0.597 cm (supernatant without inhibitor) to 0.500 cm (supernatant with inhibitor). Notably, sonicated preparations for Lon exhibited a more pronounced inhibition (from 0.237 cm without inhibitor to 0.000 cm with inhibitor). No measurable inhibitory effects were observed for the other tested proteases (DegQ, DegS, PtrB, ClpP, M20, S8/S53, and BepA) regardless of inhibitor concentration or bacterial preparation method.

**AlphaFold Structural Predictions.** AlphaFold structural predictions complemented experimental assays by providing computational insights into potential interactions between cloned proteases (DegQ, DegS, PtrB, ClpP, Lon, M20, S8/S53, and BepA) and inhibitor g6571

from *Solanum chacoense*. For example, the positive control interaction between the PrtW protease and its native inhibitor from WPP14 yielded high-confidence interaction scores (ipTM and pTM = 0.9). However, when proteases including PtrB (ipTM = 0.2, pTM = 0.6), ClpP (ipTM = 0.3, pTM = 0.5), Lon (ipTM = 0.4, pTM = 0.5), DegQ (ipTM = 0.2, pTM = 0.5), DegS (ipTM = 0.1, pTM = 0.5), S8/S53 (ipTM = 0.1, pTM = 0.8), M20 (ipTM = 0.1, pTM = 0.6), and BepA (ipTM = 0.1, pTM = 0.6) were tested against inhibitor g6571, predicted interaction confidence scores were notably lower, indicating weak predicted binding affinity. These computational predictions align closely with the limited inhibitory effects observed experimentally, underscoring the value of AlphaFold structural analyses in guiding future inhibitor-protease interaction studies.

**Summary and Media Recommendation for Cloned Protease Detection.** Comparative analysis of protease activity across five tested media revealed significant differences in their suitability for detecting cloned proteases. Medium 3 (2% skim milk supplemented with peptone and yeast extract) consistently provided the strongest detection, particularly at alkaline (pH 8, 72h) and neutral (pH 7, 72h) conditions. Medium 4 (gelatin-based medium) supported broad activity detection across varied pH and incubation times, though with slightly lower sensitivity compared to Medium 3. Medium 2 showed no measurable cloned protease activity, while Medium 1 provided limited detection restricted to specific clones. Medium 5 displayed substantial background interference from the negative control strain (*E. coli*), making it unsuitable for accurate cloned protease assessments. Based on these findings, Medium 3 is recommended as the most sensitive and reliable medium for screening and quantifying recombinant protease activity. However, due to challenges in reproducing these results, the data presented should be interpreted cautiously and considered indicative rather than conclusive. Further experiments with increased replicates are necessary to validate these observations and conclusively confirm protease activities.

## Discussion

The primary goal of this study was to evaluate whether protease inhibitors cloned from *Solanum chacoense* could effectively inhibit proteases cloned from *P. carotovorum* WPP14. Initial assays to detect cloned protease activities employed traditional skim milk media (Medium 1), but this approach encountered multiple limitations. These included inconsistent results due to variable medium clarity, protein aggregation caused by autoclaving, and challenges in reliably adjusting and maintaining alkaline pH conditions (pH ≥ 8). To address these issues, several optimized media formulations incorporating alternative substrates (casein, gelatin, and modified skim milk) were developed and systematically evaluated under various experimental conditions. This optimization process resulted in enhanced clarity, reproducibility, and sensitivity of protease detection, providing clearer insights into protease behavior and interactions with inhibitors.

Protease activity assays demonstrated a significant influence of temperature, substrate type, and pH on proteolytic activity. Specifically, unfiltered culture supernatants from wild-type *P. carotovorum* exhibited the highest proteolytic activity at room temperature (~25°C) and 18°C, forming larger and clearer proteolytic halos compared to assays performed at 37°C. Cell lysates obtained by sonication showed minimal or undetectable activity across the tested conditions, suggesting that intracellular proteases might require more specific or stringent conditions, possibly including higher temperatures, to become clearly detectable. The modified skim milk medium at pH 8 notably improved clarity and proteolytic visibility compared to traditional skim milk formulations, likely due to enhanced protein solubility and stability, facilitating more accurate and reproducible enzyme assays (Feng et al., 2014).

Despite these media optimizations, evaluating cloned protease activities proved challenging. Initial protease gene constructs, cloned without promoters and ribosome binding sites

(RBS), produced limited and inconsistent protease activity, detectable primarily for clones DegQ and PtrB on skim milk agar. Subsequent assays on optimized media (Medium 3: enriched skim milk agar with peptone and yeast extract; Medium 4: gelatin-based medium with peptone and yeast extract; Medium 5: casein-based medium) detected broader protease activity for eight cloned proteases. However, these positive preliminary results were inconsistently reproducible across repeated experiments. To address reproducibility issues, protease genes were recloned using redesigned primers incorporating promoters and RBS sequences aimed at enhancing expression and translation. Although successful cloning and correct gene insertion were confirmed by PCR and sequencing, no protease activity was detected in assays employing these redesigned constructs.

The inability to reliably detect cloned protease activity likely stemmed from multiple technical and biological challenges commonly encountered in heterologous protein expression systems. These include differences in protein expression efficiency among bacterial strains (e.g., *E. coli* JM109 versus DH5α) (Rosano & Ceccarelli, 2014), unsuitable promoter or RBS strengths leading to insufficient or improperly folded protein production (Terpe, 2006), formation of inclusion bodies (Singh et al., 2015)(Singh et al., 2015), absence of adequate secretion mechanisms (Choi & Lee, 2004), or suboptimal choice of expression vectors (Rosano & Ceccarelli, 2014). Prior studies indicate that successful expression alone does not ensure detectable extracellular protease activity, since secretion typically requires specialized transport machinery absent in standard laboratory strains of *E. coli*. Co-expression of secretion-related genes such as *prtD*, *prtE*, and *prtF*, as demonstrated in *Erwinia chrysanthemi* (now *Dickeya dadantii*), can enhance extracellular secretion and subsequent protease detection (Létoffé et al., 1990). Additionally, incorporating appropriate signal peptides, short amino acid sequences guiding proteins through secretion pathways, might enhance secretion efficiency and facilitate detection (Choi & Lee, 2004).

Alternative approaches, including evaluating intracellular protease activity through cell lysis or employing bacterial hosts with native secretion pathways similar to *P. carotovorum*, should also be considered to enhance protease detection (Marits et al., 1999; Murata, 1991).

To overcome the experimental limitations encountered in the protease inhibitor assays, complementary computational analyses were conducted using structural predictions generated by AlphaFold. These analyses specifically focused on assessing the strength of predicted interactions between inhibitor g6571 and the cloned proteases, quantified using AlphaFold-derived interaction scores (ipTM and pTM). The resulting predictions indicated moderate to low binding affinities, suggesting that inhibitor g6571 is likely to interact only weakly or transiently with the targeted proteases, rather than forming stable, strong complexes. This computational result is consistent with the experimentally observed limited inhibitory activity, supporting the reliability of these predictions and their potential to inform future assay optimization or inhibitor selection (Jumper et al., 2021; Moreno Amador et al., 2019; Varadi et al., 2022). Thus, future work should focus on refining assay methodologies, optimizing inhibitor formulations, and exploring alternative inhibitors to enhance protease inhibition potential.

During annotation and characterization of cloned proteases, ambiguity was identified concerning the classification of L-asparaginase, commonly misannotated as "Peptidase T2" in major databases (e.g., ASAP, InterPro, NCBI, UniProt). This misclassification arises from structural similarities between L-asparaginases and glycosylasparaginases (true MEROPS T2 proteases), despite distinct catalytic functions. Unlike glycosylasparaginases, L-asparaginases hydrolyze free L-asparagine rather than peptide bonds, thus aligning with amidohydrolases (EC 3.5.1.1) (Da Silva et al., 2022; Kumar et al., 2011). Clarifying this ambiguity is crucial for accurate database annotation and preventing future misinterpretations.

## Conclusion

Collectively, this study provides a detailed characterization of proteolytic activities exhibited by cloned proteases from *P.* carotovorum WPP14, highlighting the intricate relationships between environmental conditions (temperature, substrate type, and pH), enzyme specificity, expression challenges, and inhibitor efficacy. Although protease inhibitors cloned from *Solanum chacoense* showed limited predicted inhibitory potential under the tested conditions, structural modeling suggests there remains considerable scope for optimizing their effectiveness. Therefore, future research should prioritize refining inhibitor designs, developing improved assay methodologies, and conducting context-specific evaluations to enhance the practical application of protease inhibitors for controlling bacterial virulence and mitigating soft rot diseases caused by *P. carotovorum*.

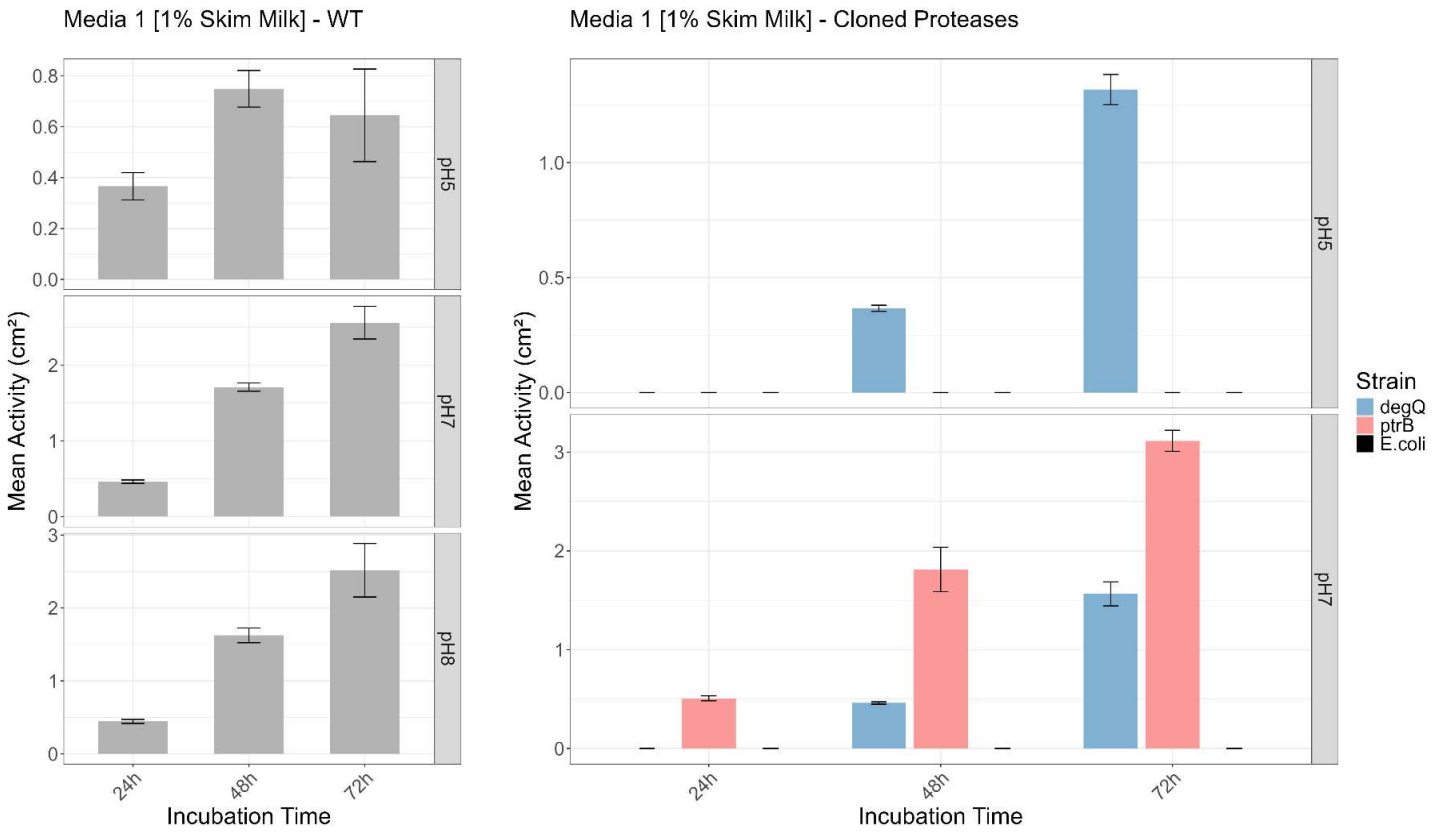


***Figure 1. Protease activity of cloned proteases DegQ and PtrB compared to WT (P. carotovorum WPP14) on Medium 1 (1% skim milk agar, supernatant, RT), measured at pH 5, 7, and 8 across incubation periods (24h, 48h, 72h).*** DegQ exhibited activity at pH 5 and 7, while PtrB showed activity only at pH 7, mainly at 72h. Statistical analysis (ANOVA, $p < 0.05$) indicated significant interactions among strain, incubation time, and pH. Data represent mean ± SD.

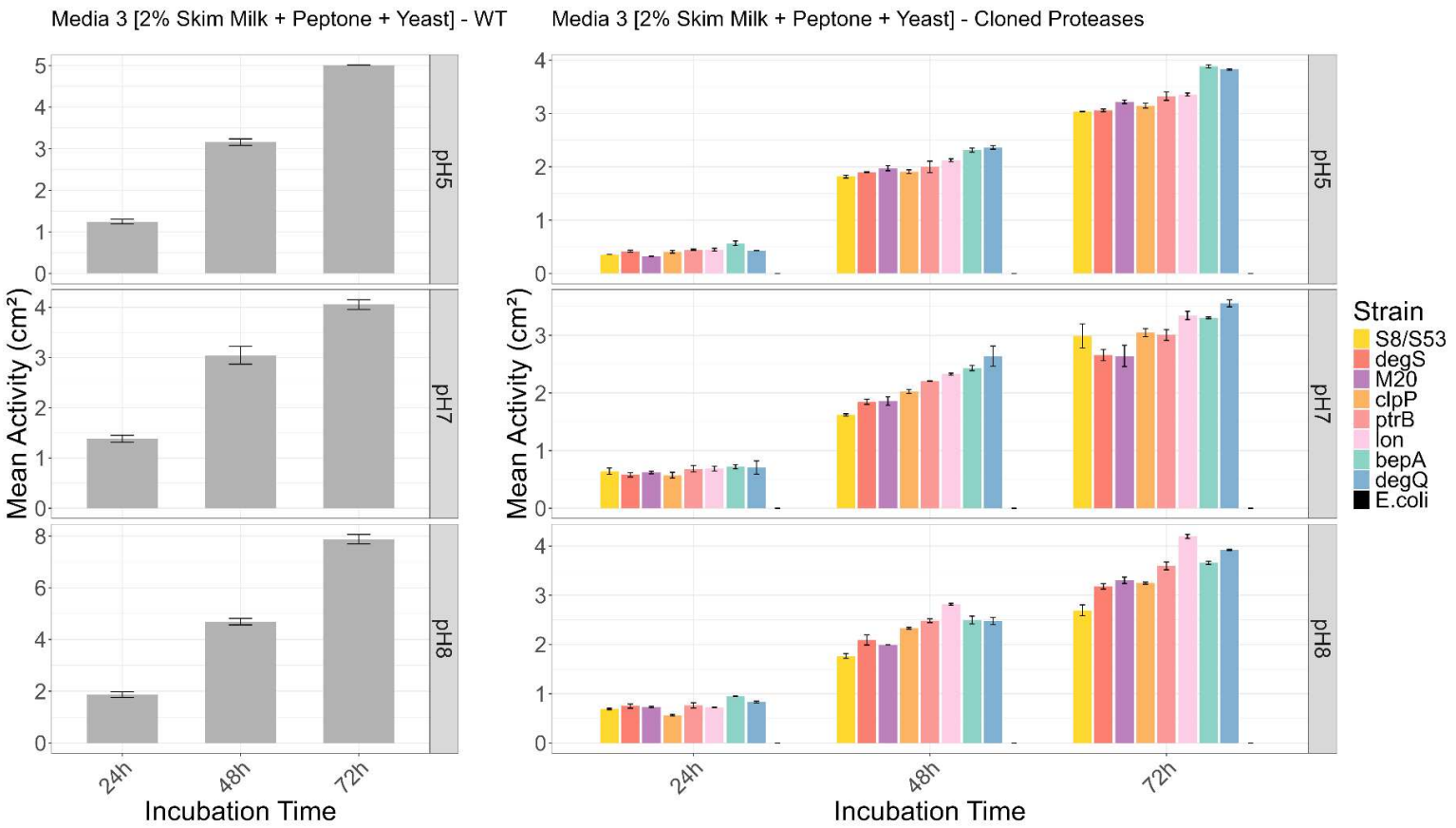


***Figure 2. Protease activity of wild-type (WT) and cloned proteases from* P. carotovorum *WPP14 on Medium 3 (2% skim milk supplemented with peptone and yeast extract, RT, supernatant) across incubation times (24h, 48h, 72h) and pH conditions (pH 5, 7, 8).*** Protease activity consistently increased with extended incubation, peaking at 72 hours. Several cloned proteases (BepA, DegQ, DegS, PtrB, ClpP, Lon, M20, and S8/S53) exhibited substantial activity across all tested pH levels, with activities comparable to or exceeding WT at ***pH 5 and pH 7 (72h).*** Data represent mean ± SD.

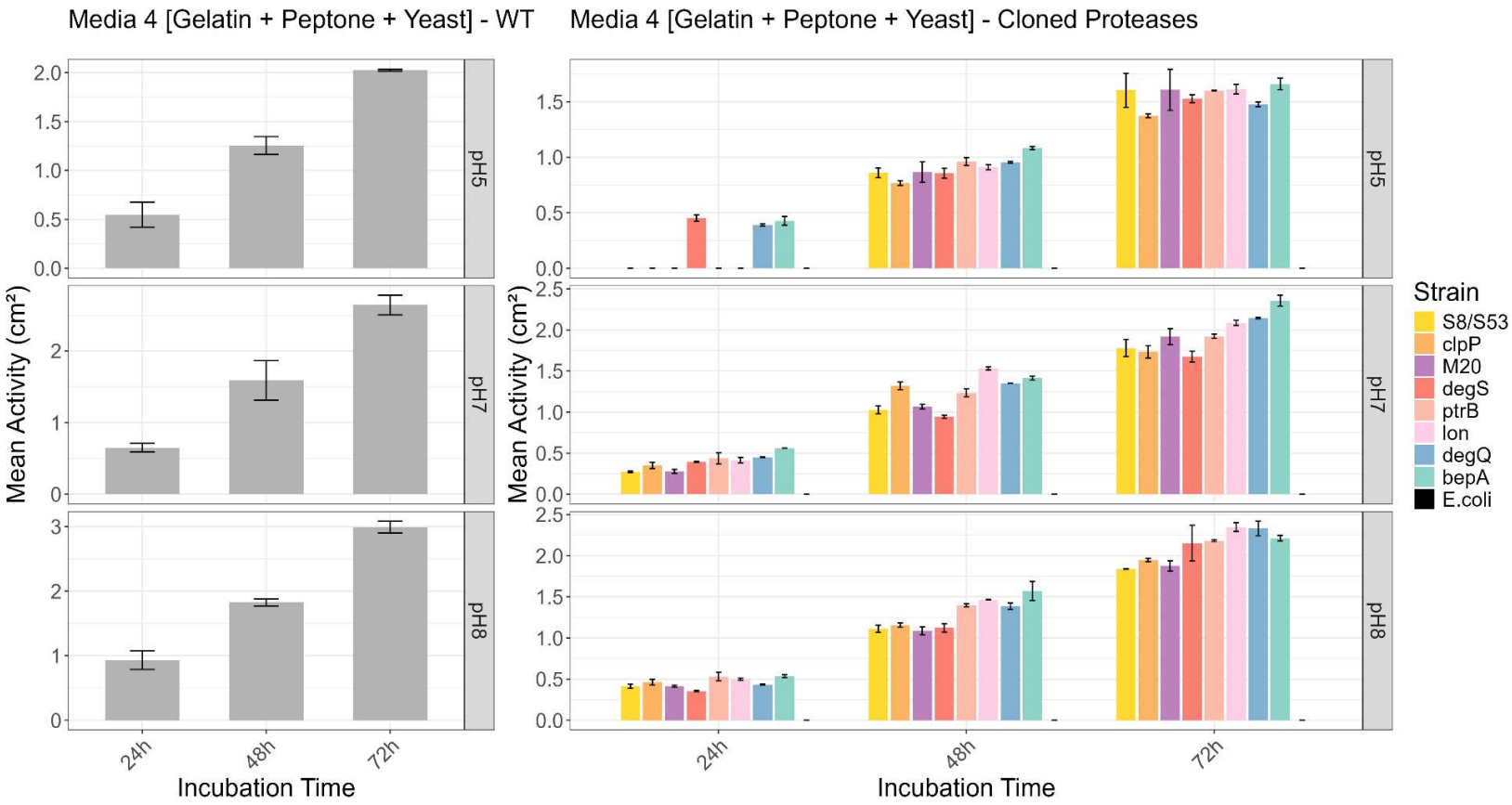


***Figure 3. Protease activity of cloned proteases compared to wild-type* (P. carotovorum *WPP14*) *on Medium 4 (gelatin-based medium supplemented with peptone and yeast extract, supernatant inoculum, RT*).** Activity was measured across pH 5, 7, and 8 at incubation durations of 24h, 48h, and 72h. Clones including ***DegQ, DegS, PtrB, ClpP, Lon, M20, S8/S53, and BepA*** exhibited reproducible activity, particularly at longer incubation times (72h). Statistical analysis (ANOVA, $p < 0.001$) confirmed incubation time as the only significant factor affecting activity. Data represent mean ± SD.

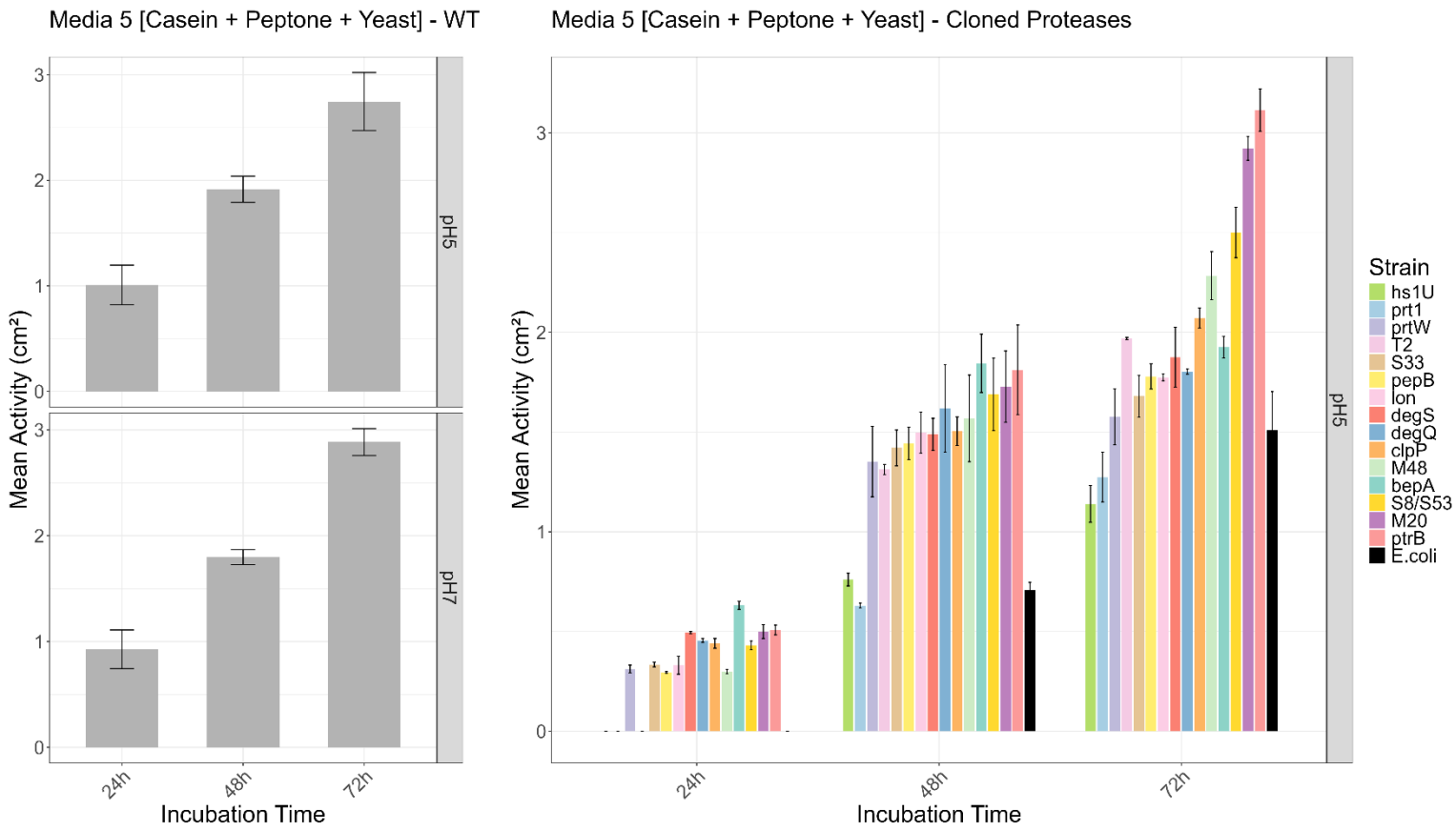


***Figure 4. Protease activity of cloned proteases compared to wild-type* P. carotovorum *WPP14 on Medium 5 (casein with peptone and yeast extract, supernatant, RT).*** Background activity from negative control (E. coli) at pH 5 raised concerns about nonspecific caseinolysis. Cloned strains showed no activity at pH 7 or 8, while the wild-type exhibited clear halos at pH 5 and 7. Data represent mean ± SD.

**Table 2. Protease Activity on Traditional Skim Milk Agar (1%) (Medium 1)**

| Strain | Sterilization | Supernatant (Filtered) | Supernatant (Unfiltered) | Sonicated Cells | Optimal pH | Optimal Temperature |
|---|---|---|---|---|---|---|
| *E. coli* | M/A | – | – | + | 7 | 37°C |
| WT (WPP14) | M/A | + | + | + | 7 > 5 | RT |
| **Metalloproteases** | | | | | | |
| Pro1 (Prt1) | Autoclave | – | – | – | – | – |
| Pro2 (PrtW) | Autoclave | – | – | – | – | – |
| Pro8 (BepA) | Autoclave | – | – | – | – | – |
| Pro9 (M20) | Autoclave | – | – | – | – | – |
| Pro13 (M48) | Autoclave | – | – | – | – | – |
| Pro14 (PepB) | Autoclave | – | – | – | – | – |
| **Serine Proteases** | | | | | | |
| Pro3 (PtrB) | Autoclave | – | – | + | 7 | RT |
| Pro4 (Lon) | Autoclave | – | – | – | – | – |
| Pro5 (ClpP) | Autoclave | – | – | – | – | – |
| Pro6 (DegQ) | Autoclave | – | + | + | 7 > 5 | RT |
| Pro7 (DegS) | Autoclave | – | – | – | – | – |
| Pro10 (S8/S53) | Autoclave | – | – | – | – | – |
| Pro12 (S33) | Autoclave | – | – | – | – | – |
| **Threonine Proteases** | | | | | | |
| Pro15 (HslU) | Autoclave | – | – | – | – | – |

**Table 3. Protease Activity on Modified Skim Milk Agar (2%) (Medium 2)**

| Strain | Sterilization | Supernatant (Filtered) | Supernatant (Unfiltered) | Sonicated Cells | Optimal pH | Optimal Temperature |
|---|---|---|---|---|---|---|
| *E. coli* | M/A | + | – | NA | 7 | 37°C |
| WT (WPP14) | M/A | + | + | NA | 8, 7 | RT, 18°C |
| **Metalloproteases** | | | | | | |
| Pro1 (Prt1) | M/A | – | – | NA | – | – |
| Pro2 (PrtW) | M/A | – | – | NA | – | – |
| Pro8 (BepA) | M/A | – | – | NA | – | – |
| Pro9 (M20) | M/A | – | – | NA | – | – |
| Pro13 (M48) | M/A | – | – | NA | – | – |
| Pro14 (PepB) | M/A | – | – | NA | – | – |
| **Serine Proteases** | | | | | | |
| Pro3 (PtrB) | M/A | – | – | NA | – | – |
| Pro4 (Lon) | M/A | – | – | NA | – | – |
| Pro5 (ClpP) | M/A | – | – | NA | – | – |
| Pro6 (DegQ) | M/A | – | – | NA | – | – |
| Pro7 (DegS) | M/A | – | – | NA | – | – |
| Pro10 (S8/S53) | M/A | – | – | NA | – | – |
| Pro12 (S33) | M/A | – | – | NA | – | – |
| **Threonine Proteases** | | | | | | |
| Pro15 (HslU) | M/A | – | – | NA | – | – |

**Table 4. Protease Activity on Enhanced Skim Milk Agar with Peptone and Yeast Extract (Medium 3)**

| Strain | Sterilization | Supernatant (Filtered) | Supernatant (Unfiltered) | Sonicated Cells | Optimal pH | Optimal Temperature |
|---|---|---|---|---|---|---|
| *E. coli* | M/A | + | – | – | 8 | 37°C |
| WT (WPP14) | M/A | + | + | – | 8 > 7 > 5 | RT > 18°C > 37°C |
| **Metalloproteases** | | | | | | |
| Pro1 (Prt1) | M/A | – | – | – | – | – |
| Pro2 (PrtW) | M/A | – | – | – | – | – |
| Pro8 (BepA) | M/A | – | + | – | 8 > 7 > 5 (*) | RT, 37°C |
| Pro9 (M20) | M/A | – | + | – | 8 > 7 > 5 | RT, 37°C |
| Pro13 (M48) | M/A | – | – | – | – | – |
| Pro14 (PepB) | M/A | – | – | – | – | – |
| **Serine Proteases** | | | | | | |
| Pro3 (PtrB) | M/A | – | + | – | 8 > 7 > 5 | RT, 37°C |
| Pro4 (Lon) | M/A | – | + | – | 8 > 7 > 5 (*) | RT |
| Pro5 (ClpP) | M/A | – | + | – | 8 > 7 > 5 | RT, 37°C |
| Pro6 (DegQ) | M/A | – | + | – | 8 > 7 > 5 (*) | RT, 37°C |
| Pro7 (DegS) | M/A | – | + | – | 8 > 7 > 5 (*) | RT, 37°C |
| Pro10 (S8/S53) | M/A | – | + | – | – | – |
| Pro12 (S33) | M/A | – | – | – | – | – |
| **Threonine Proteases** | | | | | | |
| Pro15 (HslU) | M/A | – | – | – | – | – |

**Table 5. Protease Activity on Gelatin-Based Medium (Medium 4)**

| Strain | Sterilization | Supernatant (Unfiltered) | Optimal pH | Optimal Temperature |
|---|---|---|---|---|
| *E. coli* | M/A | – | – | – |
| WT (WPP14) | M/A | + | 8 > 7 > 5 | RT |
| **Metalloproteases** | | | | |
| Pro1 (Prt1) | M/A | – | – | – |
| Pro2 (PrtW) | M/A | – | – | – |
| Pro8 (BepA) | M/A | + | 8 > 7 > 5 | RT |
| Pro9 (M20) | M/A | + | 8 > 7 > 5 | RT |
| Pro13 (M48) | M/A | – | – | – |
| Pro14 (PepB) | M/A | – | – | – |
| **Serine Proteases** | | | | |
| Pro3 (PtrB) | M/A | + | 8 > 7 > 5 | RT |
| Pro4 (Lon) | M/A | + | 8 > 7 > 5 | RT |
| Pro5 (ClpP) | M/A | + | 8 > 7 > 5 | RT |
| Pro6 (DegQ) | M/A | + | 8 > 7 > 5 | RT |
| Pro7 (DegS) | M/A | + | 8 > 7 > 5 | RT |
| Pro10 (S8/S53) | M/A | + | 8 > 7 > 5 | RT |
| Pro12 (S33) | M/A | – | – | – |
| **Threonine Proteases** | | | | |
| Pro15 (HslU) | M/A | – | – | – |

[6]**Table 6. Protease Activity on Casein-Based Medium (Medium 5)**

| Strain | Sterilization | Supernatant (Unfiltered) | Optimal pH | Optimal Temperature |
|---|---|---|---|---|
| *E. coli* | Microwaving | + (Background) | 5 | RT |
| WT (WPP14) | Microwaving | + | 5 | RT |
| **Metalloproteases** | | | | |
| Pro1 (Prt1) | Microwaving | + (Uncertain) | 5 | RT |
| Pro2 (PrtW) | Microwaving | + (Uncertain) | 5 | RT |
| Pro8 (BepA) | Microwaving | + (Uncertain) | 5 | RT |
| Pro9 (M20) | Microwaving | + (Uncertain) | 5 | RT |
| Pro13 (M48) | Microwaving | + (Uncertain) | 5 | RT |
| Pro14 (PepB) | Microwaving | + (Uncertain) | 5 | RT |
| **Serine Proteases** | | | | |
| Pro3 (PtrB) | Microwaving | + (Uncertain) | 5 | RT |
| Pro4 (Lon) | Microwaving | + (Uncertain) | 5 | RT |
| Pro5 (ClpP) | Microwaving | + (Uncertain) | 5 | RT |
| Pro6 (DegQ) | Microwaving | + (Uncertain) | 5 | RT |
| Pro7 (DegS) | Microwaving | + (Uncertain) | 5 | RT |
| Pro10 (S8/S53) | Microwaving | + (Uncertain) | 5 | RT |
| Pro12 (S33) | Microwaving | + (Uncertain) | 5 | RT |
| **Threonine Proteases** | | | | |
| Pro15 (HsIU) | Microwaving | + (Uncertain) | 5 | RT |

[6] (+) = Clear proteolytic activity detected. (−) = No detectable proteolytic activity.
NA = Not assessed.
M/A = Both microwaving and autoclaving sterilization methods were effective.

[7]**Table 7.** AlphaFold predicted interactions between cloned proteases from *P. carotovorum* WPP14 and PI (g6571) cloned from *Solanum chacoense*. Interaction predictions were evaluated using AlphaFold3 metrics (ipTM and pTM scores), where values ≥0.8 for ipTM and ≥0.5 for pTM indicate a strong predicted inhibitory interaction. The WPP14 native inhibitor against PrtW served as a positive control.

| # | Protease | Protease Inhibitor | ipTM | pTM | Predicted Inhibition |
|---|---|---|---|---|---|
| **00** | **PrtW** | **WPP14 inh** | **0.9** | **0.9** | **Strong (Positive Control)** |
| | **Metalloprotease** | **Kunitz-type PI** | | | |
| **01** | Prt1 | g6571 (PI5) | 0.2 | 0.7 | Unlikely effective |
| **02** | PrtW | g6571 (PI5) | 0.3 | 0.7 | Unlikely effective |
| **03** | BepA | g6571 (PI5) | 0.1 | 0.6 | Unlikely effective |
| **04** | M20 | g6571 (PI5) | 0.1 | 0.6 | Unlikely effective |
| **05** | M48 | g6571 (PI5) | 0.2 | 0.4 | Unlikely effective |
| **06** | PepB | g6571 (PI5) | 0.2 | 0.7 | Unlikely effective |
| | **Serine protease** | | | | |
| **07** | PtrB | g6571 (PI5) | 0.2 | 0.6 | Unlikely effective |
| **08** | Lon | g6571 (PI5) | 0.4 | 0.5 | Unlikely effective |
| **09** | ClpP | g6571 (PI5) | 0.3 | 0.5 | Unlikely effective |
| **10** | DegQ | g6571 (PI5) | 0.2 | 0.5 | Unlikely effective |
| **11** | DegS | g6571 (PI5) | 0.1 | 0.5 | Unlikely effective |
| **12** | S8/S53 | g6571 (PI5) | 0.1 | 0.8 | Unlikely effective |
| **13** | S33 | g6571 (PI5) | 0.1 | 0.6 | Unlikely effective |
| | **Threonine protease** | | | | |
| **14** | Hs1U | g6571 (PI5) | 0.5* | 0.6 | Weak inhibition |
| | **Amidohydrolase** | | | | |
| **15** | T2(L-asparaginase) | g6571 (PI5) | 0.8*** | 0.8 | Strong inhibition |

[7] A Positive (Strong): ipTM ≥ 0.8 and pTM ≥ 0.8 (high confidence prediction).
Possible (Moderate): ipTM ≥ 0.5 and pTM ≥ 0.6 (moderate confidence).
Negative: ipTM < 0.5 or pTM < 0.6 (weak or low interaction confidence).

ipTM = 0.87 pTM = 0.9 learn more

PrtW – WPP14 inh

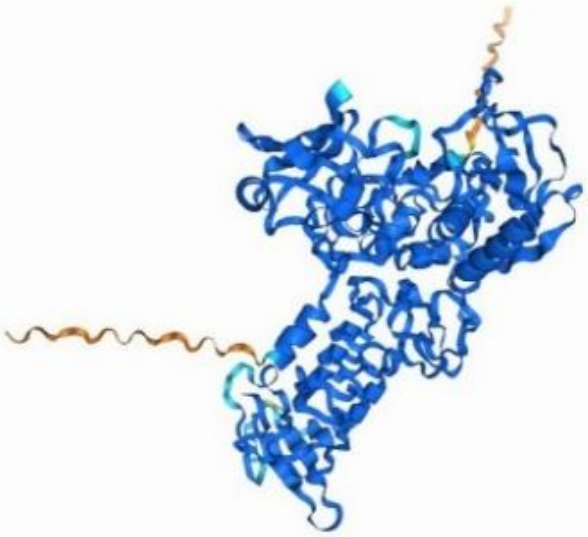

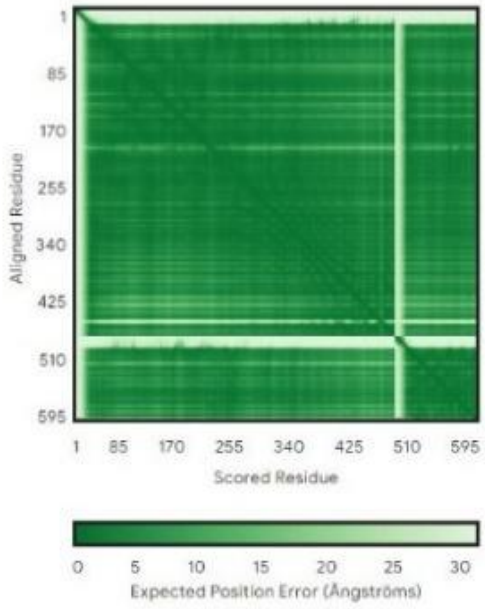


ipTM = 0.78 pTM = 0.83 learn more

T2 (L-asparaginase) – g6571 (PI5)

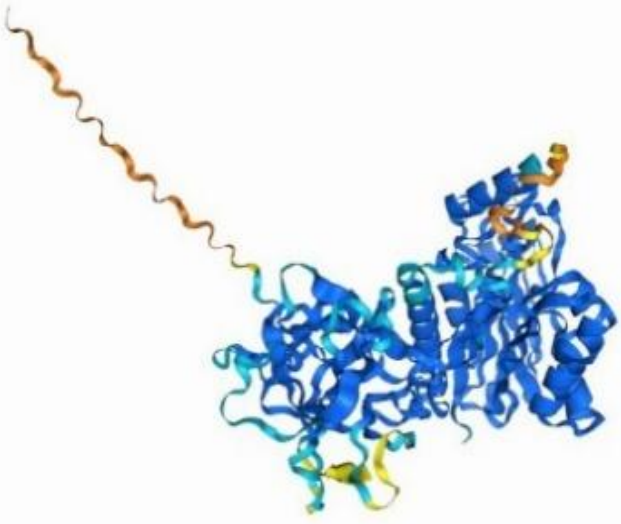

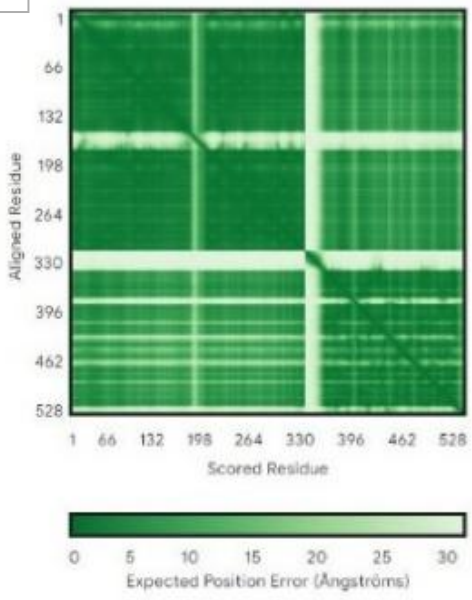

**Table 8.** AlphaFold predicted interactions between cloned proteases from *P. carotovorum* WPP14 and PI (g28531) cloned from *Solanum chacoense*. Interaction predictions were evaluated using AlphaFold3 metrics (ipTM and pTM scores), where values ≥0.8 for ipTM and ≥0.5 for pTM indicate a strong predicted inhibitory interaction. The WPP14 native inhibitor against PrtW served as a positive control.

| # | Protease | Protease Inhibitor | ipTM | pTM | Predicted Inhibition |
|---|---|---|---|---|---|
| **00** | **PrtW** | **WPP14 inh** | **0.9** | **0.9** | **Strong (Positive Control)** |
| | **Metalloprotease** | **Kunitz-type PI** | | | |
| **01** | Prt1 | G28531 (PI2) | 0.2 | 0.7 | Unlikely effective |
| **02** | PrtW | G28531 (PI2) | 0.2 | 0.7 | Unlikely effective |
| **03** | BepA | G28531 (PI2) | 0.2 | 0.7 | Unlikely effective |
| **04** | M20 | G28531 (PI2) | 0.2 | 0.6 | Unlikely effective |
| **05** | M48 | G28531 (PI2) | 0.5* | 0.5 | Weak inhibition |
| **06** | PepB | G28531 (PI2) | 0.1 | 0.7 | Unlikely effective |
| | **Serine protease** | | | | |
| **07** | PtrB | G28531 (PI2) | 0.4 | 0.6 | Unlikely effective |
| **08** | Lon | G28531 (PI2) | 0.4 | 0.5 | Unlikely effective |
| **09** | ClpP | G28531 (PI2) | 0.5* | 0.6 | Weak inhibition |
| **10** | DegQ | G28531 (PI2) | 0.5* | 0.5 | Weak inhibition |
| **11** | DegS | G28531 (PI2) | 0.4 | 0.5 | Unlikely effective |
| **12** | S8/S53 | G28531 (PI2) | 0.2 | 0.8 | Unlikely effective |
| **13** | S33 | G28531 (PI2) | 0.3 | 0.6 | Unlikely effective |
| | **Threonine protease** | | | | |
| **14** | Hs1U | G28531 (PI2) | 0.5* | 0.6 | Weak inhibition |
| | **Amidohydrolase** | | | | |
| **15** | T2(L-asparaginase) | G28531 (PI2) | 0.3 | 0.6 | Unlikely effective |

**Table 9.** AlphaFold predicted interactions between cloned proteases from *P. carotovorum* WPP14 and PI (g18987) cloned from *Solanum chacoense*. Interaction predictions were evaluated using AlphaFold3 metrics (ipTM and pTM scores), where values ≥0.8 for ipTM and ≥0.5 for pTM indicate a strong predicted inhibitory interaction. The WPP14 native inhibitor against PrtW served as a positive control.

| # | Protease | Protease Inhibitor | ipTM | pTM | Predicted Inhibition |
|---|---|---|---|---|---|
| **00** | **PrtW** | **WPP14 inh** | **0.9** | **0.9** | **Strong (Positive Control)** |
| | **Metalloprotease** | **Kunitz-type PI** | | | |
| **01** | Prt1 | G18987 (PI1) | 0.2 | 0.7 | Unlikely effective |
| **02** | PrtW | G18987 (PI1) | 0.3 | 0.8 | Unlikely effective |
| **03** | BepA | G18987 (PI1) | 0.1 | 0.7 | Unlikely effective |
| **04** | M20 | G18987 (PI1) | 0.2 | 0.7 | Unlikely effective |
| **05** | M48 | G18987 (PI1) | 0.2 | 0.5 | Unlikely effective |
| **06** | pepB | G18987 (PI1) | 0.1 | 0.8 | Unlikely effective |
| | **Serine protease** | | | | |
| **07** | ptrB | G18987 (PI1) | 0.3 | 0.7 | Unlikely effective |
| **08** | Lon | G18987 (PI1) | 0.5* | 0.6 | Weak inhibition |
| **09** | ClpP | G18987 (PI1) | 0.6** | 0.7 | Moderate inhibition |
| **10** | DegQ | G18987 (PI1) | 0.2 | 0.5 | Unlikely effective |
| **11** | DegS | G18987 (PI1) | 0.1 | 0.6 | Unlikely effective |
| **12** | S8/S53 | G18987 (PI1) | 0.2 | 0.8 | Unlikely effective |
| **13** | S33 | G18987 (PI1) | 0.1 | 0.6 | Unlikely effective |
| | **Threonine protease** | | | | |
| **14** | Hs1U | G18987 (PI1) | 0.6** | 0.6 | Moderate inhibition |
| | **Amidohydrolase** | | | | |
| **15** | T2(L-asparaginase) | G18987 (PI1) | 0.8*** | 0.9 | Strong inhibition |

ipTM = 0.49 pTM = 0.63 learn more

ClpP – g28531 (PI2)

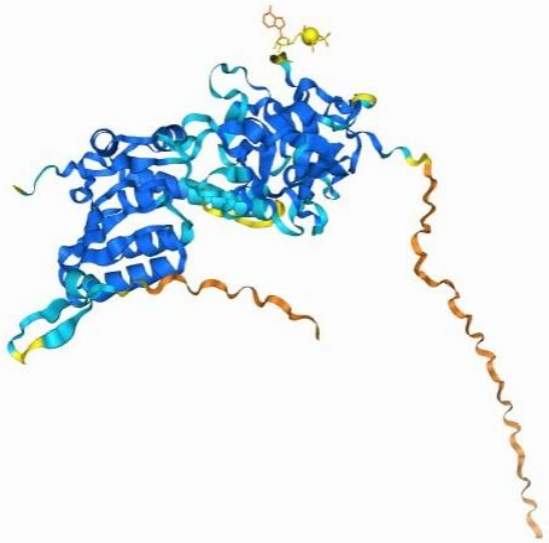

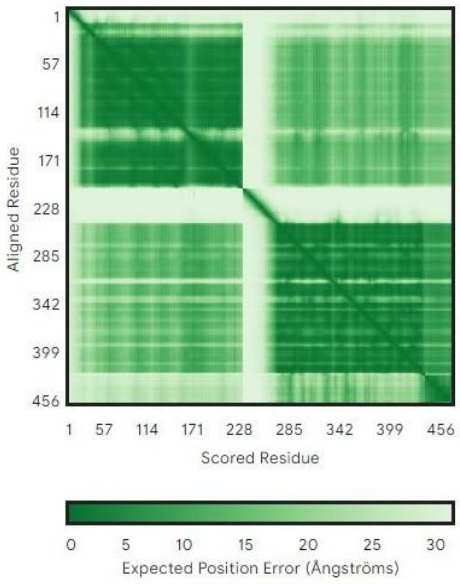


ipTM = 0.51 pTM = 0.6 learn more

Hs1U – g28531 (PI2)

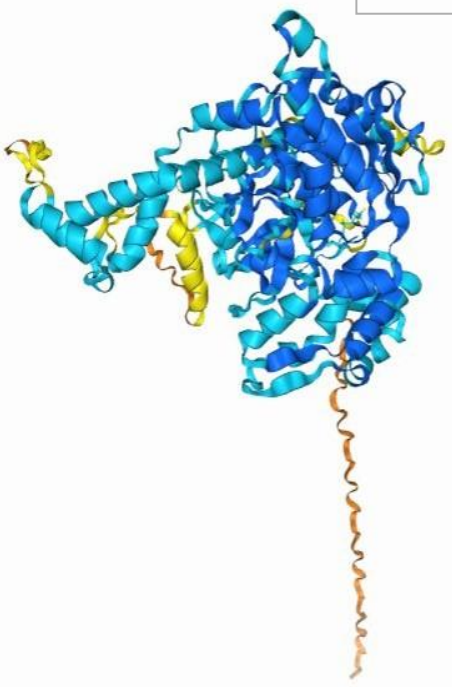

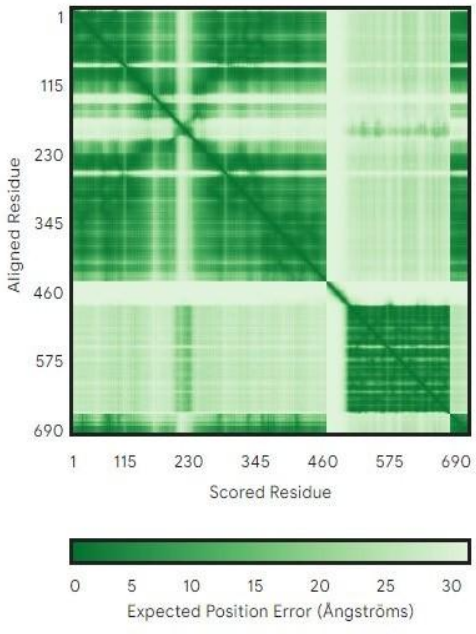

ipTM = 0.6 pTM = 0.72 learn more

ClpP – g18987 (PI1)

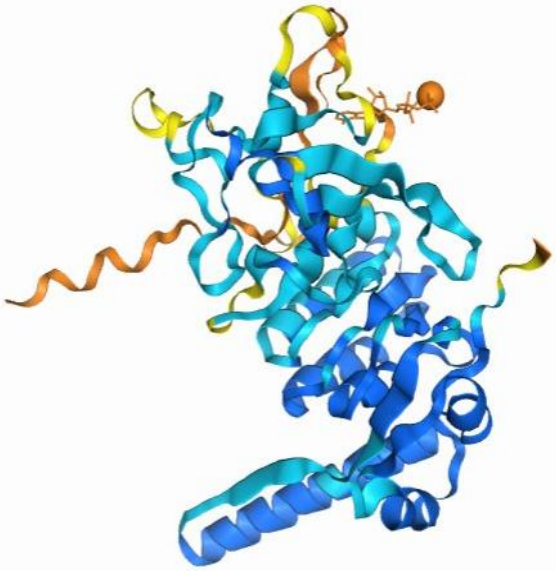

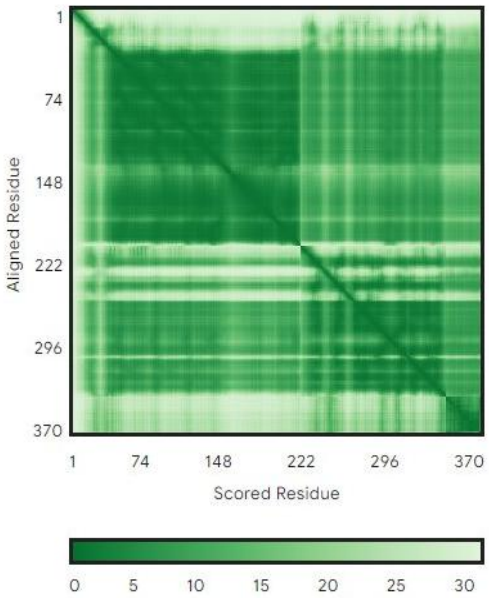


ipTM = 0.56 pTM = 0.64 learn more

Hs1U – g18987 (PI1)

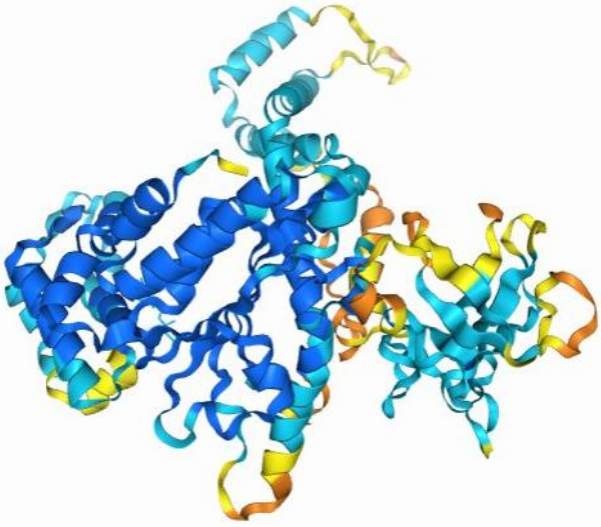

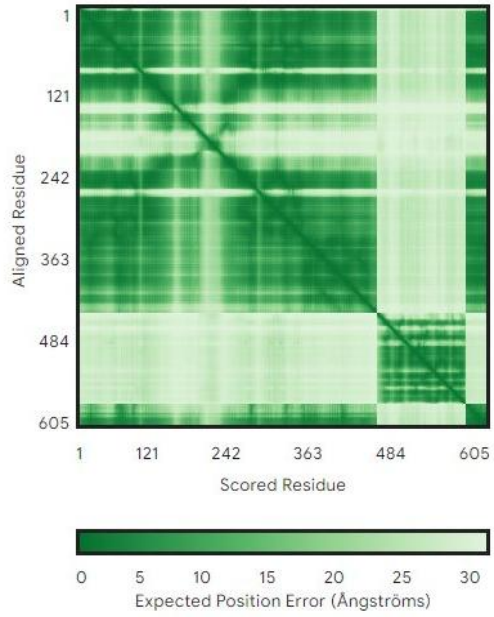

**Table 10.** AlphaFold predicted interactions between cloned proteases from *P. carotovorum* WPP14 and PI (g40384) cloned from *Solanum chacoense*. Interaction predictions were evaluated using AlphaFold3 metrics (ipTM and pTM scores), where values ≥0.8 for ipTM and ≥0.5 for pTM indicate a strong predicted inhibitory interaction. The WPP14 native inhibitor against PrtW served as a positive control.

| # | Protease | Protease Inhibitor | ipTM | pTM | Predicted Inhibition |
|---|---|---|---|---|---|
| **00** | **PrtW** | **WPP14 inh** | **0.9** | **0.9** | **Strong (Positive Control)** |
| | **Metalloprotease** | **Kunitz-type PI** | | | |
| **01** | Prt1 | G40384 (PI4) | 0.3 | 0.7 | Unlikely effective |
| **02** | PrtW | G40384 (PI4) | 0.3 | 0.7 | Unlikely effective |
| **03** | BepA | G40384 (PI4) | 0.1 | 0.6 | Unlikely effective |
| **04** | M20 | G40384 (PI4) | 0.1 | 0.6 | Unlikely effective |
| **05** | M48 | G40384 (PI4) | 0.3 | 0.5 | Unlikely effective |
| **06** | PepB | G40384 (PI4) | 0.1 | 0.7 | Unlikely effective |
| | **Serine protease** | | | | |
| **07** | PtrB | G40384 (PI4) | 0.1 | 0.7 | Unlikely effective |
| **08** | Lon | G40384 (PI4) | 0.5* | 0.6 | Weak inhibition |
| **09** | ClpP | G40384 (PI4) | 0.3 | 0.5 | Unlikely effective |
| **10** | DegQ | G40384 (PI4) | 0.2 | 0.5 | Unlikely effective |
| **11** | DegS | G40384 (PI4) | 0.2 | 0.5 | Unlikely effective |
| **12** | S8/S53 | G40384 (PI4) | 0.2 | 0.8 | Unlikely effective |
| **13** | S33 | G40384 (PI4) | 0.3 | 0.6 | Unlikely effective |
| | **Threonine protease** | | | | |
| **14** | Hs1U | G40384 (PI4) | 0.5* | 0.6 | Weak inhibition |
| | **Amidohydrolase** | | | | |
| **15** | T2(L-asparaginase) | G40384 (PI4) | 0.5* | 0.6 | Weak inhibition |

ipTM = 0.49 pTM = 0.59 learn more

Hs1U – g40384 (PI4)

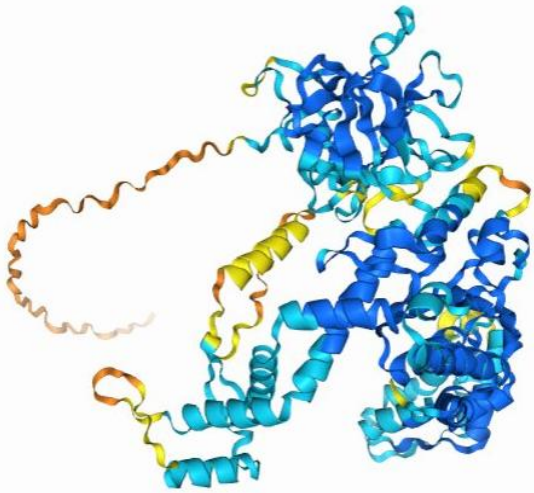

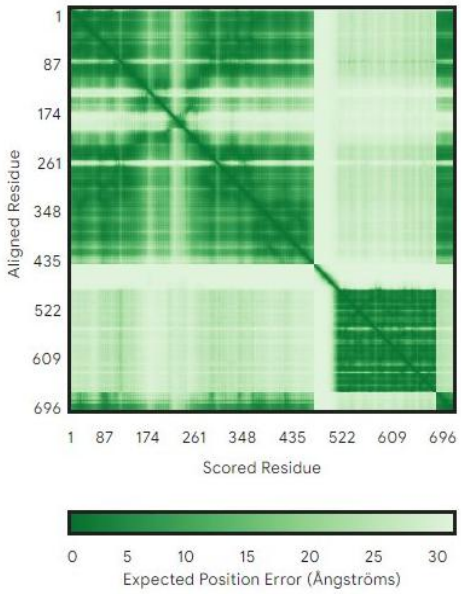


ipTM = 0.54 pTM = 0.63 learn more

T2 (L-Asparaginase) – g40384 (PI4)

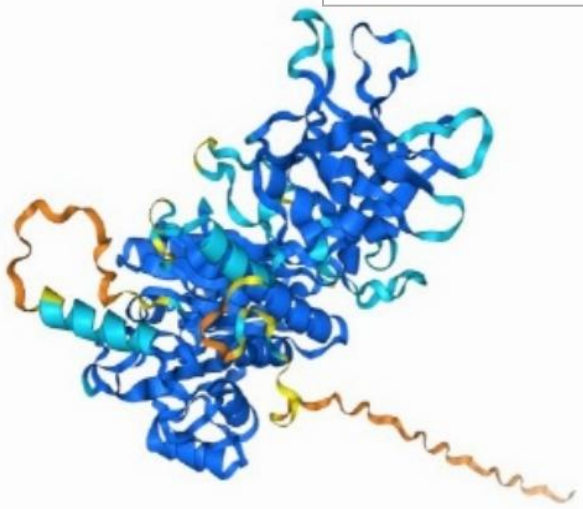

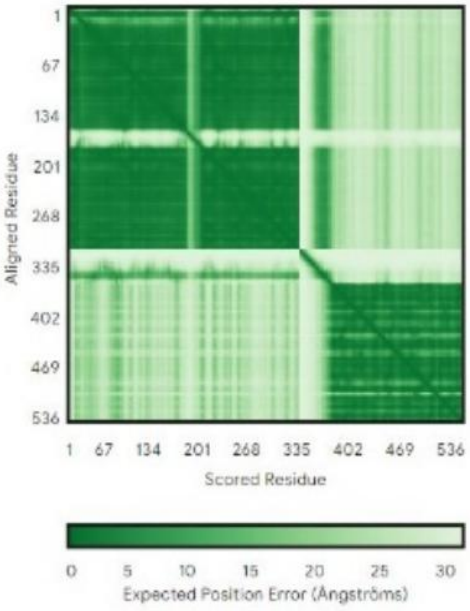

**Table 11.** AlphaFold predicted interactions between cloned proteases from *P. carotovorum* WPP14 and PI (g39249) cloned from *Solanum chacoense*. Interaction predictions were evaluated using AlphaFold3 metrics (ipTM and pTM scores), where values ≥0.8 for ipTM and ≥0.5 for pTM indicate a strong predicted inhibitory interaction. The WPP14 native inhibitor against PrtW served as a positive control.

| # | Protease | Protease Inhibitor | ipTM | pTM | Predicted Inhibition |
|---|---|---|---|---|---|
| **00** | **PrtW** | **WPP14 inh** | **0.9** | **0.9** | **Strong (Positive Control)** |
| | **Metalloprotease** | **Serine PI (Potato Type I)** | | | |
| **01** | Prt1 | G39249 (PI3) | 0.2 | 0.7 | Unlikely effective |
| **02** | PrtW | G39249 (PI3) | 0.3 | 0.8 | Unlikely effective |
| **03** | BepA | G39249 (PI3) | 0.2 | 0.7 | Unlikely effective |
| **04** | M20 | G39249 (PI3) | 0.2 | 0.7 | Unlikely effective |
| **05** | M48 | G39249 (PI3) | 0.5* | 0.6 | Weak inhibition |
| **06** | PepB | G39249 (PI3) | 0.1 | 0.8 | Unlikely effective |
| | **Serine protease** | | | | |
| **07** | PtrB | G39249 (PI3) | 0.3 | 0.8 | Unlikely effective |
| **08** | Lon | G39249 (PI3) | 0.5* | 0.6 | Weak inhibition |
| **09** | ClpP | G39249 (PI3) | 0.2 | 0.6 | Unlikely effective |
| **10** | DegQ | G39249 (PI3) | 0.6** | 0.6 | Moderate inhibition |
| **11** | DegS | G39249 (PI3) | 0.5* | 0.7 | Weak inhibition |
| **12** | S8/S53 | G39249 (PI3) | 0.2 | 0.9 | Unlikely effective |
| **13** | S33 | G39249 (PI3) | 0.3 | 0.7 | Unlikely effective |
| | **Threonine protease** | | | | |
| **14** | HslU | G39249 (PI3) | 0.6** | 0.7 | Moderate inhibition |
| | **Amidohydrolase** | | | | |
| **15** | T2(L-asparaginase) | G39249 (PI3) | 0.1 | 0.7 | Unlikely effective |

ipTM = 0.58 pTM = 0.63 learn more

DegQ – g39249 (PI3)

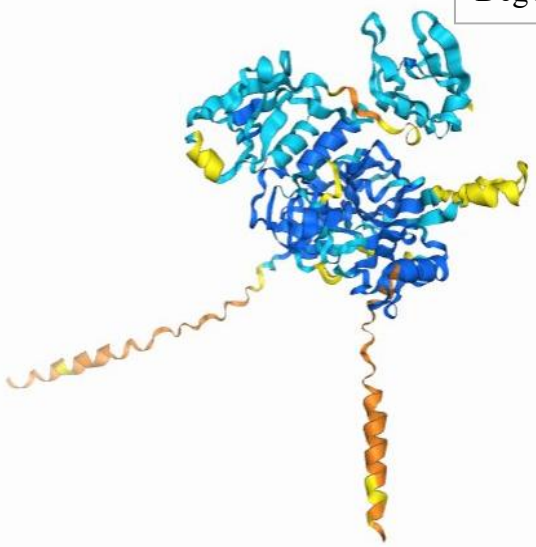

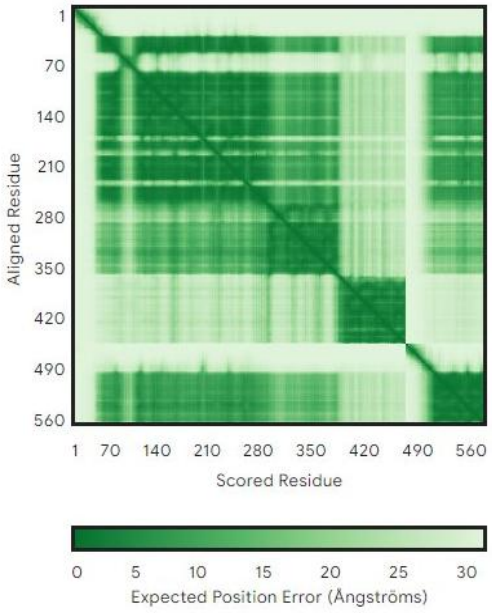


ipTM = 0.61 pTM = 0.71 learn more

Hs1U – g39249 (PI3)

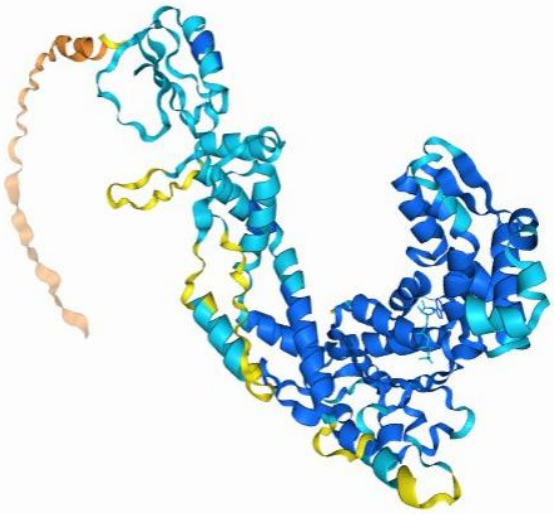

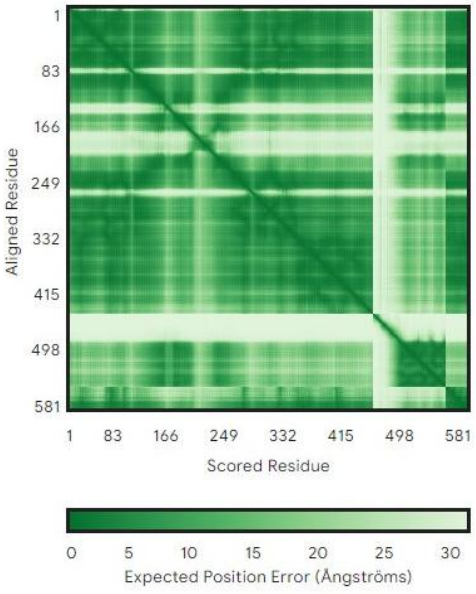

**Table 12. Summary of Cloned Proteases from *Pectobacterium carotovorum* WPP14**

| # | Protease | Enzyme Name | Biological Role | Subcellular Location | Co-factor | Optimum Conditions (pH/Temp)[8] | Species & Similarity to E. coli K-12 (%)[9] | Reference |
|---|---|---|---|---|---|---|---|---|
| | **Metalloproteases** | | | | | | | |
| 01 | Prt1 | Extracellular metalloprotease | Plant cell-wall degradation, nutrient acquisition, virulence | Secreted (extracellular) | $Zn^{2+}$, $Ca^{2+}$ | pH 6.0, 50 °C | *P. carotovorum* | (Feng et al., 2014) |
| 02 | PrtW | Extracellular metalloprotease | Plant cell-wall degradation, bacterial colonization, virulence | Secreted (extracellular) | $Zn^{2+}$, $Ca^{2+}$ | pH 7.0–8.0, ~30 °C | *P. carotovorum* | (Marits et al., 1999) |
| 03 | BepA | Beta-barrel assembly-enhancing protease | Membrane integrity, stress response, outer membrane protein quality control | Outer membrane | $Zn^{2+}$ | pH 7.0, 37 °C | *E. coli* (71%) | (Narita et al., 2013) |
| 04 | M20 | Aminoacylase/carboxypeptidase (M20 family) | Amino acid metabolism, nutrient cycling, adaptation to environmental conditions | Cytoplasm | $Zn^{2+}$, $Mn^{2+}$ | pH 7.0, 30–37 °C | General bacterial (M20 family) | (Rawlings et al., 2018) |
| 05 | M48 (HtpX) | Zn-dependent protease/chaperone | Stress adaptation, protein quality control, response to cellular stress | Periplasm | $Zn^{2+}$ | pH 7.0, 30–37 °C | *E. coli* (30%) | (Sakoh et al., 2005) |

[8] Optimal conditions derived from references specific to *Pectobacterium carotovorum* are prioritized; in their absence, conditions from closely related bacteria (e.g., *Escherichia coli*) or general bacterial literature have been included and explicitly indicated.

[9] Percent identity (%): indicates amino acid sequence similarity between the cloned protease from *P. carotovorum* WPP14 and the corresponding protease in the cited reference species (*E. coli* K-12 MG1655), as determined by BLASTp analysis.

| | | | | | | | | |
|---|---|---|---|---|---|---|---|---|
| 06 | PepB | Leucine aminopeptidase | Protein turnover, nutrient acquisition, amino acid recycling | Cytoplasm | $Mn^{2+}$ | pH 7.0–9.0, 30–37 °C | *E. coli (*76%) | (Rawlings et al., 2018) |
| | **Serine proteases** | | | | | | | |
| 07 | PtrB | Prolyl oligopeptidase (S9 family) | Protein maturation, peptide metabolism, regulation of virulence | Cytoplasm or secreted | – | pH 8.0, 30 °C | *E. coli* (62%) | (Moreno Amador et al., 2019) |
| 08 | Lon | ATP-dependent Lon protease | Stress response, protein quality control, regulation of pathogenicity | Cytoplasm | ATP | pH 7.0, 37 °C | *E. coli* (93%) | (Gottesman , 2003) |
| 09 | ClpP | ATP-dependent Clp protease | Cellular homeostasis, adaptation under stress conditions, regulation of virulence | Cytoplasm | ATP, $Mg^{2+}$ | pH 7.0, 37 °C | *E. coli* (89%) | (Kessel et al., 1996) |
| 10 | DegQ | HtrA-family serine protease | Response to envelope stress, maintaining periplasmic protein quality | Periplasmic space | – | pH 5.5–7.0, 30–37 °C | *E. coli* (70%) | (Sawa et al., 2011) |
| 11 | DegS | HtrA-family serine protease | Cellular stress signaling, regulation of periplasmic stress response pathways | Inner membrane (periplasmic side) | – | pH 6.0–7.0, 30–37 °C | *E. coli* (59%) | (Sawa et al., 2011) |
| 12 | S8/S53 | Alkaline serine protease | Protein degradation, nutrient acquisition, and possible role in host-pathogen interaction | Secreted/outer membrane | $Ca^{2+}$ | pH 8.0–10.0, 30–37 °C | General bacterial | (Rawlings et al., 2018) |
| 13 | S33 (pldB) | Serine aminopeptidase / | Protein processing, lipid metabolism, | Membrane-associated | – | pH 7.0–8.0, ~37 °C | *E. coli (*60%) | (Rawlings et al., 2018) |

| | | | | | | | | |
|---|---|---|---|---|---|---|---|---|
| | | Lysophospholipase L2 | membrane integrity, adaptation to membrane stress | | | | | |
| | **Threonine protease** | | | | | | | |
| 14 | HslU | Heat shock protease (ClpYQ complex ATPase) | Protein quality control, stress adaptation, maintenance of proteostasis | Cytoplasm | ATP | pH 7.0, 30–37 °C | *E. coli* (89%) | (Gur et al., 2011) |
| | **Amidohydrolase** | | | | | | | |
| 15 | T2[10] | L-asparaginase | Nitrogen metabolism, adaptation to environmental nutrient availability | Cytoplasm | – | pH 8.0–10.0, 40 °C | *P. carotovorum* | (Kumar et al., 2011) |

[10] T2 (L-asparaginase) is included in the table due to initial annotations classifying it as "Peptidase T2" based on structural similarities within the MEROPS database. However, functional analysis clarified it as an amidohydrolase (EC 3.5.1.1) rather than a true protease. A detailed explanation addressing this annotation ambiguity is provided in the discussion section.

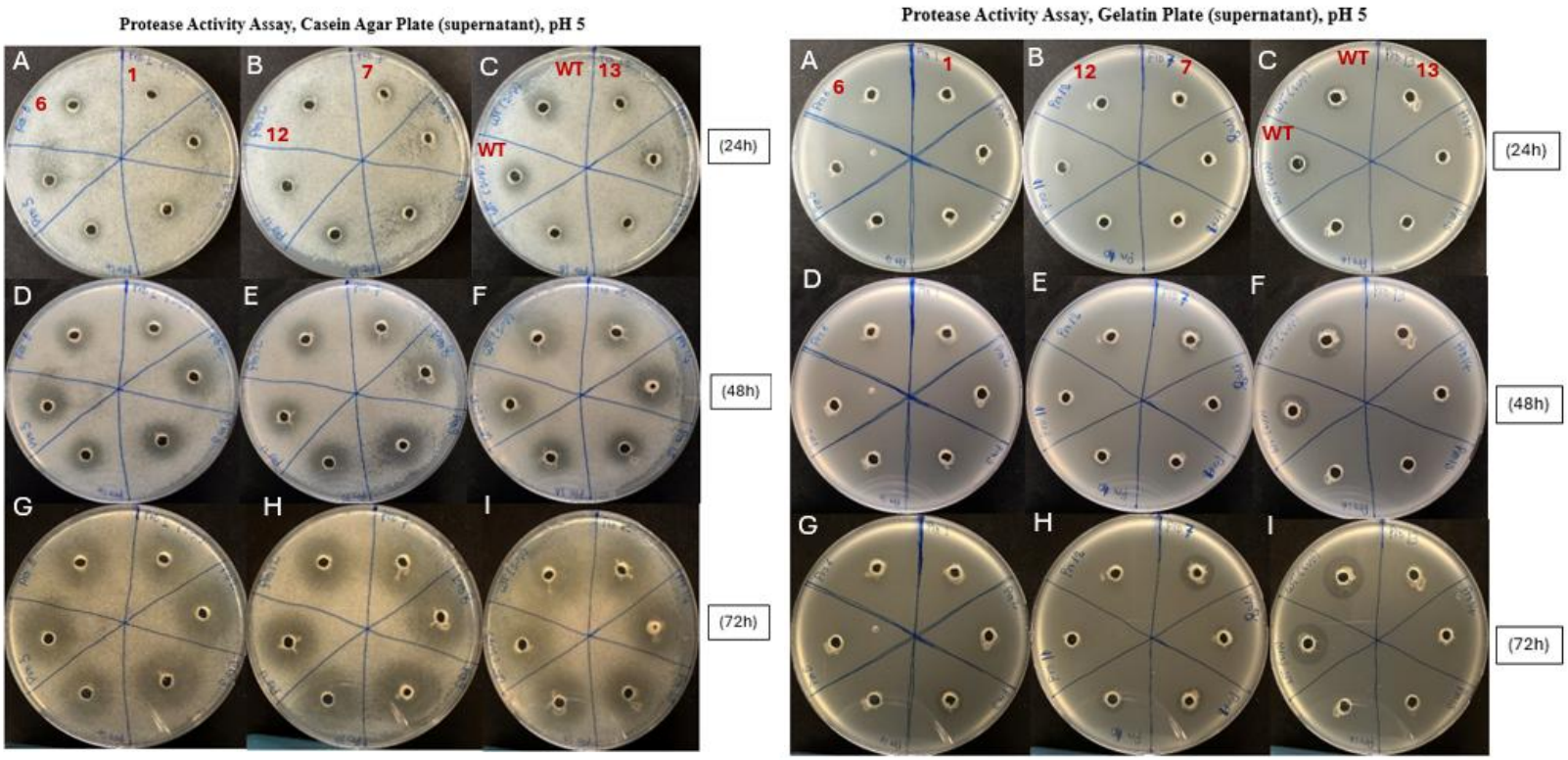


**Figure 5. Protease activity assays of cloned proteases from *Pectobacterium carotovorum* WPP14 on casein (left panel) and gelatin (right panels) agar media (pH 5, supernatant).** Activity was assessed after incubation at 24 h (A–C), 48 h (D–F), and 72 h (G–I). Tested proteases: Prt1 (Pro1), PrtW (Pro2), PtrB (Pro3), Lon (Pro5), ClpP (Pro6), DegQ (Pro7), DegS (Pro8), BepA (Pro9), M20 (Pro10), S8/S53 (Pro11), T2 (Pro12), S33 (Pro13), M48 (Pro14), PepB (Pro15), HslU (Pro16), and wild-type WPP14 (WT). Clear halos around wells indicate proteolytic activity. Among the tested substrates (skim milk, casein, gelatin), casein agar produced clearer and earlier proteolytic halos; however, significant protease activity was also detected for the negative control (*E. coli* host), demonstrating casein agar's unsuitability for accurate protease screening due to high background activity. Gelatin agar showed better specificity by not supporting background *E. coli* activity.

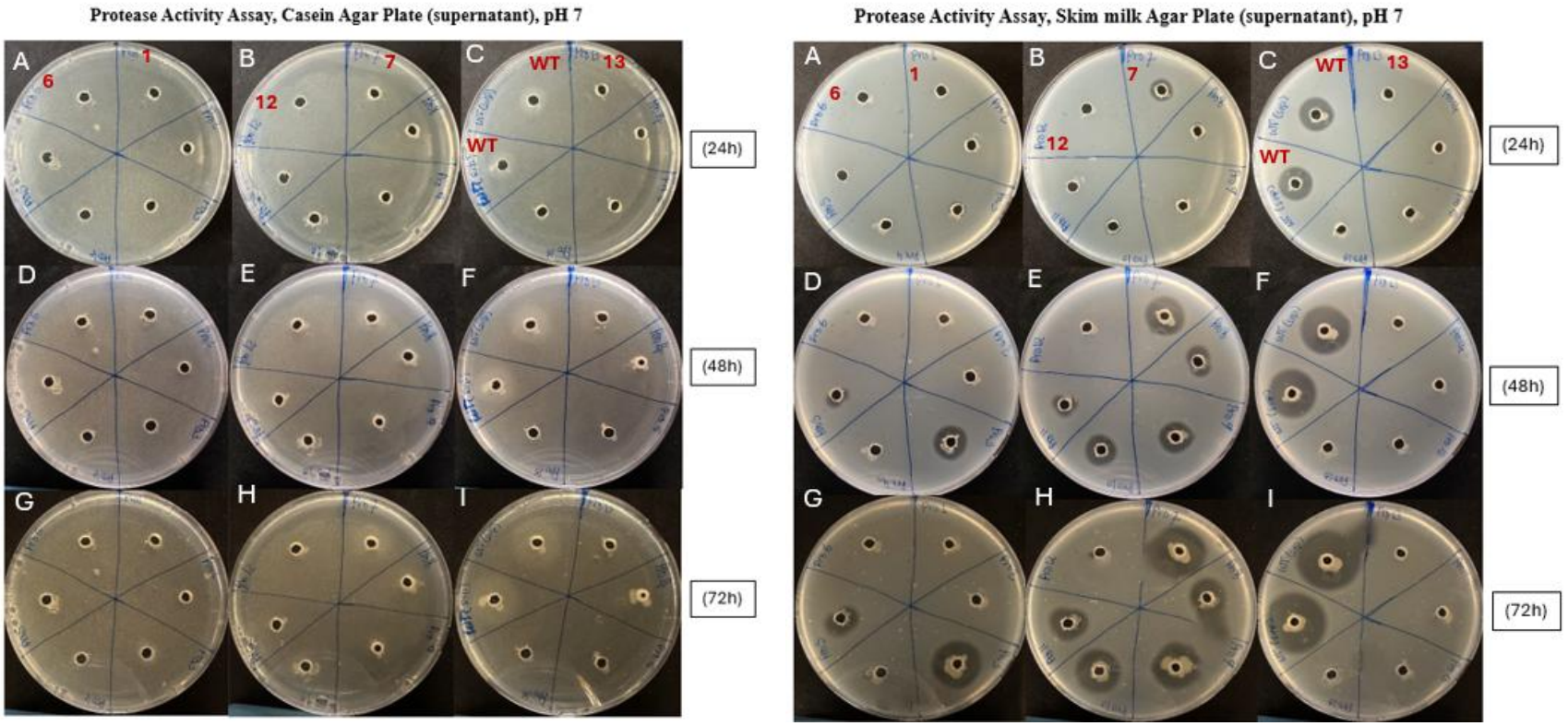


**Figure 6. Comparison of proteolytic activities of cloned proteases (Pro1–Pro16 and WT control) from *Pectobacterium carotovorum* WPP14 on casein agar (left) and modified skim milk agar (right; 2% skim milk enhanced with peptone and yeast extract), both adjusted to pH 7.0.** Plates (A–C) were incubated for 24 h, (D–F) for 48 h, and (G–I) for 72 h. Protease activity is visualized as clear halos surrounding the inoculation wells. At neutral pH (7.0), the modified skim milk agar demonstrated clear and distinct zones of proteolytic activity for several cloned proteases, indicating effective substrate hydrolysis and better visualization of protease activities. In contrast, casein agar showed minimal or no visible protease activity under these conditions, indicating it was unsuitable for reliable detection of the tested proteases from *P. carotovorum*. These findings suggest modified skim milk agar as a more appropriate medium for consistent and clear protease screening assays.

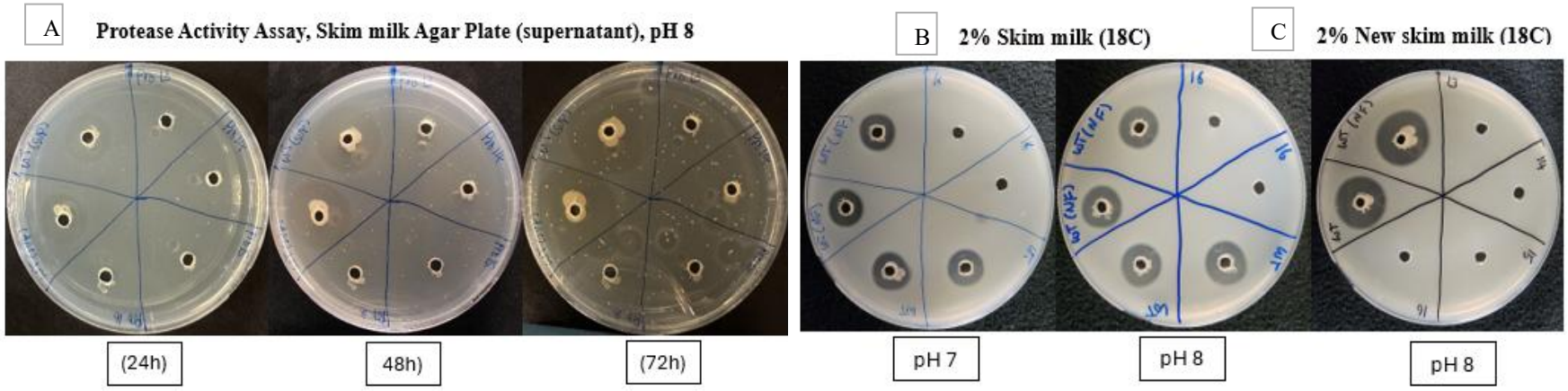


**Figure 7. Optimization of skim milk agar media for protease activity assays.** (A) Original skim milk agar media at pH 8: adjusting the pH caused the medium to become nearly transparent, significantly hindering visualization and detection of proteolytic halos. (B) Modified skim milk agar with increased skim milk concentration (2%), incubated at 18°C. At pH 7 (left), clear halos were visible; adjusting the medium to pH 8 (middle) retained sufficient opacity, enabling improved visualization of protease activity. (C) Enhanced skim milk medium supplemented with peptone and yeast extract (2% skim milk, pH 8, 18°C), showing optimal clarity, contrast, and distinct proteolytic halos, providing the most reliable and clear results for protease screening assays.

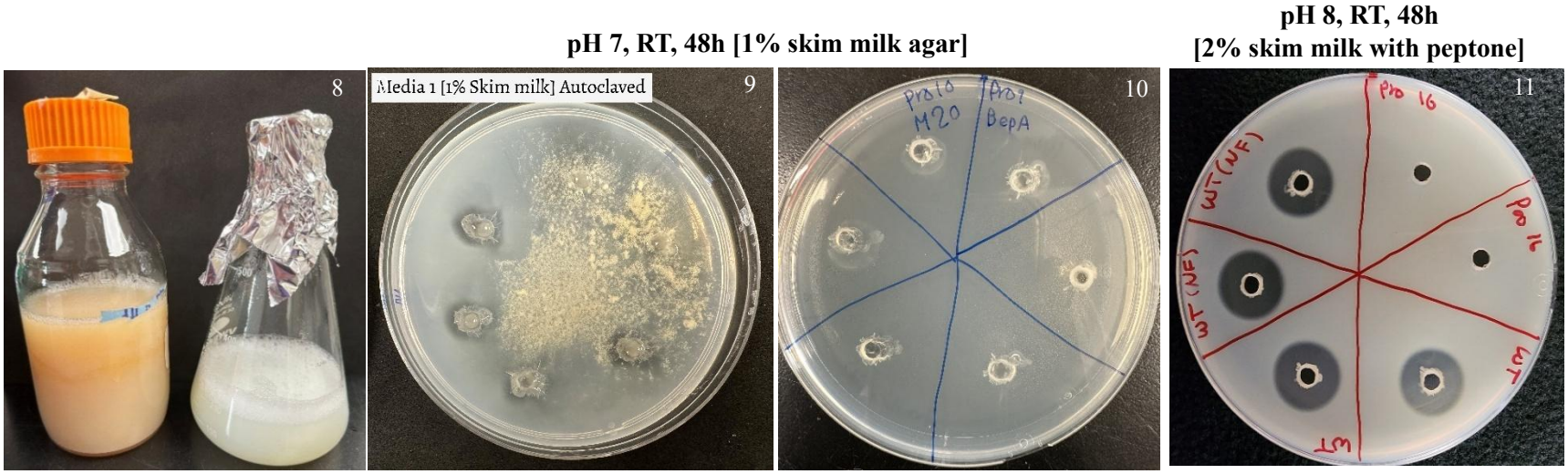


**Figure 8. Comparison of skim milk agar media preparation methods and their effects on protease activity assays.** Image (8) demonstrates the impact of autoclaving (left bottle) versus microwave-based media preparation (right flask). Autoclaving resulted in media coagulation and a browned (burnt) appearance, negatively affecting clarity, whereas microwaving preserved the media's clarity and consistency. Images (9) and (10) show protease activity assays on standard skim milk agar plates (1% skim milk, pH 7, room temperature, 48h), resulting in faint and poorly defined proteolytic halos. Image (11) illustrates optimized skim milk agar (2% skim milk enhanced with peptone and yeast extract, pH 8, room temperature, 48h), producing clear, well-defined halos that significantly enhance the accuracy and reliability of protease activity detection.

**References**


Choi, J., & Lee, S. (2004). Secretory and extracellular production of recombinant proteins using *Escherichia coli*. *Applied microbiology and biotechnology*, *64*, 625-635.

Da Silva, L. S., Doonan, L. B., Pessoa, A., De Oliveira, M. A., & Long, P. F. (2022). Structural and functional diversity of asparaginases: Overview and recommendations for a revised nomenclature. *Biotechnology and Applied Biochemistry*, *69*(2), 503-513.

Feng, T., Nyffenegger, C., Højrup, P., Vidal-Melgosa, S., Yan, K.-P., Fangel, J. U., Meyer, A. S., Kirpekar, F., Willats, W. G., & Mikkelsen, J. D. (2014). Characterization of an extensin-modifying metalloprotease: N-terminal processing and substrate cleavage pattern of *Pectobacterium carotovorum* Prt1. *Applied microbiology and biotechnology*, *98*, 10077-10089.

Figaj, D., Ambroziak, P., Przepiora, T., & Skorko-Glonek, J. (2019). The role of proteases in the virulence of plant pathogenic bacteria. *International Journal of Molecular Sciences*, *20*(3), 672.

Figaj, D., Czaplewska, P., Przepióra, T., Ambroziak, P., Potrykus, M., & Skorko-Glonek, J. (2020). Lon protease is important for growth under stressful conditions and pathogenicity of the phytopathogen, bacterium *Dickeya solani*. *International Journal of Molecular Sciences*, *21*(10), 3687.

Gottesman, S. (2003). Proteolysis in bacterial regulatory circuits. *Annual review of cell and developmental biology*, *19*(1), 565-587.

Gur, E., Biran, D., & Ron, E. Z. (2011). Regulated proteolysis in Gram-negative bacteria—how and when? *Nature Reviews Microbiology*, *9*(12), 839-848.

Joshi, J. R., Brown, K., Charkowski, A. O., & Heuberger, A. L. (2022). Protease inhibitors from *Solanum chacoense* inhibit *Pectobacterium* virulence by reducing bacterial protease activity and motility. *Molecular Plant-Microbe Interactions®. 35:825-834.*

Jumper, J., Evans, R., Pritzel, A., Green, T., Figurnov, M., Ronneberger, O., Tunyasuvunakool, K., Bates, R., Žídek, A., Potapenko, A., Bridgland, A., Meyer, C., Kohl, S. A. A., Ballard, A. J., Cowie, A., Romera-Paredes, B., Nikolov, S., Jain, R., Adler, J.,…Hassabis, D. (2021). Highly accurate protein structure prediction with AlphaFold. *Nature*, *596*(7873), 583-589.

Kessel, M., Wu, W.-F., Gottesman, S., Kocsis, E., Steven, A. C., & Maurizi, M. R. (1996). Six-fold rotational symmetry of ClpQ, the *E. coli* homolog of the 20S proteasome, and its ATP-dependent activator, ClpY. *FEBS Letters*, *398*(2-3), 274-278.

Kumar, S., Dasu, V. V., & Pakshirajan, K. (2011). Purification and characterization of glutaminase-free L-asparaginase from Pectobacterium carotovorum MTCC 1428. *Bioresource technology*, *102*(2), 2077-2082.

Létoffé, S., Delepelaire, P., & Wandersman, C. (1990). Protease secretion by Erwinia chrysanthemi: the specific secretion functions are analogous to those of Escherichia coli alpha-haemolysin. *The EMBO Journal*, *9*(5), 1375-1382.

Marits, R., Köiv, V., Laasik, E., & Mäe, A. (1999). Isolation of an extracellular protease gene of *Erwinia carotovora* subsp. *carotovora* strain SCC3193 by transposon mutagenesis and the role of protease in phytopathogenicity. *Microbiology*, *145*(8), 1959-1966.

Moreno Amador, M. D. L., Arévalo-Rodríguez, M., Durán, E. M., Martínez Reyes, J. C., & Sousa Martín, C. (2019). A new microbial gluten-degrading prolyl endopeptidase: Potential application in celiac disease to reduce gluten immunogenic peptides. *PLoS ONE*, *14*(6), e0218346.

Murata, H., McEvoy, J. L., Chatterjee, A., Collmer, A., & Chatterjee, A. K. (1991). Molecular cloning of an aepA gene that activates production of extracellular pectolytic, cellulolytic, and proteolytic enzymes in Erwinia carotovora subsp. carotovora. *Molecular Plant-Microbe Interactions*, *4(3),*, 239-246.

Narita, S.-I., Masui, C., Suzuki, T., Dohmae, N., & Akiyama, Y. (2013). Protease homolog BepA (YfgC) promotes assembly and degradation of β-barrel membrane proteins in *Escherichia coli*. *Proceedings of the National Academy of Sciences*, *110*(38), E3612-E3621.

Page, M. J., & Di Cera, E. (2008). Serine peptidases: Classification, structure and function. *Cellular and Molecular Life Sciences*, *65*(7-8), 1220-1236.

Rasband, W. S. (2025). *ImageJ*. In (Version 1.54g) [Computer software]. U.S. National Institutes of Health.

Rawlings, N. D., Barrett, A. J., Thomas, P. D., Huang, X., Bateman, A., & Finn, R. D. (2018). The MEROPS database of proteolytic enzymes, their substrates and inhibitors in 2017 and a comparison with peptidases in the PANTHER database. *Nucleic Acids Research*, *46*(D1), D624-D632.

Rosano, G. L., & Ceccarelli, E. A. (2014). Recombinant protein expression in *Escherichia coli*: advances and challenges. *Frontiers in Microbiology*, *5*, 172.

Sakoh, M., Ito, K., & Akiyama, Y. (2005). Proteolytic activity of htpx, a membrane-bound and stress-controlled protease from *Escherichia coli*. *Journal of Biological Chemistry*, *280*(39), 33305-33310.

Sawa, J., Malet, H., Krojer, T., Canellas, F., Ehrmann, M., & Clausen, T. (2011). Molecular adaptation of the degq protease to exert protein quality control in the bacterial cell envelope. *Journal of Biological Chemistry*, *286*(35), 30680-30690.

Singh, A., Upadhyay, V., Upadhyay, A. K., Singh, S. M., & Panda, A. K. (2015). Protein recovery from inclusion bodies of *Escherichia coli* using mild solubilization process. *Microbial Cell Factories*, *14*, 1-10.

Terpe, K. (2006). Overview of bacterial expression systems for heterologous protein production: from molecular and biochemical fundamentals to commercial systems. *Applied microbiology and biotechnology*, *72*, 211-222.

Varadi, M., Anyango, S., Deshpande, M., Nair, S., Natassia, C., Yordanova, G., Yuan, D., Stroe, O., Wood, G., Laydon, A., Žídek, A., Green, T., Tunyasuvunakool, K., Petersen, S., Jumper, J., Clancy, E., Green, R., Vora, A., Lutfi, M.,…Velankar, S. (2022). Alphafold protein structure database: Massively expanding the structural coverage of protein-sequence space with high-accuracy models. *Nucleic Acids Research*, *50*(D1), D439-D444.

Vermelho, A. B., Meirelles, M. N. L., Lopes, A., Petinate, S. D. G., Chaia, A. A., & Branquinha, M. H. (1996). Detection of extracellular proteases from microorganisms on agar plates. *Memorias do Instituto Oswaldo Cruz*, *91*, 755-760.

# Chapter 5 - Dickeya and Musicola


## Summary

*Dickeya* and *Musicola* are gram-negative pathogens belonging to the family Pectobacteriaceae, widely recognized for causing significant soft rot diseases in diverse plant hosts globally. Historically grouped within the genus Erwinia, recent taxonomic revisions have separated these genera based on genetic, biochemical, and pathogenic characteristics. *Dickeya* species exhibit broad host ranges, infecting economically important crops and grasses, with some strains even displaying insect pathogenicity. In contrast, *Musicola*, recently reclassified from *Dickeya*, currently comprises fewer species isolated primarily from tropical and subtropical regions, and exhibits fewer characterized virulence mechanisms. Reliable isolation and identification methods for *Dickeya* heavily depend on pectate-based selective media, notably Crystal Violet Pectate (CVP). Despite their utility, such media often miss non-pectolytic strains and newly described *Musicola* species, indicating the need for improved detection methods. Molecular detection tools such as PCR assays offer specificity but require broader validation to ensure effectiveness across all species. This chapter synthesizes existing knowledge on the isolation, biochemical differentiation, and molecular identification methods of *Dickeya* and *Musicola*, highlighting current limitations and suggesting areas requiring future research to enhance detection accuracy and pathogen management strategies.


## Introduction

*Dickeya* and *Musicola* are gram-negative soft rot pathogens in the family Pectobacteriaceae, which is in the order Enterobacteriales. They are facultative anaerobes and have rod-shaped cells with peritrichous flagella. *Dickeya* and *Musicola* cells are catalase positive and

oxidase negative and they ferment glucose and positive in the Voges-Proskauer test. Comprehensive reviews on isolation and identification of *Dickeya* species (Czajkowski et al. 2015; Humphris et al. 2015) and *Dickeya* biology are available (Hugouvieux-Cotte-Pattat et al. 2020b; 2023).

The taxonomy of this order and the families and genera within have changed considerably in the last two decades. All soft rot enterobacteria were previously classified as *Erwinia*, including *Dickeya*, *Musicola*, and *Pectobacterium*. In 2005, *Erwinia chrysanthemi* was transferred to the genus *Dickeya* and the six *E. chrysanthemi* pathovars were elevated to six similarly named species or subspecies (Samson et al. 2005). Later, *Dickeya* and *Pectobacterium* were moved from Enterobacteriaceae to the new family Pectobacteriaceae (Adeolu et al. 2016). Subsequently, several new species were subsequently reported. The history of these changes and biology supporting them are described in detail by Hugouvieux-Cotte-Pattat et al. (2023). Recently, *Dickeya paradisiaca* was moved to the new genus, *Musicola* and a second *Musicola* species, *M. keenii*, was also described (Hugouvieux-Cotte-Pattat et al. 2021). Insufficient data is available for *Musicola* for a full chapter on this genus, so it is included in this chapter.

*Dickeya* causes soft rot, blackleg, yellowing, and wilt diseases of a wide variety of angiosperms (Ma et al. 2007; Charkowski, 2018). New hosts are reported regularly for *Dickyea* and many *Dickeya* strains are broad host range necrotrophic pathogens. Unlike *Pectobacterium*, *Dickeya* species cause diseases on multiple species of grasses, including rice and maize, and particular *Dickeya* species are associated with grasses, including *D. zeae*, *D. oryzae*, and *D. parazeae* (Hugouvieux-Cotte-Pattat et al. 2023). Some species, such as *D. aquatica*, *D. lacustris*, and *D. unidicola*, are present in water, but have not yet been found to cause disease outbreaks (Hugouvieux-Cotte-Pattat et al. 2023).

*Dickeya* is among the most economically important bacterial pathogens and its importance in potato pathology increased over the past decade (Toth et al. 2011; Curland et al. 2021). *Dickeya* is frequently found with *Pectobacterium* and these two genera can be synergistic in causing plant disease (Ge et al., 2021). Therefore, when it is important to test for the presence of *Dickeya*, such as in seed potato production, samples should also be tested for *Pectobacterium* to better evaluate risk. The aggressiveness of *Dickeya* on plants can vary by strain type, host, and assay used and the genetic reasons for this variation remain mostly undescribed. With the exception of *Dickeya dianthicola* and *Dickeya solani* in potato and *Dickeya zeae* in rice, the distribution, ecology, and epidemiology of *Dickeya* species is almost entirely unexplored, so important questions about host specificity, survival in the environment, and transmission between hosts remain unanswered.

The two species in *Musicola* were both isolated from plants in tropical or subtropical regions, with *M. paradisiaca* isolated from banana and *M. keenii* isolated from tomato (Hugouvieux-Cotte-Pattat et al. 2021). They encode fewer plant cell wall degrading enzymes than *Dickeya*, lack the T1SS, T3SS, T4SS, and T6SS. Other than this, essentially nothing is known about the epidemiology, pathogenicity, or other aspects of the biology of *Musicola* species.

The main pathogenicity factors of *Dickyea* are the copious plant cell wall degrading enzymes they produce, including pectate lyases, polygalacturonases, proteases, cellulases, and xylanases (Van Gijsegem et al., 2021). One exception is *D. poaceiphila*, which encodes few pectate lyases and which may rely on other virulence factors. The *Dickeya* plant cell wall degradative enzymes are regulated by plant cell wall fragments and acyl-homoserine lactone-based quorum sensing (Charkowski et al. 2012). Other virulence factors, such as the type III secretion system and various secondary metabolites also play an important role in *Dickeya*-plant interactions (Charkowski et al. 2012). In addition to being spread by water and plant propagation, *Dickeya*

species are also spread by insects and may be a member of the microbiome for some insect species (Rossman S. et al. 2018). Some *Dickeya* also produce insect toxins and are insect pathogens (Grenier, A.M. 2006).

**Isolation Techniques using Differential and Semi-selective Media**

*Dickeya* is a xylem, root, or tuber-dwelling pathogen that can also be isolated from water, soil, roots, and wilted and macerated plant organs. It can be found at low levels on potato tubers, where it mainly colonizes lenticels. *Dickeya* is not a phyllosphere colonist and is generally not isolated from leaf or fruit surfaces. Standard isolation methods, such as allowing bacteria to stream from diseased plant organs into water or buffer, work well for *Dickeya* isolation. Diseased plant samples also host many secondary invaders, so lesion edges should be used for *Dickeya* isolations when possible.

Pectate-based media are typically used to isolate *Dickeya* from environmental samples. The semi-selective medium Crystal Violet Pectate (CVP) is the most commonly used medium for *Dickeya* isolation and multiple recipes for crystal violet pectate have been described (Woodward and Robinson 1990; Perombelon and Burnett 1991; Hyman et al. 2001; Bdliya et al. 2004; Hélias et al. 2012). CVP inhibits growth of Gram-positive bacteria via inclusion of crystal violet and promotes growth of *Dickeya* though addition of the carbon source pectate. The medium is solidified primarily by adding calcium, which cross-links the pectate to form a gel. This gel is degraded by pectinases produced by *Dickeya* and the *Dickeya* colonies form characteristic deep pits in the CVP medium. The source of pectate used in the medium will affect both whether the medium solidifies and the plating efficiency of the medium, so the pectate source used to develop each specific medium should be used and other pectates should not be substituted without validation in the particular medium recipe being used.

Pierce and McCain (1992) modified Miller Scroth (MS) medium to select for pectolytic enterobacteriaceae, including *Dickeya*. MS medium is a semi-selective medium that is useful for isolating plant-colonizing enterobacteriaceae, but it is difficult to differentiate pectolytic and non-pectolytic enterobacteriaceae on this medium. However, when solidified primarily with calcium pectate rather than agar, *Dickeya* will form pits on Miller Scroth Pectate (MSP) medium.

Researchers almost exclusively use pectate-based media to isolate *Dickeya*, which may skew our knowledge of this genus since if non-pectolytic *Dickeya* clades exist, researchers will not isolate them with pectate-based media. Other semi-selective media for *Dickeya* that are not based on ability to degrade pectate are available. Lee and Yu (2006) modified nutrient agar with glycerol and manganese (NGM) and developed a medium that promotes production of indigoidine, a blue compound produced by most *Dickeya* but that is rarely produced by other plant-associated bacteria.

To isolate *Dickeya* from diseased plant tissue, either homogenize or crush a small sample from the edge of a lesion in sterile water or quarter strength Ringer's solution. The antioxidant diethyldithiocarbamic acid (DIECA) may be added to water, buffer, or enrichment medium at 5% vol:vol to protect cells during isolation and enrichment (Toth et al. 2011). Streak or spread the bacterial suspension onto selective medium. Although *Dickeya* grow well at 36°C, they produce pectinases best at lower temperatures, so the CVP should be incubated at 23 to 28°C. All growth media for *Dickeya* isolations are semi-selective, and secondary invaders compete well with *Dickeya* in diseased plants, therefore *Dickeya* colonies may not be the prevalent colony type on growth media.

*Pectobacterium* is often present with *Dickeya* in plant samples and *Pectobacterium* strains typically grow faster than *Dickeya*, so if isolation is the only method used for diagnosis and

detection of soft rot pathogens, *Dickeya* may be missed in samples. PCR-based assays may be used to confirm that *Dickeya* and/or *Pectobacterium* is present in samples with soft rot or blackleg symptoms prior to strain isolation to determine which genera should be sought during isolation.

If *Dickeya* is present in healthy-appearing plant samples, it is most likely in the xylem tissue of lower stems or in the roots, so stem or root sections should be used for isolation. When isolating from healthy-appearing tubers, a small core from the stem end of the tuber and a portion of the tuber periderm should be used (Czajkowski et al. 2009). The stem end of the tuber has higher concentrations of *Dickeya* when tubers are infested, while a higher proportion of tubers are likely to carry *Dickeya* in the periderm. The cores and periderm portions may be soaked in sterile water or quarter strength Ringer's solution to allow the bacteria to ooze into the water or they may be crushed in water or quarter strength Ringer's solution prior to isolations.

*Dickeya* are rarely present at high levels in environmental samples, such as soil, water, insect, or asymptomatic plants. The *Dickeya* cells in environmental samples may be stressed, so extraction from samples in a buffer and enrichment prior to use of selective media is often required for isolation. For best results, quarter strength Ringer's buffer should be used to isolate *Dickeya* environmental samples. This suspension is then streaked or plated onto CVP or other selective medium and incubated at 23 to 28°C. If the bacteria are present at low levels, the suspension can be inoculated into a pectate-based enrichment broth and incubated, often under anaerobic conditions, for one to five days at 36°C. Samples from the enrichment broth may then be streaked or spread onto selective medium. If water samples are being tested, *Dickeya* can be concentrated prior to enrichment by centrifugation (Humphris et al. 2015) or filtration.

Pure cultures can generally be obtained by streaking bacteria from pits that form on CVP onto nutrient agar (NA) or casamino acid-peptone-glucose (CPG) medium (Kelman 1954).

*Dickeya* becomes unculturable within a few days when grown on some common agar media, such as Luria Bertani (LB) or when it is stored at cool temperatures (4 to 10°C). Therefore, isolates should be stored as soon as a pure culture is obtained. Isolates may be stored indefinitely at -80°C by suspending cells in cryovials filled with 20% vol:vol glycerol or in cryovials on ceramic beads (Copan Diagnostics). It is crucial that vigorous cells are stored, so only cells from freshly streaked plates that are incubated for no more than one day should be used for stored cultures.

**A)Selective and Nonselective Media used for *Dickeya* Isolation**

**1.Crystal Violet Pectate (CVP) medium**

The recipes from Hélias et al. (2012) are provided here because Dipecta pectin is currently commercially available (Agdia Inc). Some previously described recipes use pectins that are no longer being produced.

***i.Single-layer CVP (SL-CVP) medium***

| Mix A | In 500 mL of distilled water |
|---|---|
| $CaCl_2 \cdot H_2O$ | 1.02 g |
| Tryptone | 1.0 g |
| Tri-sodium citrate | 5.0 g |
| Sodium nitrate | 2.0 g |
| 0.1% crystal violet* | 1.5 mL |
| Agar | 4.0 g |

| Mix B | In 500 mL of distilled water |
|---|---|
| 5 M NaOH | 2.8 mL |
| Pectin | 18.0 g |

*corrected from error in original publication

Add each ingredient in the order listed and dissolve each ingredient before adding the subsequent one on the list. For mix B, add the pectin slowly and heat the solution to 80 to 100°C while stirring to dissolve the pectin before autoclaving. Autoclave the two solutions at 121°C for 15 min. Carefully pour mix A into mix B while the solutions are still hot and swirl to mix

the solutions together. Pour the medium into Petri dishes. Dry the medium in a biosafety hood or laminar flow hood to eliminate condensation prior to using the CVP. This medium should be stored at 4°C prior to use. CVP medium will be grey when properly prepared.

***ii.Double-layer CVP (DL-CVP) medium***

| Basal Layer | In 1000 mL of distilled water |
|---|---|
| $CaCl_2 \cdot H_2O$ | 5.5 g |
| Tryptone | 1.0 g |
| $NaNO_3$ | 1.6 g |
| 0.1% Crystal violet* | 1.5 mL |
| Agar | 15.0 g |
| **Top Layer** | **In 800 mL of distilled water** |
| 5% EDTA (pH 8.0) | 2.0 mL |
| 5 M NaOH | 4.8 mL |
| Pectin | 20.0 g |

*corrected from error in original publication

Add each ingredient in the order listed and dissolve each ingredient before adding the subsequent one on the list. For the top layer, add the pectin slowly and heat the solution to 80 to 100°C while stirring to dissolve the pectin before autoclaving. Autoclave the two solutions at 121°C for 15 min. Pour the basal layer into Petri dishes (approximately 15 mL per dish in 20 mM dishes) and allow the medium to set. Then pour the top layer (approximately 7 mL per dish in 20 mM dishes). Dry the medium in a biosafety hood or laminar flow hood to eliminate condensation prior to using the CVP. This medium should be stored at 4°C prior to use. CVP medium will be grey when properly prepared.

**2)Nutrient Glycerol Manganese (NGM) medium (Lee and Yu 2006)**

| | per L |
|---|---|
| Nutrient agar (Becton Dickinson) | 23.0 g |
| Glycerol | 10.0 mL |
| $MnCl_2 \cdot 4H_2O$ | 0.4 g |

A purple precipitate (indigoidine) will form in the middle of *Dickey*a colonies grown on NGM.

**3)Miller Scroth Pectate (MSP) medium (Pierce and McCain 1992)**

| | per L |
|---|---|
| Mannitol | 10.0 g |
| Nicotinic acid | 0.5 g |
| L-asparagine | 3.0 g |
| $K_2HPO_4$ | 2.0 g |
| $MgSO_4 \cdot 7H_2O$ | 0.2 g |
| Sodium taurocholate | 2.5 g |
| Tergitol 7 (sodium heptadecyl sulfate) | 0.1 mL |
| 2% Nitrolotriacetic acid | 10.0 mL |
| 0.5% Bromthymol blue | 9.0 mL |
| 0.5% Neutral red | 2.5 mL |
| 1% Thallium nitrate | 1.75 mL |
| 0.33% $CoCl_2$ | 50.0 mL |
| 1 N NaOH | 20.0 to 35.0 mL |
| MOPS | 4.0 g |
| 10% $CaCl_2 \cdot 2H_2O$ | 12.0 mL |
| Agar | 4.0 g |
| Sodium pectate | 18.0 g |

Heat the water to 80 to 90°C while stirring and add ingredients in the order listed. The amount of NaOH added will vary depending on the batch of pectate used. The final pH should be 7.5 to 7.7. Since calcium pectate will begin to solidify at 70°C, the medium must not be allowed to cool prior to autoclaving. When properly prepared, MSP medium is a blue-green color.

**4)Pectate enrichment medium (PEM; adapted from Meneley (1975); van der Wolf et al. (1998); Perombelon and Kelman (1980))**

| | per L |
|---|---|
| $MgSO_4$ | 0.64 g |
| $(NH_4)_2SO_4$ | 2.16 g |
| $K_2HPO_4$ | 2.16 g |
| Sodium polypectate | 3.40 g |

Heat while stirring until the pectate is dissolved and then adjust the pH to 7.2. Autoclave the PEM at 121°C for 15 min in small batches and do not re-use individual batches after opening the aliquot.

**5)Casamino acid-peptone-glucose (CPG) medium (Kelman 1954)**

| | per L |
|---|---|
| Casamino acids | 1.0 g |
| Peptone | 10.0 g |
| Glucose | 10.0 g |
| Agar | 18.0 g |

**6)Nutrient Agar (NA) medium**

| | per L |
|---|---|
| Peptone | 5.0 g |
| Yeast extract | 3.0 g |
| Agar | 18.0 g |

Adjust to pH 7.0 and autoclave for 15 min at 121°C prior to pouring into Petri plates.

**7)Ringer's solution**

| | per L |
|---|---|
| NaCl | 2.25 g |
| KCl | 0.105 g |
| $CaCl_2 \cdot 6H_2O$ | 0.12 g |
| $NaHCO_3$ | 0.05 g |

Dilute the stock solution to quarter strength in water. Sterilize by autoclaving at 121°C for 15 min. Tablets to prepare Ringer's solution can be purchased from Oxoid.

**Differentiation of Commonly Isolated Genera**

The semi-selective media used to isolate *Dickeya* or *Musicola* will also, in most cases, isolate the closely related pectolytic genus Pectobacterium, which tends to grow more quickly than *Dickeya* or *Musicola*. Biochemical differences between *Dickeya* and *Pectobacterium* can be used

to differentiate these two genera (Table 1). Of these assays, NaCl sensitivity and pellicle formation in SOBG are the simplest and least expensive differential assays.

***Table 1***. *Biochemical assays used to differentiate Dickeya and Pectobacterium*

| Test | *Dickeya* | *Pectobacterium* |
|---|---|---|
| **Phosphatase activity** | + | - |
| **Indole production** | + | v- |
| **Erythromycin sensitivity** | + | v- |
| **NaCl sensitivity** | + | - |
| **Pellicle formation in SOBG** | + | - |
| **Indigoidine production** | + | - |

v-= variable, but most strains are negative for this phenotype

Biochemical assays can also be used to differentiate Dickeya species (Table 2). However, due to variability within species and the relatively frequent discovery of new species in this genus, classification by sequence analysis is more accurate and useful than classification by phenotype. Multiple primer sets for multi-locus sequence analysis (MLSA) have been described and all of the reported MLSA of *Dickeya* appear to work well (Table 3) (Ma et al. 2007; Marrero et al. 2013; Kim et al. 2009). Importantly, MLSA results are more robust if multiple genes are used; sequence from a single gene should not be used to identify Dickeya isolates to species level.

**Diagnostic Media and Tests**

Assays marked with an asterisk are commercially available through scientific supply companies such as Sigma-Aldrich, bioMérieux, or Thermo Scientific.

**A.Biochemical tests, in addition to pitting on CVP, to confirm that the isolate is a *Dickeya/Musicola* or a *Pectobacterium* species**

**Flagellar Stain Flagellar Stain**

Prepare flagellar stain (Kodaka et al. 1982):

Solution 1:

| | |
|---|---|
| 5% carbolic acid | 10.0 mL |
| Tannic acid | 2.0 g |
| Saturated aluminum potassium sulfate | 10.0 mL |

Solution 2:
Saturated crystal violet in ethanol

The two solutions can be stored separately or mixed and stored as the final flagellar stain solution.

Streak the culture onto NA medium. Carefully transfer a portion of a colony to a drop of water on a glass slide and let the slide dry at ambient temperature. Stain the slide for 5 min, then wash with water for 2 min. Dry the slide at ambient temperature and observe under oil immersion. Growth medium and temperature can affect flagellation of strains and optimal conditions for *Pectobacterium* flagella production are unknown.

**Catalase**

Grow isolate on nutrient agar for 2 days. Suspend a colony in a small test tube in 100 µL of freshly prepared 3% $H_2O_2$ plus 1% Triton X-100 in water. Bubbles indicate that catalase is present (Iwase et al. 2013; Lemberg and Foulkes 1948).

**Oxidase***

Grow isolate on NA for 2 days and transfer bacteria with a platinum or plastic loop to filter paper. Iron present in other types of loops will cause a false positive result with this assay. Add a drop of 1% aqueous tetramethyl-p-phenylenediamine dihydrochloride. Development of a purple color within 10 minutes indicates that oxidase is present (Kovacs 1956).

**Oxidative Fermentation Test – Glucose***

Prepare Hugh and Leifson O-F medium (Hugh and Leifson 1953):

per L

| | |
|---|---|
| NaCl | 5.0 g |
| $K_2HPO_4$ | 0.3 g |
| Bromothymol blue | 30.0 mg |
| Agar | 5.0 g |
| Glucose | 10.0 g |

Adjust to pH 7.1 before autoclaving and sterilize medium at 121°C for 15 min. Filter-sterilize a 10% glucose solution and add 10 mL per L of the glucose solution to the medium. Pour the medium into sterile test tubes and allow it to solidify. Stab-inoculate the bacteria halfway into the medium in the tube and cover the medium with sterile mineral oil to create anaerobic environment in the tube. Incubate the medium at 28°C for at least 48 hours. If the medium turns yellow, the glucose in the medium was fermented.

**Nitrate Reduction (Griess Reaction)***

Prepare Nitrate Broth:

| | per L |
|---|---|
| Peptone | 5.0 g |
| Yeast extract | 3.0 g |
| Potassium nitrate | 1.0 g |

Prepare nitrate broth and dispense 10 mL aliquots into test tubes and autoclave at 121°C for 15 min. Also prepare reagent A (0.8 g of sulfanilic acid in 100 mL of 5 N acetic acid; store in the dark at room temperature for up to 3 months) and reagent B (0.6 g of N,N-Dimethyl-1-naphthylamine in 100 mL of 5 N acetic acid; store under refrigeration in the dark for up to 3 months).

Inoculate the medium with 1 mL of a freshly-grown culture or with a large amount of bacteria swabbed from a fresh agar plate. Add sterile mineral oil to the top of the medium to create anaerobic conditions. Incubate the tubes at 28°C for 48 hours. Add 125 µL of reagent

A, 125 µL of reagent B, and a small amount of zinc powder and mix thoroughly. If the medium turns pink or red, nitrate reduction occurred (Hageman et al. 1971).

**β-galactosidase**

Streak the bacteria onto a nutrient agar plate spread with 80 µL of a 2% solution of 5-bromo-4-chloro-3-indolyl-β-D-galactopyranoside (X-gal) in dimethyl formamide (DMF) or dimethyl sulfoxide (DMSO and 10 µL of a 1 M isopropyl β-D-1-thiogalactopyranoside (IPTG) solution. If the colonies turn blue, β-galactosidase activity is present.

**H2S***

Prepare Triple Sugar Iron (TSI) agar slants, but omit the 5 g of NaCl:

| | per L |
|---|---|
| Peptone | 15.0 g |
| Lactose | 10.0 g |
| Sucrose | 10.0 g |
| Beef extract | 3.0 g |
| Yeast extract | 3.0 g |
| Glucose | 1.0 g |
| Ferric ammonium citrate | 0.5 g |
| Sodium thiosulfate | 0.3 g |
| Phenol red | 24.0 mg |
| Agar | 12.0 g |

Adjust pH to 7.3 and autoclave at 121°C for 15 min. Pour media into sterile test tubes and allow the tubes to solidify into agar slants. Inoculate the medium by stabbing a bacterial colony to the bottom of the tube and also spreading bacteria onto the slant. Incubate for up to 48 h at 28°C. If $H_2S$ gas is produced, large bubbles will form in the agar slant, pushing the agar upward.

**L-arabinose*, D-galactose, D-glucose*, glycerol, D-mannose, D-ribose, and sucrose*.**

Prepare Phenol Red Broth, but omit the 5.0 g of NaCl:

| | per L |
|---|---|
| Casein peptone | 10.0 g |
| Carbohydrate | 10.0 g |
| Phenol red | 18.0 mg |

Adjust pH to 7.4, dispense the medium into sterile test tubes and autoclave at 121°C for 15 min. Inoculate the culture tubes and incubate them at 23 to 28°C for up to 48 hours. If the medium turns yellow, the carbohydrate was used by the bacterium.

**Urease***

Prepare Christensens's Urea Broth, but omit the 5.0 g of NaCl:

| | per L |
|---|---|
| Urea | 20.0 g |
| $KH_2PO_4$ | 2.0 g |
| Peptone | 1.0 g |
| Glucose | 1.0 g |
| Phenol red | 12.0 mg |

Adjust pH to 6.7, dispense the medium into sterile test tubes and autoclave at 121°C for 15 min. Inoculate the culture tubes and incubate them at 23 to 28°C for up to 48 hours. If the medium turns pink, urease was produced (Christensen 1946).

**Acid from adonitol***

Prepare 1.0% peptone broth and add bromocresol purple (30 mg $L^{-1}$) as an indicator. Add adonitol to 1.0% final concentration, adjust to pH 7.0, filter sterilize, and dispense into sterile test tubes. Inoculate tubes with the isolate and incubate 48 hours at 23 to 28°C. If the medium turns yellow, acid was produced.

**Acetoin production***

Prepare MR-VP Broth:

| | per L |
|---|---|
| Peptone | 7.0 g |
| Glucose | 5.0 g |
| $K_2HPO_4$ | 4.0 g |

Adjust pH to 6.9, dispense the medium into sterile test tubes and autoclave at 121°C for 15 min. Inoculate the culture tubes and incubate them at 23 to 28°C for up to 48 hours. Add 200 µL of Barritt's solution A (6 g of α-naphtholin in 100 mL of 95% ethanol) and 200 µL of Barritt's solution B (16 g of KOH in 100 mL of water). Shake gently. If a red color appears, acetoin was produced (Levine 1916).

**Biochemical tests to differentiate *Dickeya* or Musicola from *Pectobacterium***

***Phosphatase activity***

Prepare a 10% solution of phenolphthalein diphosphate sodium in water and add 100 µL per 20 mL NA medium and pour into Petri plates. Stab inoculate isolates on the medium and incubate for 48 hours at 23 to 28°C. Place a drop of concentrated ammonia in the lid of the Petri dish or a glass plate and invert the medium over it. Colonies that turn pink have phosphatase activity. Glass Petri dish covers should be used for this assay since the ammonia may soften plastic dish covers (Barber et al. 1951; King 1943).

***Indole production****

Prepare a medium containing 10.0 g tryptone, 1.0 g L-tryptophane, and 18.0 g agar per liter. Stab inoculate isolates into the medium and incubate for 48 hours at 23 to 28°C. Pipet 20 µL of p-dimethylamino-cinnamaldehide (1.0% wt:vol in a 10.0% HCl

solution) onto filter paper. Smear a colony onto the treated filter paper. A blue-green color within 10 seconds indicates that indole was produced.

***Erythromycin sensitivity***

Add an overnight culture of the isolate to 5.0 mL of molten nutrient agar cooled to 50°C and pour the suspension onto a NA plate. After the medium has solidified, place a filter disk with 15.0 µg of erythromycin onto the agar surface. Incubate for 48 hours at 23 to 28°C. A zone of inhibition indicates erythromycin sensitivity.

***NaCl sensitivity***

Inoculate isolate into a test tube containing Luria-Bertani plus NaCl liquid medium (10.0 g tryptone, 5.0 g yeast extract, 10.0 g NaCl per L). A lack of growth indicates sensitivity to NaCl.

***Pellicle formation (Yap et al., 2005)***

Prepare SOBG medium:

| | per L |
|---|---|
| Tryptone | 20.0 g |
| Yeast extract | 5.0 g |
| NaCl | 0.5 g |
| $MgSO_4$ (anhydrous) | 2.4 g |
| KCl | 0.186 g |
| 40% vol:vol glycerol in water | 50.0 mL |

Combine all ingredients except glycerol solution and autoclave at 121°C for 15 min. After medium is cool, add filter-sterilized glycerol solution. Dispense the medium into test tubes and inoculate with a bacterial colony. Incubate the culture for 72 hours at 23 to 28°C without shaking. A thick mat at the liquid-air interface indicates pellicle formation.

***Indigoidine production (Lee and Yu, 2006)***

Streak culture onto NGM medium and incubate for 48 hours at 23 to 28°C. Formation of a blue pigment indicates indigoidine production.

**Biochemical tests to determine species or biovar identification of *Dickeya* isolates**

**1) Growth at 39°C**

Spot or streak isolates onto NA or CPG and incubate at 39°C for 2 days. Colony formation indicates growth at 39°C.

**2) Use of carbon sources, such as D-arabinose*, melibiose, raffinose*, mannitol*, β-gentiobiose, polygalacturonate, and D-tartrate**

Prepare Phenol Red Broth, but omit the 5.0 g of NaCl

| | per L |
|---|---|
| Casein peptone | 10.0 g |
| Carbohydrate | 10.0 g |
| Phenol red | 18.0 mg |

Adjust pH to 7.4, dispense the medium into test tubes and autoclave at 121°C for 15 min. Inoculate the culture tubes and incubate them at 23 to 28°C for up to 48 hours. If the medium turns yellow, the carbohydrate was used by the bacterium.

**Pathogenicity and Virulence Assays for *Dickeya* and *Musicola***

*Dickeya* pathogenicity assays used in laboratory or greenhouse settings have not been validated with field experiments and information on *Musicola* pathogenicity is sparse. *Dickeya* will macerate plant tissue from many species when stab-inoculated into tubers, fruit, or succulent leaves. Plant organs may be surface sanitized by soaking in 10% bleach for 10 minutes and then air-dried in a biological safety cabinet or laminar flow hood. However, some plants commonly used for *Dickeya* assays, such as endive leaves, may be too delicate to surface sanitize. The tuber, leaf, or fruit is

then stab inoculated by either swabbing a toothpick across a freshly grown nutrient agar culture and stabbing it into the plant or by wounding the plant and pipetting 1 to 5 µL of a bacterial suspension into the wound. The plant parts should be placed into closed containers, such as plastic bags, and incubated at 23 to 28°C for 48 to 72 hours.

Stems of potted plants can be inoculated with *Dickeya* by wounding the stem, inoculating the wound with bacteria, and covering the wound with petroleum jelly or by winding parafilm around the wound. For efficient symptom development, plants should be kept at 100% humidity for 24 hours after inoculation.

Variability in symptom severity is common. Plant age, plant variety, tuber size, oxygen level, and plant nutrition can all affect results. The most reproducible method for comparing virulence among strains is to inoculate individual plants or plant parts with a dilution series of the bacterial isolate being investigated and determining the concentration that causes disease in half of the inoculated plants (Lethal Dose of 50% of the plants or $LD_{50}$).

Plant cell wall degrading enzymes are required for *Dickeya* pathogenicity and activities of these enzymes can be measured with semi-quantitative plate-based assays (Jahn et al. 2008; Chatterjee et al. 1995).

**Pectate Lyase Assay Medium:**

| | per L |
|---|---|
| Polygalacturonic acid (ICN Biomedical) | 10.0 g |
| Yeast extract | 10.0 g |
| 100 mM $CaCl_2$ | 3.8 mL |
| 1M Tris-HCl (pH 8.0) | 100.0 mL |
| Agar | 15.0 g |

Prepare medium and autoclave at 121°C for 15 min. Pour medium into petri plates and allow to solidify. Make wells in medium with a no. 2 cork borer and seal with molten 0.8% wt/vol

agar melted in water. Add culture or culture supernatant to wells and incubate at 28°C for 24 to 36 hours. Flood plant with 4 N HCl. Zones of clearing indicate pectate lyase activity.

**Cellulase Assay Medium:**

| | per L |
|---|---|
| Carboxymethyl cellulose | 1.0 mL |
| 250 mM $Na_3PO_4$ | 100.0 mL |
| 1 M $CaCl_2$ | 3.8 mL |
| 1M Tris-HCl (pH 8.0) | 100.0 mL |

Adjust to pH 7.0 and and autoclave at 121°C for 15 min. Pour medium into petri plates and allow to solidify. Make wells in medium with a no. 2 cork borer and seal with molten 0.8% wt/vol agar melted in water. Add culture or culture supernatant to wells and incubate at 28°C for 24 to 36 hours. Flood plant with 0.1% congo red for 45 min and then wash with 1 M NaCl. Clear zones indicated cellulase activity.

**Protease Assay Medium:**

| | per L |
|---|---|
| Powdered milk or gelatin | 30.0 g |
| Nutrient broth | 4.0 g |
| Agar | 15.0 g |

Prepare medium and autoclave at 121°C for 15 min. Pour medium into petri plates and allow to solidify. Make wells in medium with a no. 2 cork borer and seal with molten 0.8% wt/vol agar melted in water. Add culture or culture supernatant to wells and incubate at 28°C for 24 t0 36 hours. Zones of clearing will develop and indicate protease activity.

**Polymerase Chain Reaction (PCR) Assays for Detection and Identification of *Dickeya* and *Musicola* Species**

Detection and identification assays that capture all species within the *Dickeya* genus are useful for plant production since *Dickeya* is a broad host range pathogen and any *Dickeya* species present

in irrigation water or plant propagules has the potential to cause losses. Although *Dickeya* is commonly present in some plant production systems, such as potato production, and its presence is not always well-correlated with disease. If both *Dickeya* and *Pectobacterium* are present, disease is more likely to occur, therefore it is best to test for both genera in production systems where these pathogens are common.

Although *D. aquatica* can decay plants in laboratory settings but has not yet been observed to cause disease problems in agricultural production. Since *D. aquatica* is common in water, it is important to determine which *Dickeya* species is present in water when testing irrigation water for *Dickeya* since *D. aquatica* may not be a significant concern for farmers.

There remains much work to do in order to validate PCR assays for *Dickeya* species. There are no reported PCR assays that can detect all *Dickeya* species that do not also detect *Musicola*. There are not PCR assays designed to specifically detect most of the individual *Dickeya* species. In addition, there are numerous cases where PCR assays were validated with all species known at the time and with field samples, but were later shown to fail when new strains or species were discovered. There are also no PCR assays that detect just the *Musicola* genus or its two species. PCR assays developed for the *Dickeya* or *Musicola* genera and all the of the known species are essential for studying the epidemiology and host range of these pathogens.

The first *Dickeya* PCR assay described was the *pelADE* primer set developed by Nassar et al. (1996), which amplifies a 420-bp fragment from a conserved set of pectate lyase genes (Table 4), demonstrates some of the challenges of PCR assays developed for *Dickeya*. The original description of this assay uses an unusually high primer annealing temperature (72°C) and only 25 amplification cycles, which is relatively low. Other researchers who have used this primer set have adjusted the annealing temperature and/or the cycle number used (for example, see Tsror et al.

(2012)). Although this assay is still widely used, it commonly amplifies spurious DNA fragments from water samples and false positive results frequently occur with the *pelADE* PCR assay when water samples are tested.

A useful subset of other primer sets that were subsequently developed are described in Table 4 and the species that they are likely to detect are described in Table 5 and Table 6. Since none of the primers described for *Dickeya* have yet been tested with all known *Dickeya* species, the information shown in Table 5 and Table 6 is based partially on experimental data and partially on DNA sequence analysis. Unfortunately, there are multiple examples of primers developed for *Dickeya* that have failed in practice (for example, see van der Wolf et al. 2014b), so field sample validation is essential

**Table 2**. Dickeya and Musicola species names and differential phenotypesA

| | | | Carbon Sources | | | | | | Enzyme Activity | | |
|---|---|---|---|---|---|---|---|---|---|---|---|
| Species name | Reference | Growth at 39°C | Mel | Man | Xyl | Ino | Gal | PGA | Pel | Cel | Prt |
| *D. aquatica* | Parkinson et al. (2014) | + | + | - | - | + | - | + | + | + | W |
| *D. chrysanthemi* | Samson et al. (2005) | + | + | + | + | + | NT | + | + | + | + |
| *D. dadantii* subsp. *dadantii* | Samson et al. (2005); Brady et al. (2012) | + | + | + | + | + | - | + | + | W | W |
| *D. dadantii* subsp. *dieffenbachiae* | Samson et al. (2005); Brady et al. (2012) | + | - | + | + | + | - | + | + | + | + |
| *D. dianthicola* | Samson et al. (2005) | - | + | + | + | + | + | + | + | + | W |
| *D. fangzhongdai* | Tian et al. (2016) | + | + | + | + | + | - | + | + | + | + |
| *D. lacustris* | Hugouvieux-Cotte-Pattat et al. (2019) | + | + | - | + | + | - | + | + | + | + |
| *D. oryzae* | Wang et al. (2020) | - | + | + | + | + | - | + | + | + | + |
| *D. parazeae* | Hugouvieux-Cotte-Pattat and Van Gijsegen (2021) | + | + | + | + | + | - | + | + | + | W |
| *D. poaceiphila* | Hugouvieux-Cotte-Pattat et al. (2020a) | + | + | + | + | - | - | - | W | - | W |
| *D. solani* | van der Wolf et al. (2014a) | + | + | + | + | + | + | + | + | + | + |
| *D. undicola* | Oulghazi et al. (2019) | + | + | + | + | + | + | + | + | + | + |
| *D. zeae* | Samson et al. (2005) | + | + | + | + | + | - | + | + | + | + |
| *M. paradisiaca* | Hugouvieux-Cotte-Pattat et al. (2021) | + | + | - | - | - | - | + | W | + | - |
| *M. keenii* | Hugouvieux-Cotte-Pattat et al. (2021) | + | - | - | + | + | + | + | W | + | - |

[A]Phenotype information is from the references shown, plus phenotypes compiled by Hugouvieux-Cotte-Pattat et al. (2023), Parkinson et al. (2014), Samson et al. (2005), and van der Wolf et al. (2014a). Where published data conflict, the most recent data are shown. Notations include Mel (melibiose), Man (mannitol), Xyl (xyliton), Ino (my-inositol), Gal (galactonic acid), PGA (polygalactonic acid), Pel (pectate lyase), Cel (cellulase), Prt (protease), + (positive), – (negative), W (weak), and NT (not tested).

**Table 3**. Primer sets used for MLSA of Dickeya and Musicola

| Gene | Primers (5' -> 3') | Reference |
|---|---|---|
| ***dnaA*** | CCT ATC GYT CGA ACG TGA A | Marrero et al. (2013) |
| | CTG CTC GAT TTT GCG GCA G | |
| ***dnaA*** | CCT ATC GCT CSA AYG TGA A | Marrero et al. (2013) |
| | CTG CTC RAT YTT RCG GCA G | |
| ***dnaJ*** | GAT TTA CGC TAC AMC ATG GA | Marrero et al. (2013) |
| | TTC ACG CCR TCR AAR AAR Y | |
| ***dnaX*** | TAT CAG GTY CTT GCC CGT AAG TGG | Marrero et al. (2013) |
| | TCG ACA TCC ARC GCY TTG AGA TG | |
| ***gyrB*** | TAA GTT YGA CGA YAA CTC STA YAA RGT | Marrero et al. (2013) |
| | CCC CTT CCA CCA GGT ASA GTT C | |
| ***gapAD***[A] | AAG TGA AAG ACG GTC ACC TGG T | Hugouvieux-Cotte-Pattat |
| | CGA TCA GGT CCA GAA CCT TGT T | et al. (2021) |
| ***gapAM***[A] | AAG TGA AAA ATG GCA ATC TGG TCG T | Hugouvieux-Cotte-Pattat |
| | CGA TCA GGT CCA GAA CCT TGT T | et al. (2021) |
| ***recN*** | AGT AAC TTC GCC ATY GTG CGC GA | Marrero et al. (2013) |
| | AGT AAC TTC GCC ATY GTG CGC GA | |
| | CMA GRG TRT TRA TGC ARG AYT TTA C | Ma et al. (2007) |
| ***acnA*** | GAT CAT GGT GGT RTG SGA RTC VGT | |
| ***gapA*** | ATC TTC CTG ACC GAC GAA ACT GC | Ma et al. (2007) |
| | ACG TCA TCT TCG GTG TAA CCC AG | |
| ***icdA*** | GGT GGT ATC CGT TCT CTG AAC G | Ma et al. (2007) |
| | TAG TCG CCG TTC AGG TTC ATA CA | |
| ***mdh*** | CCC AGC TTC CTT CAG GTT CAG A | Ma et al. (2007) |
| | CTG CAT TCT GAA TAC GTT TGG TCA | |
| ***mtlD***[B] | GGC CGG TAA TAT CGG CCG TGG | Ma et al. (2007) |
| | CAT TCG CTG AAG GTT TCC ACC GT | |
| | or | |
| | CTG YTG GAT GCI CTS AAC MGY CG | |
| | TCC ACR GCR GAA TCW ACR AAT CC | |
| ***pgi***[B] | TGG GTC GGC GGC CGT TAC TC | Ma et al. (2007) |
| | TGC CTT CGA ATA CTT TGA ACG GC | |
| | or | |
| | CTG TCY ACC AAT GCS AAA GCC G | |
| | CAG CAG GAT GGA GTT GGT CGG | |
| | or | |
| | TCT YTI GGI TTT GAK AAY TTT GA | |
| | YGC CGC YGI AAA TTC IGC TC | |
| ***proA*** | CGG YAA TGC GGT GAT TCT GCG | Ma et al. (2007) |
| | GGG TAC TGA CCG CCA CTT C | |

[A]The *gapA* primers from Hugouvieux-Cotte-Pattat et al. 2021 amplify only from *Dickeya* (*gapAD*) or *Musicola* (*gapAM*)

[B] Ma et al. (2007) primers were designed to amplify target genes from all enterobacteria. Each of the two *mLtD* and three *pgi* primer sets may only amplify from a subset of *Dickeya*. The primer sets most likely to amplify *Dickeya* DNA are listed first.

**Table 4.** Primers that detect *Dickeya* species. Details on PCR conditions for each set of primers are in the cited references.

| Primers, 5' – 3' | Target Gene | Product Size in bp | Reference |
|---|---|---|---|
| Conventional PCR | | | |
| SR3F GGTGCAAGCGTTAATCGGAATG<br>SR1cR AGACTCTAGCCTGTCAGTTTT | 16S rDNA | 119 | Toth et al. (1999b) |
| SR1F ATGAGTCTGATATTTGG<br>SR1R1 AGCGTMCTRADMRGMTTTTT | *rsmC* | 299 | Kabir et al. (2020) |
| Dda1F TGTTGGACGCAATACAGRGAAAG<br>Dda1R TCACTCTCCATAGGTGGCATG | *hyp* | 157 | Kabir et al. (2020) |
| ADE1 GATCAGAAAGCCCGCAGCCAGAT<br>ADE2 CTGTGGCCGATCAGGATGGTTTTGTCGTGC | *pelD*, *pelE* | 420 | Nassar et al. (1996)<br>Tsror et al. (2012) |
| 5A GCGGTTGTTCACCAGGTGTTTT<br>5B ATGCACGCTACCTGGAAGTAT | *pecS* | 497 | Chao et al. (2006) |
| pelZ-1-F ATGAAACATACCCTTCTGTTTGC<br>pelZ-1-R TTATTCCAGATCTTTGGCCAT | *pelZ* | 1263 | Lee et al. (2006) |
| Real-Time PCR | | | |
| Df AGAGTCAAAAGCGTCTTG<br>Dr TTTCACCCACCGTCAGTC | *tRNA* | 133 | Laurila et al. (2010) |
| ECHf GAGTCAAAAGCGTCTTGCGAA<br>ECHr CCCTGTTACCGCCGTGAA<br>Probe ECH CTGACAAGTGATGTCCCCTTCGTCTAGAGG | *tRNA* | 86 | Pritchard et al. (2013) |
| DICg-F1 wf ATTATCTCTGCATTGTCGAAACCAAGAACAC<br>DICg-R1 wf AAATTATTTCTTGTCTTTCAGCCAGGTGAGC<br>DICg-P ATGATGCAAGGGCTGTTACCATGAAAGC | galactose ABC transporter | 150 | Dobhal et al. (2020) |
| Fw109 GCGCGCAGCACTHGAT<br>Rv109 CGACGGCACGCTCAGAAT<br>Probe P109 AAGCCGCGGAAAT | ferrodoxin subunit | 51 | Zijlstra et al. (2020) |
| Fw284 TGTGCGTTTTCGGGCTASTC<br>Rv284 CCYTGTCTTCTGTTATCAATTCATTAAC<br>Probe P284 AACCAGAATAAGGCCC | *kup/ravA* intergenic region | 70 | Zijlstra et al. (2020) |
| DIA-Af GGCCGCCTGAATACTACATT<br>DIA-Ar TGGTATCTCTACGCCCATCA<br>Probe ATTAACGGCGTCAACCCGGC | oxidoreductase | 102 | Pritchard et al. (2013) |

| | | | |
|---|---|---|---|
| Ddia-F1 wf TCTACTATTTTGTGAGCTTGGCATCAAGGAA<br>Ddia-R1 wf TTATAACATTCCGTCGTCCAACAAAATGCAG<br>Ddia-P CAAGGCCGAACTGCTGGCGATGTAT | alcohol dehydrogenase | 181 | Dobhal et al. (2020) |
| SOL-Cf GCCTACACCATCAGGGCTAT<br>SOL-Cr ACACTACAGCGCGCATAAAC<br>Probe CCAGGCCGTGCTCGAAATCC | *nifU/nifX* intergenic region | 101 | Pritchard et al. (2013) |
| SOL-Df GCCTACACCATCAGGGCTAT<br>SOL-Dr CACTACAGCGCGCATAACT<br>Probe CCAGGCCGTGCTCGAAATCC | *nifU/nifX* intergenic region | 100 | Pritchard et al. (2013) |
| dsf GCGAACTTCAACGGTAAA<br>dsr CAGAGCTACCAACAGAGA<br>Probe CTCTGCTGGACGGTTC | *fliC* | 112 | Van Vaerenbergh et al. (2012) |
| DfF CTTCGCCGCCCAGGTATTTT<br>DfR ATCAGGGCGTGACCTTCGTT<br>Probe TGCTGCAGACTCGATCAGGTTCTGA | *fusA* | 135 | Tian et al. (2020) |
| LAMP | | | |
| Dd-FIP GGAATTCGGCAATCACGCGGATGTTTCCATCGGTGCTCACA<br>Dd-BOP GCCGTTGCGAATGGCAAGGATGTTGAAGGCCATTCCAGC<br>Dd-F3 TGACTCACGCAATTGAAGCG<br>Dd-B3 GCGAATGCACATAGCCAAGA<br>Dd-LF AACGCGGAGTGGTCTGTCAG<br>Dd-LB TCAAGGCGCGCGAAATGATGG | alcohol dehydrogenase | | Ocenar et al. (2019) |
| AD-F CGCAATACGCCTAAAGATCAA<br>AD-R GAAAGGTCGGCACATTCAGT<br>Df-F3 CGCCGTTTCGGCTTCAA<br>Df-B3 CCGGAACATCCGCGAAC<br>Df-FIP GAATCTGCGGCGTGGTGGGG-AACGGCATACTGTGCGTATT<br>Df-BIP TATTGCTGCTGTTCTGGGG-AGCGAACTGATGCCGGTAA<br>Df-LF GCGGCACAAAGCAGCAACGA<br>Df-LB GGACTCAGCCGTTCGATGCA | major facilitator superfamily transporter | | DeLude et al. (2022) |
| RPA | | | |
| DIC-RPA-F GCATTGTCGAAACCAAGAACACCACGCAGAACGA<br>DIC-RPA-R/Biosg/ATGCCGCTGTCTTTCAGCCAGGTGAGCGCACTT<br>DIC-RPA-LP /FAM/TAGCGTCGTTACACCTTTAATGATGCAAGG/Internal dSpacer/CTGTTACCATGAAAGCTA/Spacer | *mglA/mglC* intergenic region | 137 | Boluk et al. (2020) |

**Table 5.** *Dickeya* species detected by each primer set listed in Table 7.4. None of the primers sets have been tested on all of the listed species and genera, so the details in the table are based on both published data and BLAST results.

| | Conventional PCR | | | | | | Real-Time PCR | | | | | | | | | | |
|---|---|---|---|---|---|---|---|---|---|---|---|---|---|---|---|---|---|
| Primer | SR3F Sr1cR | SR1F SR1R1 | Dda1F Dda1R | ADE1 ADE2 | 5A 5B | pelZ1F pelZ1R | Df Dr | ECHf ECHr ECH | DICg-F1 DICg-R1 DICg-P | Fw109 Rv109 P109 | Fw284 Rv284 P284 | DIA -A | Ddia-F1 Ddia-R1 Ddia-P | SOL-C | SOL-D | dsf dsr | DfF DfR |
| *D. aquatica* | + | - | - | - | - | + | +/- | - | + | - | - | - | - | - | - | - | - |
| *D. chrysanthemi* | + | + | - | + | + | + | + | + | + | + | + | - | - | - | - | - | - |
| *D. dadantii* | + | + | + | + | + | + | + | + | + | + | + | - | - | +/- | +/- | +/- | - |
| *D. dianthicola* | + | + | + | + | + | + | + | + | + | + | + | + | + | - | - | - | - |
| *D. fangzhongdai* | + | + | + | + | + | + | + | + | + | + | + | - | - | - | - | +/- | + |
| *D. lacustris* | + | +/- | - | na | na | na | +/- | na | + | - | - | - | - | - | - | - | - |
| *D. oryzae* | + | + | + | + | +/- | - | + | + | + | + | - | - | - | - | - | - | - |
| *D. parazeae* | + | + | + | + | +/- | - | + | + | + | + | + | - | - | - | - | - | - |
| *D. poaceiphila* | + | + | + | + | + | - | + | + | + | + | + | - | - | - | - | - | - |
| *D. solani* | + | + | + | + | + | + | + | + | + | + | + | - | - | + | + | + | - |
| *D. undicola* | + | + | + | + | + | - | + | + | + | - | - | - | - | - | - | - | - |
| *D. zeae* | + | + | + | + | +/- | + | + | + | + | + | + | - | - | - | - | - | - |
| *Musicola* | + | + | - | - | - | - | - | +/- | + | +/- | +/- | - | - | - | - | - | - |
| *Pectobacterium* | + | + | - | - | - | - | - | - | - | - | - | - | - | - | - | - | - |

+/- means that primers have a mismatch within the last 2 nucleotides of the 3' end of primer or other mismatches that likely affect primer annealing or that the region that the assay was designed to detect is missing in some strains. na = means that genome sequence for this region was unavailable.

**Table 6**. *Dickeya* species detected by each LAMP and RPA primer set listed in Table 7.4. None of the primers sets have been tested on all of the listed species and genera, so the details in the table are based on both published data and BLAST results.

| | LAMP | | RPA |
|---|---|---|---|
| Primer | Dd | AD/Df | DIC |
| *D. aquatica* | +/- | - | + |
| *D. chrysanthemi* | - | - | + |
| *D. dadantii* | - | - | + |
| *D. dianthicola* | + | - | + |
| *D. fangzhongdai* | - | + | + |
| *D. lacustris* | - | - | + |
| *D. oryzae* | - | - | + |
| *D. parazeae* | - | - | + |
| *D. poaceiphila* | - | - | + |
| *D. solani* | - | - | + |
| *D. undicola* | - | - | + |
| *D. zeae* | - | - | + |
| *Musicola* | - | - | + |
| *Pectobacterium* | - | - | - |

+/- means that primers have a mismatch within last 2 nt of primer or other mismatches that affect primer annealing or that the region that the assay was designed to detect is missing in some strains. NT = not tested.

## Culture Preservation

**Table 7** Culture collections that contain *Dickeya* and *Musicola* type strains

| Species | Culture Collection | Type Strain |
|---|---|---|
| *D. aquatica* | Belgian Coordinated Collections of Microorganisms | LMG 27354 |
| | CIRM-CFBP Collection des Bactéries Associées aux Plantes | CFBP 8348 |
| | DSMZ German Collection of Microorganisms | DSM 105346 |
| *D. chrysanthemi* | American Type Culture Collection | ATCC 11663 |
| | Belgian Coordinated Collections of Microorganisms | LMG 2804 |
| | CIRM-CFBP Collection des Bactéries Associées aux Plantes | CFBP 2048 |
| | DSMZ German Collection of Microorganisms | DSM 4610 |
| | International Collection of Microorganisms | ICMP 5703 |
| *D. dadantii* subsp. *dadantii* | Belgian Coordinated Collections of Microorganisms | LMG 25991 |
| | CIRM-CFBP Collection des Bactéries Associées aux Plantes DSMZ | CFBP 1269 |
| | German Collection of Microorganisms | DSM 18013 |
| | International Collection of Microorganisms | ICMP 1544 |
| *D. dadantii* subsp. *dieffenbachiae* | Belgian Coordinated Collections of Microorganisms | LMG 25992 |
| | CIRM-CFBP Collection des Bactéries Associées aux Plantes | CFBP 1246/2051 |
| | DSMZ German Collection of Microorganisms | DSM 18013 |
| | International Collection of Microorganisms | ICMP 1568 |
| *D. dianthicola* | Belgian Coordinated Collections of Microorganisms | LMG 2485 |
| | DSMZ German Collection of Microorganisms | DSM 18054 |
| | International Collection of Microorganisms | ICMP 6427 |
| *D. fangzhongdai* | CIRM-CFBP Collection des Bactéries Associées aux Plantes | CFBP 8607 |
| | DSMZ German Collection of Microorganisms | DSM 101947 |
| | International Collection of Microorganisms | ICPM 24519 |
| *D. lacustris* | Belgian Coordinated Collections of Microorganisms | LMG 30899 |
| | CIRM-CFBP Collection des Bactéries Associées aux Plantes | CFPB 8647 |
| *D. oryzae* | Japan Collection of Microorganisms | JCM 33020 |
| *D. parazeae* | Belgian Coordinated Collections of Microorganisms | LMG 32070 |
| | CIRM-CFBP Collection des Bactéries Associées aux Plantes | CFBP 8716 |
| *D. poaceiphila* | Belgian Coordinated Collections of Microorganisms | LMG 2468 |
| *D. solani* | Belgian Coordinated Collections of Microorganisms | LMG 25993 |
| | CIRM-CFBP Collection des Bactéries Associées aux Plantes | CFBP 8199 |
| | DSMZ German Collection of Microorganisms | DSM 28711 |
| | International Collection of Microorganisms | ICMP 24505 |
| *D. undicola* | Belgian Coordinated Collections of Microorganisms | LMG 30903 |
| | CIRM-CFBP Collection des Bactéries Associées aux Plantes | CFBP 8650 |
| *D. zeae* | Belgian Coordinated Collections of Microorganisms | LMG 2505 |
| | DSMZ German Collection of Microorganisms | DSM 18068 |
| | International Collection of Microorganisms | ICMP 5704 |
| *M. keenii* | Belgian Coordinated Collections of Microorganisms | LMG031880 |
| | CIRM-CFBP Collection des Bactéries Associées aux Plantes | CFBP 8732 |
| *M. paradisiaca* | Belgian Coordinated Collections of Microorganisms | LMG 2542 |
| | CIRM-CFBP Collection des Bactéries Associées aux Plantes | CFBP 4178 |

**References**


Adeolu, M., Alnajar, S., Naushad, S., and S. Gupta, R. 2016. Genome-based phylogeny and taxonomy of the 'Enterobacteriales': proposal for Enterobacterales ord. nov. divided into the families *Enterobacteriaceae*, *Erwiniaceae* fam. nov., *Pectobacteriaceae* fam. nov., *Yersiniaceae* fam. nov., *Hafniaceae* fam. nov., *Morganellaceae* fam. nov., and *Budviciaceae* fam. nov. International Journal of Systematic and Evolutionary Microbiology 66:5575–5599.

Barber, M., Brooksbank, B. W. L., and Kuper, S. W. A. 1951. Staphylococcal phosphatase, glucuronidase and sulphatase. Journal of Pathology 63:57–64.

Bdliya, B. S., Langerfeld, E., and Rudolph, K. 2004. A modified crystal violet pectate (CVP) medium for detection and isolation of soft rot *Erwinia* spp. from plant materials / Ein modifiziertes Kristallviolett-Pektat (CVP)-Medium zum Nachweis und zur Isolierung von Nassfäule erregenden Envinia-Arten aus Pflanzenmaterial. Zeitschrift für Pflanzenkrankheiten und Pflanzenschutz / Journal of Plant Diseases and Protection. 111:506–515.

Boluk, G., Dobhal, S., Crockford, A. B., Melzer, M., Alvarez, A. M., and Arif, M. 2020. Genome-informed recombinase polymerase amplification assay coupled with a lateral flow device for in-field detection of *Dickeya* species. Plant Disease 104:2219-2224.

Brady, C. L. , Cleenwerck, I., Denman, S., Venter, S. N., Rodríguez-Palenzuela, P., Coutinho, T. A., and De Vos, P. 2012. Proposal to reclassify *Brenneria quercina* (Hildebrand and Schroth 1967) Hauben et al. 1999 into a new genus, *Lonsdalea* gen. nov., as *Lonsdalea quercina* comb. nov., descriptions of *Lonsdalea quercina* subsp. *quercina* comb. nov., *Lonsdalea quercina* subsp. *iberica* subsp. nov. and *Lonsdalea quercina* subsp. *britannica* subsp. nov., emendation of the description of the genus *Brenneria* , reclassification of *Dickeya dieffenbachiae* as *Dickeya dadantii* subsp. *dieffenbachiae* comb. nov., and emendation of the description of *Dickeya dadantii*. International Journal of Systematic and Evolutionary Microbiology 62:1592-1602.

Chao, Y. C., Feng, C. T., Ho, W. C. 2006. First report of aglaonema bacterial blight caused by *Erwinia chrysanthemi* in Taiwan. Plant Disease 90:1358

Charkowski, A., Blanco, C., Condemine, G., Expert, D., Franza, T., Hayes, C., Hugouvieux-Cotte-Pattat, N., Solanilla, E.L., Low, D., Moleleki, L., Pirhonen, M., Pitman, A., Perna, N., Reverchon, S., Palenzuela, P.R., San Francisco, M., Toth, I., Tsuyumu, S., van der Waals, J., van der Wolf, J., Van Gijsegem, F. Yang, C.-H., Yedidia, I. 2012. The role of secretion systems and small molecules in soft-rot enterobacteriaceae pathogenicity. Annual Review of Phytopathology 50 : 425-449

Charkowski, A. O. 2018. The changing face of bacterial soft-rot diseases. Annual Review of Phytopathology 56:269-288.

Chatterjee A., Cui Y., Liu Y., Dumenyo C. K., Chatterjee A. K. 1995. Inactivation of *rsmA* leads to overproduction of extracellular pectinases, cellulase, and proteases in *Erwinia carotovora* subsp. *carotovora* in the absence of the starvation/cell density-sensing signal, N-(3-oxohexanoyl)-L-homoserine lactone. Applied and Environmental Microbiology 61:1959-1967.

Christensen, W. B. 1946. Urea decomposition as a means of differentiating *Proteus* and *Paracolon* cultures from each other and from *Salmonella* and *Shigella* Types 1. Journal of Bacteriology. 52:461–466.

Curland, R. D., Mainello, A ., Perry, K.L., Hao, J.J., Charkowski, A.O., Bull, C.T., McNally, R.R., Johnson, S.B., Rosenzweig, N., Secor, G.A., Larkin, R.P., Gugino, B.K., Ishimaru, C.A. 2021. Species of *Dickeya* and *Pectobacterium* isolated during an outbreak of blackleg and soft rot of potato in Northeastern and North Central United States. Microorganisms 9: 1733.

Czajkowski, R., Grabe, G. J., and van der Wolf, J. M. 2009. Distribution of *Dickeya* spp. and *Pectobacterium carotovorum* subsp. carotovorum in naturally infected seed potatoes. Eur Journal of Plant Pathology 125:263–275.

Czajkowski, R., Pérombelon, M. C. M., Jafra, S., Lojkowska, E., Potrykus, M., van der Wolf, J. M., et al. 2015. Detection, identification and differentiation of *Pectobacterium* and *Dickeya* species causing potato blackleg and tuber soft rot: a review: Detection of soft rot Enterobacteriaceae. Annals of Applied Biology 166:18–38.

DeLude, A., Wells, R., Boomla, S., Chuang, S.-C., Urena, F., Shipman, A., Rubas, N., Kuehu, D. L., Bickerton, B., Peterson, T., Dobhal, S., Arizala D., Klair, D., Ochoa-Corona, F., Ali, M. E., Odani, J., Bingham, J. P., Jenkins. D. M., Fletcher, J., Stack, J. P., Alvarez, A. M., Arif, M. 2022. Loop-mediated isothermal amplification (LAMP) assay for specific and rapid detection of *Dickeya fangzhongdai* targeting a unique genomic region. Scientific Reports 12: 19193.

Dobhal, S., Boluk, G., Babler, B., Stulberg, M. J., Rascoe, J., Nakhla, M. K., Chapman, T. A., Crockford, A. B., Melzer, M. J., Alvarez, A. M., Arif, M. 2020. Comparative genomics reveals signature regions used to develop a robust and sensitive multiplex TaqMan real-time qPCR assay to detect the genus *Dickeya* and *Dickeya dianthicola*. Journal of Applied Microbiology 128:1703-1719.

Ge, T. L., Ekbataniamiri, F., Johnson, S. B.; Larkin, R. P., Hao, J. J. 2021. Interaction between *Dickeya dianthicola* and *Pectobacterium parmentieri* in potato infection under field conditions. Microorganisms 9:316.

Grenier, A. M., Duport, G., Pages, S., Condemin, G., Rahbe, Y. 2006. The phytopathogen *Dickeya dadantii* (*Erwinia chrysanthemi* 3937) is a pathogen of the pea aphid. Applied and Environmental Microbiology 72:1956-1965.

Hageman, R. H., McNamara, A. L., Meeker, G. B., and Shaw, P. D. 1971. Use of a dissimilatory nitrate reductase from *Escherichia coli* and formate as a reductive system for nitrate assays. Journal of Agricultural Food Chemistry 19:229–231.

Hélias, V., Hamon, P., Huchet, E., Wolf, J. V. D., and Andrivon, D. 2012. Two new effective semiselective crystal violet pectate media for isolation of *Pectobacterium* and *Dickeya*: Isolating pectolytic bacteria on CVP. Plant Pathology 61:339–345.

Hugh, R., and Leifson, E. 1953. The taxonomic significance of fermentative versus oxidative metabolism of carbohydrates by various Gram-negative bacteria. Journal of Bacteriology 66:24–26.

Hugouvieux-Cotte-Pattat, N., Jacot-des-Combes, C., and Briolay, J. 2019. *Dickeya lacustris* sp. nov., a water-living pectinolytic bacterium isolated from lakes in France. International Journal of Systematic and Evolutionary Microbiology 69:721–726.

Hugouvieux-Cotte-Pattat, N., Brochier-Armanet, C., Flandrois, J.-P., and Reverchon, S. 2020a. *Dickeya poaceiphila* sp. nov., a plant-pathogenic bacterium isolated from sugar cane (*Saccharum officinarum*). International Journal of Systematic and Evolutionary Microbiology 70:4508–4514.

Hugouvieux-Cotte-Pattat, N. Condemine, G., Gueguen, E., and Shevchik, V. E. 2020b. *Dickeya* plant pathogens. eLS. Pettis, G. (ed), Chichester, UK: John Wiley & Sons, pp. 1–10.

Hugouvieux-Cotte-Pattat, N., des-Combes, C. J., Biolay, J., and Pritchard, L. 2021. Proposal for the creation of a new genus *Musicola* gen. nov., reclassification of *Dickeya paradisiaca* (Samson et al. *2005) as Musicola paradisiaca comb.* nov. and description of a new species *Musicola keenii* sp. nov. International Journal of Systematic and Evolutionary Microbiology 71:005037.

Hugouvieux-Cotte-Pattat, N. and Van Gijsegen, F. 2021. Diversity within the *Dickeya zeae* complex, identification of *Dickeya zeae* and *Dickeya oryzae* members, proposal of the novel species *Dickeya parazeae* sp. nov. International Journal of Systematic and Evolutionary Microbiology. 71: 005059.

Hugouvieux-Cotte-Pattat, N., Pédron, J., and Van Gijsegem, F. 2023. Insight into biodiversity of the recently rearranged genus *Dickeya*. Frontiers in Plant Science 14:1168480.

Humphris, S. N., Cahill, G., Elphinstone, J. G., Kelly, R., Parkinson, N. M., Pritchard, L., et al. 2015. Detection of the Bacterial Potato Pathogens *Pectobacterium* and *Dickeya* spp. Using Conventional and Real-Time PCR. In *Plant Pathology*, Methods in Molecular Biology, ed. Christophe Lacomme. New York, NY: Springer New York, p. 1–16.

Hyman, L. J., Sullivan, L., Toth, I. K., and Perombelon, M. C. M. 2001. Modified crystal violet pectate medium (CVP) based on a new polypectate source (Slendid) for the detection and isolation of soft rot erwinias. Potato Research 44:265–270.

Iwase, T., Tajima, A., Sugimoto, S., Okuda, K., Hironaka, I., Kamata, Y., et al. 2013. A simple assay for measuring catalase activity: A visual approach. Scientific Reports. 3:3081.

Jahn C. E., Willis D. K, Charkowski A. O. 2008. The flagellar sigma factor FliA is required for *Dickeya dadantii* virulence. Mol Plant-Microbe Interact 21:1431-1442.

Kabir, M. N., Taheri, A., and Dumenyo, C. K. 2020. Development of PCR-based detection system for sot rot Pectobacteriaceae pathogens using molecular signatures. Microorganisms 8:358.

Kelman, A. 1954. The relationship of pathogenicity of *Pseudomonas solanacearum* to colony appearance in a tetrazolium medium. Phytopathology. 44:693-695 pp.

Kim, H.-S., Ma, B., Perna, N. T., and Charkowski, A. O. 2009. Phylogeny and virulence of naturally occurring type III secretion system-deficient *Pectobacterium* strains. Applied and Environmental Microbiology 75:4539–4549.

King, E. J. 1943. Preparation of phenolphthalein phosphate. Journal of Pathology 55:311–314.

Kodaka, H., Armfield, A. Y., Lombard, G. L., and Dowell, V. R. 1982. Practical procedure for demonstrating bacterial flagella. Journal of Clinical Microbiology 16:948–952.

Kovacs, N. 1956. Identification of *Pseudomonas pyocyanea* by the oxidase reaction. Nature 178:703.

Laurila, J., Hannukkala, A., Nykyri, J., Pasanen, M., Hélias, V., Garlant, L., et al. 2010. Symptoms and yield reduction caused by *Dickeya* spp. strains isolated from potato and river water in Finland. European Journal of Plant Pathology 126:249–262.

Lee, Y.-A., Chen, K.-P., and Hsu, Y.-W. 2006. Characterization of *Erwinia chrysanthemi*, the soft-rot pathogen of white-flowered calla lily, based on pathogenicity and PCR-RFLP and PFGE analyses. Plant Pathology 55:530-536.

Lee, Y.-A., and Yu, C. P. 2006. A differential medium for the isolation and rapid identification of a plant soft rot pathogen, *Erwinia chrysanthemi*. Journal of Microbiological Methods. 64:200–206.

Lemberg, R., and Foulkes, E. C. 1948. Reaction between catalase and hydrogen peroxide. Nature 161:131–132.

Levine, M. 1916. On the significance of the Voges-Proskauer reaction 1. Journal of Bacteriology 1:153–164.

Ma, B., Hibbing, M. E., Kim, H.-S., Reedy, R. M., Yedidia, I., Breuer, Jane, et al. 2007. Host range and molecular phylogenies of the soft rot enterobacterial genera *Pectobacterium* and *Dickeya*. Phytopathology 97:1150–1163.

Marrero, G., Schneider, K. L., Jenkins, D. M., and Alvarez, A. M. 2013. Phylogeny and classification of *Dickeya* based on multilocus sequence analysis. International Journal of Systematic and Evolutionary Microbiology 63:3524–3539.

Meneley, J. C. 1975. Establishment of an inactive population of *Erwinia carotovora* in healthy cucumber fruit. Phytopathology 65:670.

Nassar, A., Darrasse, A., Lemattre, M., Kotoujansky, A., Dervin, C., Vedel, R., et al. 1996. Characterization of *Erwinia chrysanthemi* by pectinolytic isozyme polymorphism and restriction fragment length polymorphism analysis of PCR-amplified fragments of *pel* genes. Applied and Environmental Microbiology 62:2228–2235.

Ngwira, N., and Samson, R. 1990. *Erwinia chrysanthemi*: description of two new biovars (bv. 8 and bv. 9) isolated from kalanchoe and maize host plants. Agronomie 10:341–345.

Ocenar, J., Arizala, D., Boluk, G., Dhakal, U., Gunarathne, S., Paudel, S., Dobhal, S., Arif, M. 2019. Development of a robust, field-deployable loop-mediated isothermal amplification (LAMP) assay for specific detection of potato pathogen *Dickeya dianthicola* targeting a unique genomic region. PLoS One 14: e0218868.

Oulghazi, S., Pedron, J., Cigna, J., Lau, Y. Y., Moumni, M., Van Gijsegen, F., Chan, K. G., and Faure, D. 2019. *Dickeya undicola* sp. nov., a novel species for pectinolytic isolates from surface waters in Europe and Asia. International Journal of Systematic and Evolutionary Microbiology 69:2440-2444.

Parkinson, N., DeVos, P., Pirhonen, M., and Elphinstone, J. 2014. *Dickeya aquatica* sp. nov., isolated from waterways. International Journal of Systematic and Evolutionary Microbiology 64:2264–2266.

Perombelon, M. C. M., and Burnett, E. M. 1991. Two modified crystal violet pectate (CVP) media for the detection, isolation and enumeration of soft rot erwinias. Potato Research 34:79–85.

Perombelon, M. C. M., and Kelman, A. 1980. Ecology of the soft rot erwinias. Annual Review of Phytopathology 18:361–387.

Pierce, L., and McCain, A., H. 1992. Selective medium for isolation of pectolytic *Erwinia* sp. Plant Disease 76:382.

Potrykus, M., Sledz, W., Golanowska, M., Slawiak, M., Binek, A., Motyka, A., et al. 2014. Simultaneous detection of major blackleg and soft rot bacterial pathogens in potato by multiplex polymerase chain reaction. Annals of Applied Biology 165:474–487.

Pritchard, L., Humphris, S., Saddler, G. S., Parkinson, N. M., Bertrand, V., Elphinstone, J. G., et al. 2013. Detection of phytopathogens of the genus *Dickeya* using a PCR primer prediction pipeline for draft bacterial genome sequences: *Dickeya* diagnostics from draft bacterial genome sequences. Plant Pathology 62:587–596.

Rossman, S., Dees, M. W., Perminow, J., Meadow, R., Brurberg M.B. 2018. Soft rot Enterobacteriaceae are carried by a large range of insect species in potato fields. Applied and Environmental Microbiology 84:e00281.

Samson, R., Legendre, J. B., Christen, R., Fischer-Le Saux, M., Achouak, W., and Gardan, L. 2005. Transfer of *Pectobacterium chrysanthemi* (Burkholder et al. 1953) Brenner et al. 1973 and *Brenneria paradisiaca* to the genus *Dickeya* gen. nov. as *Dickeya chrysanthemi* comb. nov. and *Dickeya paradisiaca* comb. nov. and delineation of four novel species, *Dickeya dadantii* sp. nov., *Dickeya dianthicola* sp. nov., *Dickeya dieffenbachiae* sp. nov. and *Dickeya zeae* sp. nov. International Journal of Systematic and Evolutionary Microbiology 55:1415–1427.

Sławiak, M., van Beckhoven, J. R. C. M., Speksnijder, A. G. C. L., Czajkowski, R., Grabe, G., and van der Wolf, J. M. 2009. Biochemical and genetical analysis reveal a new clade of biovar 3 *Dickeya* spp. strains isolated from potato in Europe. European Journal of Plant Pathology 125:245–261.

Tian, Y., Zhao, Y., Yuan, X., Yi, J., Fan, J., Xu, Z., et al. 2016. *Dickeya fangzhongdai* sp. nov., a plant-pathogenic bacterium isolated from pear trees (*Pyrus pyrifolia*). International Journal of Systematic and Evolutionary Microbiology 66:2831–2835.

Tian, Y., Zhao, Y.-Q., Chen, B.-H., Chen, S., Zeng, R., Hu, B.-S., Li, X. 2020. Real-time PCR assay for detection of *Dickeya fangzhongdai* causing bleeding canker of pear disease in China. 19: 898-905.

Toth, I. K., Hyman, L. J., and Wood, J. R. 1999. A one step PCR-based method for the detection of economically important soft rot *Erwinia* species on micropropagated potato plants. Journal of Applied Microbiology 87:0158-166.

Toth, I. K., Wolf, J. M. van der, Saddler, G., Lojkowska, E., Hélias, V., Pirhonen, M., et al. 2011. *Dickeya* species: an emerging problem for potato production in Europe. Plant Pathology 60:385–399.

Tsror, L., Erlich, O., Hazanovsky, M., Ben Daniel, B., Zig, U., and Lebiush, S. 2012. Detection of *Dickeya* spp. latent infection in potato seed tubers using PCR or ELISA and correlation with disease incidence in commercial field crops under hot-climate conditions: Detection of *Dickeya* spp. latent infection in potato seed tubers. Plant Pathology 61:161–168.

van der Wolf, J. M., Perombelon, M. C. M., and Scottish Crop Research Institute. 1998. *Methods for the detection and quantification of erwinia carotovora subsp. atroseptica on potatoes: a laboratory manual*. Dundee: Scottish Crop Research Institute.

van der Wolf, J. M., Nijhuis, E. H., Kowalewska, M. J., Saddler, G. S., Parkinson, N., Elphinstone, J. G., et al. 2014a. *Dickeya solani* sp. nov., a pectinolytic plant-pathogenic bacterium isolated from potato (*Solanum tuberosum*). International Journal of Systematic and Evolutionary Microbiology 64:768–774.

van der Wolf, J. M., de Haas, B. H., van Hoof, R., de Haan, E. G., and van den Bovenkamp, G. W. 2014b. Development and evaluation of Taqman assays for the differentiation of *Dickeya* (sub)species. European Journal of Plant Pathology 138:695–709.

Van Gijsegem, F., Hugouvieux-Cotte-Pattat, N., Kraepiel, Y., Lojkowska, E., Moleleki, L. N., Gorshkov, V., and Yedidia, I. (2021). Molecular interactions of *Pectobacterium* and *Dickeya* with plants. In: Plant diseases caused by *Dickeya* and *Pectobacterium* species. Eds. F. Van Gijsegem, J. M. van der Wolf and I. K. Toth (Cham, Switzerland: Springer International Publishing), 85–147.

van Vaerenbergh, J., Baeyen, S., De Vos, P., and Maes, M. 2012. Sequence diversity in the *Dickeya fliC* gene: phylogeny of the *Dickeya* genus and TaqMan® PCR for *D. solani*, new biovar 3 variant on potato in Europe ed. Sunghun Park. PLoS ONE. 7:e35738.

Wang, X., He, S.-W, Guo, H.-B., Han, J.-G., Thin, K.-K., Gao, J.-S., Wang, Y., Zhang, X.-X. 2020. Dickeya oryzae sp. Nov., isolated from the roots of rice. International Journal of Systematic and Evolutionary Microbiology 70:4171-4178.

Woodward, E. J., and Robinson, K. 1990. An improved formulation and method of preparation of crystal violet pectate medium for detection of pectolytic erwinia. Letters in Applied Microbiology 10:171–173.

Yap, M.-N., Yang, C.-H., Barak, J. D., Jahn, C. E., and Charkowski, A. O. 2005. The *Erwinia chrysanthemi* type III secretion system is required for multicellular behavior. Journal of Bacteriology 187: 639-648.

Zijlstra, C., Groenenboom–De Haas, L., Krijger, M., Verstappen, E., Warris, S., de Haan, E., and van der Wolf, J., Development and evaluation of two TaqMan assays for generic detection of *Dickeya* species. European Journal of Plant Pathology 156:311-316.